Analytical Applications

of

Sensor Arrays

and

Virtual Instrumentation

Francisco J. Sáez de Viteri Alonso

Ldo. en Ciencias Químicas

Thesis Submitted in Accordance with the Requirements for the degree of

Doctor of Philosophy

Dublin City University   **Ollscoil Chathair Bhaile Átha Cliath**

School of Chemical Sciences

Supervisor: Dr. Dermot Diamond

August 1995

Declaration

I hereby certify that this material, which I now submit for assessment on the programme of study leading to the award of **DOCTOR OF PHILOSOPHY** *is entirely my own work and has not been taken from the work of others save and to the extent that such work has been cited and acknowledged within the text of my work.*

Signed: _____   *I.D. No.: 91700221*

Dublin, 31st of August, 1995.

For my dear parents and sister

For Idoia.

To the memory of Txentxo

A genius is somebody who knows more and more

about less and less.

Until he/she eventually knows everything…about nothing

Anonymous

Acknowledgments

This thesis will not be complete without recognising the help and support from many people, organisation and institutions. To all of them my most sincere thanks.

- First of all to my parents, to whom I am dedicating this thesis, for their moral support, understanding and continuous push forward. And also for all the money transfers from Bilbao to Dublin. Paradoxically enough, they might be closer to the red convertible.

- I must thank my sister for being always there for me, even at worst of times, bearing my bad temper in all so many occasions. I cannot forget her strength and determination through no matter how painful situation.

- I Also want to thank Idoia for the continuous understanding and trust, specially in the last stages of this thesis, both at home and a few thousand miles away. As well, because I spent so much money in telephone bills I had none left to go out and I worked longer hours.

- To my grandparents, thanks a million for the help to buy my portable computer. I made very good use of it.

- I must, indeed, thank my supervisor Dr. Dermot Diamond for his guidance throughout the research and the compilation of the thesis, and all the extra workload

in correcting my written "inglis". Also to Dermie the "fiddler" and Tara for all the much enjoyed Irish tunes washed down with Guinness.

- I want to thank future Dr. Dave Kelly for his friendship since I arrived to Ireland. Also for those sometimes long, sometimes too short coffee and cigarette breaks while writing up this thesis. Best plastic pizza I ever had.

- Thanks to Dr. Eddie Forouzan and Dr. Jeff Debbab for their friendship and help while I was in The Lone Star State. What's up, dudes?

- Thanks to Dr. Margaret Hartnett and Dr. Eithne Dempsey for their useful discussions and ideas which helped me all throughout this research.

- Thanks to all the technicians in the School of Chemical Sciences at Dublin City University for bearing me all these years when I wanted something and I wanted it right away. Special thanks to Veronica Dobbyn, Mick Burke, Maurice Burke, Damien McGuirk and "g'day" Fintan Keogh.

- I also want to thank Brendan Roycroft (Pfizer Pharmaceuticals) for his ideas and discussions over the Continuous Monitoring software, and all the times he invited me for lunch.

- I want to thank Dr. Steve Harris for synthesising, always with a smile, some chemical compounds which I used in this research.

Contents

Figures

Tables

List of Abbreviations

ADC	Analogue to Digital Converter
ASCII	American Standard Code for Information Interchange
BIA	Batch-Injection Analysis/Analyser
CIN	Code Interface Node
CRT	Cathodic Ray Tube
DAC	Digital to Analogue Converter
DIO	Digital Input/Output
DMA	Direct Access Memory
DOA	di(2-ethylexyl) adipate
DOS	Disk Operating System
DOS	di(2-ethylexyl) sebacate
DSP	Digital Signal Processing
e.m.f.	Electro-motive force
FI	Flow-injection
FIA	Flow-injection Analysis/Analyzer
FID	Flame Ionisation Detection/Detector
GUI	Graphical User Interface
I/O	Input/Output
ISE	Ion-Selective Electrode
KTpClPB	Potassium tetrakis(p-chlorophenyl)borate
LAN	Local Area Network

LCD	**Liquid Crystal Display**
LSB	**Least Significant Bit**
MSB	**Most Significant Bit**
MSM	**Mixed Solution Method**
o-**NPOE**	**ortho-Nitrophenyl Octyl Ether**
PC	**Personal Computer**
PCMCIA	**Personal Computer Micro Channel Interface Architecture**
PVC	**Poly Vinyl Chloride**
QB	**Quick BASIC**
RAM	**Random Access Memory**
RIC	**Relative interferent contribution**
ROM	**Read Only Memory**
SAD	**Sensor Array Detection/Detector**
SSM	**Single Solution Method**
THF	**Tetrahydrofuran**
VDU	**Visual Display Unit**
VI	**Virtual Instrument**

Glossary of Symbols

∞	Infinity.
a	Ion activity.
a_{ik}	Activity of the ionic species k in solution i.
$\overline{B}$	Average bias.
β	Stability, or complexation, constant in membrane.
β^v	Stability, or complexation, constant in water.
C	Neutral carrier.
C_k	Concentration of species k.
ΔE	Potential difference.
ΔG	Free energy of Gibbs.
Δt	Time interval.
δt	Time instant.
E_{elec}^0, E_j^0	Standard electrode potential.
E_B	Boundary potential.
E_{cell}	Galvanic cell potential.
E_D	Diffusion potential.
E_{elec}, E_j	Electrode potential.
E_M	Membrane potential.
E_{ref}	Reference electrode potential.
Ex	Ion exchanger.

ε	Error.
F	Faraday constant.
f	Activity coefficients. Also, number of factors.
$f(x), g(x)$	Function f or g of the independent variable x.
$f'(x)$	First derivative of function $f(x)$.
H	Quantisation interval.
i	Solution index.
k	Integer number.
k	Primary ion. Also, distribution coefficient.
K	Overall distribution coefficient.
K^*_{jkl}	Conditional selectivity constant of electrode j, selective for k, against the interfering ion l.
K_{jkl}	Selectivity coefficient of electrode j, selective for k, against the interfering ion l.
l	Interfering ion. Also, number of activity levels.
λ	Parameter.
M	Metal.
M^{z+}	Metal ion of charge z.
n	Natural number.
$\boldsymbol{R}$	Group of the real numbers.
R	Gas constant.
$\vec{r}$	Response vector
r	Response (component of $\vec{r}$). Also correlation coefficient.

R^+	Organic cation.
R_n	Resistor n.
S	Subgroup of R.
S_j	Sensitivity (slope) of electrode j.
t	Time.
T	Absolute temperature (K).
u	Ion mobility.
V	Sample volume.
x	Independent variable. Also, abscissa.
y	Value of a particular function $f(x)$ or $g(x)$.
y'	Value of the first derivative function $f'(x)$.
z	Ionic charge.

Abstract

Analytical Applications of Sensor Arrays and Virtual Instrumentation

Francisco J. Sáez de Viteri Alonso

An ammonium detection system using Ion-Selective Electrodes (ISEs) in Flow-Injection Analysis (FIA) is described. Because of the low selectivity of the nonactin ammonium selective electrode towards some common ions, different selectivity enhancement techniques have been examined. A Sensor Array Detector (SAD) which comprises ISEs selective for ammonium, sodium, potassium and calcium was used. A modified form of the Nikolskii-Eisenman Equation is proposed in which the charge power function of the interfering ion activity is linearised. Selectivity is quantified for the PVC membrane electrodes (NH_4^+, Na^+, K^+, Ca^{2+}) in terms of constants rather than conventional coefficients. These constants and other electrode parameters such as cell constant and slope are estimated by means of the FIA-SAD approach.

The SAD response was modeled *via* the Nikolskii-Eisenman equation with SIMPLEX regression model. The applicability of the resulting values for these parameters is demonstrated through the determination of unknowns by direct solution of the system of modified Nikolskii-Eisenman equations describing the array response. The results show that the use of an array of ISEs under FIA regimes for the detection of ammonium in the concentration range 10^{-4} to 10^{-2} mol dm^{-3} gives a much higher improvement in the determination of ammonium in aqueous samples than the use of a single ammonium electrode in steady-state or kinetic measurements. This approach is suitable for use in real-time monitoring applications where batch calibration techniques cannot easily be implemented.

Computer controlled laboratory instrumentation is of growing importance both in research and in industry. Different hardware and software approaches may be chosen which allow the development of high quality products. Last trends in hardware and software strategies are analyzed and some general guidelines are given for instrumentation development. The graphical compiler LabVIEW 3.0 for instrumentation from National Instruments is presented and evaluated in terms of flexibility and low cost for the production of virtual instrumentation for research, biomedical applications and industrial environmental monitoring.

Preface

When I first sat down to write this thesis I had the idea that it was going to be pretty straightforward to explain the ideas and results obtained during the previous three and a half years. Soon I realised that, even if the results and theories behind them were not too much trouble, the ideas and why they were applied were much reluctant to sit nicely in paper. Besides, the task of linking them one another was specially troublesome.

Giving my brain a bit of credit, I preferred to think that this was indeed a very difficult job because of the different aspects involved in this research. Flow-injection electrochemistry, sensor arrays, chemometrics, electronics, computer interfacing, software development and engineering design are areas of knowledge on their own right, which I had to put to work together to achieve the goals of this research. Luckily enough for me and because of time and space limitations, only the areas of sensor array detectors for chemical analysis and scientific software applications are greatly detailed, the rest of them being described only in their application to this research.

Nevertheless, an introductory chapter on electronics and computing gives a brief overview on signals, computer hardware and software, and signal interfacing. It does not intend to give formal technical knowledge but to clarify and describe some concepts, and to set the scene for the idea of scientific interfacing and software designed further developed during the following chapters.

Chapter 2 deals with the theory of ion-selective electrodes (ISEs), particularly of neutral carrier ISEs, in which this research was focused. Also the applicability of these sensors for analysis purposes in terms of optimum experimental circumstances and analytical technique used (batch measurements or flow-injection analysis-FIA) is described for systems where single electrodes, or perhaps an array of electrodes treated as individual sensing units, are used as the sensing element of the analytical system.

The following chapter describes the theory and application of detector arrays formed by a number of ISEs in which the response of each of the electrodes is treated as a component of the overall response of the sensor array, and it is used to support and complement the response of the remaining electrodes in the array. Either Batch or FIA experimental setups can be used, the latter being the most appropriate for the increased accuracy in the prediction capability and a number of advantages and possibilities discussed, specially for self-diagnosis "intelligent" analysers.

The application of the above described system to the analysis of ammonium is described in detail in Chapter 4, and demonstrates the advantages of using detector arrays for the analysis of ionic species in samples where the background matrix contains high and varying levels of interferents. The striking prediction capabilities of a detector array in FIA regime are compared to those of other experimental setups and the results discussed. Also new theoretical findings on the behaviour of ISEs in flowing systems are described and discussed.

These analysis techniques would be impossible to implement without the need of digital multichannel acquisition devices because of the necessity of simultaneously reading of the array of sensors with very high precision. The latest technology in plug-in acquisition cards for microcomputers allows implementation of this task by interfacing the analytical system to a desktop computer, and nowadays also a to a portable notebook, and enabling data acquisition and system control in digital format straight to and from the computer.

Obviously, specialised software is needed for this purpose and, in Chapter 5, a software compiler specially designed for the development of acquisition and control programmes for scientific purposes is described. LabVIEW for WINDOWS, which is the name of this commercial package, allows the generation of very high quality interfacing software in little time, with a superb graphical interface which recreates in the computer screen forms and shapes of instruments (real or imaginary) which are controlled graphically to generate a *virtual instrument* which only exists within the computer architecture.

In the following, and last, Chapter 6, this graphical programming environment is put to work in the design and development of virtual instrumentation for three different applications, which cover analytical research, biomedical *in-vivo* monitoring and industrial environmental analysis. These applications demonstrate the possibilities of this graphical language compiler in terms of computing power, ease of design, flexibility and modularity. Different examples of the graphical interface are shown throughout this chapter, and Appendix E shows their graphical code.

I did not enjoy writing this thesis and I wonder if anybody ever did, but I will say that I really enjoyed my time thoroughly during these three and a half previous years. Of course, working in the lab always has its ups and downs but as an overall result I will say it was fun.

Finally, I will say that I really tried to write this thesis as "user friendly" as possible but, as it will be obvious, a doctoral thesis does not give too much room for amenity and fun. Nevertheless, this is the final product which will probably be the version 2001 by now.

1. Electronics and Computing

Since the development of analogue electric meters, the chemist has been using such devices to measure properties in chemical systems. Signals from transducers and probes were measured with these meters to translate a physical or chemical property into a number representing the magnitude of that property. Data logging was usually *via* an analogue strip chart recorder or oscilloscope. These measurement systems continued to evolve slowly up to c.a. 1950.

With the invention of digital electronics, and its rapid evolution during 1970's and 80's, the philosophy and the practicality of system interfacing changed completely. Small and simple digital meters often incorporated facilities to allow data logging to other devices and mainframe computers, which could be used for digital storage and data processing. Electronic devices were available to perform signal acquisition and control to and from these mainframes but, in the chemistry field, it was the development of microcomputers that really boosted the concept of computer interfacing. The drop in the cost of computing power and the availability of specialised acquisition and control electronic equipment from secondary manufacturers made the use of dedicated computers for process control and data acquisition economically viable.

The development of software, both for general purpose and for specific applications, has also seen a dramatic evolution in the basic concept of programme design, appearance and flexibility. The idea of close and self sufficient programmes written in now obsolete sequential line codes has given way to the latest interactive and flexible applications generated with object oriented graphical programming compilers.

This chapter presents a general overview of signals types in chemical instrumentation followed by a discussion of computer architecture and interfacing hardware for communications and signal acquisition. Computer software, operating systems and compilers are also discussed in terms of performance, appearance and simplicity of user design.

1.1 Signals

In general, signals can be described as a function of any variable x which describes quantitatively an occurring phenomenon. Mathematically this can be represented as

$$y = f(x)$$

<div align="right">Eq. 1.1</div>

where y is the magnitude of the signal, x is the independent variable and f is the relationship between both. Throughout this work, signals will be referred as functions of time t unless otherwise stated. Signals can also be functions of more that one variable (e.g. time t and position x), but only bidimensional signals will be discussed. In the scientific world a signal is a function that describes the magnitude of a physical variable

or property associated with a system. In the instrumentation world, the word *signal* makes reference to streams of electrons traveling through conductive wires. The characteristics of these electron streams (voltage difference, current, etc.) are often related to the response of a transducer to a physical or chemical property in a system. Signals can be grouped in continuous-time and discrete-time depending on the characteristics of the time variable t during the interval t_2-t_1 where the signal exists.

1.1.1 Continuous-Time Signals

Continuous-time signals, also known as analogue signals[1], are those signals which, during the time interval t_2-t_1 where they exist, the independent variable t can take any value from the group of the real numbers R. Continuous-time signals can be represented as;

$$y = f(t) \quad \forall t_1 < t < t_2 \quad t \in R \qquad \textbf{Eq. 1.2}$$

where y is the value of the time dependent function f at time t. This means that, while the values of the magnitude $f(t)$ may be discontinuous (i.e. $y'=f'(t)=\infty$ in, at least, one point),

Figure 1.1: Continuous-time and discrete-time signals.
A signal defined in a continuous time domain (a) exists for any value of time, while the discrete-time type (b) only exists at particular time values and during a short period of time δt.

3
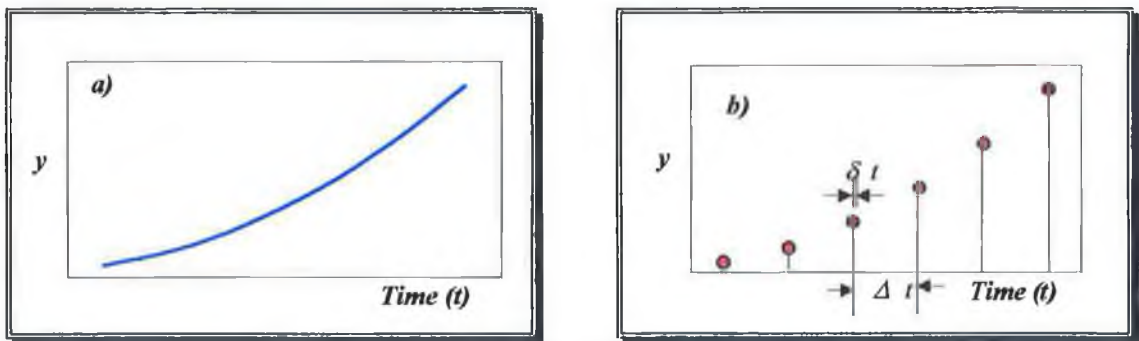
the function g from where t takes its values ($t=g(x)$) is continuous in the interval t_2-t_1.
Figure 1.1a shows an example of a continuous-time signal.

1.1.2 Discrete-Time Signals

Discrete-time signals are described as those signals which only exist during sampling periods of instants δt in the time interval t_2-t_1 where they are defined. In this type of signal the time variable t can only take values from S, a subgroup of R. Mathematically,

$$y = f(t) \quad \forall t_1 < t < t_2 \quad t \in S \subset R \qquad \qquad \textbf{Eq. 1.3}$$

In this case, the magnitude $f(t)$ can be continuous or discontinuous, but the function from where t takes its values is discontinuous. Figure 1.1b shows a discrete-time signal where the time variable t takes values equally spaced Δt during the sampling instant δt. The value of the time increment Δt can be a variable resulting in signals that present non-homogeneous spacing between samples.

1.1.3 Quantised Signals

In Sections 1.1.1 and 1.1.2, signal types were discussed in terms of the continuity characteristics of the time variable t and the continuity of the values of the phenomenon or physical magnitude y used to classify signals as continuous and discrete. Continuous signals are those whose magnitude $f(t)$ can take any real value R. Therefore the function from which y takes its values from is a continuous function. Quantised or discrete signals

are those whose magnitude $f(t)$ can only take values which are multiples of a positive number called the quantisation interval, H [2].

$$y = f(t) \quad \forall t_1 < t < t_2 \quad y = kH \qquad (\text{k=}\pm1, \pm2,..., \pm\text{n}) \qquad \text{Eq. 1.4}$$

Figure 1.2a shows a continuous $y=\sin^2(t)$ signal and the representation of its quantised equivalent (Figure 1.2b) with a quantisation interval H equal to 0.1 units (the quantisation interval units are identical to those of the signal magnitude y). It can be appreciated how the intervals between steps are not time dependent (Δt is not constant), and the duration of a particular step depends on whether the continuous signal has reached the next possible quantisation level, $y=(k+1)H$. From the theoretical point of view the parameter H of a quantised signal can take any real value. Its only when this signals are related to some other phenomenon that the value of the quantisation interval has critical importance (e.g. for electric signals, the value of the quatisation interval H will be dictated by the resolution of the data sampling device). When a quantised signal, either analogue or digital, is used to represent a continuous signal, the closest the interval H is to zero the better the quantised signal can reproduce the magnitude values of the continuous one. In fact, high H values and sampling periods Δt translate to loss of information. For high quantisation interval values the magnitudes of the continuous and quantised signals may differ considerably and truncation of the continuous signal may occur. This aspect of the quantisation interval H will be further discussed, for electric signals, in Section 1.4.1.1

Figure 1.2: Example of a sinusoidal ($\sin^2(t)$) and its equivalent quantised signal.
The resolution of the quantised signal is dictated by the quantisation interval. High quantisation interval values may truncate important information of the continuous that will not appear in the quantised equivalent. In this example the interval H=0.1 units.
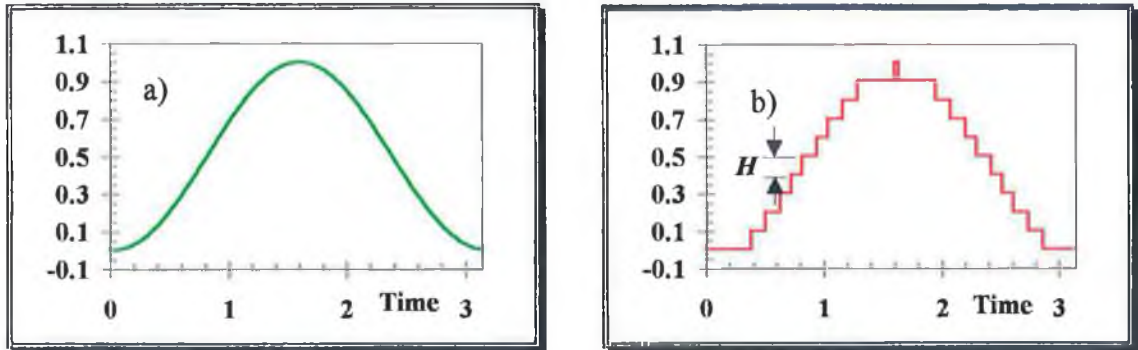
Because of the difference between continuous and quantised signals lies in the continuity of the signal magnitude $f(t)$ (not t), quantised signals exist both as continuous-time and discrete-time signals, and a conversion from continuous to quantised for a discrete-time signal will have an equivalence in the example shown in Figure 1.2. Discrete time signals which have been quantised are called digital signals[1,3].

1.1.4 Analogue Signals

As described previously in Section 1.1.1 analogue signals are those which are defined in a continuous time period. From the instrumentation point of view, the main components of an analogue signal are the level, shape and frequency, and signals can often be classified in terms of which of these components is the dominant one, although it is very common to find signals in which there is no dominant contribution from any of them, and important contributions to the information content are carried in one, two or all three components[4].

(i) Level

The magnitude of an analogue signal has a single value for each point in the time interval t_2-t_1. The level of a signal can be described as the relative position of a general trend to an arbitrary zero value. Magnitudes representing, for example, ambient temperature or cruising speed have the signal level as main information component. In fact, small and quick variations of the magnitudes of these signals will be almost certainly be related to noise effects or artifacts. Figure 1.3 shows a representation of the variation of temperature with time. Gradual changes of temperature are represented by the general trend of the temperature values. The figure shows two distinctive trends, a decrease in the temperature followed by a stabilisation stage.

Later in this thesis a biomedical system (Section 6.3) and an environmental monitoring system (Section 6.4) are described in which the valuable information resides in the general trends of the signals experimentally acquired.

Figure 1.3: Level signal: Variation of temperature with time.
A decrease in the magnitude followed by stabilisation are the two trends in this level signal.
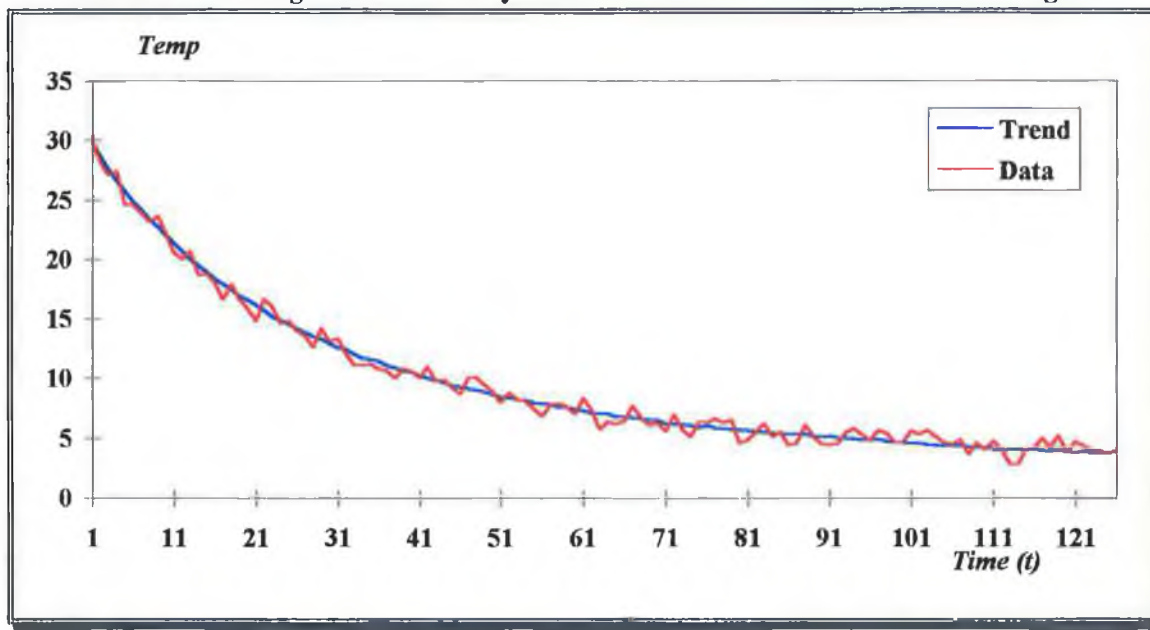
(ii) Shape

The shape of a signal can be defined as the relative position of the magnitude values with respect to the other values in the signal. If the main information component is in this inter-relationship among values, but not the relative position to an outside reference (e.g. zero-level) the signal is considered a pure shape signal[4]. This means, for example, that the absolute values of the magnitude can be modified with offset procedures with no change in the signal information. Figure 1.4 shows the variation with time of the response of an Ion-Selective Electrode with respect to a reference voltage (baseline) in a flow-injection analysis (FIA) system. Comparisons of the electrode potential at different points of the signal gives the information about the system.

Figure 1.4: Variation of an ISE e.m.f. with respect to a baseline voltage.
The shape of the traces also carry important fundamental information about the electrochemical system.
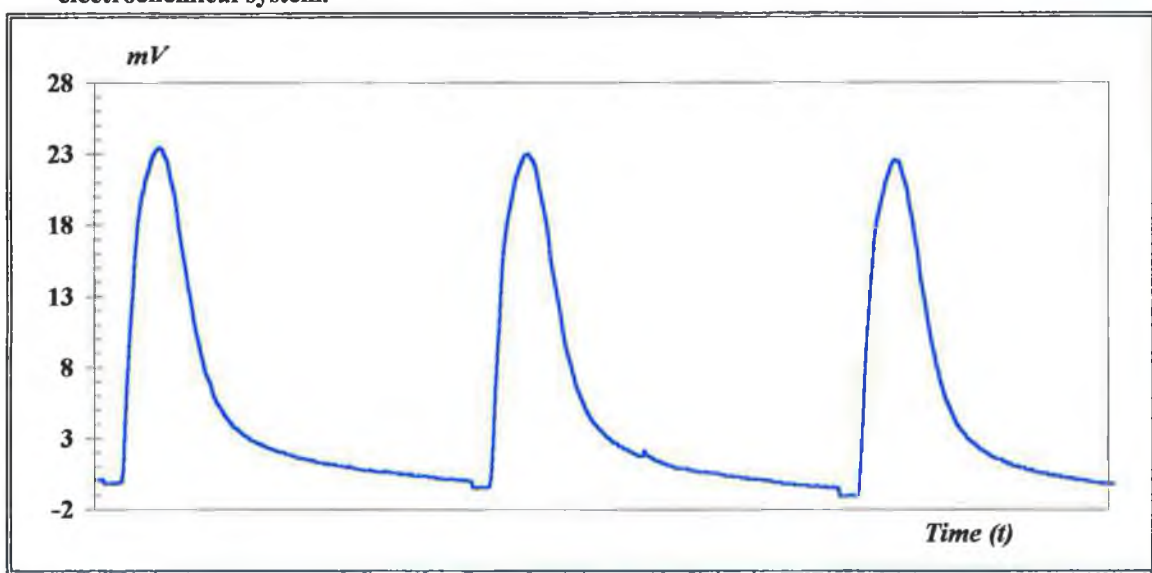
(iii) Frequency Signals

Periodic repetitions of shapes of signals can give information about how frequently particular events happen in time. Level or shape may not be of interest and only the

frequency component carries information about the phenomenon. Figure 1.5 shows a signal in the time domain with level and shape components but which only carries valuable information in the frequency component. Very often these frequency signals are transformed from the time domain into the frequency domain which facilitates the interpretation of the information content. In theory, any signal defined in the time domain can be represented as a convolution of sinusoidal waves with different frequencies and amplitudes.

Figure 1.5: Frequency signal: $y=\sin (t/2)*\cos(8*t)$.
In pure frequency signals valuable information is carried in the frequency component, while level and shape are not of importance.
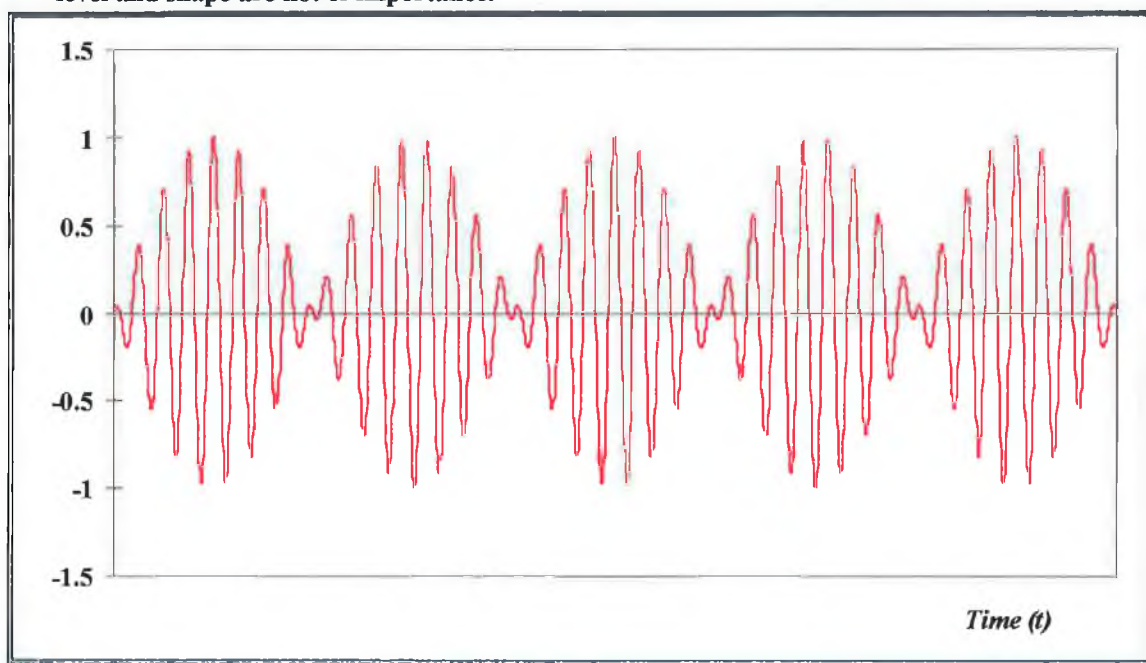
1.1.5 Digital Signals

Strictly speaking, and as explained in Section 1.1.3, digital signals are quantised signals which exist in a discontinuous time domain. In the electrical world, digital signals are

described as current spikes of very short duration traveling through conducting wires. The signal is quantised so as only two signal levels are possible, current "yes" or current "no". In Boolean algebra, when a clause is happening, it is tagged as TRUE or, inversely, FALSE if it is not. If the same nomenclature is used for digital signals, TRUE will refer to whenever there is current in the wire and FALSE will mean that the former clause is not happening. Indeed, depending on the frequency and duration of these TRUE/FALSE stages digital signals can be classified in TRUE/FALSE, single pulse and pulse train signals.

(i) TRUE/FALSE Signals

In fact, all digital signals are of the TRUE/FALSE type at some stage (i.e. all kids present TRUE/FALSE levels), but only those with low frequency switch will be considered in this class. In these signals the duration of the TRUE period is somewhat of the same order as the FALSE stages. Figure 1.6a shows a representation of a TRUE/FALSE signal. Typical applications are in the actuation and monitoring of the ON/OFF switching state in electric devices such as contact switches, valves, solenoids, indicators (LEDs), etc.

(ii) Single Pulse Signals (one-shot)

These signals only maintain the TRUE state during a short period of time δt after which they switch back to the zero-current state. The duration of the time interval δt is an integer multiple of the update time of the system generating the signal. The most

common applications are for triggering events in third systems. Figure 1.6b shows the time profile of a single digital pulse.

(iii) Pulse Train Signals

Pulse train signals, as Figure 1.6c shows, are series of current pulses traveling along a wire. Both the duration of each pulse and the time lapse between pulses is also an integer multiple of the system update time. They find applications in event counting and rate/frequency measurements.

Figure 1.6: Digital signals and their variations with time.
a) TRUE/FALSE signal. b) Pulse signal. c) Pulse train signal
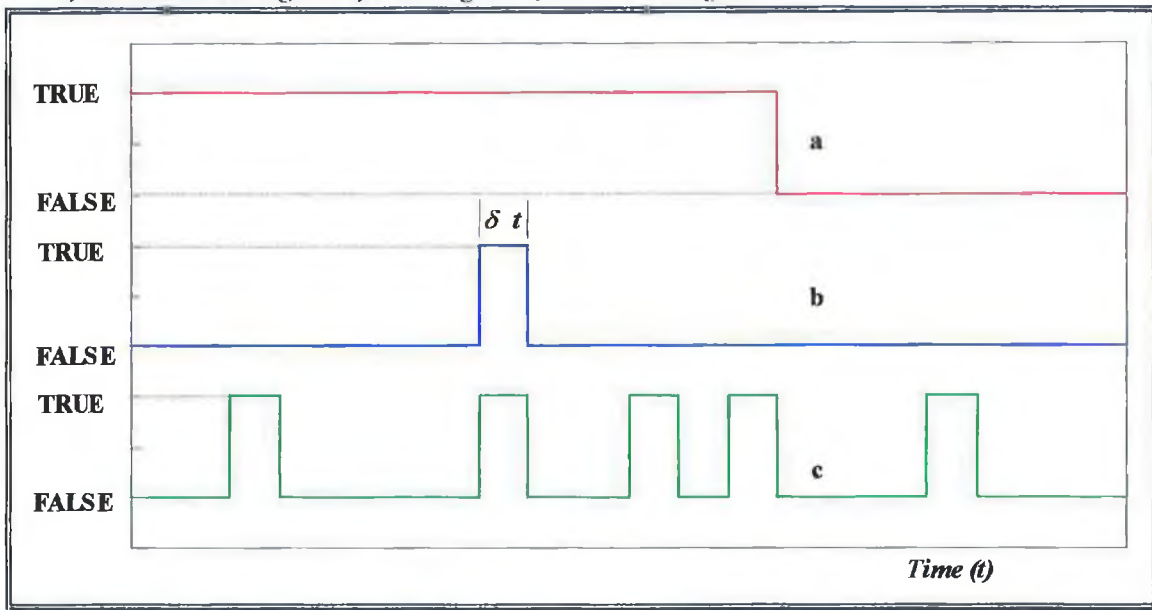
1.2 Hardware

Real signals need some kind of physical hardware to be generated or acquired. Hardware can be divided into analogue and digital systems. Before microprocessors were available, equipment functioned in an analogue fashion. Acquisition, processing and data presentation dealt with analogue signals and functioned in an analogue manner. Microprocessors, linked to analog-to-digital converters (ADC) allowed the signal to be acquired and handled in a digital fashion, and instruments incorporating this hardware could perform better signal processing and more elaborate presentations and displays than their analogue counterparts. Besides, data processed in a digital fashion provided the critical advantage of easy storage and retrieval. Using magnetic supports (hard drives, floppy disks or tapes) the information could be permanently stored with no loss of information or precision of the measurements.

Stand-alone systems with dedicated internal microprocessors were originally developed to solve specific problems in particular applications. Instruments like chromatographs, spectrometers or potentiostats are some examples of instruments that were, until recently, built only as physical stand-alone instruments. As these instruments developed, the electronics evolved into more and more complex forms as the processing power increased. This created a situation where powerful instruments were very specialised and with very little flexibility. Large amounts of money had to be spent in buying instruments that would perform only one task.

However, in recent years, the availability of microcomputers and the development of specialised high performance interface electronics has had a major impact in analytical instrumentation. Sophisticated pieces of equipment need not be dedicated to a single task, and inevitably they need computers to assist in the process of data processing and data presentation. In cases where only an analogue signal is available, the PC will need an interface board to convert analogue signals to digital before processing, whereas in cases where the instrument provides a digital output port a communications device is needed to transfer the digitised signals into the computer memory. This next-to-computer approach is more cost-effective as standard electronics circuitry is used , which allows a higher degree of flexibility than the stand-alone systems, in the sense that the same computer might be linked to a second system and it will also allow for more specialised and custom designed data processing and data presentation options for the user.

1.2.1 Computer Architecture

A number of different microcomputer systems are available in the market which, in essence, are able to perform the same type of processes. While this research only focuses on IBM PC and PC compatible computers (PCs), these could be substituted with other systems such as SUN or Macintosh.

1.2.1.1 Processor

The PC series are based on 8086 series processor which has rapidly evolved in the last decade through the 80286, 80386 and 80486 to develop the new state-of-the-art Intel Pentium main processor. An important attribute of the series is the back compatibility they present. Performance and speed are substantially increased through the series, maintaining the characteristics of the PC system and therefore, except in very few occasions, programmes written for an earlier processor version will perform identically (except for the enhanced speed) in the fastest of the series. In those cases when a very large number of calculations have to be performed, mathematical co-processors can be added into the main computer structure to increase the calculation speed.

1.2.1.2 Memory

The memory of a computer is its ability to store information so that it is readily available to the processor. Random Access Memory (RAM), i.e. the memory which allows the computer to store information while the computer is switched on, is used to store experimental data as it is acquired. RAM memory is usually divided into Base Memory and Upper Memory areas. The Base Memory are the lowest 640 KBytes and are used by the Disk Operating System (DOS) and DOS based applications. If a particular DOS application needs extra memory it can swap the contents of the Base Memory with the Upper Memory area to the Extended or Expanded Memory, depending on how this Upper area is configured. WINDOWS environment, which will be further discussed in this chapter (Section 1.3.3), facilitates this operations to an extent that the computer user

and, in general, the programmer need not to worry about these operations. The amount of memory installed in a computer is probably, after the type of processor, the factor that most affects the performance of a PC in terms of the internal processing speed. Also the access time, i.e. the time needed to make the information available to the processor, has an important role in the computer's performance, specially for very heavy operations and processes.

1.2.1.3 Peripherals

Peripherals, i.e. modems, printers or plotters, even the disk drives and particularly graphics cards, will have an effect on the overall performance of the computer. A slow peripheral will mean that the processor will have to wait for the device to complete a specific operation before it can continue with the process. For applications where continuous data storage/retrieval are needed, slow drives will considerably lengthen the operation time.

In particular, operations concerning the update of information in visual display units (VDUs), usually a monitor, may slow down the computation process to a great extent. To prevent this, graphics accelerator cards with local bus and dedicated graphics processor and memory can be installed to work in parallel with the basic computer hardware.

1.2.2 Input/Output Ports and Interface Boards

Obviously, these peripherals treated in Section 1.2.1.3 need a way to receive or send information to the microprocessor. This is done through Input/Output (I/O) ports or interface boards which can be already built into the computer architecture or connected to it, as with the communications ports. Other devices which may not be considered as peripherals may also use the same type of communications, such as connections to local area networks (LANs) or mainframes. In addition, more specialised protocols for data transfer among devices will require also extra hardware to support the process. General Purpose Interface Bus (GPIB) cards are, without doubt, the most illustrative example. Not all the devices that one may desire to communicate to and from a computer will have inherent communications capabilities, like a recorder or an analogue switch, and therefore can only be capable of very basic I/O functions. In those cases, data acquisition boards will be the only approach to achieving data transfer.

1.2.2.1 Communications Ports

Standard I/O ports are present in every PC computer. Some are specific I/O ports for selected devices like VDUs, keyboards or docking stations for portable computers. Furthermore, general purpose I/O sockets are available for a variety of external devices like plotters, printers, mice, optic pens, etc. and can be also used for long distance communication to mainframe computers. These ports are present not only in computers, but also in many "intelligent" instruments which use them to interact with one another.

Data passed through this communication ability can be sent either in series or in parallel along the wires that make the physical support for the port-to-port communication.

1.2.2.1.1 Serial (RS-232) Communication

Serial communication is very slow in comparison to other data transfer protocols, and it is only used when slow data transfer rates can be accepted. The standard configuration internationally accepted by manufacturers, allows communication between devices. Information is sent in a one-bit-at-a-time mode through a single line. For each byte (7 or 8 bits plus parity), control signals are included at the beginning (start) and at the end (stop bits), making the protocol even slower. The maximum data transmission rate with standard serial ports is 19200 bits s^{-1}. If data can only travel through the line in one direction, the device will be either sending or receiving information at any point in time. This serial type is called Half-Duplex (HDX). Using two physical lines the devices can communicate to each other sending and receiving information simultaneously. This is the Full-Duplex (FDX) serial type and can multiplying by two the data transmission rate.

As an example, the ASCII (American Standard Code for Information Interchange) code 75, which corresponds to the character "K", translates to 1001011 (LSB first) in binary code. The serial protocol will send a start bit, then 1, then another 1, then 0 and so on, finishing with a parity bit and stop bits (Figure 1.7). A "1" means that the voltage in the communication line is HIGH (+3 V in American RS232 and +6 V in European CCITT V24) with respect to ground[5], and "0" means that the line voltage is LOW (logic zero).

The first bit of the ASCII character to be sent is always the Least Significant Bit (LSB), ending with the Most Significant Bit (MSB).

As serial communications can be used over very long distances (in comparison to other communication types) it is usually utilised for data transfer to computers and devices in remote locations, although signals boosters may be needed to ensure high/low signal requirements are met.

Figure 1.7: Diagram of serial communication.
The transfer of the ASCII character "K" (ASCII 75, binary 1001011) is done by sending a start bit followed by 7 bits (actual information) and a parity check bit for error checking.
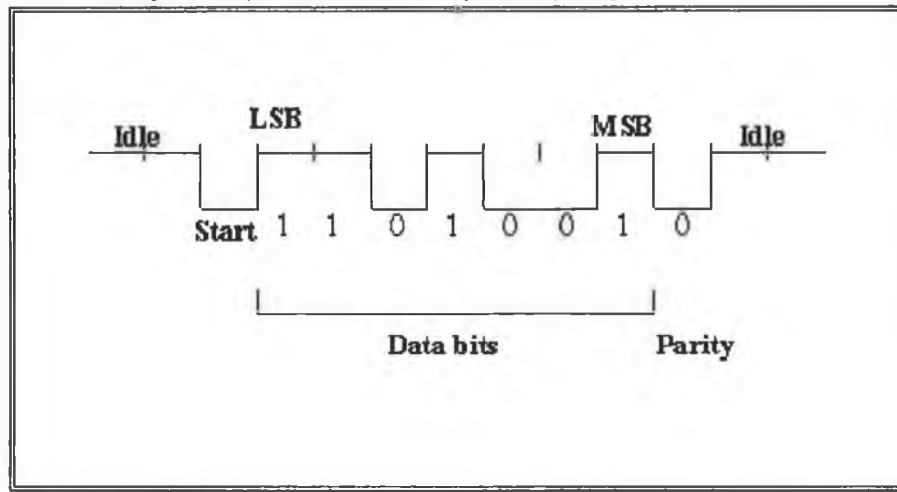
1.2.2.1.2 Parallel Communication

(i) Printer Port

Taking the same example as in the previous section, transmission of the character "K" (ASCII 75) is achieved in parallel communication by sending simultaneously all the bits that compose the character "K" through eight parallel data lines (extra lines are needed for the control signals). This way, the same character will be transferred in one go as

each wire carries only one bit position. This communication type is used only over short distances but offers much higher data transfer rates than serial ports. Typical uses are for data transfer to printers or backup devices (tape streamers).

(ii) Modified Printer Port

Communication through the printer port was, until recently, not very important in the scientific world as it was not really used for scientific data communication. But with the new portable technology, devices and peripherals that were normally connected inside the computer and which do not fit in the small portable volume can be externally connected and powered *via* the parallel ports. Data acquisition boards for field measurements, like the new DAQPad-1200 from National Instruments[6], are rising new possibilities for fast data transfer through parallel communications. As well as serial ports, additional parallel hardware can be obtained for applications requiring it. There is a certain degree of configuration incompatibility among parallel port types which renders the direct connection of intelligent instruments from different manufacturers difficult or impossible. This has generated the necessity for a standard parallel communications protocol like the IEEE/GPIB protocol.

(iii) GPIB/IEEE Protocol

General Purpose Interface Bus (GPIB) or IEEE 488 bus was developed some 20 years ago and allows interconnection of a maximum of fifteen intelligent instruments to a supervisor computer[5]. Only one packet of information can be carried by the bus at one time, so the computer controls which instrument is sending the data and which one is

receiving it, to avoid data corruption. For the information to be transmitted three conditions need to be satisfied;

- The instrument sending the data is ready to transmit.

- The device receiving is ready to read.

- The bus is empty of data.

In theory the bus can transmit up to one KBytes s^{-1} through a 24-wire shielded cable[5]. Eight of those wires are information lines, as in the normal parallel ports, and eight are control lines. The remaining eight lines are grounds. Communication is limited to distances of several meters between stations, and around 30 m in total for a network (i.e. realistically, the communication is restricted to a single room).

1.2.2.2 Plug-in Data Acquisition Boards

As noted before, data acquisition cards are needed in those systems where the computer cannot communicate digitally with the external device. These cards digitise electronic signals and can also generate digital or *pseudo*-analogue (hybrid type) signals. Each interface board manufacturer offers a wide range of products to suit any applications, from the "cheap" 8 bit I/O card for teaching purposes to the very expensive high performance boards. General purpose acquisition cards are also available which are designed to suit an average application and present a standard number of functions.

In general, instrument detectors, sensors, transducers, etc., provide analogue signals which can be digitised using I/O cards fitted inside a computer[7]. Standard features in a

12-bit general purpose card, which gives a discrimination of 1:4096, will be 16 analogue input channels (8 in differential mode), 2 analogue outputs, 8 digital I/O channels, and some kind of triggering and frequency reading facilities. The standard input range is often variable (see Section 1.4.1.1) so better resolution can be obtained in a narrower input range. Higher resolution 16-bit cards are also available. They are more expensive and present higher settling times, and will not be standard equipment unless very high resolution is really needed. Two acquisition cards, the RTI-815 from Analog Devices and the AT-MIO-16DL from National Instruments, were used at different stages of this research.

1.3 Software

Section 1.2 was dedicated to the physical part of the interfacing world. On its own it will not be able to do anything as software must be available to control it. Software is physically supported in the hardware and can be described as the interface between the hardware and the user, talking to both and receiving information from both.

1.3.1 The Operating System

The operating system is the lowest level software. It performs the most basic actions, such as read/write functions to peripherals, memory management, or keyboard and language selection. The operating system is stored on disks (floppy or hard disks) for the PC architecture, although some different computer systems have it fixed in Read Only

Memory (ROM) chips which start the computer up as soon it is switched on. In recent years the trend has been to move from the command type structure to graphical environments, as they are regarded as being more "user friendly". MS-DOS (DOS from now onwards), Microsoft WINDOWS Environment (WINDOWS), and OS/2 are typical examples of this increase in user friendliness towards graphical operating environments which are much more intuitive to use and need less technical knowledge. Not only the ease to use changes with the evolution of the operating systems. Performance is also important and designers and software engineers spend much effort in improving the performance of each new version.

DOS is the least friendly of the three. Its structure is command oriented, and the user needs to type, without mistakes, the commands in a blank computer screen. Awkward command and parameters are used and an extensive list of instructions and switches have to be learned. For example, a number of different switches can be added to commands and programs at different positions so that different functions or operations are executed. Apart from the unfriendliness, a major drawback DOS presents is its inability to perform more than one task at a time. This means that if a number of applications need to be run they will only be able to do it in series, one after another.

In contrast, WINDOWS and OS/2 are graphical operating systems, based in a "drag-and-drop" or "click and double-click" operations. The user sails through a series of icons representing computer objects such as drives, files, directories and so on. These systems are very intuitive with a high degree of user friendliness which increases user

productivity. Furthermore, the multitasking capabilities of these systems make them much more powerful than the old DOS. The term "multitask" will have to be explained as it represents slightly different concepts for WINDOWS than for OS/2. WINDOWS is a high level system that "sits" on DOS. This means that it uses DOS while it provides a higher degree of user friendliness. Using DOS means that the main processor only performs one task at a time, but WINDOWS can have several applications opened and running at a time, switching the use of the processor from one to the other every 50 milliseconds (typically) which has the effect, in a bigger time frame, of a multitasking capability. OS/2, on the other hand, allows different applications to share the processing power at the same time, in a real multitasking fashion. Very recently, a new version of WINDOWS called WINDOWS '95 has been released. This version is a full operating system on its own with many of the characteristics of OS/2, such as multitasking, and does not need the support of DOS as the base operating system.

1.3.2 DOS Based Software

In this section, any programme or code which runs directly on top of the DOS system is included. The most important characteristic is that there are no multitasking possibilities, and the maximum memory available to this applications is the 640 KBytes of base memory.

1.3.2.1 Line Oriented Code

Line oriented code developed from the very first computer programming techniques in which the instructions were input to the computer in series. The instructions or commands were executed in the same order they were input, usually following the numbers the command lines started with. Very low level programming languages, machine code or assembly were used to design the programmes. Eventually, a number of different higher programming languages (BASIC, C, FORTRAN, etc.) appeared based on more recognisable (language based) commands. For some of them, each time the code was executed the commands were interpreted into low level machine code and the operation performed. Drawbacks of these early interpreters included the need to have the command interpreter code in memory at all times to convert the code, and the need to perform the conversion every time the programme was executed. The most popular interpreted languages evolved towards the concept of compiled languages. These compiled languages retained the basic structure of the interpreted languages with the advantage that when the code was compiled a machine code version of the programme was generated. The need to perform the translation operation only once, writing the machine code to a executable file and the freedom to use this file without the compiler code in memory made these language compilers very popular among serious computer programmers.

QuickBASIC

BASIC has always been one of the most popular line oriented programming languages because of its similarity to written English. It started as an interpreted programming
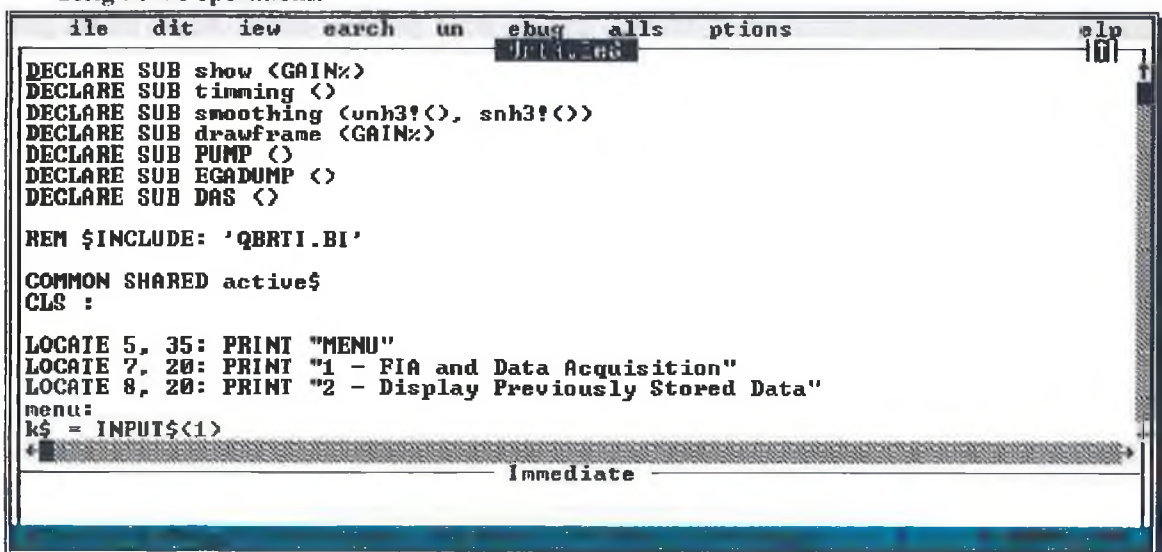
language in a numbered-line command code type, slow and very limited in its possibilities. The natural evolution step was to design a BASIC compiler to take advantage of the simplicity of the language, increasing the execution speed and possibilities. Microsoft marketed QuickBASIC (c.a. 1989) as a compiled version of the obsolete GWBASIC interpreted language. Figure 1.8 shows the workspace for the version 4.5 of the compiler. Run-time code is written in an editor-like page where the commands follow one another in series, being executed in order except when the code states a jump in the programme. The top part of the compiler shows a drop down menu to select operations and options at design time.

This compiler was used at the early stages of this research because of its computation possibilities, specially in the PC microcomputer based on the 286 processor, its

Figure 1.8: Microsoft QuickBASIC 4.5 workspace.
Typical aspect of a DOS based compiler for the most common programming languages. The programme code consists of a series of lines containing instructions and parameters which are executed successively. On the top row a menu allows the user to select the compilers design-time operations.

```
   ile    dit    iew    earch    un    ebug    alls    ptions                      elp

 DECLARE SUB show (GAIN%)
 DECLARE SUB timming ()
 DECLARE SUB smoothing (unh3!(), snh3!())
 DECLARE SUB drawframe (GAIN%)
 DECLARE SUB PUMP ()
 DECLARE SUB EGADUMP ()
 DECLARE SUB DAS ()

 REM $INCLUDE: 'QBRTI.BI'

 COMMON SHARED active$
 CLS :

 LOCATE 5, 35: PRINT "MENU"
 LOCATE 7, 20: PRINT "1 - FIA and Data Acquisition"
 LOCATE 8, 20: PRINT "2 - Display Previously Stored Data"
 menu:
 k$ = INPUT$(1)

 ─────────────────────────── Immediate ───────────────────────────
```

resemblance with the known GWBASIC, and the availability of external libraries necessary to develop the instrumentation software for data acquisition and control (See Chapter 4).

1.3.2.2 Object Oriented Code

Some DOS compilers use a different approach to the programming technique in the sense that apart from commands, objects are used for designing an application. The code is, in essence, line oriented and, in fact, the basics of the programming technique is a line oriented language which is used to define high level command or objects which are then used to generate the programme. This type of compiler is usually very specialised and developed for a particular area of application.

LabWINDOWS

This product was developed by National Instruments for designing software for instrumentation applications. LabWINDOWS is an object oriented compiler which uses a number of libraries written in C or BASIC to generate high level commands or objects that can easily be used to develop software applications for instrumentation and control. These objects are used in conjunction with the language usual commands, with the advantage that as the compiler uses the computer's extended memory the applications are not limited to the base memory, being able to use up to 16 MBytes. Applications developed with this compiler that are too big to run under DOS can still be executed in a run-time LabWINDOWS environment.

1.3.3 WINDOWS Based Software

Nowadays, the great majority, if not all, of the commercial application packages for PC microcomputers are based on the WINDOWS environment. Similarly, computer programmers are developing their applications using compilers which are based on the environment, and which allow the creation of programmes that incorporate the powerful features of WINDOWS. This important trend has rendered DOS-based applications and compilers so obsolete that users will travel far to run these applications under WINDOWS, reduced to a small square in the computer screen.

(i) Visual BASIC

Visual BASIC is a general purpose compiler which functions within the WINDOWS environment. This package is a more advanced version of BASIC than, for instance QuickBASIC (Section 1.3.2.1), as it includes the concept of objects (WINDOWS type objects) in the programming possibilities as well as the traditional command lines. There is a close interaction among the different line code sub-programs and windows, controls and other objects which enables powerful applications with a very high quality Graphical User Interface (GUI) to be easily created.

(ii) LabVIEW

This graphical compiler was specially designed by National Instruments (Austin TX, USA) for developing scientific instrumentation software in an easy, professional and reliable way. LabVIEW comes with a number of structures, arithmetic functions and subroutines ready to use which are represented as icons. This icons are interconnected to

generate a code diagram which resembles an electronic circuit. In addition, there are a number of libraries designed for signal generation and processing, statistics, digital filters, etc, which can easily be incorporated into the user interface.

The LabVIEW environment comes with control drivers only for National Instruments I/O cards and installation and set-up can be done in ten minutes. Nevertheless, other manufactures I/O cards can also be used if drivers are written for them, as LabVIEW accepts links to interface code written in C++. LabVIEW was first introduced for Macintosh systems in 1986, and subsequently extended for PCs and SUN Sparkstations. This work only deals with the PC version of the software LabVIEW for WINDOWS (LabVIEW from now), but it is important to know that the software is portable between the three platforms. This means that Sub VIs written on PC, Macintosh or SUN platform can be used in any of the other two without changes. LabVIEW can also generate stand-alone executable "*.EXE" files which run under WINDOWS on any PC 386 DX or higher with 8 MBytes RAM memory. However, for software development a 486 DX or DX2 is recommended. Detailed discussion on this graphical compiler and its possibilities is given in Chapters 5 and 6.

1.3.3.1 DOS vs. WINDOWS Software

The first main difference any computer user will notice about WINDOWS software in comparison to DOS based software is that the GUI is standard for any application and even the strangest application will look familiar in this environment.

On the contrary, DOS software always depended on the programmers ability, and time and effort spent on it, to produce relatively user friendly applications which are, at the most, acceptable in terms of the GUI. In terms of computer speed, the more complex the GUI is, obviously the more resources are used-up. In other words, WINDOWS slows down the computational speed, as the processor has to be shared with the environment to produce and update the graphical displays. Therefore, applications that need heavy calculations and fairly lengthy "number crunching" processes are usually much faster, if memory limitations do not impair it, when developed with DOS based compilers. Besides, in these applications, the GUI is usually kept to a minimum, as there is little or no interaction with the user. As noted before, multitasking is possible within the WINDOWS environment and a number of applications can be running at the same time. Furthermore, these applications can dynamically share data and interact one with each other through applications dynamic data exchange.

Dynamic Data Exchange (DDE)

Windows applications (clients) can define objects in them which represent operations, data sets, charts, files, etc. which are objects defined in some other application (server). This data sharing is done through Dynamic Data Exchange (DDE) which allows internal data transfer among applications in WINDOWS. Objects designed in one programme which refer to objects in another application will create links between the applications through which the client will receive the information from the server. This information can be updated manually, at the user's request, or automatically, each time the information changes. With this system, a number of applications running in a interactive

mode can assure that they all have access to the new information as soon as it is updated. The inter-application links are created either when the application is launched (automatic), or when the embedded object is called up by the user (manual).

1.4 Signal Interfacing

1.4.1 Signal Acquisition

Section 1.2.2 describes devices that allow the computer to interface to, and communicate with, external devices. More in particular, in Section 1.2.2.2, a series of electronic devices which allow computers to handle raw signals are described. This section notes a few guidelines to be considered when this devices are utilised to acquire signals.

Table 1.1: Characteristics of ADC converters in terms of the number of bits.

No. of bits	No. of Steps (bitnumber)	Resolution (V bit^{1}) in a 0 to 10 V input range
8	255	39.1×10^{-2}
12	4095	2.44×10^{-3}
16	65535	1.5×10^{-4}
n	$2^n - 1$	$10/(2^n - 1)$

1.4.1.1 ADC Resolution

Converting an analogue signal into a digital one is a process which is limited by the card used. The ability of the card to discriminate between to consecutive levels of an analogue signal will depend on the ADC resolution which is measured in "bits". The higher the

number of bits, the more the ADC can count, and the signal input range can be divided into a higher number of steps. Table 1.1 shows the number of steps and the effect in the card resolution depending on the number of bits.

ADC Gain

If the system deals with small signal levels it is very probable that the card discrimination (2.44 mV for 12-bit ADC) will not be good enough. Acquisition cards usually present the possibility of increasing the discrimination by reducing the signal input range. This is called gain. The card now will narrow the range, discarding any signal outside it and applying the full 2^n steps to the incoming signal. The most common gains are as shown in Table 1.2. The gain values refer to the reduction factor applied to the input range. In many cases, offset procedures, as described in Section 1.4.1.3, can be used to fully employ the precision of the ADC chip.

Table 1.2: Variation with gain of the acquisition resolution of a 12-Bit card (standard input range 0 to 10 volts).

Gain	*1*	*2*	*5*	*10*	*100*	*500*
Input Range (V)	10	5	2	1	0.1	0.02
Resolution ($V\,bit^{-1}$)	2.44×10^{-3}	1.22×10^{-3}	4.88×10^{-4}	2.44×10^{-4}	2.44×10^{-5}	4.88×10^{-6}

1.4.1.2 Sampling Frequency

Depending on the card model, version and gain in operation, the maximum sampling frequency will vary, but usually is in the thousands of cycles per second, typically from 20 to 100 KHz. For applications dealing with relatively slowly changing signals this fast acquisition rate will only generate enormous amounts of unnecessary data which will pile

up in the storing devices. Hence, the data acquisition rate must be reduced to a more appropriate frequency, usually by software control. In contrast, for signals with high frequency components the system will have to acquire the signal at a high enough rate so that no information is lost. Figure 1.9 shows how, for signals that contain high frequency information, a slow sampling rate will miss some of the information conveyed in the signals. A properly chosen scan rate of at least twice the frequency of the highest frequency component o the signal (Nyquist criterion) will allow a proper and more effective acquisition of the signal, maintaining the information completely with low number of samples.

Figure 1.9: Effect of the sampling rate in acquiring signals with high frequency components. Decreasing the sampling frequency has a negative effect in the proper acquisition of the information in the signal.
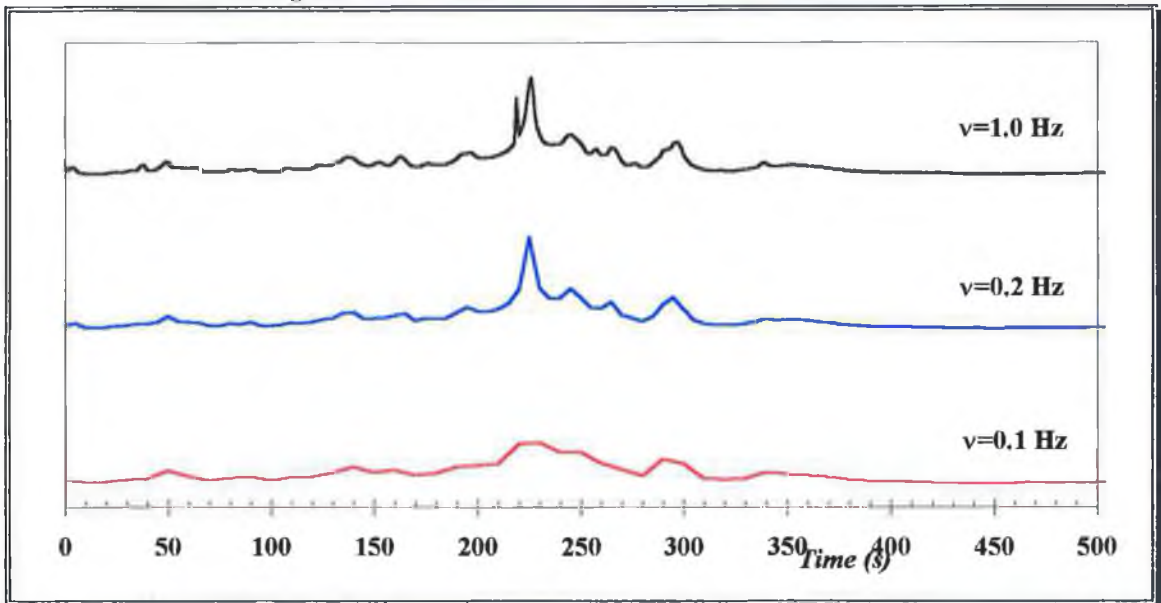
1.4.1.3 Signal Conditioning

Quite often the signal to be acquired does not match the input specifications of the acquisition card, and it has to be modified in some way. This can be in order to protect the information to be read or to protect the hardware itself, as extreme signal conditions may result in electronics damage. A standard acquisition card (Analog Devices' RTI-800 series or National Instruments' AT-MIO series) will have a maximum signal input range of ±10 volts. Normally, the electronics are protected to stand, with no damage, input voltages up to 35 volts. If the signal to be acquired exceeds the 10 volt limit it will have to be proportionally reduced to match the requirements. On the other hand, if the precision of the card is not good enough for a particular signal, or the signal variations are so small that are outside the possibilities of the card, the signal will have to be amplified. Figure 1.10a shows the schematics of an electronic circuit for signal amplification. It is based on a operation amplifier integrated circuit with two resistors R_1 and R_2 connected to it. The net gain of this circuit depends on the values of the resistors, being its value the quotient R_2/R_1.

Figure 1.10: Signal amplifier and voltage follower schematics.
a)This simple signal amplifier is based on a op-amp integrated circuit. The output signal with respect to ground is given by the formula $y=-(R_2/R_1)x$. Gain=$-R_2/R_1$. b) To ensure that the electrode e.m.f. measurements are taken in zero-current conditions, the signal from the ISEs is conditioned with operational amplifiers connected as voltage followers. The circuit's net gain is 1.
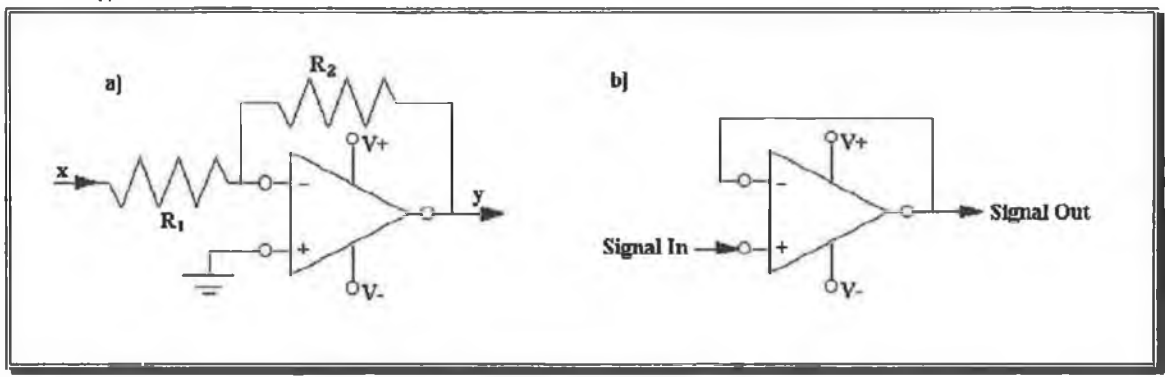
Throughout this research, signals generated by potentiometric devices have been captured with Analogue-to-Digital Converter (ADC) cards. The input voltage was always under 500 millivolts, well within the 0 to 10 volt ADC converter input range. Zero-current measures must be taken to properly read the signal generated by these sensors and, although the input impedance of the card used was very high (>100 MΩ for the RTI-815 and 1 GΩ for the AT-MIO-16DL), operational amplifiers (op-amps) were used, as voltage followers or pre-amplifiers, to convert to low impedance and reducing the load in the measured system. Figure 1.10b describes the set-up for these pre-amplifiers.

The op-amps used for the conditioning circuitry were of the CA 3140 AE type fed with symmetrical $\pm$ 5 volts, which provided a very high input impedance of 1 TΩ, ideal for this application, a very low input current (2 pA) and a high speed performance[8]. The typical output impedance of these op-amps is 60 Ω.

Shielding and Filtering

Reducing the noise in the signals can be achieved by preventing the signals to be exposed to noise (passive reduction). Environmental noise pick-up can be greatly reduced by placing the electronic system inside earthed metal boxes and transmitting all the signals through earthed screened cables.

Signal filtering (active reduction) is applied to reduce noise already convoluted with the signal information, but it must be carefully applied, as it can distort unexpected features which are part of the signal if the filter "thinks" they are noise. A number of different

filtering techniques can be used, like high pass, low pass, band pass filters or Fourier Transform filters, and each technique has different filter designs to choose from. The characteristics of the signal to be filtered will determine which filter or combination of filters is optimum.

Signal Offset

Signals which vary within very narrow values while the overall level is high will be difficult to acquire with precision if the pre-acquisition gain of the card has to be kept at a low value so that the signal is not amplified over the maximum acquisition range (typically 10 V). This signals can be assumed to be the addition of two signals. One component gives the signal level and a second component carries the signal information. Therefore the first component can be subtracted with no loss in information. Now the signal level is smaller and a higher gain and therefore higher global precision could be used to read it.

Figure 1.11 shows an example of the benefits in precision an offset procedure can generate. For a standard 12-bit acquisition card the resolution of the analog-to-digital converter is 2.44 mV for a typical 10 volt input range. Signals which present voltages varying around +500 mV (Figure 1.11a) are acquired with a global resolution of 2.44 mV when the pre-amplifier (amplifier stage before the ADC) gain is set to 1. If the variation of the signal magnitude is not two high (no more than a few mV decades), the signal can be pre-amplified with a gain of 10 (Figure 1.11b) or lower, if available, to give a better global signal resolution when the acquisition data are digitally converted to the

original signal levels, provided that the new signal does not exceed the card's input range (see Table 1.2 for resolution values). Because the amplifier multiplies the global magnitude of the signal, the level of the signal is also amplified, in this case form ~500 mV to ~5000 mV. Selecting the next higher gain typically available for these cards (100) will increase the signal level to around 50 V which will be outside the acquisition range.

Applying an offset procedure to the original signal means the reduction of the signal level close to 0 volts, so that subsequent amplification stages do not increase the signal over the input range of the card. In this example, an offset of -300 mV applied to the original signal lowers its magnitude close enough to zero-level. The resulting signal can be amplified with a higher gain of 100 and still lie within the 10 V input range (Figure 1.11c), enhancing the acquisition resolution to 0.0244 mV bit^{-1}

Figure 1.11: Example of an offset procedure performed on a electrochemical system. **The signal at the output of the circuit is expressed by the relation $y=x$-offset. This circuit may be used, as shown in the graph, to reduce the absolute magnitude values and apply a higher discrimination factor in the acquisition of the signal.**
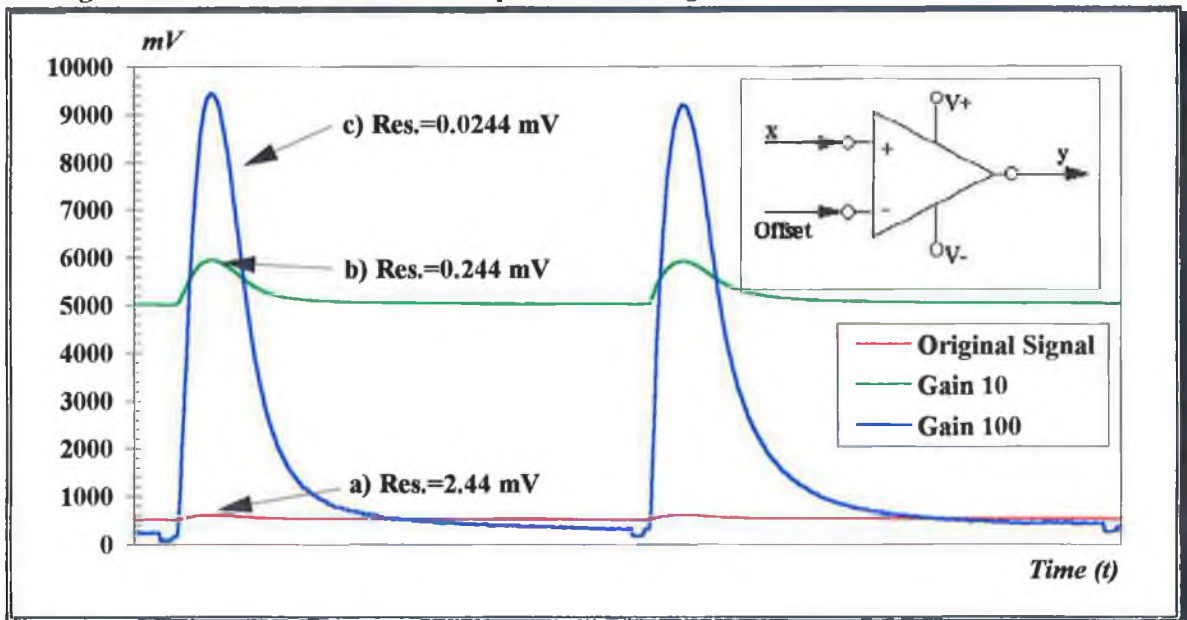
This technique can be sometimes useful for common mode noise rejection. As the output from the circuit is the subtraction of the offset from the signal, in those cases where the noise components both in the signal and offset are the same the output signal will filtered and clear of that component.

1.4.2 Instrument Actuation

Signals and how to acquire them has been the topic of discussion in the previous sections. Signal generation is a different aspect of the acquisition cards. The brand and model of the card will determine the signal output characteristics as the number of digital and analogue outputs, output range, and so on. Both Analog Devices and National instruments card used in this work have two analogue output channels but, while the RTI-815 has 8 digital outputs, the AT-MIO-16DL has 32.

1.4.2.1 Digital Control

The number of ON/OFF functions a computer can control is determined by how many of the digital ports in the data acquisition card are configured as output. A high/low (TRUE/FALSE) signal carries the information to activate a particular switch

(i) TTL Compatible Signals

Transistor-Transistor Logic (TTL) signals are digital signals use to actuate a transistor controlled function. Devices which present external control port usually need TTL signal in the inputs to switch the operations. As described previously (Section 6.2.1.1) the

peristaltic pump use in the FIA system was controlled through a remote port *via* two TTL signals.

(ii) Relays

Other systems which do not support TTL signals can be activated with other additional devices as relays. This approach can also be applied for high voltage, high power or AC ON/OFF signals. A relay was controlled from a digital port to activate/deactivate the mains power supply to the FIA system. TTL compatible relays can also be used to add some kind of logic compatibility to small devices. A logic quad-gated power driver chip was used to allow TTL-compatible control of the injection port of the same FIA system.

1.4.2.2 Analogue Control

Devices that are actuated gradually, i.e. have a number of different steps or levels between the lowest and highest, can often be actuated if an analogue value is sent to a remote control port. Devices like speed selectable pumps, temperature controllers and so on can be controlled by this method.

Also, the analogue ports can be used for signal generation, sending signal waves to control the level of a particular magnitude during a determined time span. Signals generated with this technique are of the quantised type (Section 1.1.3), which means that the signal voltage output is generated in steps, and therefore, depending on the time constant of the magnitude to control, the actuation may also be in steps. The FIA peristaltic pump speed was controlled this way. In this case, the steps of the incoming

signal were negligible in comparison with the steps of the pump, as the signal resolution was below 4μl min^{-1} and the internal digital potentiometer's step was around 80 μl min^{-1}.

Signal Amplifiers

Analogue output channels have limitations in terms of the signal output characteristics. Limited voltage and current ranges (0 to 10 V and 2 mA for RTI-815 and AT-MIO-16DL) means that the signals have to be externally modified to match the specifications of the application. High voltage operational amplifiers could be used in applications where the voltage output from the card has to be multiplied for high voltage applications, like a ceramic piezo positioner ($\pm$ 200 V) for Scanning Electrochemical Microscopy (SECM). Similar approach can be used for low-power high-current applications[2].

1.5 References

[1] Kamen, Edward W. "*Introduction to Signals and Systems*" Macmillan Publishing Company, New York, **1990**.

[2] Kwakernaak, Huibert; Sivan, Raphael " *Modern Signals and Systems*" Prentice Hall, Englewood Cliffs, New Jersey, **1991**.

[3] Ziemer, R.E.; Tranten, W. H.; Fannin, D. R.; "*Signals and Systems: Continuous and Discrete*" Macmillan Publishing Company, New York, **1989**. 2 Ed.

[4] "*Data Aquisition Seminar*" National Instruments, *Jan.* **1994**.

[5] Morris, A. S.; "*Principles of Measurement and Instrumentation*" Prentice Hall International (UK) Inc, Englewood Cliffs, Hertfordshire, **1993**.

[6] Instrumentation Reference and Catalogue 1995, National Instruments, sec. 3, p 75.

[7] Sáez de Viteri, F. J.; Diamond, D. *Anal. Proc., Chem. Comm.* **1994**, *(31)*, 229-232.

[8] Harris Semiconductors: Operational Amplifiers CA3140A, CA3140 specifications sheet. Harris Corporation, **1990**, *Section 3*, 122-125.

2. Ion-Selective Electrodes

2.1 Introduction

As a general definition, the term *Electrochemistry* refers to the branch of chemistry which studies chemical reactions and processes in which electric charges are involved, either applied to produce chemical reactions or as a result of them. These processes, which can be of very different nature, have been used in the analytical field for many years and have led to the development of very distinctive techniques like potentiometry, voltammetry, amperometry, coulometry and the recently developed scanning electrochemical microscopy (SECM)[1,2].

Potentiometry, which is the focus of this research, deals with the electromotive force (e.m.f.) generated in an galvanic cell where a spontaneous chemical reaction is taking place. In the last twenty years or so this technique has widened its areas of application, especially in the analytical fields, as selective potentiometry techniques were being developed. Selective potentiometry deals with the use of the e.m.f. response of electrodes which are selective to groups of species to determine analytical parameters in sample matrices. The glass-membrane electrode was the first ISE to be discovered and characterised, and its selectivity for H^+ ions made it widely used for pH measurements.

The technique rapidly became very popular and different glass compositions were used to induce selectivity to other ions. This technique evolved to the development of different sensing membranes and materials, and a whole series of different selective electrodes was developed, all based on the same principle as the glass electrode. Solid-state, gas sensing electrodes or the liquid and polymer membrane electrodes are amongst the selective electrochemical probes available today. Enzymes and proteins are also used as selective materials in ISEs for biochemical species as part of special electrode setups[3].

Apart from the continuous development and improvement on the chemistry side of these sensors, techniques to enhance the sensor performance and robust response theories to explain their behaviour have been elaborated, thus increasing the range of applications and giving a better understanding of the electrochemistry involved.

Numerous applications appear continuously in the literature describing new selective materials, new techniques and new fields of application for potentiometric electrochemistry using ISEs, both in the chemical[4,5,6,7] and biochemical fields[8].

2.2 Potentiometry

It is known that when a metal M is immersed in a solution containing its own ions M^{z+} an electric potential is developed on the metal surface as the following process occurs:

$$M^{z+}_{(aq)} + ze^- \rightleftharpoons M_{(s)} \qquad \text{Eq. 2.1}$$

This generates an electrode potential (E) which depends on the activity of the metal ions in solution and the number of electrons involved in the process, and which can be expressed as;

$$E_{elec} = E_{elec}^0 + \frac{RT}{zF} \ln a_{M^{z+}}$$

Eq. 2.2

where E_{elec} is the electrode potential in volts, R is the gas constant, T is the absolute temperature and F is the Faraday constant. $a_{M^{z+}}$ is the activity of the metal ions in solution, z is the number of electrons involved in the process and E_{elec}^0 is the standard electrode potential, which is the value of the potential the electrode presents when $a_{M^{z+}} = 1$. At 25 °C, and correcting from natural to decimal logarithm, Eq. 2.2 takes the form

$$E_{elec} = E_{elec}^0 + \frac{59.16}{z} \log a_{M^{z+}}$$

Eq. 2.3

also known as the Nernst equation which states that, for a ten-fold or decade change in the activity of a monovalent cation ($z=1$), a theoretical potential change of 59.16 millivolts should be expected. This potential change can only be measured against a reference electrode, of stable potential, which completes the electrochemical cell. The electrode potential is calculated by measuring the e.m.f. of the cell and subtracting the known reference electrode potential as in the following expression:

$$E_{elec} = E_{cell} - E_{ref}$$

Eq. 2.4

The hydrogen electrode is the standard reference electrode, but more practical secondary reference electrodes such as calomel or silver/silver chloride are usually utilised[9].

2.3 The Nikolskii-Eisenman Equation

Ion-Selective Electrodes (ISEs) are potentiometric devices characterised by the fact that the electrochemical response is usually dominated by one ionic species present in the solution, known as the primary ion. Other species which contribute to the response (ideally to a lesser extent) are called interfering ions or interferents.

Although these electrodes are often very selective, they are never specific, which means that the response produced by the primary ion, is supplemented by contributions arising from interferents in the sample matrix[10]. Therefore direct potentiometry on samples containing interferents is not possible if the results are interpreted *via* the Nernst equation (Eq. 2.3).

But even if the Nernst theory is not suitable for direct potentiometry, measurements still can be accurately performed if the contribution from the interfering ions to the ISE potential are somehow included in the electrode model.

Figure 2.1 shows schematically a typical membrane based galvanic cell[*]. Three different parts must be distinguished in the membrane; the two boundary or outer surfaces and the

---

[*] Superscript (") refers to a solution of constant (fixed) ion activity which is equivalent to the electrode's internal electrolyte. Superscript (') refers to a solution of variable activity equivalent to the sample solution.

bulk of the membrane. When the membrane is placed between two solutions containing

an ionic species, k, at two different levels of activities (a'_k and a''_k) a potential E_M is

created across it. Assuming that;

1. The only forces involved in the process are concentration and electrical forces. No temperature or pressure gradients exist across the membrane.

2. The membrane is in thermodynamic equilibrium, internally and with the two solutions at both sides.

3. Both solutions (' and ") are prepared in the same solvent, and

4. That the standard potentials of all the chemicals remain constant with time and space within the membrane,

Figure 2.1: Schematic diagram of a selective membrane cell.
a) Selective membrane. b) aqueous solutions containing ionic species. c) reference electrodes. d) high impedance voltammeter. See text for explanation of ion activities.
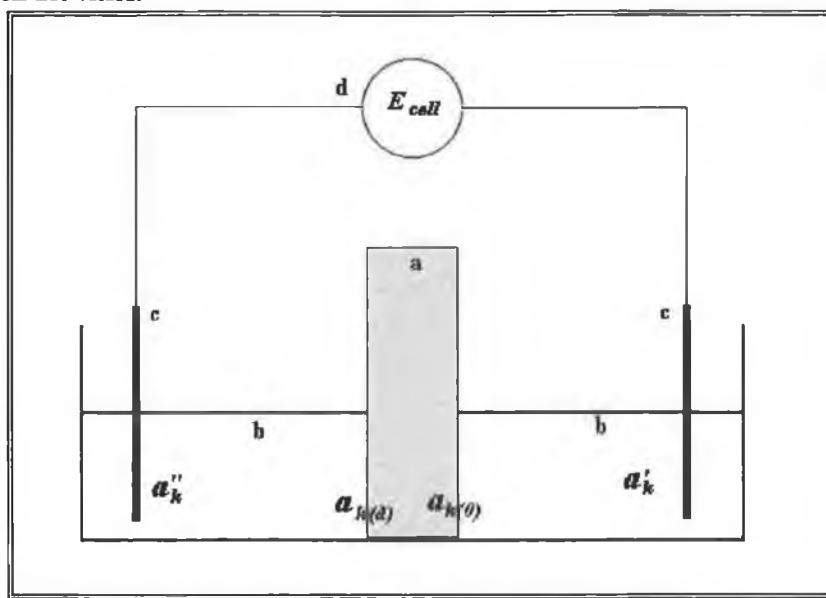
the overall membrane potential (E_M) can be described, in an ideal membrane, as a sum of the boundary potentials E_B' and E_B'' (outer surfaces), and the diffusion potential E_D (bulk of membrane)[11] as in

$$E_M = \left(E_B' - E_B''\right) + E_D \qquad \textbf{Eq. 2.5}$$

where $E_B' = \dfrac{RT}{zF}\ln\dfrac{a_k'}{a_{k(0)}}$, $E_B'' = \dfrac{RT}{zF}\ln\dfrac{a_k''}{a_{k(d)}}$ and $E_D = \dfrac{RT}{zF}\ln\dfrac{u_k a_{k(0)}}{u_k a_{k(d)}}$.

Overall,

$$E_M = \left(\dfrac{RT}{zF}\ln\dfrac{a_k' a_{k(d)}}{a_k'' a_{k(0)}}\right) + \left(\dfrac{RT}{zF}\ln\dfrac{u_k a_{k(0)}}{u_k a_{k(d)}}\right) \qquad \textbf{Eq. 2.6}$$

$a_{k(d)}$ and $a_{k(0)}$ are the activities of the primary ion k in the membrane phase at the internal and external boundaries respectively, and a_k'' and a_k' are the activities of the ion k in the internal and external solutions. u_k is the ion mobility in the bulk of the membrane. For the ideal case where $a_{k(d)} = a_{k(0)}$ and assuming identical mobilities for all the similar species permeating into the membrane (i.e. $E_D \Rightarrow 0$ or it is constant), the expression for the membrane potential is reduced to:

$$E_M = \dfrac{RT}{zF}\ln\dfrac{a_k'}{a_k''} \qquad \textbf{Eq. 2.7}$$

In a disposition where the k^{z+}-selective membrane is set-up as an electrode j, the activity of the ionic species at one side of the membrane remains constant (electrode's internal

solution of ion activity $a_k^{''}$) and Eq. 2.7 reverts to the expression of the Nernst theory as in Eq. 2.2:

$$E_j = \frac{RT}{zF}\ln\frac{1}{a_k^{''}} + \frac{RT}{zF}\ln a_k^{'} = E_{elec}^{0} + \frac{RT}{zF}\ln a_k^{'}$$

<div align="right">**Eq. 2.8**</div>

If the variable solution contains a permeating interfering ion l of the same charge as the primary species, k, the membrane potential (Eq. 2.7) can be expressed as

$$E_{jk} = \frac{RT}{zF}\ln\frac{u_k k_k a_k^{'} + u_l k_l a_l^{'}}{u_k k_k a_k^{''}} = E_{jk}^{0} + \frac{RT}{zF}\ln\left(a_k^{'} + \frac{u_l k_l}{u_k k_k}a_l^{'}\right)$$

<div align="right">**Eq. 2.9**</div>

where k_k and k_l are the distribution coefficients of the ionic species k and l between the aqueous and membrane phases and $a_l^{'}$ is the activity of the interfering ion l in the sample solution. The ratio $\frac{u_l k_l}{u_k k_k}$ effectively defines the contribution of the interfering ion l to the overall electrode response, and it is usually represented as the potentiometric selectivity coefficient K_{jkl}. A more generalised expression, known as the Nikolskii-Eisenman equation includes contributions from a number of interfering ions of different charges in the same solution (i);

$$E_{ij} = E_j^{0} + S_j \log\left(a_{ik} + \sum_l K_{jkl} a_{il}^{z_k/z_l}\right)$$

<div align="right">**Eq. 2.10**</div>

Where E_{ij} is the potential measured in the electrode j for a given solution i, E_j^{0} is the standard electrode (half cell) potential, S_j is the electrode slope, a_{ik} is the activity of the primary ion k, and a_{il} is the activity of any interfering ion l in the same sample i. z_k and z_l

are the charges on the primary and interfering ions and K_{jkl} is the selectivity coefficient of the electrode j against the interfering ion l, and it is defined as

$$K_{jkl} = \frac{u_l k_l}{u_k k_k} = \frac{u_l}{u_k}\left(_e K_{jkl} \right)$$

Eq. 2.11

where u_l and u_k are the ion mobilities in the membrane phase and $_e K_{jkl}$ is the equilibrium constant of the reaction shown in Eq. 2.12[9]:

$$l_{(aq)}^{zl+} + k_{(mem)}^{zk+} \rightleftharpoons l_{(mem)}^{zl+} + k_{(aq)}^{zk+}$$

Eq. 2.12

The summation factor $\sum_l K_{jkl} a_{il}^{zk/zl}$ in Eq. 2.10 is the error arising from the net contribution of all interferents. Figure 2.2 shows the theoretical response of the Nikolskii-Eisenman semilogarithmic equation for a primary ion activity range of 10^{-9} to 10^{0} mol dm^{-3} with an arbitrary total contribution of background interferents of 10^{-4} mol dm^{-3} ($E_j^0 = 100$ mV, S_j = Nernstian).

From the above equation (Eq. 2.10), the most useful ISEs are clearly those which are very selective ($K_{jkl} \Rightarrow 0$) against a wide range of common interfering ions as for these electrodes $\sum K_{jkl} a_{il}^{zk/zl} \Rightarrow 0$, and hence changes in the measured potential (E_{ij}) can be related with confidence to variations in the primary ion activity alone. Three situations can be differentiated in terms of the relative values inside the logarithm in Eq. 2.10.

- **Case 1;** $a_{ik} \gg \sum_l K_{jkl} a_{il}^{zk/zl}$: This is the ideal case in which the contribution of the sample interferents, l, is negligible in comparison to the primary ion k. Graphically, it

can be related to the ascendant part of the Nikolskii-Eisenman response curve in Figure 2.2 which rises with constant slope. In this case direct potentiometry can be performed on a sample, relating the electrode potential to the primary ion activity as in the following equation:

$$a_{ik} = 10^{\frac{E_{ij} - E_j^0}{S_j}}$$

Eq. 2.13

- **Case 2;** $a_{ik} \approx \sum_l K_{jkl} a_{il}^{z_k/z_l}$: In situations where the net contributions of the interferents is of the same order than the contribution of the primary ion, direct potentiometry (Section 2.6.4.1) cannot be used for analysis unless the value of the summation term for interferent contribution is known and this value remains constant

Figure 2.2: Example of the theoretical response of an ideal ISE.
The curve represents the Nikolskii-Eisenman response for an ISE with the following parameters. E_j^0 =100 mV. S_j =59.16 mV decade^{-1}. Overall contribution of the summation term equals 10^{-4} mol dm^{-3}.
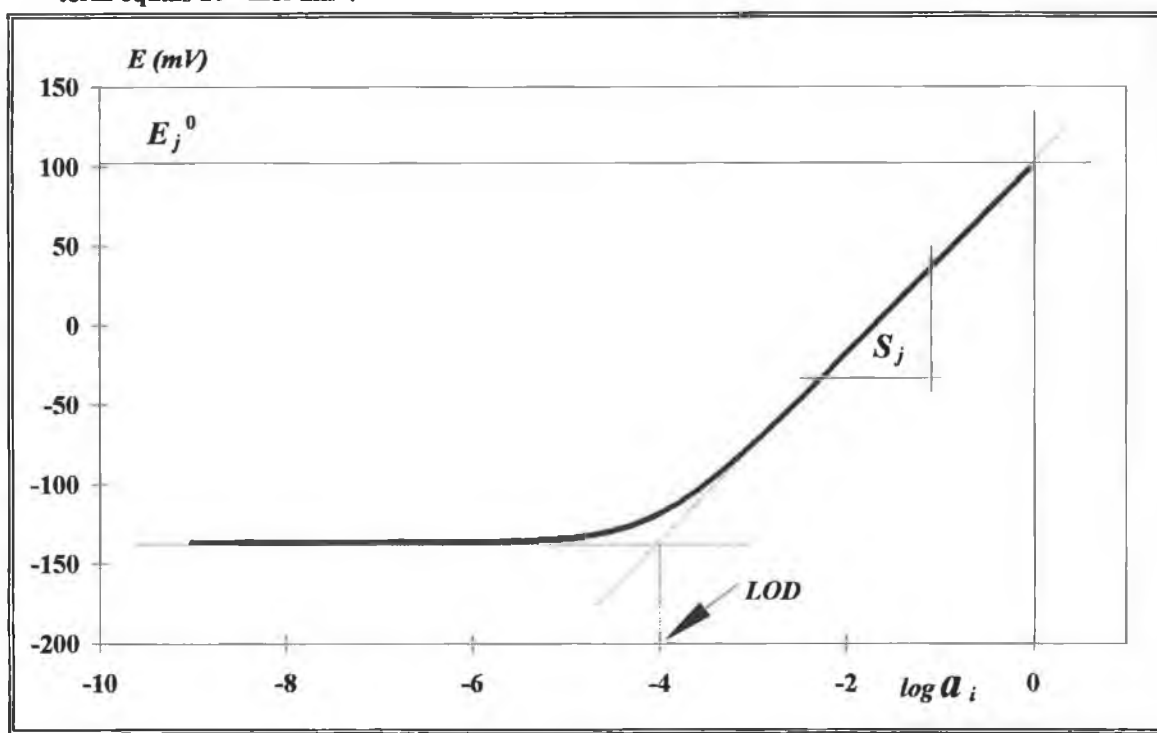
for both in standards and unknown samples. In this case, the standards must contain a constant background of interferent ions. The calibration curve obtained with this series of standards contains the information and correction for the effect of this particular interferent background, and accurate prediction of unknowns with this calibration curve can only be guaranteed for samples with the same background composition.

If the presence of interferents cannot be considered constant from sample to sample in terms of occurring species and activity levels, analysis on an individual basis can still be performed on the samples using techniques like standard addition (Section 2.6.4.2).

If additional information is available on the activity of one or more of the interfering ions, the contribution of the summation term can be reduced and direct potentiometry can still be done on a sample set without the need of applying standard addition on each sample, provided that the remainder of the summation term stays constant. In these cases, the Nikolskii-Eisenman equation can be extended to

$$E_{ij} = E_j^0 + S_j \log\left(a_{ik} + K_{jkl_1} a_{il_1}^{z_k/z_{l1}} + K_{jkl_2} a_{il_2}^{z_k/z_{l2}} + \ldots + \sum_l K_{jkl} a_{il}^{z_k/z_l} \right) \qquad \textbf{Eq. 2.14}$$

Electrode parameters like the selectivity coefficient for the particular interferents corrected, as well as the activity of those interferents, are needed to apply this correction process. This way, a quantitative background interferent correction can be achieved with the terms corresponding to $l_1, l_2, \ldots,$etc. so that the term $\sum_l K_{jkl} a_{il}^{z_k/z_l}$ is

negligible or constant (with the same value than in the standards), or inaccuracies arise.

In Figure 2.2, this case is represented by the curved portion of the theoretical electrode response. Chapter 3 will discuss in detail the implications of extending the Nikolskii-Eisenman equation for a number of particular interferents.

- **Case 3;** $a_{ik} << \sum_l K_{jkkl} a_{il}^{z_k/z_l}$: In this case accurate determination of the primary ion is not possible, as its response is masked by the contribution from interferents. Separation and preconcentration techniques like ion-chromatography[12] or gas diffusion[13] processes must be used previous to the determination of the target species. The part of the Nikolskii-Eisenman ideal response with zero slope in Figure 2.2 represents this third case.

2.4 Types of ISEs

In this section, an overview of the most common electrode types is presented. All of them are considered as ISEs, as they are potentiometric devices selective for ionic species. Other more complex designs exist which combine some characteristics from different types, but cannot be considered relevant from the theoretical point of view.

- **Glass Electrodes:** pH-glass electrodes have been widely used since the early 1930's to quantify the presence of H^+ in solution. These electrodes operate upon the fact that when a glass membrane is immersed in a solution containing these species an ion

exchange mechanism with the fixed SiO^- groups is initiated[14]. The glass material is made of a solid silicate matrix where the alkaline metal cations present high mobility. In the area where this glass membrane is in contact with an aqueous solution its surface becomes hydrated to a depth of about 100 nm and the alkali metal cations (principally Na^+) from the matrix (M^+) can be exchanged for other ions in the solution, preferably H^+, creating a potential across the membrane which is a linear function of the pH of the solution.

$$M^+_{(glass)} + H^+_{(aq)} \rightleftharpoons H^+_{(glass)} + M^+_{(aq)}$$

<div align="right">Eq. 2.15</div>
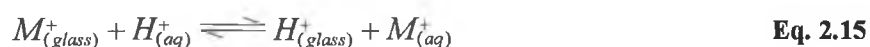
Doping the glass membrane with different proportions of aluminum oxide can produce glass membrane electrodes selective for other metallic ions like lithium, sodium, potassium, silver or ammonium[15].

- **Solid State Electrodes:** The glass membrane from the glass electrode can be replaced with other solid materials to produce electrodes with selectivity for other ions. Single crystals can be used as selective materials, as is the case of the fluoride ion-selective electrode which is based on a lanthanum fluoride crystal. Other crystalline materials can also serve as selective membranes when pressed into disks or dispersed in suitable polymers.

- **Gas Sensing Electrodes:** These electrodes consist of a glass pH electrode covered with a hydrophobic gas permeable membrane (GPM) and buffer solution filling the space between the electrode and the membrane. When the membrane is immersed in

a solution containing acidic/basic gaseous species (e.g. NH_3, CO_2, SO_2, NO_2), they diffuse through the membrane, dissolving in the buffer solution and inducing a change in pH which is detected by the glass electrode[3].

As an example, Figure 2.3 illustrates the functioning mechanism of an NH_3 gas selective probe. Changing the pH of a sample solution containing NH_4^+ ions to pH~9 or higher induces the formation of NH_3 gas. This species can diffuse across the gas permeable membrane, which changes the pH of the buffer at the other side of the membrane. Changes in H^+-activity of this internal solution are sensed by a pH glass electrode and its response is related to the activity of NH_4^+ ions in the original sample solution through the use of standard NH_4^+ solutions.

Similar gas sensor arrangements can be obtained by using a NH_4^+-selective ISE to develop the response to ammonium ions instead of a glass electrode to measure changes in pH, which prevents the interference of other gases like CO_2 or NO_2[16,17].

Figure 2.3: Chemical equilibria involved in an ammonia-selective gas-sensing probe. See text for details on the equilibria and gas-diffusion mechanism. GPM = gas permeable membrane.
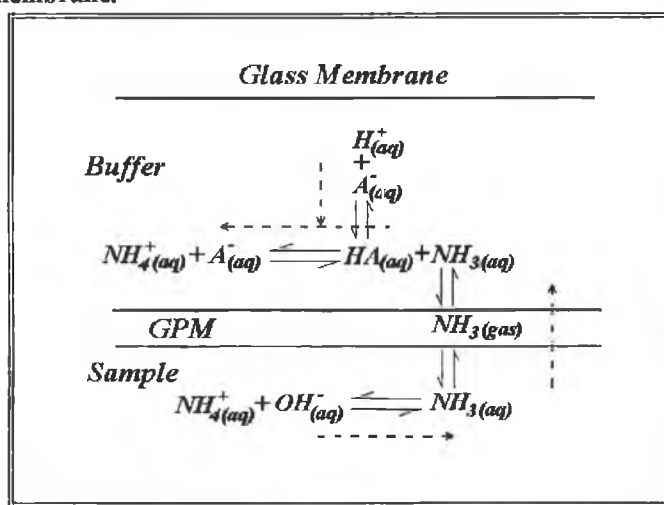
- **Liquid Ion-Exchange Electrodes:** The membrane of these electrodes is a solution of a hydrophobic anion and a cation dissolved in a organic solvent which is immiscible with water[14]. This solution can either impregnate a hydrophobic membrane or be dissolved in a polymer structure (e.g. poly(vinyl chloride)-(PVC)). In the presence of an aqueous solution containing the primary ion, the membrane exchanges cations with the solution, and Eq. 2.12 transforms to:

$$Ex - l_{(mem)} + k_{(aq)}^+ \rightleftharpoons Ex - k_{(mem)} + l_{(aq)}^+ \qquad \text{Eq. 2.16}$$
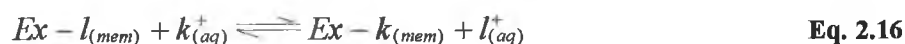
where Ex is the ion exchanger, and k^+ and l^+ are the two cations involved in the process. The selectivity characteristics of these membrane systems are almost exclusively explained by the extraction properties of the solvent used in the membrane. Assuming equal mobilities for similar ionic forms with distribution coefficients k_k and k_l, the selectivity coefficient of Eq. 2.11 can be rewritten as:

$$K_{jkl} = \frac{k_l}{k_k} \qquad \text{Eq. 2.17}$$

The distribution coefficients depend on the free energy of hydration, $\Delta G^0_{hyd,k^+}$, and solvation of the ions in the membrane, $\Delta G^0_{solv,k^+}$, and its magnitude is given by the equation[11]:

$$k_k = e^{\left(\frac{\Delta G^0_{hyd,k^+} - \Delta G^0_{solv,k^+}}{RT} \right)} \qquad \text{Eq. 2.18}$$

Because the hydration term is the dominant in Eq. 2.18, low free energy of hydration favours inclusion into the membrane. Thus, large organic cations such as acetylcholine, tubocurarin or lipophilic quaternary ammonium ions (R^+) can be determined in the presence of high levels of inorganic cations in biological applications[11]. The typical selectivity series for cationic species coincides with the Hofmeister lyophilic series:

$$R^+ > Cs^+ > Rb^+ > K^+ > Na^+ > Li^+$$
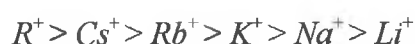
Ion-exchange electrodes selective for anions also present a typical selectivity pattern which corresponds to a similar liophilic series for anions. This selectivity mechanism is usually employed for anion selective electrodes, as designing 3D cavities (see next entry) formed with positively polarised groups remains an elusive goal. Hence, electrodes for environmentally important species such as NO_3^- and Cl^- tend to be based on ion-exchangers or inorganic materials.

- **Neutral Carrier ISEs:** These electrodes are similar to the ion-exchange ISEs, but the active species are neutral molecules, C, dissolved in the organic solvent and the complexation species formed, k^+C, are electrically charged:

$$k^+_{(aq)} + C_{(mem)} \rightleftharpoons k^+C_{(mem)} \qquad \textbf{Eq. 2.19}$$

These neutral carriers or *ionophores* are commonly macrocyclic structures that coordinate cations in and out of a solution and must comply with the following requirements[11]:

1. The ionophore must present polar and non-polar groups.

2. Upon complexation the polar groups should form a stable internal cavity suitable for ion coordination. The lipophilic groups should shell the coordination sphere and ensure sufficient solubility of the complex in the lipophilic membrane.

3. The coordination sphere should present no more than 12 coordination sites, preferably 5 to 8.

4. Higher selectivities can be obtained if the coordination sphere is fixed to a rigid molecular structure. For a periodic series, the cation that best fits the cavity is the one preferred by the ionophore.

5. The size of the ionophore should be small to present high mobility, but sufficiently big to assure enough solubility in a lipophilic medium.

Only this type of sensing electrode is used in this research and the term *ISEs* will be referring to neutral carrier type electrodes from now on, unless otherwise stated. Theory, discussion and applications will also focus mainly on neutral-carrier ion-selective electrodes.

2.5 Trends in ISEs

ISE theory predicts that the most accurate results are always obtained when only the primary ion is present in the sample or when the effect of the interferents in the electrode response is negligible ($\sum_l K_{jkl} a_{il}^{z_k/z_l} \Rightarrow 0$). Ion separation techniques like chromatography or gas-diffusion previously mentioned cannot always be applied as different problems may require different approaches. But still, ISEs are an inexpensive, time effective and reliable technique for routine ion analysis in aqueous samples.

During the last 20 years or so, a number of different approaches have been used in trying to overcome the general selectivity problems that occur with ISEs, either because of the high K_{jkl} values or because the sample matrix contains high and variable levels of interferents, or both. In the first case, an increase in the electrode selectivity may allow accurate determination of the presence and activity of a particular ion in solution, provided that the situation is either case 1 ($a_{ik} \gg \sum_l K_{jkl} a_{il}^{z_k/z_l}$) or case 2 ($a_{ik} \approx \sum_l K_{jkl} a_{il}^{z_k/z_l}$) as described in Section 2.3.

The following Section (2.5.1) covers the increase in thermodynamic selectivity, while Section 2.7.2.2 deals with the enhanced selectivity derived from kinetic measurements. If the problem faced is high and variable levels of interferents, higher selectivity will not solve the problem and an ISE array approach will have to be used. Very high selectivity may, in fact, be an obstacle for the use of a particular ISE in a Sensor Array Detector (SAD) approach as explained in detail in Chapter 3.

2.5.1 Potentiometric Selectivity

As previously described in Section 2.4, ion-exchange electrodes present cation selectivity which depends on the lipophilicity of the ionic species and its distribution coefficient between the membrane and the aqueous phase.

In contrast, neutral carrier based ISEs owe their selectivity to the reversible process shown in Eq. 2.19 which can be considered equivalent to the distribution of the ion k^+ in both the membrane and aqueous phase. The equilibrium of that reaction is governed by the constant K_k which is the overall distribution coefficient and its value

$$K_k = \beta_{kC} k_k a_C \qquad \text{Eq. 2.20}$$

depends on the stability constant of the ion-carrier complex in the membrane solvent, β_{kC}, the distribution coefficient (k_k) of the free ion between the membrane and the solution, and the activity of free carrier molecules, a_C, in the membrane[11].

In order to avoid magnitudes of stability constants in membrane solvent media, the reaction shown in Eq. 2.19 can be studied as a consecutive number of subprocesses, namely:

1. Migration of the free carrier ligands to the boundary surface with the aqueous solution as in Eq. 2.21. This process is determined by the distribution coefficient of the free ligand between membrane and aqueous phase, k_C.

2. Complexation, in aqueous phase, between the ionic species k^+ and the carrier molecule C (Eq. 2.22), being β_{kC}^w the stability constant of the formed complex in the aqueous phase.

3. Migration of the complex k^+C into the membrane (Eq. 2.23). The distribution coefficient of the ion-carrier complex, k_{kC}, controls this equilibrium.

$$C_{(mem)} \xrightleftharpoons{1/k_C} C_{(aq)}$$ **Eq. 2.21**

$$k_{(aq)}^+ + C_{(aq)} \xrightleftharpoons{\beta_{kC}^w} k^+C_{(aq)}$$ **Eq. 2.22**

$$k^+C_{(aq)} \xrightleftharpoons{k_{kC}} k^+C_{(mem)}$$ **Eq. 2.23**
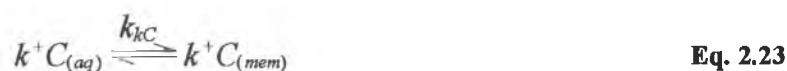
From this series of equilibria the overall distribution coefficient can be redefined as

$$K_k = \beta_{kC}^w k_{kC} \frac{a_C}{k_C}$$ **Eq. 2.24**

In the frequent case where the electrochemical cell considered contains a second ion of the same charge, l^+, which can also permeate the membrane, and assuming equal mobilities for the complexes k^+C and l^+C, Eq. 2.11 can be re-written for neutral carrier membranes as

$$K_{jkl} = \frac{K_l}{K_k} = \frac{\beta_{lC}^w k_{lC} \dfrac{a_C}{k_C}}{\beta_{kC}^w k_{kC} \dfrac{a_C}{k_C}} = \frac{\beta_{lC}^w k_{lC}}{\beta_{kC}^w k_{kC}}$$ **Eq. 2.25**

which is consistent with Eq. 2.12 for neutral carrier membranes and quantifies the following competition equilibrium of the parallel complexation reactions with either ionic species

$$k^+C_{(mem)} + l^+_{(aq)} \xrightleftharpoons{K_{jkl}} l^+C_{(mem)} + k^+_{(aq)}$$ **Eq. 2.26**
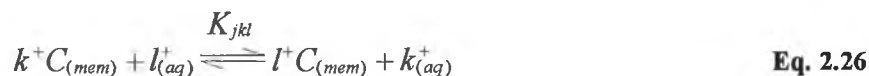
Improvement in the behaviour of the potentiometric selectivity of single ISE probes may be possible by modifying the electrode in terms of the active carrier molecules and the composition of the final membrane cocktail.

2.5.1.1 *Neutral Carriers*

Neutral carriers or *ionophores* are the selective molecules which make a polymer membrane sensitive to ions by selectively extracting ions from the sample solution into the membrane, and thereby modifying the potential across it. These molecules present or form a polar internal cavity with electron donor atoms which coordinate and hold the ion. The coordination mechanism is controlled by size, and the neutral carrier is more selective towards the ion, within the same period, that best fits the molecular cavity. Bigger ions will not be able to access the coordination sites, and the bonding of smaller ions to the coordination atoms will be too weak to form stable complexes. The type of molecules used as neutral carriers are widely variable, and range from crown-ethers[18] derivatives to calixarenes[19,20,21] or complex macromolecules and antibiotics like valinomycin[22] or nonactin[23,24,25].

Eq. 2.25 clearly shows the dependence of the potentiometric selectivity of a neutral carrier based electrode on the stability constant of the complexes formed between the carrier ligand and the ions, and the relative selectivity for two different ions is proportional to the ratio of these stability constants.

2.5.1.2 *Optimum Cocktail Membrane*

In general, these selective membranes consist of the neutral carrier or ionophore, the polymer, usually poly-vinyl chloride (PVC), and a plasticiser which acts as the organic solvent. The role of the PVC matrix is to provide an inert solid support structure in which the rest of the components are embodied. The relative proportions of the components affects membrane parameters like electrode slope, selectivity against interferents, active life, etc. Different plasticisers, like *ortho*-Nitrophenyl Octyl Ether (*o*-NPOE), di(2-ethylexyl) sebacate (DOS) or di(2-ethylexyl) adipate (DOA) will affect differently the lipophilicity of the PVC membrane, which alters the distribution coefficients (k) of the different species. The more hydrophilic plasticisers, like *o*-NPOE, will have higher distribution coefficients and higher activity of ions inside the membrane (Eq. 2.20), but will also mean that the ligand will leach out to the aqueous phase more easily, reducing the working life of the electrode.

Other additives are used if they improve the membrane parameters, like potassium tetrakis(4-chlorophenyl)borate (KTpClPB) which functions as an anion excluder, preventing negative charged ions getting into the polymer membrane and helping to obtain a more ideal Nernstian response. However, a minimum amount should be used as

the exchanger anions have their own cation exchanger selectivity (Hoffmeister series) which may conflict with the desired selectivity.

2.5.2 Array of ISEs

Another trend which has been developed in recent years is to utilise an array of ISEs to detect, quantify and compensate for a number of interferents present in the sample matrix. Thus, if the technique is implemented for the analysis of a target ion (e.g. NH_4^+) in a high and varying background of interferents (e.g. K^+, Na^+ and Ca^{2+}) a Sensor Array Detector (SAD) formed of a number of ISEs selective for the main analyte plus the interferents (i.e. ISEs for NH_4^+, K^+, Na^+ and Ca^{2+}) is used to analyze the sample. For a given electrode the remaining ISEs are used to compensate for the interferents, allowing precise determination of both target analyte and interferents.

This multicomponent analysis technique can compensate for the contributions of main interferents in each single ISEs and provides a fast, inexpensive and viable way to simultaneously determinate a number of ions in samples containing widely varying amounts of these species. Chapter 3 explains in greater detail all concerning with the implementation of applications based on this multivariate analysis technique.

2.6 Analysis with ISEs

This section deals with some considerations that must be kept in mind when using ISEs for ion analysis. Electrochemical measurements must be made at zero current and in

previous Quadrant (valve) voltammeters were used. These were large, high power systems which, although accurate, were not portable and required considerable warm-up periods. More recently, op-amp based instruments with very high input impedance (typically ~1 TΩ) have been developed. These devices allow potentiometric readings in near-zero current conditions.

Another consideration is the fact that these potentiometric devices function in a logarithmic fashion, being the change in potential related to the logarithm of the ion activity (Eq. 2.3) with a maximum theoretical sensitivity (in the best case of ion charge being +1) of 59.16 mV for a tenfold change in ion activity at 25 °C. This means, that for a minimum error of 1%, the reading instrument used must have a discrimination factor of at least 0.25 mV.

2.6.1 ISE Requirements

A number of characteristics are required from an ISE so it can be consider a suitable sensor for quantitative ion analysis. Of these, slope, selectivity, limit of detection and electrode working life are probably the most important.

2.6.1.1 Slope

This is a measure of the sensitivity of the electrode, and the closer it is to the Nernstian value of $59.16/z_k$ mV decade^{-1} (Eq. 2.3) the more ideal the electrode behaviour is. In determinations with single ISEs the electrode working range will be determined by the

activity window of the primary ion where the electrode response is a straight line (in logarithmic scale).

2.6.1.2 *Limit of Detection*

The limit of detection (LOD) can be used to compare the performance of different electrodes at low primary ion activities. It is defined as the value of primary ion activity where the activity of the primary ion equals the summation term for interferents in the Nikolskii-Eisenman equation (Figure 2.2), i.e. the contribution of all the interferents equals the contribution of the primary ion[11]. At this point,

$$a_{ik} = \sum_{l} K_{jkl} a_{il}^{z_k/z_l}$$

<div align="right">**Eq. 2.27**</div>

Comparing the difference in response from primary ion only (E_{ik}) to mixed behaviuor (E_{ikl}),

$$\Delta E_i = E_{ikl} - E_{ik} = S_j \log\left(a_{ik} + \sum_{l} K_{jkl} a_{il}^{z_k/z_l} \right) - S_j \log a_{ik}$$

$$\Delta E_i = S_j \log \frac{2a_{ik}}{a_{ik}} = S_j \log 2$$

<div align="right">**Eq. 2.28**</div>

This means that the LOD for an electrode selective for a single charged ion is the activity level corresponding to where the mixed response deviates from the primary response by 17.8 mV (17.8/z_k for a $z+$ charged ion k). Limit of detection does not mean limit of determination, and ISEs can be used to analysis of activities below the LOD with the appropriate methodology.

2.6.1.3 Selectivity

Selectivity coefficients give an idea of the degree of discrimination of an electrode to ions in solution other than the primary ion (see also Section 2.5.1). The smaller the coefficient is the better selectivity the ISE presents. However, values are far from constant and depend on the activity range studied and the measurement technique used[26,27].

As an example, if the overestimation accepted for the total primary ion concentration is a maximum of 5% then, for binary mixtures where primary (k) and interfering (l) ions ($z_k = z_l$) are present in the solution at the same level the electrode used should have a selectivity coefficient $K_{jkl} = 5 \times 10^{-2}$ or lower.

2.6.1.4 Electrode life

The working life of an ISE can vary from a few days to a few months, and will depend on factors such as the analysis technique used, the matrix of the samples analysed and membrane composition, the lipophilicity of the plasticiser used being the prime factor affecting the life time of the PVC membrane electrodes[11]. With these sensors, deterioration of the selective species, or leaching out of one or more components into the aqueous samples will produce a gradual decrease of the electrode slope and eventually null response. An important parameter to consider during the active life of the electrode is how long the ISE can be use between calibrations without significant changes in the electrode parameters that will affect the accurate prediction of unknowns.

2.6.2 Sample Requirements

Samples to be analysed using a single electrode approach must comply with a number of requirements which are discussed below.

2.6.2.1 Activity

As explained in Section 2.2 the response of an ISE is related to the activity, not concentration, of the ions in solution. The analyst must always bear in mind what the relationship between activity and concentration is and how it varies from solution to solution. This relationship is defined as:

$$a_i = \gamma_i C_i$$

Eq. 2.29

where γ_i is the activity coefficient of the ionic species i in a particular solution. Several theories exist to explain this relationship, all of them relating the values of the activity coefficient to the ionic strength of the solution. The Davies equation, used in this research, states that this relationship is expressed by:

$$\log \gamma_i = -A\left(\frac{z_i^2 \sqrt{I}}{1 + \sqrt{I}} + cI \right)$$

Eq. 2.30

where z_i is the ionic charge of the species and A and c are parameters which take the values of 0.51 and 0.15 for water solutions at 25 °C[28]. I is the ionic strength of the solution which is defined as a contribution of all the ionic species i present in the sample:

$$I = \frac{1}{2}\sum_i z_i^2 c_i$$

<div align="right">**Eq. 2.31**</div>

The Davies equation is an extended form of the Debye-Hückel equation with the advantage that the correction term at the end validates it for ionic strengths up to $I=0.6$ mol dm^{-3} (see Figure 2.4) [29].

The activity of the primary ion must, of course, be high enough to be within the dynamic range of the ISE. The minimum activity that can be accurately analysed will depend on the type and activities of interferents present in the sample and the electrode selectivity. The activity value corresponding to the LOD of the electrode will give a rough idea of the lowest activity, although high error is to be expected in the determination from a calibration graph of the activity of the primary ion in the vicinity of the LOD (~100%).

Figure 2.4: Effect of the ionic strength on the activity of single ion solutions. Deviation from the ideal relationship (a) for a single-charged ion (b), for a double-charged (c) and a triple-charged ion (d) as calculated from the Davies formalism (Eq. 2.30).
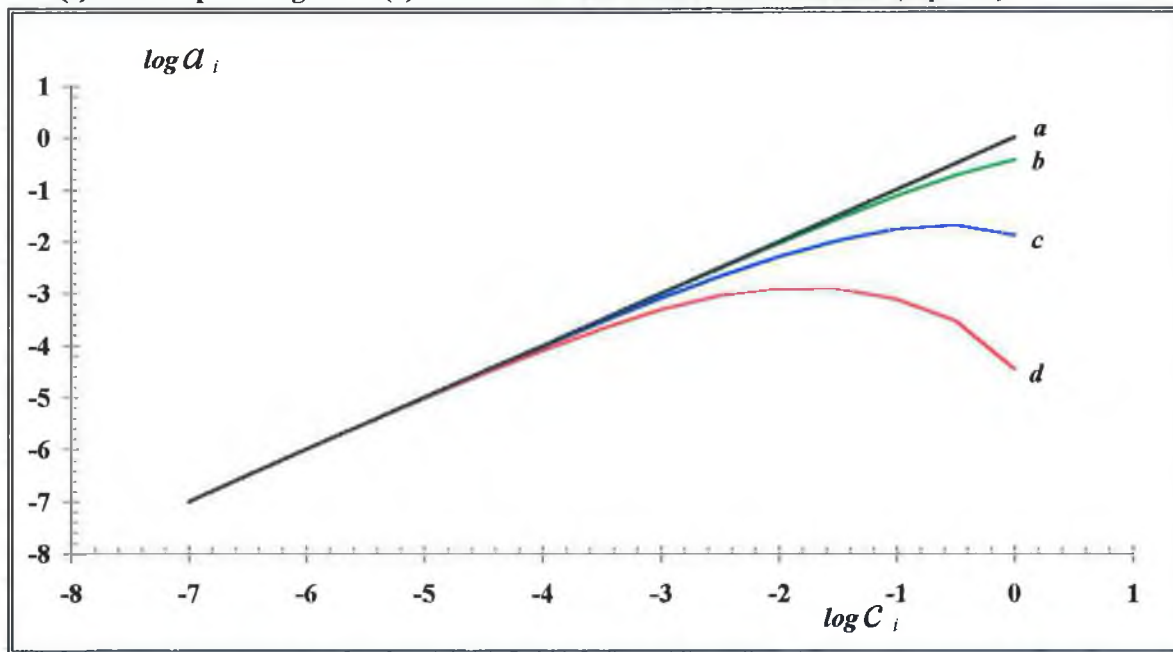
Other factors like indifferent ions will not induce response in the ISE but will alter the ionic strength of the solution and therefore the activity coefficients. Formation of charged complexes between the primary ion and ligands in the sample will lead to under-estimation of total-ion concentration, as this will reduce the free ion activity, to which the electrodes are responsive. On the other hand, where the analyst is interested in the free ion activity rather than total concentration (as often is the case in physiology and biochemistry studies) ISEs may be the only suitable analytical method.

2.6.2.2 Interferents

The activities of interferents in the sample should, ideally, be much smaller than that of the target analyte, in which case they can usually be neglected. However, if the levels of the interferents are known and constant and their contribution to the ISE response is significant, direct potentiometry can still be used if some correction for this contribution is applied. If the ions presents and the activity levels are unknown and variable, analysis of the target analyte can be performed, on a sample to sample basis, with a standard addition (Section 2.6.4.2) or sensor array techniques (Chapter 3). These particular cases depend on the ratio between the contribution to the sensor response from the primary ion and the bulk of interferents as discussed in Section 2.3.

2.6.2.3 Matrix Effects

The presence in the sample matrix of other species than interferents, like proteins or lipids, may create suspensions or gels of high molecular weight particles which can affect the proper performance of the ISE by deteriorating the membrane or dissolving its

components, therefore reducing considerably its working life. In addition, the presence of macromolecules like proteins or long chain lipids may coat the membrane and eventually block the active electrode surface. In flowing systems this same effect may produce clogging of the narrow flow conduits.

Chelates or other complexing agents may favour the development of side reactions which will interfere the proper determination of the analyte by reducing the level of activity of the free ion.

2.6.3 Calibration and Characterisation

There is no significant difference between the conventional calibration and characterisation procedures for batch and flow-injection single ISE systems. In the former, the e.m.f. values represent the potential of the whole of the electrochemical cell and, as the potential of the reference electrode (E_{ref}) remains constant, the variations in the cell potential from solution to solution can be related to variations on the e.m.f. of the working ISE alone ($E_{(ISE)}$).

$$E_{(cell)} = E_{(ISE)} - E_{(ref)}$$

<div align="right">**Eq. 2.32**</div>

This also applies to flow-injection analysis (FIA) systems employing ISEs as detectors, with the difference that the analytical result does not correspond to the overall e.m.f. of the galvanic cell, but the increment in potential of two different solutions, i.e. peak height. This is because in flow-injection systems, the contribution to the cell potential of

the reference electrode and the lowest standard (when present in the carrier solution) are offset to a baseline referred as zero-potential (Eq. 2.33). Therefore, when only the carrier solution is being presented to the electrode the response of the system is;

$$E_{(carrier)} = E_{(ISE,carrier)} - E_{(ref,carrier)} = 0$$ **Eq. 2.33**

and for the sample analysed;

$$E_{(sample)} = E_{(ISE,sample)} - E_{(ref,carrier)}$$ **Eq. 2.34**

Therefore the response corresponding to a particular sample *i* measured in comparison to the response of the carrier solution should be treated as

$$\Delta E_{(peak)} = E_{(sample)} - E_{(carrier)} = E_{(ISE,sample)} - E_{(ISE,carrier)}$$ **Eq. 2.35**

The general characteristics of an ISE are usually obtained by studying the steady-state response to a wide range of primary ion activity, typically between 10^{-7} to 10^{-1} mol dm^{-3} This calibration gives general electrode parameters like the standard electrode potential, slope and LOD. Observing the response to solutions containing interfering ions will provide information about the selectivity coefficients. If very precise measurements are needed in a particular application, a different calibration set more focused on the sample range can be designed, giving information on how the electrode behaves in that specific activity range.

It is important to know the effect of ionic strength of the solutions on the activity of the ions in the standards. This effect increases exponentially with concentration and is much stronger for multiple charged ions. A correspondence graph between activities (a_i) and concentration (C_i) is shown in Figure 2.4 which was constructed using the Davies relationship (Eq. 2.30). For singly charged ions (b) the deviation from the ideal relationship (a) and the 1:1 ratio only becomes apparent when the concentration of the ion in a single ion solution increases over c.a. 10^{-2} mol dm^{-3}. This deviation is more dramatic for doubly-charged (c) and triply-charged ions (d). Modifying the calibration solutions so that they contain the same high concentration of an indifferent ion gives a constant ionic strength in the whole calibration and therefore constant activity coefficients. Electrode potentials or potential changes can then be directly related to the ion concentration, but sometimes at a cost of reduced electrode sensitivity, as the slope may decrease due to a reduction of the chemical activity of the free ions.

2.6.4 Analysis and Prediction

A brief description of the analysis techniques used with single ISE systems and their methods for determining unknowns are given in the following sections. Each one is particularly appropriate for particular interferent conditions, also described.

2.6.4.1 Direct Potentiometry

After sample treatment and preconcentration, if needed, direct potentiometry involves presenting the sample to the ISE and recording the change in electrode or the cell

potential, depending on the analysis technique used. The response is used to calculate the activity of the primary ion either graphically, from a calibration curve like Figure 2.2, or theoretically, from the Nikolskii-Eisenman equation.

The first method requires the matrix of the calibration solutions and the samples to be matched and with constant activities of the interferents, as the only variable allowed is the activity of the primary ion. This technique is ideal for samples which only contain the primary ion or some interferents at negligible levels. If the contribution of the interferents to the electrode response cannot be neglected, the second method can provide some degree of correction if the summation term $\sum_l K_{jkl} a_{il}^{z_k/z_l}$ is known and constant from sample to sample (Case 2, Section 2.3: $a_{ik} \approx \sum_l K_{jkl} a_{il}^{z_k/z_l}$). This method is specially indicated for analysis of samples where the interfering ions maintain a constant level, as the summation factor can be calculated during electrode characterisation. The activity of the primary ion could be calculated from the extension of Eq. 2.13;

$$a_{ik} = 10^{\frac{E_{ij}-E_j^0}{S_j}} - \sum_l K_{jkl} a_{il}^{z_k/z_l} \qquad\qquad \textbf{Eq. 2.36}$$

In practise, this procedure is not usually utilised and the of the primary ion activities are predicted graphically from a calibration curve.

2.6.4.2 Standard Addition

This technique allows the reduction of the contribution of interferents when used with each sample. The sample is analysed directly with the ISE and the potential recorded. After that, a volume of a solution containing a known concentration of the primary ion is

added. This solution is presented again to the ISE. The change in response is only related to the change in the activity of the primary ion and from the Nikolskii-Eisenman equation the difference in electrode potential can be explained as;

$$\Delta E_{ij} = E_{ij}^{'} - E_{ij} = S_j \log\left(\frac{a_{ik}^{'}}{a_{ik}}\right)$$

Eq. 2.37

where $E_{ij}^{'}$ and $a_{ik}^{'}$ are the electrode response and activities after the primary ion addition. From Eq. 2.37 it derives that the initial primary ion activity in the sample can be determined from the equation:

$$a_{ik} = \frac{a_{std}V_{std}}{V_i + V_{std}}\left(10^{\frac{\Delta E_{ij}}{S_j}} - \frac{V_i}{V_i + V_{std}}\right)^{-1}$$

Eq. 2.38

a_{std} being the activity of the volume (V_{std}) of the standard solution added and V_i being the initial volume of the sample. If a relatively small aliquot ($V_{std} \Rightarrow 0$) of high primary ion concentration standard solution is added, the volume can be considered constant and the activity of the primary ion in the original sample is given by the simplified equation;

$$a_{ik} = \frac{V_{std}a_{std}}{V_i}\left(10^{\frac{\Delta E_{ij}}{S_j}} - 1\right)^{-1}$$

Eq. 2.39

2.7 ISE-FIA Systems

Ion-Selective electrodes can be used as detectors for two fundamentally different analysis methods, batch measurements and flow-injection analysis. Although the chemical

composition of membranes do not differ significantly, factors as thickness, the type and architecture of the electrode body and the membrane position can affect dramatically the overall response behaviour. Thus, membranes from the same production cocktail used in batch and flow analysis will show very different response characteristics and different electrode parameters in FIA and batch measurements. Also, different possible flowing geometries (Figure 2.6) in FIA affect the ISE response, which indicates that the overall detector characteristics do not solely depend on the analysis technique, but also on the way the sample is presented to the electrode membrane.

The traditional batch analysis approach involved dipping a bench-type ISE and a reference electrode into the solutions and reading the electrochemical cell potential after the steady-state is allowed to develop (typically 1 to 3 minutes). This assures that the full electrode response to the primary ion is obtained. But as well as the primary ion, the interferents in the sample also generate a complete response and contribute to their maximum extent to the overall electrode potential. In batch measurements, the cell potential obtained is related to a calibration curve or to a electrode response equation from which unknowns can be estimated. Electrode potential drift constitutes a serious problem, as it cannot be compensated for unless the ISE is re-calibrated.

When a membrane in equilibrium with the primary ion is exposed to a solution of higher primary ion activity, a fast initial change in membrane potential occurs (boundary potential), followed by a slower potential settling towards the steady-state *plateau* which can typically take between 1 to 3 minutes (diffusion potential). The first effect is

kinetically limited and is mainly a response caused by the primary ion due to the faster rate of exchange of these ions compared to interferents, which gives some degree of kinetic selectivity[30]. This fast initial response depends on how the sample is presented to the membrane (e.g. stirring rate) and as it is not very reproducible in steady-state measurements it cannot be exploited for analysis purposes.

On the other hand, when the potential settles the exchange process is thermodynamically controlled (Figure 2.5a). The equilibrium involves a competition mechanism between primary ion and interferents to complex the free ligands, and therefore the exchange selectivity in steady-state will depend on the stability constants of the ion-ligand complexes formed in the membrane (see Section 2.5.1). This steady-state potential, E_{SS}, is the only part of the ISE response in batch regime reproducible enough to be related to the ion activity in the solution.

Figure 2.5: Theoretical response of an ISE to the primary ion.
Response a) represents the development of the response of ISEs in batch measurements. The potential generated E_{SS} is maximum when the steady-state equilibrium is reached. For flow-injection measurements (b), the concentration is related to the potential E_{FIA} observed at the maximum of the transient electrode response.
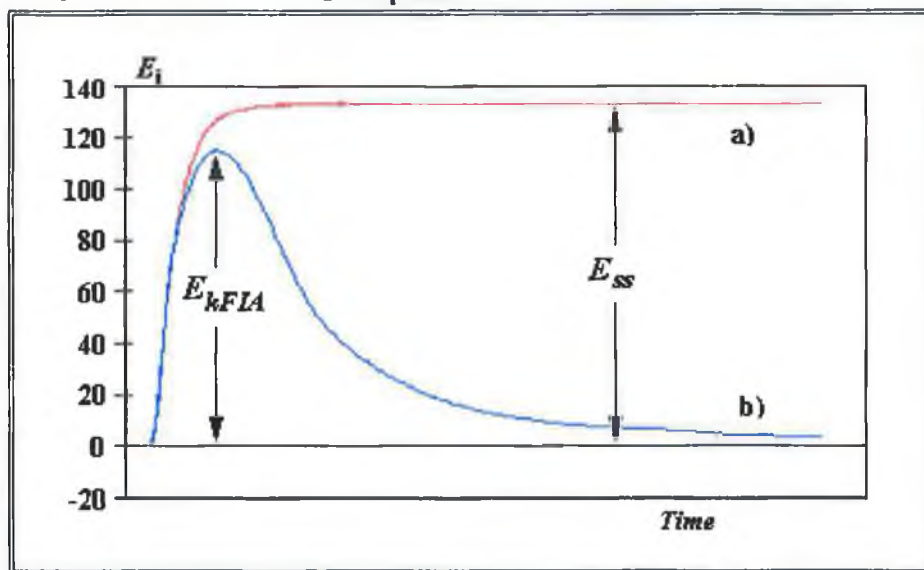
In flow-injection systems[31,32], the sample is transported to the electrode active surface through tubes of small diameter. The sample only occupies a small section of the flow between two sections of a carrier or conditioning solution that pushes the sample to the detector. When the electrode sees the sample "plug" a potential is developed (typically in less than 30 seconds) related to that of the carrier solution containing a lower concentration of the primary ion. In this situation, the potential developed in the electrode rarely reaches the steady-state and a sub-Nernstian response is to be expected. This is a comparative technique, in opposition to the global batch analysis method, in so far as the potential maximum (i.e. peak height) is always measured against a baseline which is the electrode response to the conditioning solution instead of the e.m.f. of the galvanic cell for that solution. Hence, as signal drift occurs, both baseline and peak are affected and, because the analytical measurement is the difference between these two, the drift is inevitably subtracted out.

One of the most important features of flow-injection systems is that the hydrodynamic characteristics of the sample through the conduits is very reproducible. This reproducibility generates the same variation of the potential with time in every sample injection, and any point in the potential profile could be related (in theory) to the ion activity[33]. Flow-injection systems are in essence kinetic systems and, as the steady-state is not reached, the slope of the electrode response is smaller than in batch measurements. In most cases, depending on the composition of the membrane cocktail, the electrode lifetime will be longer in flow-injection techniques because the electrode membrane is in

contact with the sample only a few seconds, being washed and re-conditioned immediately after the response is developed.

Figure 2.6 shows the most common geometries, both for batch and flow-injection systems. The typical design for a bench-type electrode and its components appears in Figure 2.6a. An internal reference electrode, usually Ag/AgCl, is immersed in a solution containing a fixed concentration of the primary ion (typically 0.1 mol dm^{-3}). This solution is in contact with the internal surface of a selective membrane, creating a constant potential at the inner side. The electrode body is immersed in the sample solution and a potential, which depends on the activity of ions in the solution, is created across the membrane. The architecture and components of ISEs for flow systems is essentially the same, and only changes the way the sample is presented to the electrode[34].

Figure 2.6: Ion-Selective Electrode geometries.
a) Bench or dip-type electrode for batch measurements. b) ISE geometries for flow systems;
***i*) Flow-through. *ii*) Flow-past. *iii*) Tangential. *iv*) Wall-jet.**
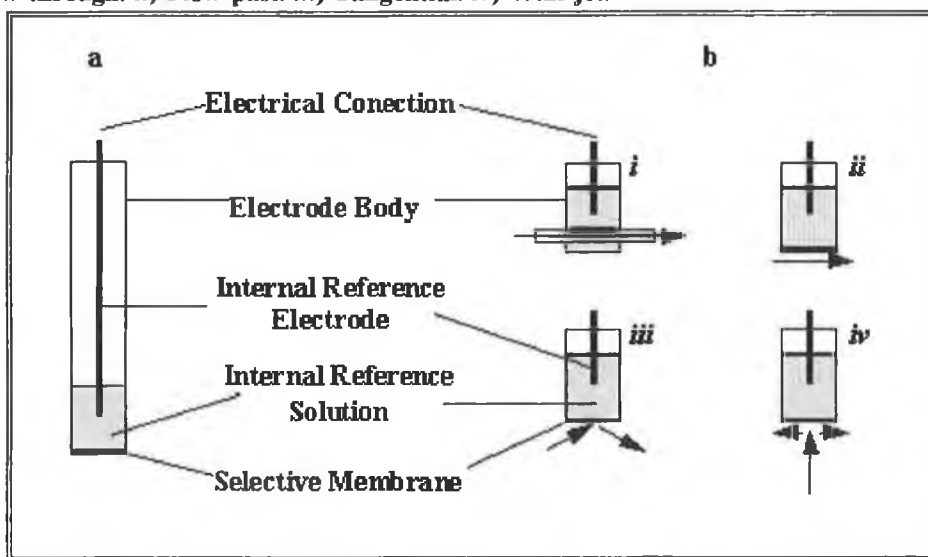
Figure 2.6b shows the most common designs for flow-injection ISEs. In the flow-through (*i*) and flow-past geometries (*ii*) the sample crosses the electrode body through a small conduit in which part (or the whole) of the wall has been replaced with the selective membrane[35,36], and the sample passes along the electrode making contact with the surface of the membrane. In the tangential electrode (*iii*) the sample strikes the membrane at an angle between 0° and 90°. In and out-flow angles usually have the same value. In Figure 2.6b type *iv*, or wall-jet, the sample reaches the membrane at an angle of 90° and exits at the sides[37].

2.7.1 Batch vs. FIA Systems

This section deals with some of the well known advantages of using FIA systems instead of steady-state batch analysis. These features are solely dependent on the technique itself and independent of the detector type used. Figure 2.7 show a simple FIA set-up which can be used with an ISE as the detector.

Figure 2.7: Set-up diagram for the FIA system with single ISE detector.
The minimum set-up for a FIA system must consist of the following parts: a) Pump.
b) Injection Port. c) Detector: ISE and reference electrode. d) Measuring device.
The different stream lines carry: e) Reference electrode internal electrolyte. f)
Carrier. g) Sample.
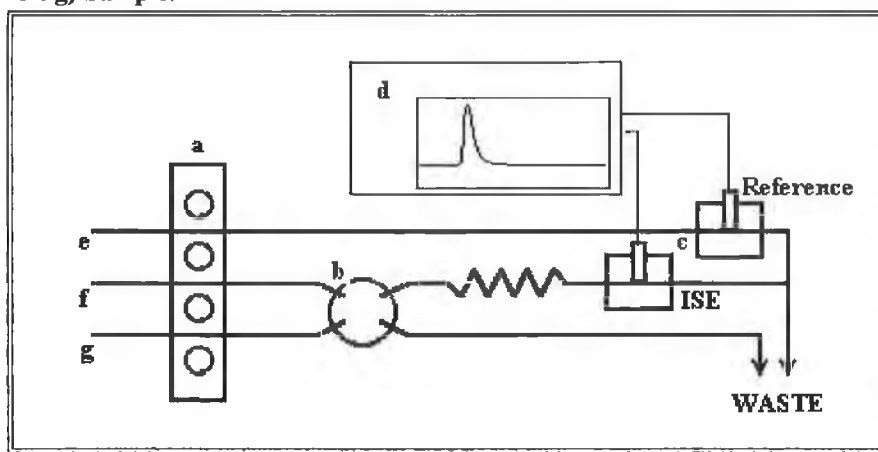
2.7.1.1 Reproducibility

Because of the friction and mixing that happens inside the systems conduits, the "square wave" injected into the carrier in the injector port is modified as it travels along to the detector. The concentration gradient created around the bulk of the sample, which depends on the flow rate and the distance traveled, creates a response in the detector which is not square and presents a rising and tailing stages typical from the FIA traces[31,32,33].

For the same experimental conditions, this gradient created is very reproducible, as the sample always travels the same distance, and the analysis are expected to have very high experiment reproducibility not only at the *pseudo* equilibrium reached at the top of the peak (although this tend to be more reproducible), but also during the rise and decay of the transient signal. This characteristic of flow-injection systems allows the use of the kinetically limited initial electrode response for analytical applications in cases where the rate of exchange of interfering ions is significantly slower than that of the primary ion.

2.7.1.2 Reagent Consumption

The volume of sample injected into the carrier stream will vary depending on the application but is usually between 25 and 200 microlitres. This volume is much smaller than the millilitre scale which is usually the case in batch analysis.

For applications were the sample is available in very small quantities, or it is very precious, e.g. blood serum, it can be injected straight into the detector or into a carrier

stream with reagents for derivatisation previous to analysis. In the opposite case, where the sample is inexpensive and available in large quantities, e.g. sea water, the reagents can be injected in very small volumes into the sample, reducing the amount of reagent needed for the analysis.

2.7.1.3 Sample throughput

Compared to other flowing techniques which use continuous or air-segmented flows the speed of the carrier along the FIA conduits is very high. The flow rate used is typically between 0.5 to 1.5 mL min^{-1} or even higher. which means that at flow rate of 1.0 mL min^{-1} (typical) a sample volume of 100 μL only stays in contact with the detector during 6 seconds, time during which the response maximum, which is related to the sample concentration, is developed. FIA systems with detectors which do not chemically interact with the samples, or with fast hysteresis cycles, can produce sample rates of 120 samples min^{-1} or higher.

2.7.1.4 Sensor Life Span

As seen above, the proportion of analysis time the detector is in actual contact with the sample is very small, and the remaining time is being washed by the buffer or conditioning solution used as carrier. In those cases where the target analyte is present in a sample matrix which may contain species capable of damaging or reducing the sensor's ability to detect the analyte, a FIA set-up will increase considerably the working life of the detector.

In some cases it may happen that the high hydrophilicity of the membrane components, i.e. relatively low distribution coefficient between aqueous and membrane phases, causes some of the membrane components to leach out of the membrane phase, being washed away in the carrier. This will inevitably cause a deterioration of the electrode membrane faster than usual.

2.7.1.5 *Kinetic Measurements*

Because of the very high reproducibility all along the FI trace this technique is particularly suitable for kinetic studies[38,39] where the sample has some type of chemical interaction with the detector. This characteristic of the FIA systems is thoroughly exploited in some of the more advanced FIA setups like double injection[40], stopped-flow[33] or reverse flow[41] systems.

2.7.2 ISE-FIA Advantages

As described above, FIA presents a number of inherent advantages. In addition, the response characteristics that ISEs present when used in FIA mode generate a new set of features which must be taken into account and which represent a dramatic advantage over the steady-state batch measurements.

However, FIA is additionally attractive from the point of view of analytical potentiometry for several reasons outlined below.

2.7.2.1 Sensor Conditioning

Because the selectivity mechanism involves ion complexation in the boundary region between the membrane and the aqueous solution, the electrodes must be conditioned regularly to ensure that the membrane-solution interface is stable. In conventional batch analysis this conditioning must be done after a few number of measurements (if not after every single one). This is obviously very time consuming and it can increase considerably the experimental time for sample analysis.

On the other hand, in FIA systems the carrier solution is continuously washing through the detector between analysis, which helps to stabilise the boundary potential in the boundary region. If the buffer contains a low concentration of the primary ion, an exchange equilibrium is established between the membrane and the solution, and once the initial equilibrium is established, the membrane responds faster to higher concentrations of primary ions in the sample. When the sample leaves the membrane surface, any interferent ions which may have entered the membrane will exchange more easily with the primary ion in the carrier solution.

2.7.2.2 Enhanced Selectivity

As discussed before, the response kinetics of the ISE to the primary ion is usually faster than to the interferents. This characteristic generates a kinetically enhanced selectivity in the first stages of the development of the electrode response[42,43]. In contrast batch procedures where the measurements are taken from the signal *plateau* once the steady-state is reached do not benefit from this advantage.

Figure 2.8 shows a diagram of the batch (a_k & a_l) and flow-injection (b_k & b_l) potential profiles for two single ion solutions containing the primary ion (a_k & b_k) and an interfering ion (a_l & b_l) at an activity level so that the steady-state responses are equal in both solutions. Theoretically, the Nikolskii-Eisenman equation assumes a logarithmic additive contribution from both primary ion and interferent. In a binary solution containing both the primary ion and the interferent at these activities, the response will be incremented as

$$\Delta E_{ij} = S_j \log\left(\frac{a_{ik} + K_{jkl}a_{il}}{a_{ik}}\right) = S_j \log 2 \qquad \textbf{Eq. 2.40}$$

Eq. 2.40 clearly indicates that for the batch experiment, the contribution to the potential from the interferent ion is 30% of the electrode slope.

Figure 2.8: Kinetic-enhanced selectivity in ISEs.
In flow-injection systems, the difference in electrode response time to the primary ion and the interferents can significantly increase the selectivity for the primary ion in comparison to batch techniques (see text).
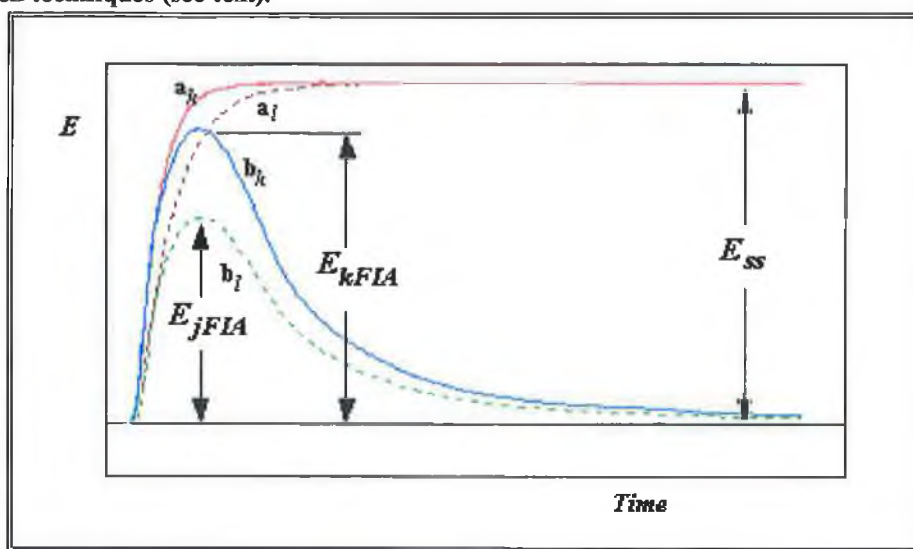
In flow-injection measurement, the response of the ISE to the interfering ions in the binary solution is smaller because of the slower initial response to the interferents, and will be reduced even further because of the added effect of ion competition. In general, the slower the response kinetics is for an interfering ion, in comparison to the primary ion, the greater the difference between the steady-state and the kinetically enhanced selectivity.

2.8 ISE Applications

Numerous publications on neutral carrier and ion-exchanger based ISEs and their applications can be found in specialised publications as part of the general area of chemical sensors[4,5,6] or as a class of its own[7]. Other reviews comprise the use of potentiometric selective electrodes for water analysis[44] and biochemical applications[8]. General guidelines for the use of ISEs for environmental applications[45] and as detectors for flow systems[46] have also been reported.

Hundreds of articles on particular applications of ISEs are available in the literature but, because this section does not intend to be an exhaustive compilation of ISE applications and reviews, only general reviews have been considered, and the following sections are compiled mainly from these referenced articles.

2.8.1 Target Species

Table 2.1 summarises the most usual active species used for the selective detection of the commonly occurring inorganic cations and anions with membrane-based potentiometric sensors. There are many more references in the literature to species like organic ions, proteins and enzymes, vitamins, drugs, medicines and other species of complex molecular composition which can also be detected with ISEs.

Table 2.1: Active species for cation-selective membranes.
Columns on the left indicate the target analyte, and on the right, the active materials for the selective electrodes are shown [4,5,6,7].

Inorganic Cations			
H^+	N,N-dioctylaniline and Tridecylamine	$Cu(II)$	Dithiocarbamates, thiuram sulfides
Ammonium	Nonactin, narasin, monensin, salinomycin	Ag^+	monothia-crown ethers
Li^+	1,10-phenantrolines, crown ethers, formazans, isatin oximates	$Ni(II)$	bis(2-ethylexyl)phosphate
Na^+	Calix[4]arene esters and amides, crown ethers, cyclodextrins	$Zn(II)$	tetradecylammonium tetrathiocyanatozincate
K^+	Pyridine macrocycle, valinomycin, bis-crown ethers	$Pb(II)$	Tetraphenylborate surfactant complexes
Cs^+	Calix[6]arene derivatives	$Fe(III)$	1,7-dithia-12-crown-4
Ca^{2+}	ETH series, lipophilic hexapeptides	$Tl(III)$	Butylrhodamin β-tetrachlorothallate
Mg^{2+}	Acyclic aspartamides	$Au(III)$	Butylrhodamin β- and tetraphenylpyridinium tetrachloroaurates
Ba^{2+}	Barium (tetraphenyl borate-Antarox CO-880 complex)	$U(VI)$	Uranyl bis(phosphates)
Inorganic Anions			
Clhloride	Silver chloride-silver sulfide	Perchlorate	Berberine hydrochloride, N-ethylbenzo thiazole-2,2'-azaviolene perchlorate
Iodide	Vitamin B_{12} derivatives	Phosphate	bis(p-chlorobenzyl)tin dichloride
Nitrite	Tetraalkvitin compounds	Thiocyanate	nitron-thiocyanate complex
Sulphite	bis(diethyldithiocarbamato) mercury(II)	Chlorocromate	Quaternary ammonium chlorocromate
Carbonate	ion-exchanger-derivatised benzoic acid ester complex	Periodate	Berberine periodate

2.8.2 Analytical Techniques

Apart from the traditional batch mode for single electrode potentiometry, ISEs are commonly used as detectors potentiometric titrations, where the electrodes are used to detect the end-point of the titration. Batch-Injection Analysis is a relatively new technique which has already made the most of ISEs, using them for fundamental kinetic measurements and SAD applications.

Most of the flow analysis techniques can benefit from the wide variety of ISEs and target species for which these are available. In chromatography, ISEs are not often applied, except for ion detection after column separation, and more complex ones like the detection of enantiomer with chiral crown ether based membranes. Air segmented continuous analysers and Flow-Injection systems routinely use ISEs as electrochemical detectors.

From all these techniques, FIA is probably the one that makes the most of the characteristics of these sensors, and an increasing number of papers describing complex systems where arrays of ISEs are used for multivariate determination of a number of cations (also mixed cations and anions) can be found in the literature[47].

2.8.3 Process Application

ISEs find areas of application in almost any process where the detection and/or determination of ionic species is needed. Table 2.2 gives a schematic summary of process

applications, classified in different areas of chemistry, which can be found in the literature

cited above.

Table 2.2: Review of processes where membrane ISEs find applications as potentiometric detectors.

Fundamental Studies	**Environmental**
• Determination of ion conductance	• Analysis of effluents
• Determination of stability constants	• Determination of contaminants in waste water streams
• Determination of diffusion coefficients of ions in soil	• Monitoring of nuclear waste containment
	• Analysis of pH in rain water
• Determination of kinetic parameters of enzymatic processes	• Analysis of drinking water
	• Soil analysis
Industrial Processes	**Fundamental Analysis**
• Pharmaceutical analysis	• Multicomponent analysis
• Fermentation control	• Analysis of organofluoride compounds
• Determination of boric acid in plating baths	• Determination of trace level impurities in nuclear materials
• Measurement of Na^+ and K^- in Spanish wines.	• Potentiometric titrations
• Determination of the chloride content of fresh concrete	• Enantiomer selectivity
Biochemical Applications	**Clinical Analysis**
• Microsampling of biochemical systems	• Analysis of Na^+, K^+, Li^+, Ca^{2+}, CO_2, amines in:
• Antigen and antibody monitoring	Saliva
• Analysis of ions inside cells	Tissue
	Amniotic fluid
• Determination of H_2O_2 from biological processes	Whole blood
	Plasma
Petroleum Industry	Urine

2.9 References

[1]   Wipf, D. O.; Bard, A. J. *Analyst* **1994**, *119*, 719-726.

[2]   Wipf, D. O.; Bard, A. J. *J. Electrochem. Soc.* **1991**, *138*, 469-474.

[3]   Pranitis, D. M.; Telting-Diaz, M.; Meyerhoff, M. E. *Crit. Rev. Anal. Chem.* **1992**, *23*, 163-186.

[4]   Janata, J.; Josowicz, M.; DeVaney, D. M. *Anal. Chem.* **1994**, *66*, 207R-228R.

[5]   Janata, J. *Anal. Chem.* **1992**, *64*, 196R-219R.

[6]   Janata, J. *Anal. Chem.* **1990**, *62*, 33R-44R.

[7]   Solsky, R. L. *Anal. Chem.* **1990**, *62*, 21R-33R.

[8]   Wang, J. *Anal. Chem.* **1993**, *65*, 450R-453R.

[9]   Crow, D.R. *"**Principles and Applications of Electrochemistry**"* Blackie Academic & Professional, Glasgow, UK, 1994. 4th Ed.

[10] Sáez de Viteri, F. J.; Diamond, D. *Electroanalysis*, **1994**, *6*, 9-16.

[11] Morf, W. E. *"**The principles of Ion-Selective Electrodes and of Membrane Transport**"* Elsevier Scientific Pub. Co., Amsterdam, 1981.

[12] Suzuki, K.; Aruga, H.; Shirai, T. *Anal. Chem.* **1983**, *55*, 2011-2013.

[13] Yim, H. S.; Cha, G. S.; Meyerhoff. M. E. *Anal. Chim. Acta* **1990**, *237*, 115-125.

[14] Koryta, J.; Dvorák, J.; Kavan, L. *"**Principles of Electrochemistry**"* John Wiley &Sons, Chichester, England, 1993. 2nd Ed. Ch. 6.

[15] Vogel, A. I. *"**Textbook of Quantitative Chemical Analysis**"* Longman Scientific & Technical, Essex, England, 1989, 5th Ed. Ch. 15, pp. 548-590.

[16] Pranitis, D. M.; Meyerhoff, M. E. *Anal. Chem.* **1987**, *59*, 2345-2350.

[17] Fraticelli, Y. M.; Meyerhoff, M. E. *Anal. Chem.* **1981**, *53*, 992-997.

[18] Allen, J. R.; Cynkowski, T.; Desay, J.; Bachas, L. G. *Electroanalysis* **1992**, *4*, 533-537.

[19] Forster, R. J.; Cadogan, A.; Telting Diaz, M.; Diamond, D.; Harris, S.; McKervey, M. A.; *Sensors and Actuators B* **1991**, *4*, 325-331.

[20] Cunningham, K.; Svehla, G.; Harris, S. J.; McKervey, M. A. *Analyst* **1993**, *118*, 341-345.

[21] Cadogan, A. M.; Diamond. D.; Smyth, M. R.; Deasy, M.; McKervey, M. A.; Harris, S. J. *Analyst* **1989**, *114*, 1551-1554.

[22] Ozawa, S.; Hauser, P. C.; Seile, K.; Tan, S. S. S.; Morf, W. E.; Simon, W. *Anal. Chem.* **1991**, *63*, 640-644.

[23] Pranitis, D. M.; Meyerhoff, M. E. *Anal. Chem.* **1987**, *59*, 2345-2350.

[24] Fraticelli, Y. M.; Meyerhoff, M. E. *Anal.Chem.* **1981**, *53*, 992-997.

[25] Davies, O. G.; Moody, G. J.; Thomas, J. D. R. *Analyst* **1988**, *113*, 497-500.

[26] Forster, R. J.; Diamond, D. *Anal. Chem.* **1992**, *64*, 1721-1728.

[27] Otto, M.; Thomas, J. D. R. *Ion-Selective Electrode Rev.* **1986**, *8*, 55-84.

[28] Ramette, R.W. "*Chemical Equilibrium and Analysis*" Addison-Wesley Publishing Co., 1981, p. 95.

[29] Christian, G. D. "*Analytical Chemistry*" Wiley, New York, 1986, 4th Ed., p110.

[30] Sáez de Viteri, F.J.; Diamond, D. *Analyst* **1994**, *119*, 749-758.

[31] Ruzicka, J. *Anal. Chem.* **1983**, *55*, 1040A-1053A.

[32] Ranger, C. B. *Anal. Chem.* **1981**, *53*, 20A.

[33] Ruzicka, J.; Hansen, E. H. *Anal. Chim. Acta* **1980**, *114*, 19-44.

[34] Davey, D. E.; Mulcahy, D. E.; O'Connell, G. R. *Electroanalysis* **1993**, *5*, 581-588.

[35] Meyerhoff, M. E.; Kovach, P. M. *J. Chem. Edu.* **1983**, *60*, 766-768.

[36] van Standen, J. F. *Anal. Proc.* **1987**, *24*, 331-333.

[37] Douglas, J. G. *Anal. Chem.* **1989**, *61*, 922-924.

[38] Hungerford, J. M.; Christian, G. D. *Anal. Chim. Acta* **1987**, *200*, 1-19.

[39] Hungerford, J. M.; Christian, G. D.; Ruzicka, J.; Giddings, J. C. *Anal. Chem.* **1985**, *57*, 1794-1798.

[40] Whitman, D. A.; Seaholtz, M. B.; Christian, G. D.; Ruzicka, J.; Kowalski, B. R. *Anal. Chem.* **1991**, *63*, 775-781.

[41] Frenzel, W. *Analyst* **1988**, *113*, 1039-1046.

[42] Diamond, D; Forster, R. J. *Anal. Chim. Acta* **1993**, *276*, 75-86.

[43] Lewenstam, A.; Saarinen, K. S.; Hulanicki, A. *IFCC Workshop* **1986**.

[44] MacCarthy, P.; Klusman, R. D.; Cowling, S. W. *Anal. Chem.* **1991**, *63*, 301R-342R.

[45] Fuckskó, J.; Tóth, K.; Pungor, E. *Anal. Chim. Acta* **1987**, *194*, 163-170.

[46] Pungor, E.; Tóth, K.; Hrabéczy-Páll, A. *Trends in Anal. Chem.* **1984**, *3*, 28-30.

[47] Diamond, D. *Electroanalysis* **1993**, *5*, 795-802.

3. Sensor Array Detection Systems

3.1 Introduction

The previous chapter discusses in detail the theory of ion-selective electrodes. Response characteristics and selectivity for particular species have also been discussed and compared for both batch and FIA experimental approaches, the latter being pointed out as an outstanding technique for customary analysis with ISEs. Nevertheless, and as with any experimental approach, there are some routine monitoring applications where the use of batch processes or FIA with single ISE detection cannot be used, either because of the high sample turnover expected from the technique or the unavailability of selective enough ISEs, or both. These are situations where the matrix of the sample contains interfering species at relatively high and variable levels. Methods such as standard-addition can cope with a varying sample matrix but at a much reduced analysis rate, whereas single ISE measurements in FIA regime will produce a high sample throughput but at high cost in prediction accuracy (as no compensation for a varying sample matrix is possible).

Unless very selective ISEs are available (near-specific), the error arising from the sample matrix may be unacceptably high. In a dynamic analytical situation where the matrix

contribution to the signal may change significantly, the only option (besides sample pre-treatment) is to use a number of electrodes, selective for different species, to simultaneously probe the same sample. With this approach, a Sensor Array Detector (SAD) is employed and its response characteristics modeled so that it can accurately predict the activity of a target ion in a variable background of interfering species by compensating for matrix errors in a dynamic manner.

This chapter deals with the theory behind the approach and with some of the different techniques available for its implementation. Even though the SAD approach can be used either in batch or FIA conditions, in those cases were *pseudo* real time analysis is needed, batch processes cannot meet with the sample rate required. Therefore FIA, and perhaps Batch-Injection Analysis (BIA), is the preferred experimental setup for the SAD approach.

3.2 The SAD Approach

As discussed in Section 2.3, analytical determinations of ions with single ISEs are limited to cases where experimental conditions are quite controlled, and when the sample matrix is well characterised. The use of a SAD approach enables the analyst to determine directly a target analyte in some of those cases where the characteristics of the sample matrix (high and varying levels of interferents) or the ISE characteristics (poor selectivity) do not permit single electrode measurements.

A SAD consists of a number of a sensors which generates a response pattern to the same sample. The information obtained from the detector as a whole, rather than each sensor individually, is used to generate analytical results. ISEs selective for different ions were used in this research as the sensors for the detector array. Redundant ISEs, i.e. a number of ISEs in the array selective for the same ion, could be included for fundamental studies or self-diagnosis of system performance.

Even though the overall SAD response is used for the analysis, each electrode still behaves as an ISE and therefore its behaviour obeys the Nikolskii-Eisenman theory, and Eq. 2.10 represents in general terms the response of these sensors. Thus, the overall SAD response can be explained in terms of a system of Nikolskii-Eisenman equations, each of them representing the response of one ISE. The system of equations for a n-ISE array is as follows:

$$E_{ij} = E_j^0 + S_j \log\left(a_{ik_1} + \sum_l K_{jk_1l} a_{il}^{z_{k_1}/z_l} \right) \qquad \text{Eq. 3.1a}$$

$$E_{ij} = E_j^0 + S_j \log\left(a_{ik_2} + \sum_l K_{jk_2l} a_{il}^{z_{k_2}/z_l} \right) \qquad \text{Eq. 3.1b}$$

$$E_{ij} = E_j^0 + S_j \log\left(a_{ik_3} + \sum_l K_{jk_3l} a_{il}^{z_{k_3}/z_l} \right) \qquad \text{Eq. 3.1c}$$

$$\cdots$$

$$E_{ij} = E_j^0 + S_j \log\left(a_{ik_n} + \sum_l K_{jk_nl} a_{il}^{z_{k_n}/z_l} \right) \qquad \text{Eq. 3.1d}$$

(See Glossary of Symbols for identification of variables)

These equations explain the SAD response and predictions can be made using this mathematical model once the optimum parameter values, i.e. those which minimise the error during calibration, are accurately obtained from the SAD modeling stage.

3.3 Selectivity Coefficients vs. Selectivity Constants

Ideally, the selectivity for an ISE against any interfering ion should be quantified with a single number (a selectivity constant) which is independent of the experimental conditions or the method of determination. Unfortunately, this has not been possible for a number of reasons which can be summarised as follows;

The Nikolskii-Eisenman equation contains a power ratio associated with the charges of the primary and interfering ions and the interfering ion activity. The practical determination of selectivity coefficients is usually by means of the separate solution method (SSM) or mixed solution method (MSM)[1,2]. In the case of the former, cell potentials are measured in separate solutions of the primary ion (k) and an interfering ion (l) while in the case of the latter, the cell potential is measured in a series of solutions of the primary ion made up in pure water and compared to potentials measured obtained with the same primary ion activities in a fixed background of an interfering ion. With the SSM (where the potentials in the primary and interfering ion solutions are equal) and the MSM (where the potentials obtained at equal activities of the primary ion differ by 17.8 mV for the pure and mixed solutions, respectively), the selectivity coefficient is given by;

$$K_{jkl} = \frac{a_k}{a_l^{z_k/z_l}}$$

Eq. 3.2

These methods have been used by many researchers over the past 30 years or so in order to quantify, to some degree, the selectivity of a particular electrode. However, they are unsatisfactory for a number of reasons;

- When $z_k = z_l$, K_{jkl} is simply estimated from the ratio of the primary and interfering ion activities which satisfy the conditions applying to each method. However, with the SSM, this ratio is usually not constant, as the slope for the interfering ion response is often smaller than that of the primary ion, and hence the selectivity coefficient varies over the calibration range.

- With the MSM, the point of 17.8 mV difference in the two calibration curves is difficult to locate exactly leading to imprecision in the value of the selectivity coefficient.

- In cases where $z_k \neq z_l$, the value of the selectivity coefficient becomes a function of the interfering ion activity.

In addition, neither of these methods approximates the situation encountered in real analytical situations, where the primary ion usually exists in the presence of a number of interfering ions whose activity may vary over a certain range.

Hence it is not surprising that the selectivity coefficients quoted in the literature are of very limited use, and are never regarded as being robust enough to be used in the Nikolskii-Eisenman equation to determine unknowns.

The solution to the problems outlined above lies in the definition and measurement of constants by which the selectivity of an ISE for the primary ion against interfering ions can be described. The first stage is to modify the Nikolskii-Eisenman equation so that the power-dependence of the selectivity coefficient in situations where $z_k \neq z_l$ is removed, i.e.

$$E_{ij} = E_j^0 + S_j \log\left(a_{ik} + \sum_l K_{jkl}^* a_{il} \right)$$

Eq. 3.3

The relationship between this new selectivity constant (K_{jkl}^*) and the conventional selectivity coefficient as defined by Eq. 2.10 is;

$$K_{jkl}^* = K_{jkl} a_{il}^{(z_k/z_j)-1}$$

Eq. 3.4

Hence for those cases where $z_k = z_l$, $K_{jkl}^* = K_{jkl}$

In adopting the term "constant" instead of "coefficient" to describe the parameter used for measuring selectivity, attention is drawn to the difference in definition of the two terms (the coefficient cannot be a constant under any conditions if $z_k \neq z_l$). However, the value of the constant is not a *"global* constant", but rather a *"conditional* constant" whose value is constant within the constraints of the calibration design and experimental conditions used, i.e. the term "constant" is used in a similar way to the qualifications associated with most other constants used to describe experimental phenomena (e.g. the so-called "cell constant" in the Nernst equation, rate constants and equilibrium stability constants, whose values are in effect not constants, but associated with certain experimental conditions, e.g. temperature or perhaps the experimental method used, and whose values can only be estimated rather than determined exactly).

3.4 Multicomponent Analysis

Multicomponent analysis involves the determination of a number of characteristics of an unknown sample during the same analytical run. Temperature, turbidity, acidity or concentration are some examples of properties which could be analysed through multicomponent analysis. Detectors or sensors which can provide information, particularly on those variables, are needed. A ISE-SAD approach where the detector is fitted with a number of sensors selective for particular ions, or sample components, will give information about the activity levels of the ions for which the ISEs are selective. Once again, ISEs are selective but not specific and some degree of interferent contribution is to be expected. This contribution can be constructive and will help to explain the overall SAD response if it can be studied as cross-response between two electrodes, meaning that the primary ion for one ISE contributes significantly, as an interferent, to the response of a second ISE and *vice versa*. This cross-response is very important for the accurate modeling of the overall SAD response and the contribution of interferents in the different electrodes of the array[3].

Two very different situations, both in the approach and the goals, must be considered in multicomponent analysis. In a first situation, a number of ions of interest in the samples are sensed with a number of ISEs, one for each ion, and the existing information is used for interferent correction, where and if applicable, to increase the accuracy of the technique. In a second approach, only one of the ions in the solution is targeted, and a number of ISEs are included in the array to specifically seek the information needed

about the sample matrix to allow compensation for major interferents and hence improve the accuracy of the primary ion determination. These two approaches are as follows:

- **Approach 1:** The number of ISEs is equal to the number of factors of interest in the sample. As an example, determining sodium in drinking water will require a sodium-selective electrode. The variable, or factor, will be the activity of sodium ions in the water samples. On the other hand, water hardness, i.e. total calcium and magnesium, can be measured with one probe which responds to both ions. In this case, the factor will be the hardness of the water, measured as a sum of the activities of calcium and magnesium ions, not the activity of calcium and the activity of magnesium separately.

The system of Nikolskii-Eisenman equations that explain the response behaviour of the SAD is shown in the Eq. 3.5 series, where k_1, k_2, k_3,...,k_n are the primary ions for each of the electrodes and l refers to the interfering ions whose contribution cannot be corrected ($l \neq k_1$, k_2, k_3,...,k_n). High degree of selectivity will be required from the ISEs against their main interfering ions (l) because correction for their contribution to the signal cannot always be assured by the rest of electrodes in the array. For each of the sensors, this uncertainty in the model is expressed by the summation term at the end of each equation Eq. 3.5a to Eq. 3.5d). Feed-back information from other ISEs in the array does not necessarily mean an improvement in the interferent compensation, as an important interfering ion may not have a ISE selective for it in the array and hence cross-response will not exist. If this is the case, information about the activity levels of the interfering ion will not be available for compensation

leaving an important interferent contribution ($K_{jk_1l}^* a_{il}$) without correction which will increase the error in the determination.

$$E_{ij} = E_j^0 + S_j \log\left(a_{ik_1} + K_{jk_1k_2}^* a_{ik_2} + K_{jk_1k_3}^* a_{ik_3} + \ldots + \sum_l K_{jk_1l}^* a_{il} \right) \qquad \text{Eq. 3.5a}$$

$$E_{ij} = E_j^0 + S_j \log\left(a_{ik_2} + K_{jk_2k_1}^* a_{ik_1} + K_{jk_2k_3}^* a_{ik_3} + \ldots + \sum_l K_{jk_2l}^* a_{il} \right) \qquad \text{Eq. 3.5b}$$

$$E_{ij} = E_j^0 + S_j \log\left(a_{ik_3} + K_{jk_3k_1}^* a_{ik_1} + K_{jk_3k_2}^* a_{ik_2} + \ldots + \sum_l K_{jk_3l}^* a_{il} \right) \qquad \text{Eq. 3.5c}$$

$$\cdots$$

$$E_{ij} = E_j^0 + S_j \log\left(a_{ik_n} + K_{jk_nk_1}^* a_{ik_1} + K_{jk_nk_2}^* a_{ik_2} + \ldots + \sum_l K_{jk_nl}^* a_{il} \right) \qquad \text{Eq. 3.5d}$$

(See Glossary of Symbols for identification of variables)

In the ideal situation, the contribution of all interferents k ($k \neq$ primary ion) and l is negligible (Section 2.3, case 1), there is no cross-response, and the SAD behaviour does not need to be modeled[4]. The ion activity can be directly read from the electrode response to the sample as in Eq. 2.13.

- **Approach 2:** The alternative situation, on which this research is focused, is that in which the SAD approach is chosen as it is impossible to accurately determine the activity of a particular target analyte without correcting for the contribution of interferents present in the sample, either because they are present in high and variable levels or because the only ISEs available have insufficient selectivity, or both. Here, the analytical response of a primary electrode, i.e. the one selective for the target analyte, is assisted by a number of secondary electrodes selective for the main interferents.

The contribution $K^*_{jkl}a_{il}$ for each of the main interfering ions can be calculated and subtracted from the response of the primary electrode. As each of the ISEs follows a particular Nikolskii-Eisenman equation the SAD response is explained by the following series of equations

$$E_{ij} = E^0_j S_j \log\left(a_{ik} + K^*_{jkl_1}a_{il_1} + K^*_{jkl_2}a_{il_2} + \ldots + \sum_l K^*_{jkl}a_{il}\right) \qquad \text{Eq. 3.6a}$$

$$E_{ij} = E^0_j + S_j \log\left(a_{ih} + K^*_{jh_1k}a_{ik} + K^*_{jh_1l_2}a_{il_2} + \ldots + \sum_l K^*_{jh_1l}a_{il}\right) \qquad \text{Eq. 3.6b}$$

$$E_{ij} = E^0_j + S_j \log\left(a_{il_2} + K^*_{jl_2k}a_{ik} + K^*_{jl_2l_1}a_{il_1} + \ldots + \sum_l K^*_{jl_2l}a_{il}\right) \qquad \text{Eq. 3.6c}$$

$$\ldots$$

$$E_{ij} = E^0_j + S_j \log\left(a_{il_n} + K^*_{jl_nk}a_{ik} + K^*_{jl_nl_1}a_{il_1} + \ldots + \sum_l K^*_{jl_nl}a_{il}\right) \qquad \text{Eq. 3.6d}$$

(See Glossary of Symbols for identification of variables)

The summation term in the equations represents the error produced in each of the ISEs by the interferents present which are not modeled ($l \neq k,\ l_1,\ l_2,\ \ldots\ l_n$). This error exists because of the practical impossibility of modeling all the interferents present in the sample matrix. The analyst must decide which of these interferents will be modeled to minimise the contribution of this error term for each sensor. Even though the weight on the final determination of the target analyte of these unmodeled contributions is maximum in the equation directly affecting the target analyte, the minimisation of these errors in the secondary electrodes, although not always possible, will help to improve the prediction characteristics of the SAD. The minimisation of the summation terms corresponding to the unmodeled interferents can only be done when the decision is taken as to which ISEs will form the array

during the design step because, during prediction, there is no information available about the activities of these unmodeled ions and no corrections can be made for their contribution. In the modeling step, these terms are stripped off the Nikolskii-Eisenman equations and only the contributions of the primary ions and modeled interferents are considered. The contribution of these unmodeled terms will be regarded by the SAD model as response of the ISE's primary ion.

3.4.1 ISE Array Design

The SAD approach can be taken, as previously discussed[5], either for specific determinations of a number of ions (approach 1) or to accurately determine a target analyte in high interfering media (approach 2). In the first case, ISEs with good selectivity are suggested unless reciprocal cross-response exists among the ISEs chosen for the analysis in question, i.e. two or more of the selected ISEs respond significantly to the other electrodes' primary ions. If this is the case, then the SAD response can be modeled using the second approach. Either case, one ISE for each ion (or variable studied) is included in the array. The SAD modeling and prediction characteristics will depend on the selectivity performance of the electrodes.

In the second approach, the response of the primary ISE selective for the target analyte is assisted with secondary ISEs which are appropriately selective for the most important interferents. The array must include these electrodes to provide information on the

activity of the interfering ions and to allow the correction for the interferent contribution $K^*_{jkl}a_{il}$ in the primary electrode.

The first step is to identify which ions in the sample matrix interfere most significantly with the determination of the target analyte. The ideal case will be to include one ISE in the array selective for each of the interferents but this is impractical since the complexity of the SAD model grows exponentially with the addition of an extra ISE. This limits the of ISE array to a number around four electrodes, meaning that for complex matrices only up to three interferents can be modeled and corrected. These electrodes should ideally display significant cross-response among them and especially with the primary ISE, as modeling small selectivity constants will be difficult to achieve, to properly model the interferent contribution both in the primary and secondary ISEs. The degree of cross-response should be high enough to be appreciable in terms of the total signal. If this requirement is not met, the modeling of the SAD response will be inaccurate, and high errors can be expected in the predictions. The best case will be that in which each of the electrodes have moderately high degree of cross-response with the other array electrodes and very little or no response to the unmodeled interferents in the sample matrix.

There are no general rules for the design of a SAD for a particular application, and the final configuration will depend upon the analytical needs, the sample matrix and the availability of adequate ISEs with the required selectivity. Usually, the values of the selectivity coefficients (K_{jkl}) for the ISEs obtained from traditional electrode characterisation can be used as guidelines to determine the right SAD configuration but,

in the end, it is to the analyst discretion to decide which interfering species will be modeled for corrections and which of the available ISEs are used for each of these ions.

3.4.2 Array Calibration

The SSM and MSM are used for characterising single ISE systems. The electrode calibration is done with a series of solutions containing the primary ion at different levels of activity. The effects studied in this calibration process are the interactions between the electrode and the primary ion. In a SAD, single ion calibration is not applicable because a higher number of interactions exist. Each ion present in the sample affects not only the response of all four electrodes in the array, but also how of other ions affect that response. The calibration procedure must explore these interactions and explain the effect of the considered species (primary ion and interferents modeled) both with the sensors and the other species. The calibration solutions or "training" set must be designed so that the necessary information is acquired during the calibration process to explain all these interactions and to produce a SAD response model that can account for those effects during prediction[6].

3.4.2.1 Factorial Design

A factorial study to design the characteristics of the training set used for SAD calibration involves studying the different variables or factors considered (ion activities) at different activity levels. For each of the sensors in the SAD, all the possible interactions are explored. In general, in a *f*-factor system where the interactions are studied at *l* different

levels, the number of calibration experiments needed is l^f. The design of the set of experiments is summarised in Table 3.1 for a linear 4-factor 2-level system where each parameter in the system is considered as a constant. The "+" and "-" symbols represent the high and low level for that particular factor. It can be appreciated how this design covers every possible permutation of high/low levels for all factors.

Table 3.1: Factorial design for a 4-factor, 2-level system.
Each of the levels of the factors in the system is studied at every possible permutation of the levels of the other factors in the system.

Experiment Number	Factor 1 level	Factor 2 level	Factor 3 level	Factor 4 level
1	+	+	+	+
2	+	+	+	-
3	+	+	-	+
4	+	+	-	-
5	+	-	+	+
6	+	-	+	-
7	+	-	-	+
8	+	-	-	-
9	-	+	+	+
10	-	+	+	-
11	-	+	-	+
12	-	+	-	-
13	-	-	+	+
14	-	-	+	-
15	-	-	-	+
16	-	-	-	-

In order to properly explore these perturbations the levels of the factors must be chosen so that a low level of a particular factor can produce an appreciable contribution to the ISE response in the presence of high levels of the remaining factors. Usually, for the primary ion of the electrode the high and low levels are chosen from the activity range limits of the application. For the interferents it is common that extremely high activities of interferents may be needed in order to produce a suitable perturbation.

Fractional Factorial Design

The major disadvantage of these calibration designs is that a very high number of experiments is needed to fully explain all the occurring interactions. Even for the simplest 2-level designs, there is an exponential increase with the number of factors. The inclusion for study of an extra factor will mean the increase in the number of experiments from 2^f to 2^{f+1} for a 2-level design.

Table 3.2: Fractional factorial design for a 2^{4-1} system.
Each of the levels of a factor is only confronted with a combination of levels of the other factors, reducing the number of experiments needed. With this method, the accuracy in the prediction may suffer.

Experiment Number	Factor 1 level	Factor 2 level	Factor 3 level	Factor 4 level
1	+	+	+	+
2	+	+	-	-
3	+	-	+	-
4	+	-	-	+
5	-	+	+	-
6	-	+	-	+
7	-	-	+	+
8	-	-	-	-

An alternative is to only study the lowest order interactions, i.e. those involving only part of the factors, and still be able to explain the analytical system with great accuracy. This can be achieved using Fractional Factorial Design techniques, in which the higher order interactions, i.e. the least significant, are disregarded altogether from the system. The experimental design for calibration becomes much simpler since a l-level f-factor system where the n highest interactions are disregarded can be explained with a l^{f-n} number of experiments. Table 3.2 shows the high/low characteristics of a set of calibration experiments for a 2-level, 4-factor system where the highest order interactions ($n=1$) have been disregarded.

This shows that the number of experiments needed for calibration is reduced from 16 (2^4) to 8 (2^{4-1}) simplifying the calibration procedure to a great extent. The fourth order interaction, i.e. those involving the four factors, are usually very weak and can be neglected with no or very little effect on the calibration.

3.4.3 Array Response Modeling

The modeling procedure is the process for which the response characteristics of a SAD are compiled into a prediction model. This model will be used to determine ion activities in unknown samples from the response generated in the array of ISEs.

Different optimisation techniques can be utilised for obtaining the model and they may differ significantly in the way they approach the chemical information. Normally, the system is known to obey a mathematical relationship between the response and the model parameters. Some of the techniques will approach the modeling of the array so that its response is modeled to a theoretical equation, optimising theoretical parameters so that the real response can be mathematically explained. Other methods, instead, are non-parametric in the sense that they do not try to fit the array response to a theoretical model but to an empirical relationship that best suits the system.

3.4.3.1 Parametric Methods

In the case of ISEs, the relationship between the electrode potential and the ion activity in the solution follows the Nikolskii-Eisenman equation. The values of the constants in this equation are the electrode parameters and they are characteristic for each ISE.

Parametric methods can be used to optimise the values of these parameters so that the difference between the experimentally obtained response and the predicted response (i.e. calculated from the characteristic Nikolskii-Eisenman equation of the ISEs) is minimum. For each of the electrodes, the standard electrode potential (E_j^0), the electrode slope (S_j) and the selectivity constants (K_{jkl}^*) are the SAD response parameters which must be optimised so that the Nikolskii-Eisenman equation characteristic of each electrode describes the calibration data from the training set with minimum error. The Nikolskii-Eisenman parameters are independent variables and each of them adds a new dimension to the space where the electrode response is defined. High dimensionality is normally the case and searching tools are used to suggest values for these parameters, which are evaluated in terms of how valid the prediction characteristics of the model are. This validity of the model suggested from a set of parameters is evaluated in terms of the magnitude of an error function, $f(\mathcal{E})$. The error function represents the error between the experimental response and the response that would be obtained from an ideal ISE with the particular characteristics of those parameters over the whole activity range covered by the s solutions of the calibration set, and can be expressed as;

$$f(\mathcal{E}) = \sum_{i=1}^{s} \mathcal{E}_i^2 = \sum_{i=1}^{s} \left(\frac{^{Exp}E_{ij} - {}^{Calc}E_{ij}}{^{Exp}E_{ij}} \right)^2$$

Eq. 3.7

where $^{Exp}E_{ij}$ is the experimental potential induced in the electrode by sample i and $^{Calc}E_{ij}$ is the theoretical value obtained from the Nikolskii-Eisenman equation

$$^{Calc}E_{ij} = {}^{Mod}E_{ij}^0 + {}^{Mod}S_j \log\left(a_{ik} + {}^{Mod}K_{jkl_1}^* a_{il_1} + {}^{Mod}K_{jkl_2}^* a_{il_2} + \ldots + {}^{Mod}K_{jkl_n}^* a_{il_n}\right) \qquad \textbf{Eq. 3.8}$$

being ${}^{Mod}E_j^0$, ${}^{Mod}S_j$ and ${}^{Mod}K_{jkl}^*$ the electrode parameters suggested by the optimisation method during the modeling procedure. The set of parameters that minimise the value of the error function will be accepted as the model parameters for that ISE and will be used for the prediction of activities.

Because the electrode parameters have fundamental significance within the Nikolskii-Eisenman theory, the optimum values give the behavioural characteristics of these ISEs in the conditions resembled by the set of calibration solutions, explaining the sensitivity and selectivity against the modeled interferent ions.

(i) Down Hill SIMPLEX

The SIMPLEX method is an optimisation tool it could be said to be based on the theory of gravity. The same way a ball rolls down a slope until it finds a valley, a SIMPLEX algorithm will search an move along a *n*-dimensional surface until it reaches a minimum[7,8]. As the searching process is limited to an area next to that were the SIMPLEX exist there is no assurance that the minimum found is the global minimum. To increase the chance of encountering the absolute minimum the algorithm should be started at different random surface locations several times, depending on the roughness of the surface and the results obtained.

The SIMPLEX is a geometrical figure with the same number of dimensions (*n* dimensions, *n*+1 vertices) as the surface it searches. The vertices take the same values as

the problem function (surface) for a given set of coordinates resulting in the algorithm being placed on the surface, "walking" down the slope towards the minimum. This is achieved by disregarding the vertix with the highest function value and taking another set of coordinates, hence maintaining the dimensionality, and calculating the new function value. To optimise the surface search the SIMPLEX can change its shape and n-dimensional volume as it moves along. These changes can be divided into four categories, with the following working strategy:

1. Reflection: The SIMPLEX reflects the vertix with the worst function value through the centre of the polygonal face defined by the best n-vertices set.

2. Elongation: If the reflection gives a better vertix then the algorithm expands in the same direction as the reflection and tries to get a better point further away.

3. One-dimension contraction: If the reflection process does not yield a better vertix, the simplex contracts the dimension of the worst vertix in an attempt to bring it closer to the best vertices.

4. Multi-dimension contraction: If none of the above operations give a better vertix, the SIMPLEX contracts in all dimensions around the vertix with the smallest function value, searching for new vertices around the coordinates for best point.

Simplex procedures can be used to search for either the minimum or maximum of a function by modifying the operational logic of the algorithm.

Figure 3.1: Down Hill SIMPLEX search of surface $z = -1/\left[Log\left(e^{y^2}\right) + Log\left(e^{x^4-x^3-x^2+x+2}\right)\right]$

a) Topographic representation of the evolution of the SIMPLEX algorithm searching a surface. b) 3D representation of the surface. The algorithm is initialised in a random location and it is able to find its way downwards to the minimum. Although this is not always the case, the SIMPLEX is able to reject a local minimum and find its way towards the lowest point in the surface
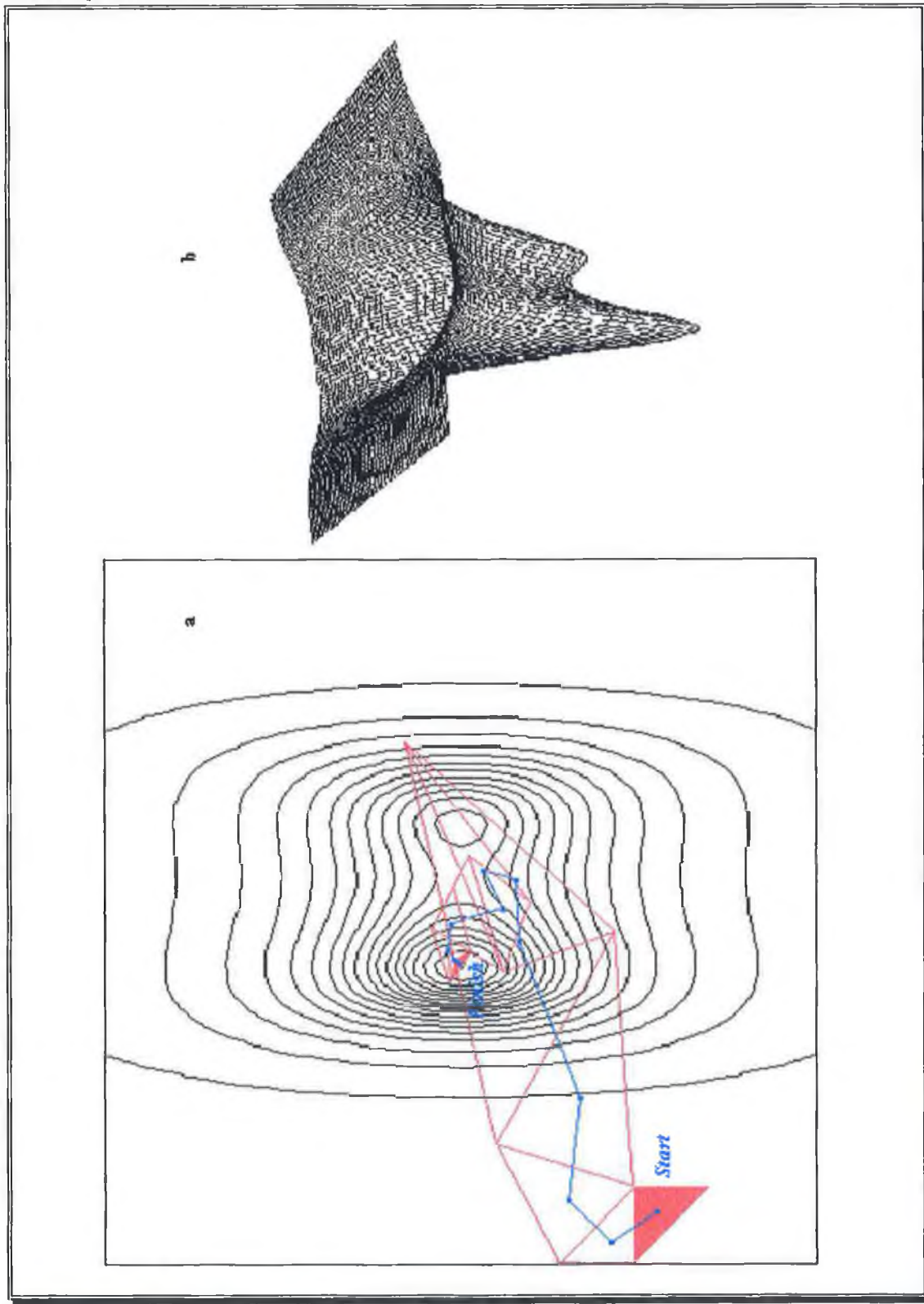
The SIMPLEX subroutine used in this research[9,10], shown in Appendix A, was a translation and adaptation to QuickBASIC of Press, Flannery, Teutolsky and Vetterling's "amoeba" subroutine[11] written in Pascal.

In a calibrated SAD composed by four ISEs, the parameters which explain the response of each detector will be the activities of the ISEs' primary ions, k. A problem function can be defined as the sum of the square relative difference between the real response to the ISEs obtained from experimental results and the response simulated with a suggested set of parameters for the system (Eq. 3.7). This function is a surface which exists in a $n+1$ dimensional space which can be searched with a SIMPLEX algorithm to find, at least, a local minimum. The coordinates for the minimum indicate the optimum set of system parameters.

(ii) Genetic Algorithms

Genetic algorithms is another parametric technique which is based on the principles that rule the evolution of living organisms[12].

Viable values of the system parameters are encoded in a series of genes or chromosomes. A finite population of these chromosomes is then allowed to breed, mutate and cross among themselves, creating the next generation. Inevitably, genes which encode bad solution to the problem are eliminated from the population as in a "survival of the fittest" regime. In the following generations, the predominant gene is that which encodes the better solution.

A global search of the problem function is possible by cross-over and random mutation of the chromosomes, which changes the "genetic makeup" of the genes. This represents an advantage over SIMPLEX optimisation in that the result obtained with this technique is the absolute minimum of the searched *n*-dimensional surface. On the other hand, this procedure is much more computationally intensive than the down hill SIMPLEX.

Research was carried out on the performance of these two parametric methods which showed that both SIMPLEX and Genetic Algorithms[13] rendered the same optimum parameters in optimisation processes involving experimental data from ISE arrays, hence giving the same prediction characteristics for the SAD system.

3.4.3.2 Non-Parametric Methods

Situations may be encountered where there may not be enough information about the system to generate a mathematical relationship to explain its behaviour. The system may also be so complicated that this relationship is just too difficult to find, or that it does not exist. In these cases, non-parametric techniques, which do not need a mathematical expression linking results and variables, are used.

Two of these methods are described in this section, Projection Pursuit and Neural Networks, which are able to obtain the values of the parameters that best suit the system by optimising the relationship between the variables and the response of the SAD obtained for a special training set (Section 3.4.2) designed for this purpose.

(i) Projection Pursuit

This regression technique permits the search of the multidimensional space of a system by reducing its dimensionality and projecting the multivariate data into two (*2D*-graphs) or three (*3D*-graphs) dimensions so that the new projected data are easier to analyze[14]. This technique has been applied for the exploration of chemical data in multivariate systems[15] and in particular to Ion-Selective Electrode SAD systems[5,16].

The projection pursuit method consists of the reduction of a number of the system dimensions into a single one. This one dimension is a linear combination of the others and contains the same information than the original four. If all the dimensions are projected into a single one, the system reduces its dimensionality to a *2-D* representation. The variables can also be grouped and projected into to independent dimensions, originating a *3-D* representation. Only *2-D* representations will be discussed. A weight factor for each of the dimensions is introduced, and the linear combination of the reduced dimension can be expressed as;

$$x = \lambda_r \vec{r}$$

<div align="right">**Eq. 3.9**</div>

Where r is the identifier of the variables to project, λ_r is the weighting parameter for each variable, and $\vec{r}$ is a vector containing the electrode response. In a four electrode SAD system, the variables projected will be the response of the four electrodes. For a system like this Eq. 3.9 expands to;

$$x = \lambda_{r1} r_{k_1} + \lambda_{r2} r_{k_2} + \lambda_{r3} r_{k_3} + \lambda_{r4} r_{k_4} \qquad \text{Eq. 3.10}$$

where k_1, k_2, k_3 and k_4 are the primary ions for the ISEs in the array.

The following procedure can used to find a particular set of λ_r parameters for each of the system variables. Arbitrary starting values must be given to all parameters at the start of the regression process. The activities of every primary ion in the training set are plotted versus abscissa as the weighted sum of the response vector $\lambda_r \vec{r}$ as in Eq. 3.10. The resulting graph is smoothed with a final-point Satvisky-Golay filter[17] and the error function of that projection was determined as;

$$f(\mathcal{E}) = \sum_{i=1}^{s} \mathcal{E}_i^2 = \sum_{i=1}^{s} \left(\frac{G_i[\lambda_r \vec{r}] - a_i}{a_i} \right)^2$$

$$\text{Eq. 3.11}$$

where a_i is the activity of the ion being modeled in the calibration solution i and $G_i[\lambda_r \vec{r}]$ is the value of the smooth at the same abscissa. The value of the error function, $f(\mathcal{E})$, and the λ_r parameters are then introduced into a down hill SIMPLEX subroutine (see Section 3.4.3.1) to obtain a new and more optimised set of parameters which are evaluated with the same procedure applied to the starting values. The process is repeated until the optimised system parameters (minimum of the error surface) are reached.

(ii) Neural Networks

Another approach which can be used for the optimisation of FIA-SAD systems is the application of Neural Networks[18,19]. These are a form of artificial intelligence which is based in the same working strategy as human nervous systems.

For this type of application a feed forward network, using a back propagation training algorithm can be used to generate a relationship between the potentials registered in each of the electrodes and the activity of one of the ions in the solution analysed. This relationship is generated during training inside the Neural Network, in the weights of the links which connect different neurons.

Training the net consists of changing the values of the neural weights to minimise a particular function. In this case this function is the error of the system when predicting the ion activities in comparison to the real activities of the ions in the solutions of the training set. Overtraining is a constant problem when using Neural Networks. This arises from fitting the noise in the signals, and it reduces the ability of the network to generalise and produce an answer for an input which was not included in the training set. These effects can be reduced by decreasing the complexity of the network using weighted weight factors which reduce the overtraining effects when testing new sets of input data.

3.4.4 Prediction

When an unknown sample is presented to the SAD, a response is obtained from each sensor in the array. These responses usually carry mixed information which has to be processed and isolated to predict the activities of the species in the sample. As discussed previously, the parametric methods use the well known Nikolskii-Eisenman relationship between the ISE response and the activities of the ions to explain the chemical system, and a series of optimised electrode parameters are obtained from the modeling

procedure. During the prediction step, these parameters are included in the model as constants and the ion activities will now be the variables to determine. The system of Nikolskii-Eisenman equations that describe the SAD behaviours can be re-written to show the dependence of the activities on the ISE parameters as follows;

$$a_{i1} = 10^{\frac{E_{ij} - E_j^0}{S_j}} - \left(K_{j12}^* a_{i2} + K_{j13}^* a_{i3} + \ldots + K_{j1n}^* a_{in} \right) \qquad \text{Eq. 3.12a}$$

$$a_{i2} = 10^{\frac{E_{ij} - E_j^0}{S_j}} - \left(K_{j21}^* a_{i1} + K_{j23}^* a_{i3} + \ldots + K_{j1n}^* a_{in} \right) \qquad \text{Eq. 3.12b}$$

$$a_{i3} = 10^{\frac{E_{ij} - E_j^0}{S_j}} - \left(K_{j31}^* a_{i1} + K_{j32}^* a_{i2} + \ldots + K_{j1n}^* a_{in} \right) \qquad \text{Eq. 3.12c}$$

$$\ldots$$

$$a_{in} = 10^{\frac{E_{ij} - E_j^0}{S_j}} - \left(K_{jn1}^* a_{i1} + K_{jn2}^* a_{i2} + \ldots + K_{jn(n-1)}^* a_{i(n-1)} \right) \qquad \text{Eq. 3.12d}$$

(See Glossary of Symbols for identification of variables)

where the ions 1, 2, 3,...,n are equivalent to k_1, k_2, k_3,...,k_n and k, l_1, l_2,...l_n for Eq. 3.5 (Approach 1) and Eq. 3.6 series (Approach 2) respectively. As explained before, contribution of uncorrected ions are not included in the model. It can clearly be appreciated at first glance the dependence of the activity of one ion on the activity levels of the other ions included in the model in a n-equation, n-variable system. Resolving the system of equations will give the activity values of the ions in the sample.

Parametric methods ultimately seek a set of optimised theoretical parameters that best explain the SAD response. For all of these techniques the prediction process involves the method above, as they only differ in the way the parameters are optimised. For non-parametric methods this does not happen, and each technique will have a different algorithm to predict new results for new data sets.

The Projection Pursuit regression technique explained in the previous section is mainly a graphical method for predicting unknowns. Once the technique has obtained the optimised set of weight factors λ_r for the response vector $\vec{r}$, the activities of a particular ion are plotted versus an abscissa which is the linear combination of the weights for each of the dimensions of the vector. The graph is smoothed and the resulting trace is the response model for that one species.

Projection Pursuit regression was used in the early stages of this research[10] to model the response of a SAD (same as in Chapter 4) for the analysis of ammonium in the ion activity range 10^{-5} to 10^{-2} mol dm^{-3}. Figure 3.2 reproduces, for illustrative purposes, the typical final projection of the ion activity versus a multivariable vector x defined as Eq. 3.10. Prediction of the ion concentration is made by composing the value of the abscissa from the response vector and reading the activity directly from the graph. A clear trend can be seen in the graph (dashed line) which suggests an increasing linear relationship between the SAD response vector and the logarithm of the ion activity. At higher SAD responses, the smooth of the projection presents a more linear shape, in accordance with the linear 2-level calibration applied to the system.

Below a value of x of around 50, a scatter which distorts the linear relationship appears. This could be explained for the small cross-response between ISEs at low ion activities (which produces low ISE response and therefore low x values). Also, the experimental error at those low activity levels is higher because of the reduced electrode sensitivity as it approaches the usual limit of detection of these devices, and the inherent decrease in

the signal-to-noise ratio. It can also be seen from the model smooth that, even if one primary ion activity can be explained by a number of SAD response combinations, a particular response from the SAD to a unknown sample can only be related to one and only one value of the logarithm of the primary ion activity.

Figure 3.2: Typical Projection Pursuit regression graph[10].
The individual data represent the projection of the ion concentrations over the response vector *x* (See Eq. 3.10). The solid line shows the smooth for this projection, which will be used for prediction polling. A general linear trend (dashed line) can be guessed for the SAD response behaviour.
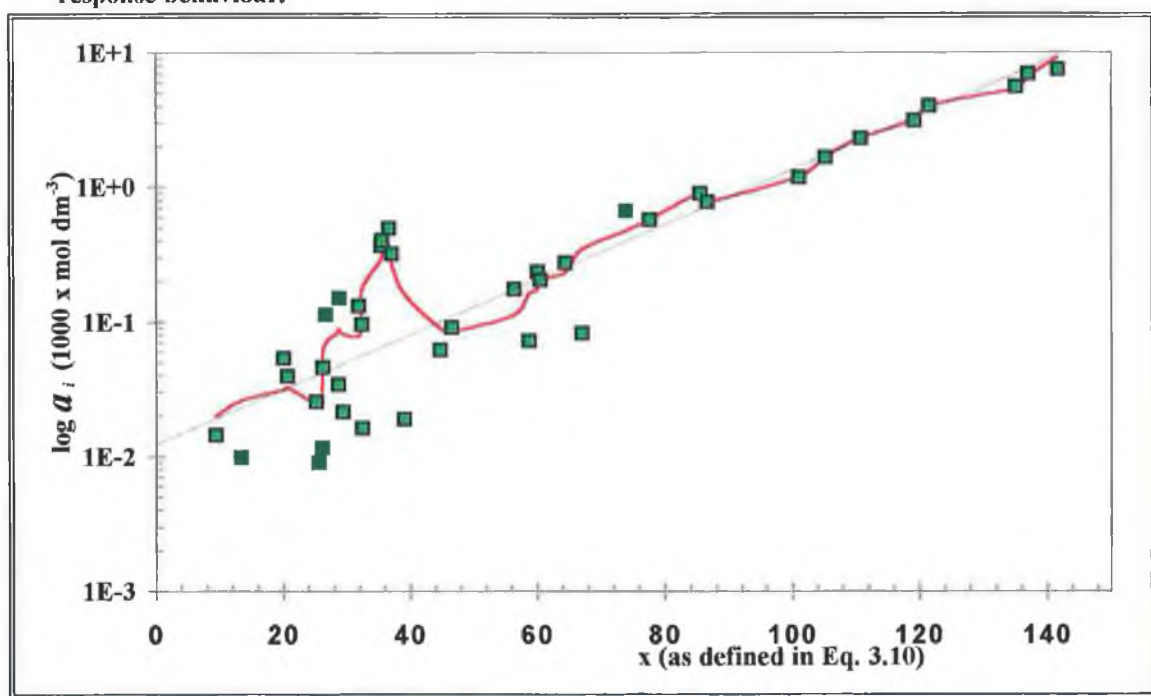
3.5 FIA-SAD Systems

In the previous section, theory and procedures behind the SAD techniques have been described for the particular case of using ISEs as sensing devices. A number of experimental methodologies, batch processes[5,20], Batch-Injection Analysis (BIA)[4,21] and Flow-Injection Analysis (FIA)[5,22], can be used as described by Diamond and co-workers.

Although these techniques are very different in their fundamental background they can all be used in conjunction with detector arrays to generate suitable experimental data for the SAD approach. Table 3.3 shows a compilation of the main characteristics of the techniques mentioned above.

In this research FIA was used at all times, unless otherwise stated, as the methodology to obtain the analytical data from the chemical system, and this section focuses on the description of the technique applied to SAD systems, mainly as opposed to batch measurements.

Table 3.3: FIA, BIA and batch process main characteristics.
The techniques best suited for SAD analysis clearly are Flow-Injection, for fundamental and kinetic studies, and Batch-Injection, mainly for kinetic measurements. FIA is the only one that can be automated completely using reasonable resources.

Characteristics	Flow-Injection Analysis	Batch-Injection Analysis	Batch Processes
Reproducibility	✓✓✓	✓✓	✓
Steady-State Measurements	✓✓	✓	✓✓✓
Kinetic Measurements	✓✓	✓✓✓	✓
Analysis Time	✓✓	✓✓✓	✓
Sample Throughput	✓✓✓	✓✓	✓
Reagent Consumption	✓	✓✓	✓✓✓
Automation	✓✓✓	✓✓	✓

3.5.1 FIA-SAD System Set-Up

Section 2.7.1 describes the set up of a FIA system where the detector used is a single ISE measured against a Ag/AgCl reference electrode. A system very similar is used for

the SAD approach in FIA mode. Basically the system remains unchanged except for the detector block. This detector is designed so it can support up to four independent PVC membrane ISEs.

A SAD detector is used with this FIA setup so the measuring device used must provide the same number of channels as the active sensors in the system. Because potentiometric measurements must be made at zero current, a set of operational amplifiers were used in this system to increase the input impedance to 1 TΩ (1 TΩ = 10^6 MΩ) so that a near-zero current status was reached (See Section 1.4.1.3). Flow pump, injector port and reference electrode serve the same purpose than single ISE detector FIA systems previously described.

Figure 3.3: FIA-SAD system diagram.
The system is in essence identical to that described in Figure 2.7 with the difference that a multichannel e.m.f. recorder is provided for simultaneous signal monitoring. For illustrative purposes the SAD is displayed as a straight line disposition.
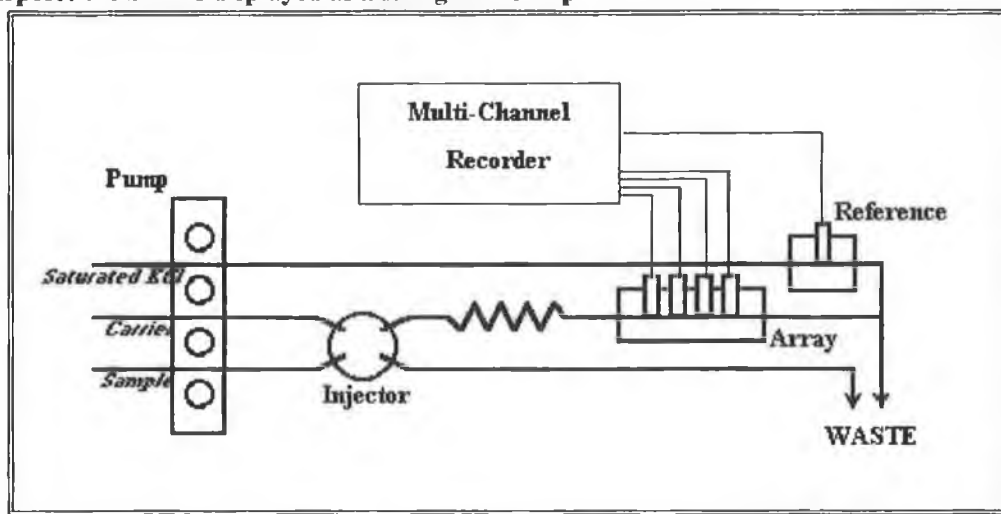
3.5.1.1 SAD Flow-Through Cells

Dealing with the concept of sensor array geometry inevitably brings the idea of a number of sensors placed in a linear disposition. The same way that in FIA the different system devices are placed sequentially along the stream conduits the idea of a number of single cell ISE flow electrodes seems the most feasible. Different types of flow cells (Figure 2.6) could be used, even for each individual cell, to form the SAD. Unfortunately problems arise when using this arrangement, as very long distances between electrodes will create an appreciable difference in the sample dispersion and the cell distance to the reference electrode will also vary considerably. Besides, some of the geometries available are only acceptable for use in single cell detectors because they destroy the sample concentration gradient in the detection site and any detector placed downstream will not see a FI sample profile.

As part of this research and to overcome the above mentioned problems, a solid flow detector block was designed which could house up to four independent ISEs in serial disposition. The use of this single flow-cell for housing all the electrodes allows for a more compact design, with much smaller inter-electrode flow paths than with serially connected in-line single electrode units. The increase in rigidity enables a more reproducible flow and dispersion characteristics inside the detector unit and therefore a much better precision in the overall system performance. The array design described here permits fabrication by machining solid material without the need for moulding dissolved polymer constituents.

The array consists of three blocks machined in Perspex (polymethylmethacrylate) arranged in a "sandwich" disposition (see Figure 3.4). The two outer pieces are identical, and each contain the sites for two of the selective PVC membranes, the internal reference solution reservoirs, the internal reference electrodes and the electrical connections. The internal reference solution meets the membrane surface at the end of a 1 mm I.D. perforation that connects the reservoir with the membrane location. The carrier stream is directed against each membrane in turn *via* a zigzag channel machined in the central portion of the sandwich such that a 0.8 mm I.D. angled perforation reflects from one

Figure 3.4: Diagram of the array block showing the 2 vs. 2 electrode "sandwich" configuration. The three Perspex pieces are assembled into place with stainless steel bolts which secures the PVC membranes in their correct location. The membranes serve as gaskets sealing the internal reservoirs from the carrier solution which is restricted to the central piece. LEGEND: I & II [identical]): External pieces designed for holding two ISEs each. III) Internal block for controlling direction of flowing stream. a) Internal filling solution reservoir. b) Liquid membrane-reservoir connection. c) PVC membrane location. d) Bolt guides. e) Bolt holes. f) Carrier stream conduit. g) Teflon tubing inlet/outlet. h) Electrical connections. Dimensions: 60x35x25 mm (LxWxH).
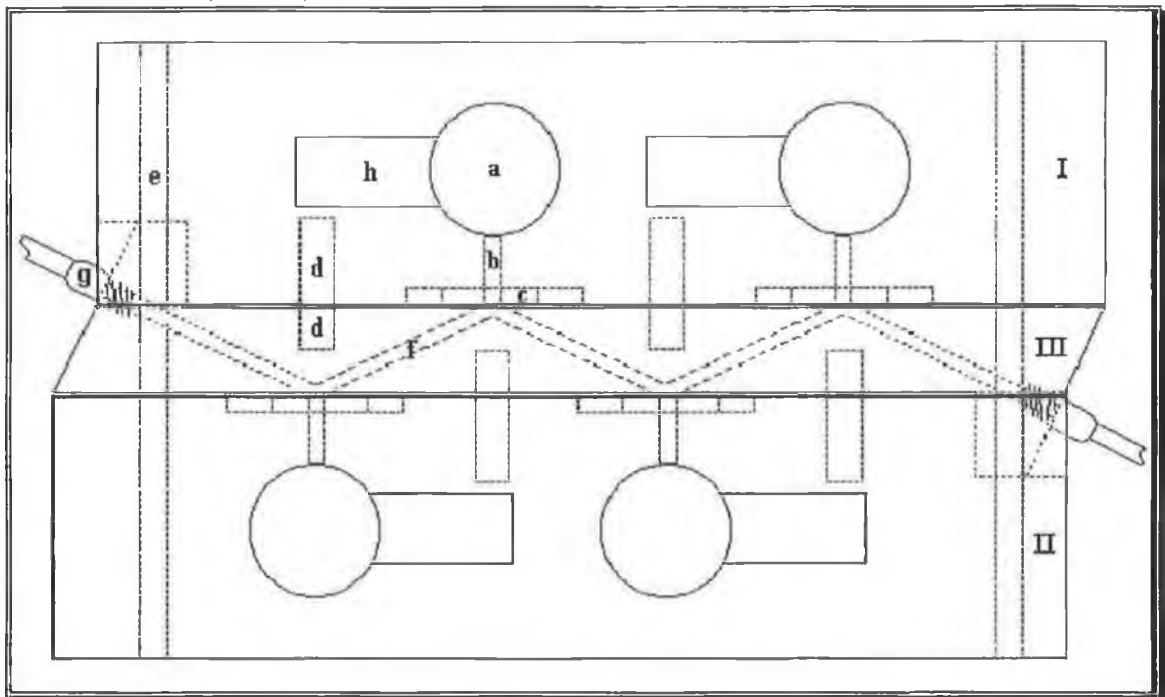
membrane surface to the next. Hence, each membrane acts as a perm-selective barrier between the flowing stream and the internal solution across which the membrane potential is developed.

This design overcomes the technical difficulties of machining long narrow channels inside a Perspex block to redirect the flowing stream from one electrode to the next, and makes the array block even more compact than for an equivalent linear design. The very small flow path between the electrodes assures that the variation in the sample plug dispersion as it passes through the flow-cell is minimised, and the high reproducibility of the flow dynamics of the system assures that the same sample profile is presented at each membrane location for each injection.

3.5.2 Self Diagnosing Systems

Full computer control and automation of the FIA-SAD system opens the possibility of building "intelligent" subroutines within the control procedures which can allow for detection of system malfunction or detector degradation.

This approach may require a number of identical sensors with the same response characteristics. Comparison of the response pattern and prediction polling characteristics, both between the equivalent ISEs and among all the SAD sensors, can identify any malfunctioning sensor and its response can be automatically discarded and a warning flagged.

Other problems arising in the operation of the FIA system can be diagnosed, e.g.:

- A drop in the flow rate because of a breakage in the tubing can be detected by an abnormal increase in the duration of the FIA traces which appears in all the sensors.

- Total lack of signal in the SAD will indicate that the system is failing to inject the sample into the carrier stream (unless the unlikely case that the sample has exactly the same composition as the carrier).

- Drifting signals at the predicted peak location indicate that the electrochemical cell is electronically open, probably because of the introduction of air during injection.

- If the above happens continuously in one detector channel it suggests that an air bubble is trapped at that sensor location.

If the SAD contains redundant ISEs, diagnosis on the working characteristics of the electrode membranes can be obtained by comparing the responses, e. g.:

- A decrease in the signal of one will indicate, among others, that the sensor is past its useful working life and has to be replaced or the that the complete sample volume does not reach the sensor site, perhaps caused by leakage (see Figure 6.9).

- Also, selective detector poisoning is suggested when only one type of the redundant sensors continuously fails to give a signal.

All of these possible events, and more, can be compiled within the system operation processes and may alert the analyst if any are detected. However, it is the analytical

chemist who, with his/her experience, will be able to diagnose a SAD system much more accurately that any "intelligent" routine.

3.6 References

[1] Moody, G.J. and Thomas, J.D.R. *"Selective Ion-Sensitive Electrodes"* Merrow, Watford, 1971.

[2] Covington, A.K. (ed.) *"Ion-Selective Electrode Methodology"* CRC Press, Boca Raton, Florida, 1979, p. 18.

[3] Beebe, K.: Uerz, D.; Sandifer, J.; Kowalski, B. *Anal. Chem.* **1988**, *60*, 66-71.

[4] Diamond, D.; Lu, J.; Chen, Q.; Wang, J. *Anal. Chim. Acta* **1993**, *281*, 629.

[5] Diamond, D.; Forster, R. J. *Anal. Chim. Acta* **1993**, *276*, 75-86.

[6] Morgan, E.: Burton, K. W.; Church, P. A. *Chemometrics and Intelligent Laboratory Systems* **1989**, *5*, 283-302.

[7] Forster, R. J.; Diamond D. *Anal. Proc.* **1991**, *28*, 117-122.

[8] Haswell, S. J. (ed) *"Practical Guide to Chemometrics"* Marcel Dekker Inc., New York, **1992**.

[9] Sáez de Viteri, F. J.; Diamond, D. *Analyst* **1994**, *119*, 749-758.

[10] Sáez de Viteri, F. J.; Diamond, D. *Electroanalysis* **1994**, *6*, 9-16.

[11] Press, H. W.; Flannery, B. P.; Teutolsky, S. A.; Vetterling, W. T. *"Numerical Recipes in Pascal: The art of Scientific Computing"* Cambridge University Press, New York, 1986.

[12] Hibbert, D. B. *Chemometrics and Intelligent Laboratory Systems* , **1993**, *19*, 277-293.

[13] Hartnett, M. V. *"The Application of Artificial Neural Networks and Genetic Algorithms to the Estimation of Electrode Response Characteristics and Stability Constants"* Doctoral Thesis, Ph.D., 1994.

[14] Friednman, J. H.; Stuetzle, W. *J. Amer. Stat. Assoc.* **1981**, *76*, 817-823.

[15] Glover, D. M.; Hopke, P. K. *Chemometrics and Intelligent Laboratory Systems* **1992**, *16*, 45-59.

[16] Beebe, K. R.; Kowalski, B. R. *Anal. Chem.* **1988**, *60*, 2273-2278.

[17] Gorry, P. A. *Anal. Chem.* **1990**, *62*, 570-573.

[18] Hartnett, M; Diamond, D.; Barker, P. G. *Analyst* **1993**, *118*, 347-354.

[19] Janson, P. A. *Anal. Chem.* **1991**, *63*, 357A-362A.

[20] Forster, R. J.; Reagan, F.; Diamond, D. *Anal. Chem.* **1991**, *63*, 876-882.

[21] Lu, J.; Chen, Q.; Diamond, D.; Wang, J. *Analyst* **1993**, *118*, 1131-1135.

[22] Forster, R. J.; Diamond, D. *Anal. Chem.* **1992**, *64*, 1721-1728.

4. FIA-SAD Applications

4.1 Introduction

The theory behind ion-selective electrode arrays for flow-injection analysis system explained in the previous chapters has been applied for real analytical applications. Detailed explanation on the experimental systems and methodologies used can be found in the following sections. The results demonstrates that this approach can be used for the analysis of ionic species in complex matrices. The theoretical and practical implications of this research are also discussed in detail.

4.2 Analysis of Ammonium

Ammonia, in the form of ammonium ions is a frequent contaminant of natural water bodies and originates mainly from the breakdown of proteins in organic matter. Under the European Community Environment Legislation[1] information on the levels of contaminants in surface waters of one member state must be available to the rest of the countries. In the case of ammonium, the levels of surface waters intended for the extraction of drinking water must not exceed 1.5 mg dm^{-3} (8.3×10^{-5} mol dm^{-3}) for water

in normal conditions, or 4 mg dm^{-3} (2.2×10^{-4} mol dm^{-3}) for water bodies in exceptional climatic or geological conditions (Council Directive 75/440/EEC of 16/06/1975)[1]. For drinking water, these regulations are much more strict, with a maximum admissible level of ammonium of 0.5 mg dm^{-3} (2.7×10^{-6} mol dm^{-3}) (Council Directive 80/778/EEC of 15/07/1980[1]. High concentrations of ammonium are usually expected in waste waters, but it can also be at dangerously levels in streams, rivers and lakes because of intensive localised farming activity. If sewage sludge is used in agriculture, ammonium must also be analysed as total nitrogen with a 6 month frequency (Council Directive 86/278/EEC of 12/06/1982)[2]. Hence, environmental regulations enforce the frequent analysis of ammonia in natural water bodies and waste water effluents for environmental monitoring purposes.

Among several instrumental methods available for the determination of the NH_4^+ / NH_3 pair, probably the ammonia gas probe (Section 2.4) is the most popular. This electrode takes advantage of the unique equilibrium between both species,

$$NH_{3(gas)} + H_{(aq)}^+ \rightleftharpoons NH_{4(aq)}^+$$

Eq. 4.1

to isolate ammonium ions and eliminate the effect of possible interferents present in the sample matrix. The procedure involves the spiking the sample with an aliquot of a strong base to modify the equilibrium shown in Eq. 4.1 towards the gaseous form which can now cross a gas-permeable membrane and redisolve in an acidic buffer solution in the probe as NH_4^+ ions. The amount of NH_3 that crosses the porous membrane is obtained

from the potential readout of an ISE which can be either selective for H^+ (glass electrode) or NH_4^+ ions (nonactin based ISEs). Interference from low molecular weight amines might be expected for this technique. The method is quite laborious, specially if a large number of samples need to be analysed on a continuous basis, and the conversion of this batch method into an equivalent automated continuous technique is far from easy.

Neutral carrier-based ISEs are, on the other hand, available for the selective determination of NH_4^+ without the need for transformation into NH_3, thus greatly simplifying the analysis procedure[3]. Unfortunately, these probes do present poor selectivity towards other ions[4,5] and high response can be expected for background species in the sample matrix. The "best-fit" mechanism behind the selectivity theory (see Section 2.5.1) explains why ions of similar dimensions will, in fact, "fool" the selective membrane and will produce a significant contribution to the electrode response. For the ammonium selective membranes, this finds its maximum effect with potassium ions due to the similar ionic radii they present (1.43 Å for NH_4^+ and 1.33 Å for K^+)[6]. In fact, the presence of potassium as a component in the background matrix renders these selective electrodes useless for many important applications (e.g. determination of NH_4^+ in estuarine water).

4.2.1 Array Design

The target of the analysis technique was the accurate determination of ammonium ions through correction of the sensor signal for important interferent contribution, as

described in Section 3.3. Potassium and sodium are species present in water samples which interfere with the response of the ammonium selective electrode, potassium being the main interferent, and sodium a secondary one.

To minimise the effect of these ions, an ISE selective for each of them was included in the SAD to provide the necessary cross-response needed for signal compensation. These three ISEs present a fairly good selectivity towards calcium ions, but as high calcium activities might be expected in water samples an extra Ca^{2+}-selective ISE was included in the array to enable the effect of calcium in hard waters on the other ISEs to be deconvoluted and corrected.

Therefore, the SAD used comprises ISEs selective for NH_4^+, Na^+, K^+ and Ca^{2+}. The ionophores used for the selective membranes were Ammonium Ionophore I (~25% nonactin), Calcium Ionophore II (ETH 129) both Selectophore® grade and Valinomycin (for potassium) obtained from Fluka (catalogue No. 09877, 21193 and 94675 respectively). The sodium ionophore *p*-tert-butyl calix[4]arene methoxyethylester[7,8] was synthesised by Dr. Steve Harris at DCU as described previously[9]. The composition of the all the membrane cocktails was 1.00% w/w ionophore, 0.35% w/w KTpClPB (Selectophore®, Fluka catalogue No. 60591), 66.00% w/w plasticiser and 32.65% w/w PVC. The plasticisers used for the membranes were; bis(2-ethylexyl) sebacate (DOS) (Selectophore®, Fluka catalogue No. 84818) for ammonium and potassium electrodes, and 2-nitrophenyl octhylether (2-NPOE) (Selectophore®, Fluka catalogue No. 73732) for sodium and calcium electrodes[4,5].

The membrane cocktail was prepared by dissolving the neutral carrier and anion excluder (KTpClPB) in the appropriate plasticiser. When the viscous solution was homogeneous and clear, 5 mL THF were added to the mixture which was stirred to obtain a more fluid solution. The cocktail was completed by adding, in small portions and while stirring continuously, the needed amount of PVC.

The membranes for the array were cast by pouring the THF cocktail solution into perfectly horizontal Petri dish plates. The vessel were covered with paper tissue and closed with a glass lid to decrease the solvent evaporation rate and thus achieve a more homogeneous membrane structure. After complete THF evaporation, square portions of 25 mm² and approximately 0.3 mm thickness were cut from the bottom of the dish to fit in the detector block.

4.2.2 Calibration

The calibration procedure required for modeling the SAD characteristics is not simple. For an array with *j* electrodes, there is an *j+1* dimensional space which contains the calibration response surface. A factorial experimental design is the most appropriate technique to quantify the effect of each variable in the model, and the interactions among them[10]. With this approach, a sequence of experiments comprising different levels (ion activities) of the factors (targeted ionic specie plus interferents modeled) is used to produce the corresponding potential responses from the SAD.

The detector consists of four different ISEs and all the cross-response effects among them are studied (for each electrode, the primary ions for the remaining ISEs will be considered as interferents). The number of factors (f) that affect the response of the electrodes are the activities of the primary ion and the three interfering ions modeled. The factors are studied at two different levels (l) which means that in a full factorial design the number of experiments needed to model the response of each ISE is 2^4 (l^f) for a 4-factor, 2-level design.

However, the number of experiments needed was significantly reduced without sacrificing the accuracy of the model by means of a fractional factorial design. With this approach, the number of experiments was reduced to 2^{4-1} by disregarding the highest order interactions among the factors, which generate less critical information about the SAD response[10]. Adoption of the fractional factorial design reduces the number of calibration solutions required to model this particular array from 64 to 32. (Note that in a practical sense, this method is limited to the use of 2 levels, as higher levels would result in very large calibration sets).

The concentration range selected for this study was 10^{-4} to 10^{-2} mol dm^{-3}, where the ISE responses are known to be Nernstian[5]. In accordance with the requirements of the fractional factorial calibration design described in Section 3.4.2.1, a total of 32 solutions were prepared to calibrate the four electrodes (Table 4.1).

For each ISE, eight solutions were used to calibrate the response, and the remaining 24 solutions were presented to the array as unknowns (test solutions) to study the

performance of the array in terms of prediction capabilities. Note that in some of these solutions, the level of interferents can be up to a hundred times higher than that of the primary ion to ensure a significant contribution to the overall signal.

The composition of the calibration sets for each electrode is summarised in Table 4.1, where the experiments with high ion level are represented by "+", and the low ion level are represented by "-". For each electrode, the primary ion activity appears in the calibration set at exactly two levels, while the interferent ions is varied slightly around two levels (+,-). This slight fuzziness in interfering ion activity gives a scatter in the final potentials, enabling the selectivity constants to be calculated more accurately.

The calibration set is divided into four sub-sets, each of eight solutions, which are used to calibrate a particular electrode. These sub-sets are selected randomly, and within each, the individual solutions are also injected randomly during the calibration process. The eight responses obtained from a particular electrode in its calibration sub-set are then selected as training sets and input the SIMPLEX optimisation procedure. The remaining 24 solutions (i.e. the training set for the other 3 ISEs) are presented to the Nikolskii-Eisenman model given by the SIMPLEX to asses the prediction performance of the SAD model.

Table 4.1: Concentration of the modeled ions in the calibration solutions.
All figures in mol dm^{-3}. Calibration sets for each electrode are ammonium (ISE 1: 1,1 - 1,8); sodium (ISE 2: 2,1 - 2,8); potassium (ISE 3: 3,1 - 3,8) and calcium (ISE 4: 4,1 - 4,8). Factorial design high/low levels are shown next to the ion concentration.

Soln.		[Ammonium]		[Sodium]		[Potassium]		[Calcium]
1,1	+	10^{-2}	+	9×10^{-3}	+	3×10^{-3}	+	8×10^{-3}
1,2	+	10^{-2}	+	3×10^{-3}	-	5×10^{-4}	-	9×10^{-4}
1,3	+	10^{-2}	-	10^{-3}	+	5×10^{-3}	-	7×10^{-4}
1,4	+	10^{-2}	-	5×10^{-4}	-	6×10^{-4}	+	3×10^{-3}
1,5	-	10^{-4}	+	7×10^{-3}	+	4×10^{-3}	-	4×10^{-4}
1,6	-	10^{-4}	+	5×10^{-3}	-	8×10^{-4}	+	2×10^{-3}
1,7	-	10^{-4}	-	2×10^{-4}	+	3×10^{-3}	+	6×10^{-3}
1,8	-	10^{-4}	-	3×10^{-4}	-	2×10^{-4}	-	2×10^{-4}
2,1	+	9×10^{-3}	+	10^{-2}	+	9×10^{-3}	+	7×10^{-3}
2,2	-	9×10^{-3}	+	10^{-2}	+	6×10^{-3}	-	6×10^{-4}
2,3	-	4×10^{-4}	+	10^{-2}	-	7×10^{-4}	+	4×10^{-3}
2,4	+	3×10^{-3}	+	10^{-2}	-	9×10^{-4}	-	8×10^{-4}
2,5	-	5×10^{-4}	-	10^{-4}	+	2×10^{-3}	+	5×10^{-3}
2,6	+	6×10^{-3}	-	10^{-4}	+	7×10^{-3}	-	10^{-3}
2,7	+	7×10^{-3}	-	10^{-4}	-	4×10^{-4}	+	6×10^{-3}
2,8	-	2×10^{-4}	-	10^{-4}	-	3×10^{-4}	-	5×10^{-4}
3,1	+	8×10^{-3}	+	8×10^{-3}	+	10^{-2}	+	8×10^{-3}
3,2	-	9×10^{-4}	-	6×10^{-4}	+	10^{-2}	+	5×10^{-3}
3,3	+	4×10^{-3}	-	8×10^{-4}	+	10^{-2}	-	7×10^{-4}
3,4	-	8×10^{-4}	+	3×10^{-3}	+	10^{-2}	-	4×10^{-4}
3,5	+	2×10^{-3}	-	9×10^{-4}	-	10^{-4}	+	9×10^{-3}
3,6	-	3×10^{-4}	+	4×10^{-3}	-	10^{-4}	+	3×10^{-3}
3,7	+	10^{-3}	+	5×10^{-3}	-	10^{-4}	-	9×10^{-4}
3,8	-	2×10^{-4}	-	4×10^{-4}	-	10^{-4}	-	3×10^{-4}
4,1	+	8×10^{-3}	+	7×10^{-3}	+	8×10^{-4}	+	10^{-2}
4,2	+	5×10^{-3}	-	7×10^{-4}	-	8×10^{-3}	+	10^{-2}
4,3	-	3×10^{-4}	+	10^{-3}	-	4×10^{-4}	+	10^{-2}
4,4	-	7×10^{-4}	-	10^{-4}	+	10^{-3}	+	10^{-2}
4,5	+	6×10^{-3}	+	6×10^{-3}	-	7×10^{-4}	-	10^{-4}
4,6	+	3×10^{-3}	-	8×10^{-4}	+	3×10^{-3}	-	10^{-4}
4,7	-	8×10^{-4}	+	2×10^{-3}	+	2×10^{-3}	-	10^{-4}
4,8	-	6×10^{-4}	-	5×10^{-4}	-	10^{-4}	-	10^{-4}

4.2.3 Array Modeling

As the activities of the selected interfering ions in the calibration solutions are known, modeling the array involves determining the selectivity constants, standard electrode potential and slope for each electrode. If these parameters can be accurately modeled, then, in a situation where the composition of the activities of the four modeled components are fluctuating, the system should be able to internally compensate for the effect of the three interferents on the primary ion signal and enable the primary ions for each electrode in the array to be accurately determined.

Using a 2-level calibration means that the global response of the electrode is fitted to a straight line between the high and low levels of the primary ion in the standard solutions. Any potential recorded in the electrodes is linearly correlated to the logarithm of the total ionic contribution and the effect from the interfering ions is calculated and subtracted from it depending on the values of the *conditional* selectivity constants (Section 3.3) which are obtained from the set of parameters which better explain the electrode response. With this linear approach only one value can be returned for the model parameters E_j^0 and S_j (intercept and slope) and for the various selectivity coefficients which minimise the error of the model. Hence this approach implicitly estimates a constant rather than a coefficient, the accuracy of which can be tested through determination of primary ion activities in test solutions of known composition.

$$E_{ij} = E_j^0 + S_j \log\left(a_{iNH_4^+} + K^*_{jNH_4^+Na^+}a_{iNa^+} + K^*_{jNH_4^+K^+}a_{iK^+} + K^*_{jNH_4^+Ca^{2+}}a_{iCa^{2+}}\right) \qquad \textbf{Eq. 4.2a}$$

$$E_{ij} = E_j^0 + S_j \log\left(a_{iNa^+} + K^*_{jNa^+NH_4^+}a_{iNH_4^+} + K^*_{jNa^+K^+}a_{iK^+} + K^*_{jNa^+Ca^{2+}}a_{iCa^{2+}}\right) \qquad \textbf{Eq. 4.2b}$$

$$E_{ij} = E_j^0 + S_j \log\left(a_{iK^+} + K^*_{jK^+NH_4^+}a_{iNH_4^+} + K^*_{jK^+Na^+}a_{iNa^+} + K^*_{jK^+Ca^{2+}}a_{iCa^{2+}}\right) \qquad \textbf{Eq. 4.2c}$$

$$E_{ij} = E_j^0 + S_j \log\left(a_{iCa^{2+}} + K^*_{jCa^{2+}NH_4^+}a_{iNH_4^+} + K^*_{jCa^{2+}Na^+}a_{iNa^+} + K^*_{jCa^{2+}K^+}a_{iK^+}\right) \qquad \textbf{Eq. 4.2d}$$

(See Glossary of Symbols for identification of variables)

The mathematical model for the SAD described in this application is a series of equations as discussed in Section 3.3 and is shown in detail in equations Eq. 4.2a to Eq. 4.2d. In the modeling procedure, the response of each factor in each of the equations is decoupled to calculate the array parameters, which are, for each electrode, E_j^0, S_j, and the *conditional* selectivity constants (K^*_{jkl}) for the interfering ions which are related to the conventional selectivity coefficients as explained in Section 3.3, Eq. 3.4.

Each equation is modeled with respect to the data obtained with the eight solutions comprising the calibration sub-set for that particular electrode. This is achieved by means of the downhill modified simplex routine, using 10^{-3} as the initial value of the three selectivity constants, and initial values for E_j^0 and S_j obtained from bench calibration experiments. The values for the standard electrode potential and selectivity constants were allowed to optimise freely, while the electrode slope was constrained within $\pm 20/z_k$ mV decade^{-1} of the theoretical slope.

The simplex routine varies the values of the selectivity constants, standard electrode potential and slope according to the rules of the algorithm until the error (ε) defined by Eq. 4.3 below falls below an arbitrary breakout value.

$$\varepsilon = \frac{\sqrt{\sum_n \left(a_{ik}^* - a_k\right)^2 / a_{ik}}}{n}$$

<div align="right">Eq. 4.3</div>

where a_{ik}^* and a_{ik} are the real and estimated activities of the primary ion k in the calibration solution i obtained *via* the model, and n is the number of solutions needed to

Figure 4.1: Flow chart of the experimental and modeling procedure used for each of the electrodes in the array.
For example, starting with the ammonium electrode modeling, eight solutions containing different concentrations of ammonium, sodium, potassium and calcium (Table 4.1: 1,1-1,8) are injected past the ISE array (Loop 1).The process is the repeated for the remaining three electrodes (Loop 2). The signal is acquired digitally, the FIA traces are processed and peak heights automatically calculated. For each ISE, the response set consists of an 4x8 array containing the response of the four electrodes to each of the eight calibration solutions. Each response set is presented to a SIMPLEX algorithm to calculate the Nikolskii-Eisenman parameters that minimise the prediction error in the eight solutions within each ISE calibration set. The starting simplex algorithm was randomly situated in different locations to avoid local minima. The Nikolskii-Eisenman equation is then reconstructed for each ISE for future unknown sample analysis. Additional details are in the text.
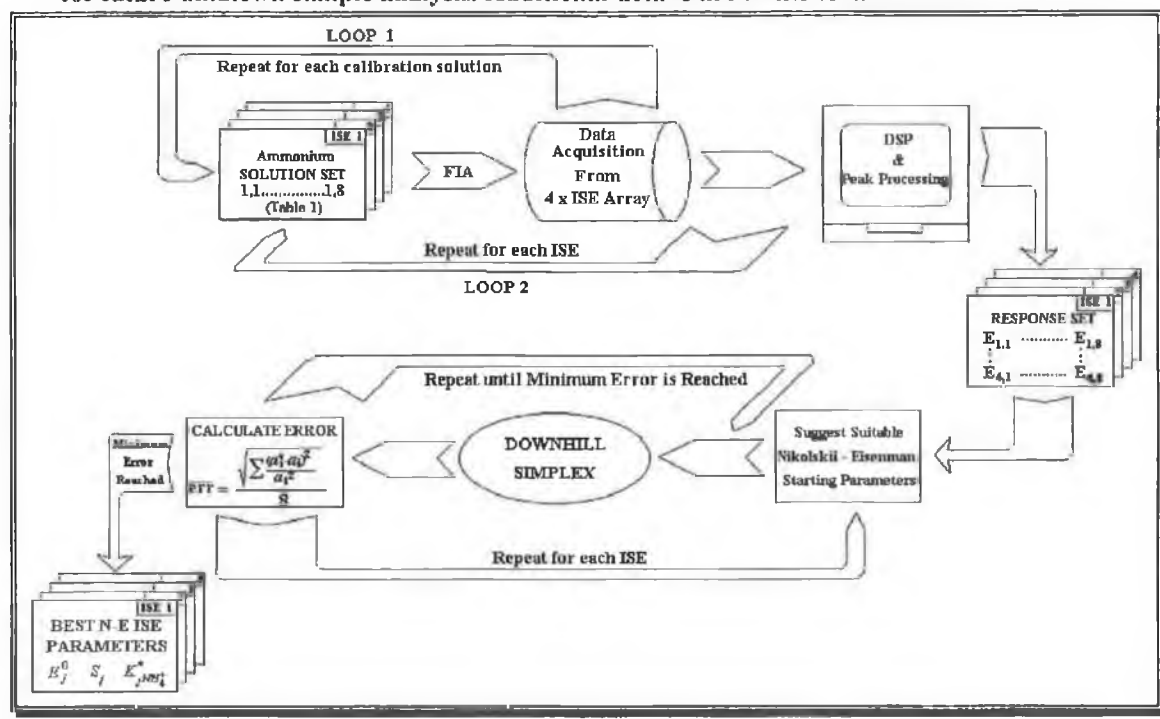
model each ISE. To obtain these parameters, the simplex uses the measured response of the electrode and the estimated model parameters to solve for the primary ion activity *via* the electrode equation (Eq. 4.2 series) above for the eight solutions in the calibration set corresponding to the particular electrode j (i.e. $n=8$).

The simplex continues to iterate until the defined maximum number of iterations is reached, or the error falls below a breakout value (typically 10^{-5} average relative square error), indicating that a satisfactory fit has been obtained. The simplex is repeated several times with different starting values for the model parameters in order to maximise the probability of finding the global minimum of the error surface. This process is repeated for each electrode using the responses obtained in their respective set of eight calibration solutions. This entire procedure was repeated with four sets of potential values to check the precision of the final model parameters obtained.

Figure 4.1 shows a schematised flow diagram of the experimental and modeling procedure used. See Section 3.4.3.1 (*i*) for detailed information on the SIMPLEX algorithm.

4.2.4 Experimental

A *tris* buffer solution (pH=7.3)[4,5] was prepared by diluting 1.387 gr dm^{-3} *tris-HCl* and 0.145 gr dm^{-3} *tris* base (90.5% w/w *tris-HCl* and 9.5% w/w *tris* base, Fluka catalogue No. 93358 and 93362 respectively) in Milli-Q water (Millipore system) to give a total *tris* concentration of 10^{-2} mol dm^{-3} ($pK_{a(tris)} = 8.24$[11]). Ammonium, sodium, potassium

and calcium chloride stock solutions were mixed and diluted with the buffer solution to give a final concentration of the cations of 10^{-6} mol dm^{-3}. The total ionic strength from the solution can be calculated as in Eq. 2.31 and while it is clear that the contribution from the added ions to the buffer is insignificant, attention must be draw to the fact that the only contribution from the *tris* buffer to the ionic strength comes from the charged species *tris-H$^+$*, which is present in the buffer at a concentration of 8.8×10^{-3} mol dm^{-3}. This solution was used as carrier stream, which was pumped at a flow rate of 1.0 mL min^{-1}.

The calibration standards were prepared with the same *tris* buffer concentration by mixing 1.0 mL of 1.0 mol dm^{-3} *tris/tris-HCl* mixture with the appropriate volume of stock solutions of the different ions and diluting them to 100 mL in volumetric flasks. As the concentration of ions in the solutions vary over a wide range, the ionic strength changes from one solution to another, and cannot be considered constant. Activity coefficients were therefore calculated for each solution using the Davies formalism (Eq. 2.30).

The activity coefficients vary in the range $\gamma=0.896$ to $\gamma=0.783$ for ammonium, sodium and potassium ions, and in the range $\gamma=0.649$ to $\gamma=0.387$ for calcium ions. For simplicity, concentrations of the ions instead of activities are used in Table 4.1 to show the levels of the ions in each of the calibration solutions. However, the corresponding activities were used in the model building calculations.

The ISE membranes were prepared as described in Section 4.2.1 and placed in the SAD block in the following sequence: NH_4^+, Na^+, K^+ and Ca^{2+}, and the internal electrolyte reservoirs were filled with chloride solutions (10^{-1} mol dm^{-3}) of the corresponding primary ion. The three pieces of the detector block were then aligned by the steel rods incorporated to the Perspex pieces and secured with bolts and nuts properly tightened. The elasticity of the PVC membranes provide self sealing characteristics to the array block which ensure a smooth and continuous flow through the inner piece. Proper flowing of carrier through the block was tested prior to the inclusion of the detector block in the FIA system, and then placed in series between the auto-injector and the carrier-reference electrolyte merging T-piece (see Figure 3.3). The internal reference electrodes were electrically connected to the input of the voltage followers for differential data acquisition *via* the AT-MIO-16DL I/O card with respect to an external Ag/AgCl flow-through reference electrode. The membranes were conditioned by continuously pumping carrier solution through the SAD block, and their potentials were allowed to stabilise prior to injection of the calibration set solutions.

The calibration solutions were presented serially to the array and each measurement repeated four times. On completion of the injection sequence, the computer will have acquired 32 FIA responses from each electrode in the array. The FIA traces were stored as ASCII files and smoothed with 2nd-order Savitzky-Golay filters[12], which in essence is a moving average smoothing technique with weighted coefficients. Bandwidths of 7 to 13 points were used, depending on the signal characteristics, to reduce the effect of noise. In-home peak processing routines were then applied to locate the peak maxima

and measure the peak heights automatically (see Section 6.2.3). The peak height values were stored together with solution and electrode identifiers. Data were stored in two files, one containing the activity of the ions in the calibration set, and the other the millivolt response of the array to these solutions. These files were presented to the SIMPLEX algorithm to calculate the optimum SAD response parameters as described previously in Section 3.4.3.1.

4.2.5 Results and Discussion

4.2.5.1 Electrode parameters.

Table 4.2 shows the output from the SIMPLEX optimisation procedure for each of the electrodes in the array. These parameters give the best fit between the primary ion activities estimated with the modified Nikolskii-Eisenman equations (Eq. 4.2 series) and the known primary ion activities as described above. Table 4.3 gives the results of a Nernstian-type calibration where each electrode is treated individually, and pure solutions of each primary ion are injected. Interestingly, the Na^+ and Ca^{2+} models return better electrode slopes (54.16 and 25.01 mV dec^{-1}, closer to the theoretical value), than the K^+ - and NH_4^+ -selective electrode values, possibly because of a slower dynamic response of the latter (see Figure 4.2 and discussion below). The NH_4^+ -selective electrode also gives a sub-Nernstian slope in the calibration with pure solutions (Table 4.3), which supports the conclusion that this is an inherent feature of the membrane used, rather than an artifact of the array calibration procedure. In every case, steady-state conditions with respect to the primary ion apply, as it can be observed from the fact that

the slopes obtained are very similar for both Nikolskii-Eisenman and Nernst electrode models.

Care must be exercised when interpreting the values of the selectivity constants obtained with the modeling approach, as different values may be obtained depending on a variety of factors such as the concentration range of the ions investigated, the experimental design employed, the composition of the PVC membrane, and the parameter chosen for optimisation (see discussion on Figure 4.8 and Figure 4.9). Other factors such as the inter-variable effect in multivariate calibration[10] or kinetic discrimination in non steady-state measurements (FIA)[13,14] will affect the selectivity constants, as well as the electrode slope or cell potential values returned by the modeling procedure (see discussion below). However, the important feature of this approach is that within the limits of the calibration design employed, these numbers appear to be constants (*conditional* constants) and can be successfully used to compensate for modeled interferent contributions to an electrode signal, in order to isolate that portion of the signal arising from the primary ion.

Table 4.2: Optimised Nikolskii-Eisenman parameters for the array of electrodes.
Data were obtained from the output of the SIMPLEX optimisation procedure. The ISE array was calibrated four times in the range 10^{-4} to 10^{-2} mol dm^{-3}, and the average values were taken. Relative standard deviation values (%) are in parenthesis ($n=4$).

ISE	$E_j^0(mV)$	$S_j(mVdec^{-1})$	$K^*_{jNH_4^+} \times 1000$	$K^*_{jNa} \times 1000$	$K^*_{jK} \times 1000$	$K^*_{jCa^{2+}} \times 1000$
NH_4^+	226.90 (0.1)	45.60 (0.4)	1000.0 (00.0)	4.7 (51.1)	173.8 (3.5)	5.2 (69.2)
Na^+	261.87 (0.9)	54.16 (1.6)	2.0 (45.0)	1000.0 (00.0)	103.2 (1.6)	14.6 (15.1)
K^+	269.28 (0.3)	52.21 (0.4)	132.8 (07.2)	1.3 (130)	1000.0 (0.0)	12.7 (128)
Ca^{2+}	125.89 (2.7)	25.01 (3.9)	0.2 (50.0)	1.5 (60.0)	7.5 (54.7)	1000.0 (0.0)

Furthermore, the constants can be used in this manner with real samples with widely varying ion levels provided that the sample matrix does not differ significantly, in species and levels, from the calibration ranges used to generate the prediction model[13,14,15]. But as long as the ion activity in the samples lies within the calibration range of the model, it will cope with dynamic variations in sample composition, which no other direct potentiometry technique, so far, can do. The limit of application of the model to matrices different from that of calibration range is given by the relative magnitude of the contribution of unmodeled interferents to the overall compared to that of the primary ion and modeled interferents. The type of ISEs used must have very good response characteristics in terms of stability, constant parameters and working life because, as the modeling procedure is not a trivial process, the SAD should be able to maintain the same response characteristics for as long as possible without recalibration.

Table 4.3: Slopes and Cell Constants obtained using single ion solutions (Nernst Calibration).
FIA conditions as for multicomponent injections. *NB: concentrations were converted to activities using the Davies formalism (Eq. 2.30) during calculation of slopes and cell constants.

C *(mol dm^{-3})*	NH_4^+	Na^+	K^+	Ca^{2+}
10^{-2}	131.2	123.7	144.9	67.1
10^{-3}	81.5	63.8	92.7	36.8
10^{-4}	36.5	21.8	37.3	13.2
S_j *(mVdec^{-1})*	47.4	51.4	54.3	27.9
E_j^0 *(mV)*	230.1	227.0	257.8	128.8

4.2.5.2 Electrode Kinetics

Figure 4.2 shows the first derivative for the response of the array to sample 3,1 (see Table 4.1). The digital nature of the electrode data obtained *via* computer techniques makes this and other sophisticated data transformation techniques relatively easy to implement. In turn, this provides a tool for investigating fundamental aspects of the membrane response mechanism, such as the ion-exchange kinetics. In this particular case, the Na^+- and Ca^{2+}-selective electrodes reach the peak maximum (first derivative crosses zero) at almost the same time, while the K^+- and NH_4^+-selective electrodes lag behind. The sodium ISE also responds faster to the sample than the other ISEs, giving a higher maximum slope in the rising portion of the FIA peak (maximum in the first derivative traces). This occurs although the sodium concentration in the sample is slightly lower than potassium or ammonium (8×10^{-3} mol dm^{-3} for NH_4^+ and K^+ to 10^{-2} mol dm^{-3} for Na^+), and despite the order of the membranes in the block being NH_4^+, Na^+, K^+ and Ca^{2+}, which causes the Na^+ electrode to see a more diffuse injected sample than the ammonium ISE.

The relatively slower response of the NH_4^+- and K^+-selective electrodes means that these ISEs are less likely to reach the true maximum potential (as would be achieved using large sample volumes or with stopped-flow measurements) before the sample plug leaves the detector. It follows that with these electrodes, the measurements are more likely to be made in a kinetic limited regime, where selectivity towards the primary ion may be enhanced due to a lower transportation rate of interfering ions across the membrane in the early stages of the signal development[13,14].

In contrast, the faster response of the Na^+- and Ca^{2+}-selective electrodes enables them to come closer to an apparent steady-state *plateau*, even though they occupy the second and fourth positions in the flow-cell, respectively. Considering the number of variables affecting the values of selectivity coefficients, it is not surprising that the literature contains widely varying estimates for electrodes[14].

However, as we use the parameters in Table 4.2 in the modified version of the Nikolskii-Eisenman equation to calculate unknowns, we are convinced that these are accurate values, at least for the experimental design and calibration range used in this investigation. Of course, the flow regime employed means that each membrane is exposed to a slightly different sample plug due to dispersion. This means that for a rigorous investigation, the positions of the membranes in the flow-cell would have to be

Figure 4.2: First derivative of the response of a 33µl plug of sample.
Sample 3,1 contains a molar ratio 8:8:10:8 of ammonium/sodium/potassium/calcium showing faster response for the sodium and calcium. The electrode positions in the flow-cell are ammonium, potassium, sodium and calcium, respectively. Each response has been normalised to account for the slightly different time of arrival of the sample plug as it passes through the cell.
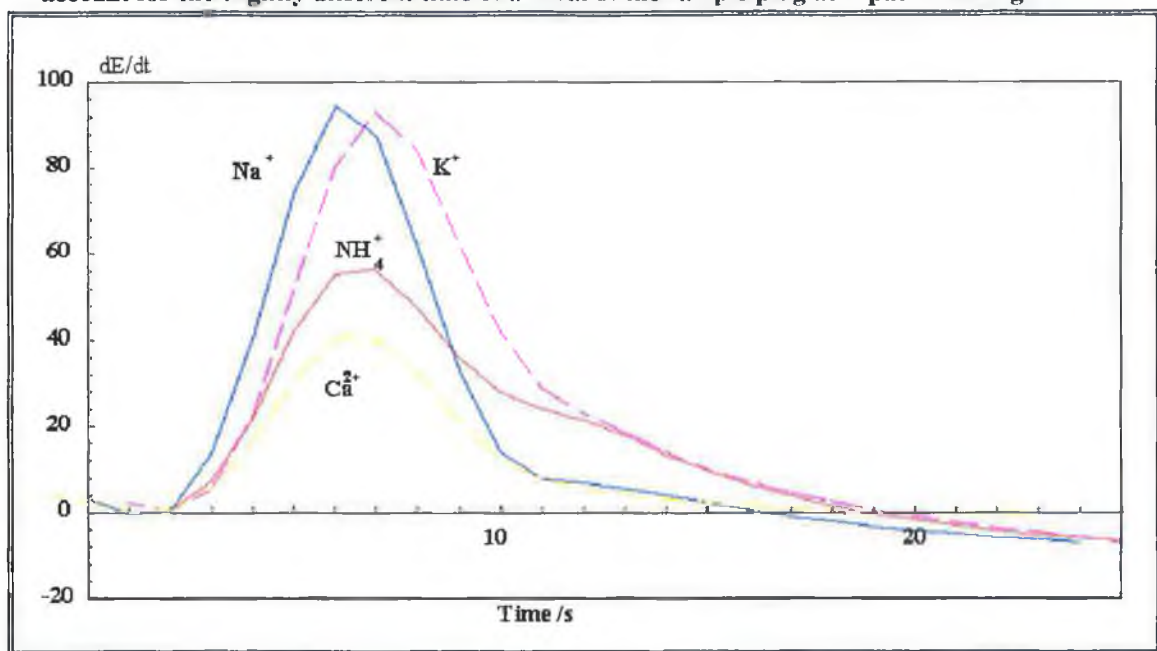
varied. On the other hand, the use of a technique like Batch-Injection Analysis might be more appropriate for fundamental studies on response kinetics using the array approach, as the sample is injected directly onto the sensor surface to give an essentially undistorted square-wave chemical impulse[16].

4.2.5.3 SAD Prediction Characteristics

Figure 4.3a-d shows the prediction characteristics of the four electrodes where the signals are corrected *via* the modeled Nikolskii-Eisenman parameters in comparison with the uncorrected Nernst approach. These corrected data were obtained by modeling the characteristics of each electrode with the 8 calibration solutions, and then presenting the remaining 24 solutions as unknowns. In contrast, the Nernst calibration parameters (Table 4.2) were obtained using pure solutions of the primary ions (injected under the same conditions as for the other solutions), and the same potentials from the 24 test solutions presented as unknowns.

A clear improvement in the prediction capability is obtained for the NH_4^+-, Na^+- and K^+-selective electrodes with the Nikolskii-Eisenman model (Figure 4.3a, Figure 4.3b and Figure 4.3c, respectively) whereas with the Ca^{2+}-ISE, the results show little difference between both models (Figure 4.3d). The results convincingly show that application of the Nikolskii-Eisenman model reduces the bias which occurs in the uncorrected (Nernstian) results for the NH_4^+-, Na^+- and K^+-selective electrodes, and to a lesser extent for Ca^{2+}-ISE (see Table 4.4). These striking improvements are in

complete agreement with earlier results produced in a study involving the use of a

different array for the analysis of plasma samples[13,14,15].

Figure 4.3: Prediction characteristics of the SAD in the concentration range 10^{-4} - 10^{-2} mol dm^{-3}. The final model is obtained when the average relative error calculated according to Eq. 4.3 (n=8) for each electrode calibration set is minimised by the SIMPLEX algorithm. It should be noted that only 8 solutions from the set are used to model each electrode, and the remaining 24 are presented as unknowns. Clear improvements are obtained for ammonium (Figure 4.3a), sodium (Figure 4.3b) and potassium (Figure 4.3c), when modeling the selectivity coefficients of the Nikolskii-Eisenman equation (colour) vs. the Nernstian approach (grey).
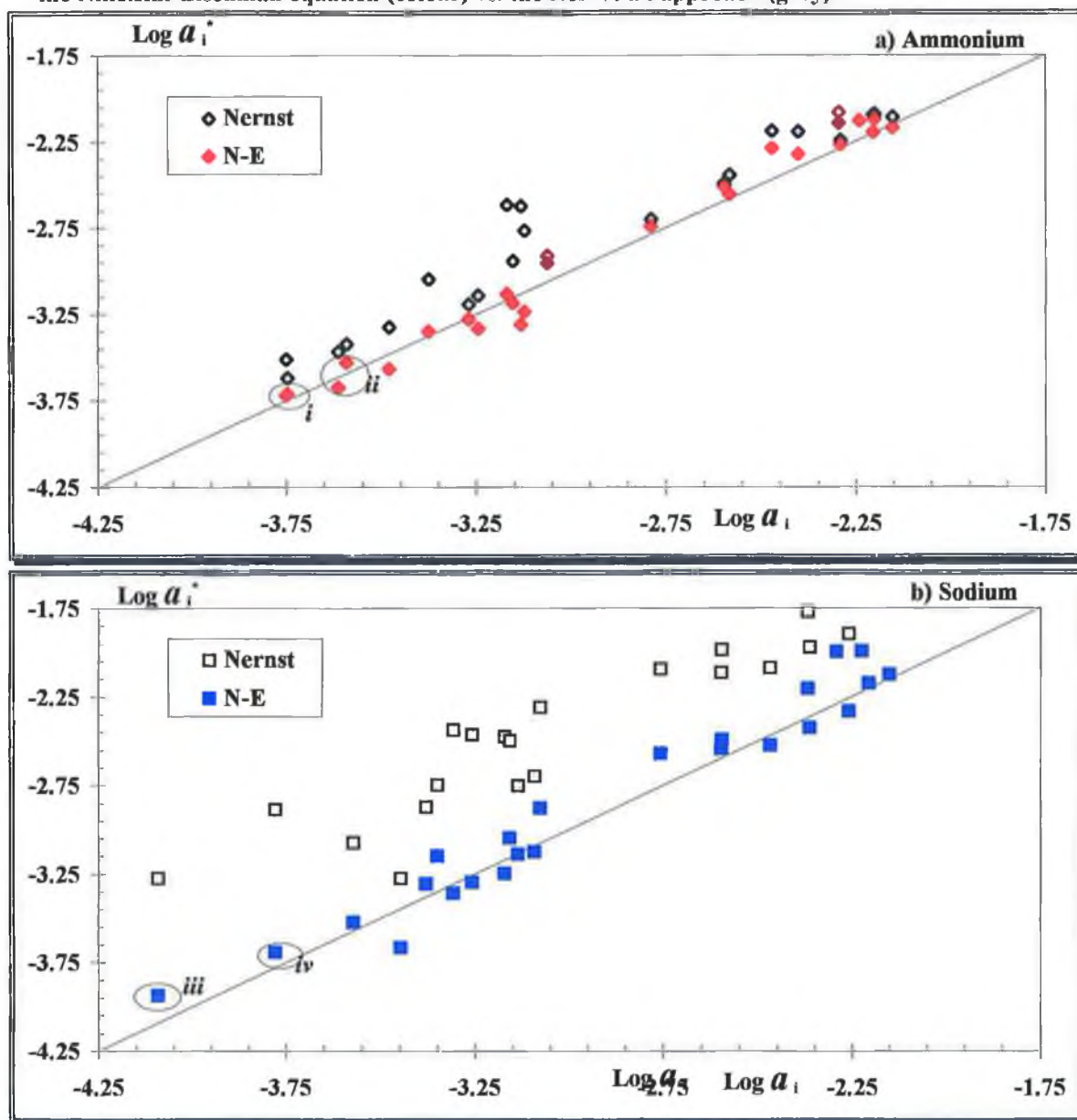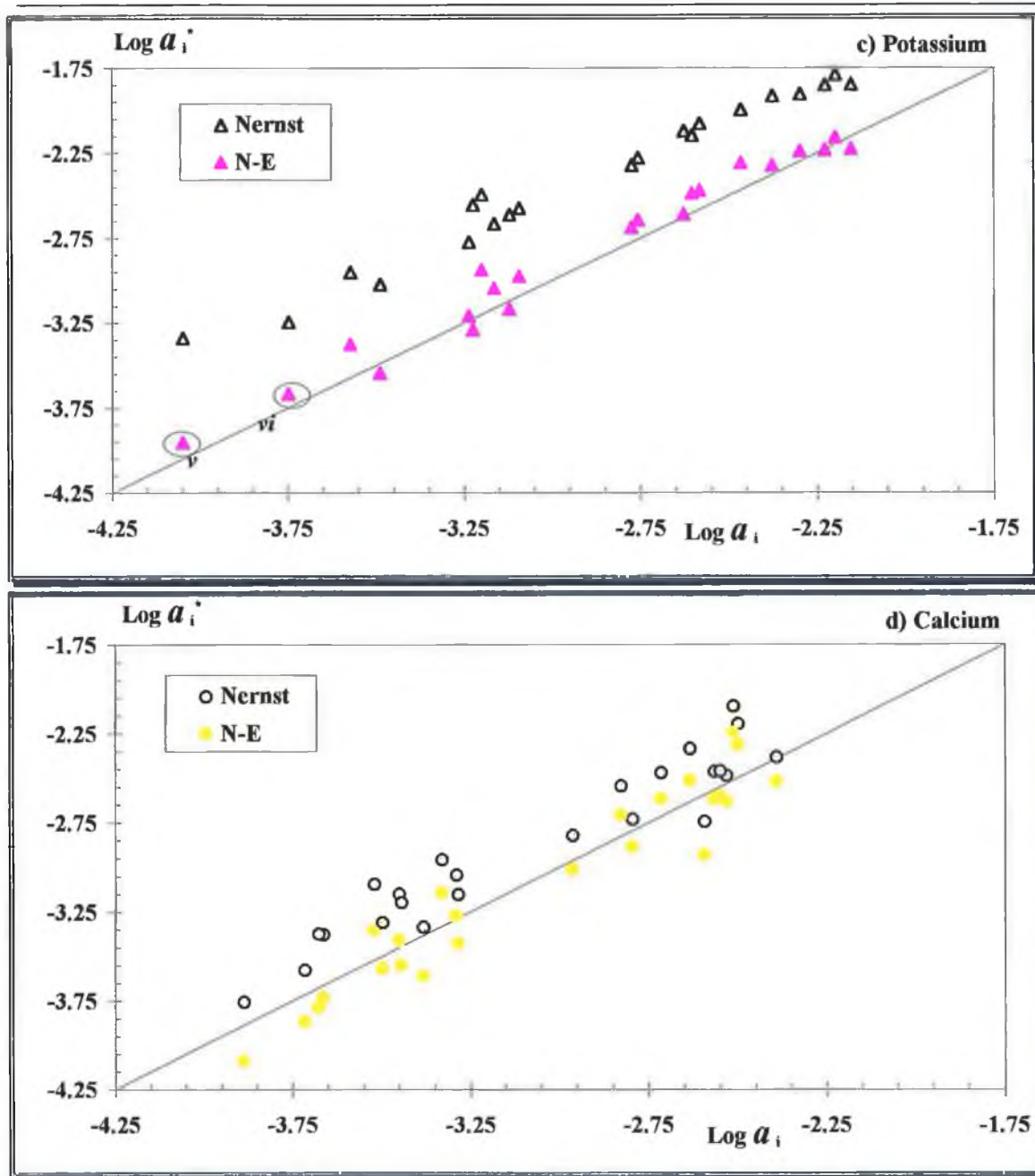
Perhaps most impressively, the array is able to compensate accurately the ammonium, potassium and sodium electrode signals at the lowest range of the primary ions tested even though the interfering ions are present in gross excess in most of these solutions. Figure 4.3a shows in the lower activity range of the diagram solutions 2,8-3,8 (marked as *i*) and 3,6-4,3 (*ii*) which present a NH_4^+ concentration of $2x10^{-2}$ and $3x10^{-2}$ mol dm^{-3}

respectively. It can clearly be appreciated how the SAD model is very capable of correcting for the contribution of the main interferent, K^+, even when this is present at a level of 150% of the ammonium concentration, (soln. 2,8), and can also correct for Na^+ at a 200% of the original ammonium concentration (soln. 3,8). Figure 4.3b shows also good prediction characteristics at low levels of sodium (*iii*) in matrices containing as much as 700% NH_4^+ and 1000% K^+ (soln. 4,4) of the sodium concentration, and as little (comparing to 4,4) as 50% NH_4^+ and 150% K^+ of the Na^+ concentration (soln. 1,7 marked as *iv*). Similar prediction characteristics are obtained for K^+ ions as is shown in Figure 4.3c. Solutions marked as *v* and *vi* refer to solutions 4,8 and 1,8 in Table 4.1.

Table 4.4 presents a statistical comparison of the model predictions and uncompensated data (Nernst model). It could seem surprising that the prediction characteristics for calcium are not as good as for the other three , but it must be taken into consideration that the Ca^{2+}-ISE presents an global selectivity better than, at least, the ammonium and potassium ISEs. This high selectivity will produce a poor modeling of the response characteristics of this particular ISE, as explained in Section 3.4.1. This last statement would explain why only limited improvement is obtained with the calcium ISE, with recovery characteristics similar to those that would be expected from uncorrected determinations. As Figure 4.3d shows the Ca^{2+}-selective ISE presents a bigger scatter in the prediction characteristics, possibly because of the lower sensitivity this electrode has, which is inherently half that of the ISEs selective for single charged ions, with additional imprecision due to the difficulty in obtaining accurate values for the selectivity constants because of good overall selectivity.

Table 4.4 indicates that the Nikolskii-Eisenman model generates, in general, a better linear model for the four ISEs than the Nernst model. Apart from this better linearity, the Nikolskii-Eisenman model also presents a huge reduction in the positive bias expected from the Nernst model as the recovery results lie very close to the ideal diagonal. This bias is defined as the difference between the predicted activity and the real activity, and gives information about the distance of the predicted data to the ideal recovery. The average bias used in Table 4.4 corresponds to the expression:

$$\overline{B} = \frac{\sum_n \left(Log a_i^* - Log a_i \right)}{n}$$

Eq. 4.4

Also, the overall error over the whole activity range is greatly reduced except for the Ca^{2+}-selective electrode. This ISE also presents better mean square error (MSE) value than for the Nernst model, but the relatively small improvement obtained is, once again, a reflection of the limited advantage of using very selective electrodes in this type of array.

Table 4.4: Statistical parameters for the ISE prediction characteristics.
From the values displayed below it can be seen how the Nikolskii-Eisenman theory can produce results with much better consistence than the Nernst approach. Values in parenthesis correspond to the response of the SAD to the same training set when modeled to the Nernst theory (no correction for interferents).

ISE	Slope	Intercept	Correlation Coeff. (r)	Average Bias $\overline{B}$	Mean Square Error
NH_4^+	1.064 (0.929)	0.204 (-0.015)	0.991 (0.970)	0.015 (0.189)	0.001 (0.006)
Na^+	1.022 (0.907)	0.112 (0.313)	0.978 (0.943)	0.048 (0.583)	0.002 (0.045)
K^+	0.970 (0.862)	-0.026 (0.097)	0.987 (0.989)	0.060 (0.497)	0.001 (0.026)
Ca^{2+}	1.073 (0.919)	0.187 (-0.057)	0.926 (0.957)	-0.038 (0.191)	0.003 (0.006)

Reduction in the technique's precision and accuracy is a common phenomenon that occurs at low activity ranges. This is caused by a decrease in the electrode slope, lower signal-to-noise ratio and errors in the measurements, which are relatively higher at low activities. From Figure 4.3 series, and more in particular from Figure 4.4 it can be appreciated that the FIA-SAD technique presents very good prediction characteristics, in terms of precision and accuracy. Furthermore, the relative error throughout the activity range shows a scatter which does not present the typical higher error trend towards lower activities. This suggests that the Nikolskii-Eisenman parameters obtained from the modeling procedure are able to cope, at least, with the decrease in electrodes slope when fitting the ISE response to a linear model.

Figure 4.4: Percentage relative error obtained during prediction polling.
The percentage error scatters regularly throughout the activity range. It can be appreciated that ammonium and potassium ISEs present a smaller overall prediction error than sodium and calcium ISEs.
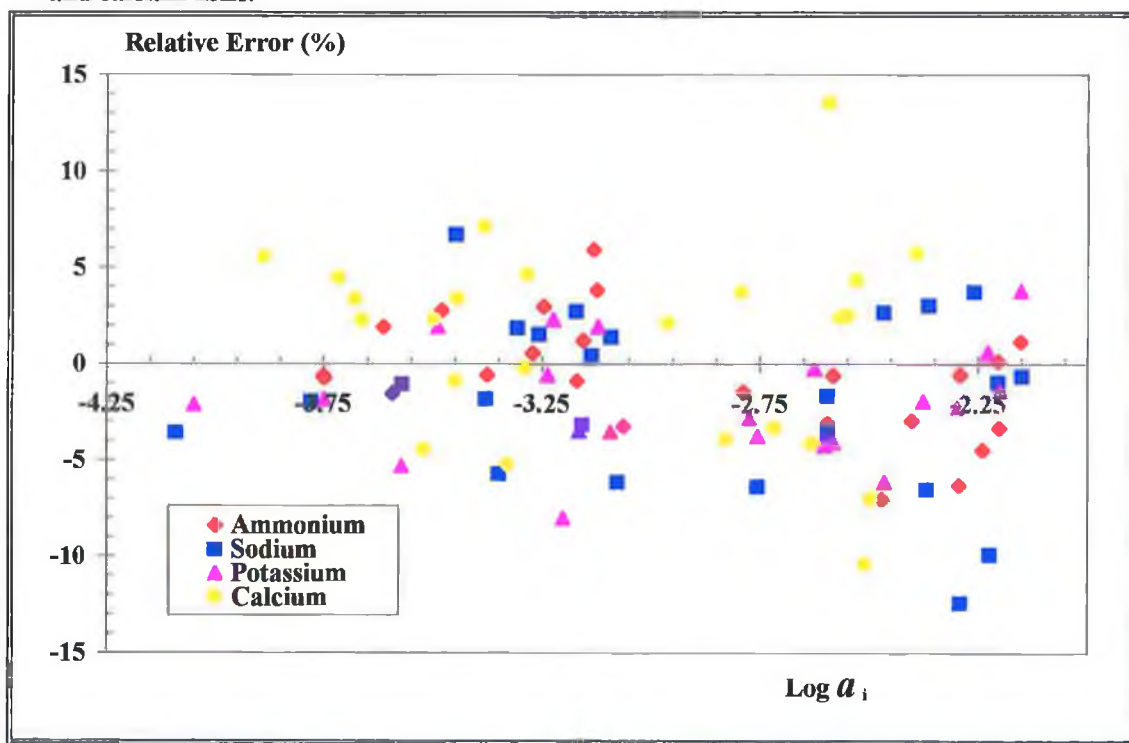
A closer look to Figure 4.4 reveals the error characteristics for the NH_4^+- and K^+-selective ISEs to be consistent with the effect expected when fitting the ISE response to a linear ($Log a_i$) model. Both electrodes show an over-determination of primary ion activity at highest level. This pattern changes at primary ion activities of around $10^{-2.2}$ mol dm^{-3} where the relative error is negative, which indicates maximum under-determination around $Log a_i = 10^{-2.5}$ mol dm^{-3} and gradually increasing to zero ($Log a_i = 10^{-3.5}$ mol dm^{-3}). These effects are not so clear for Na^+- and Ca^{2+}-ISEs probably because of the poorer modeling characteristics of the electrodes.

Figure 4.5: Relationship between Nikolskii-Eisenman and the best linear model fitted to it. Fitting the Nikolskii-Eisenman model (blue) to a linear best fit (red) inevitably generates error in the activity determination, specially in those areas where the models differ most (middle and extremes). It can be appreciated how the same electrode potential is related to under determined activities (a_{lin}) using the linear model, comparing to the real model (a_{N-E}).
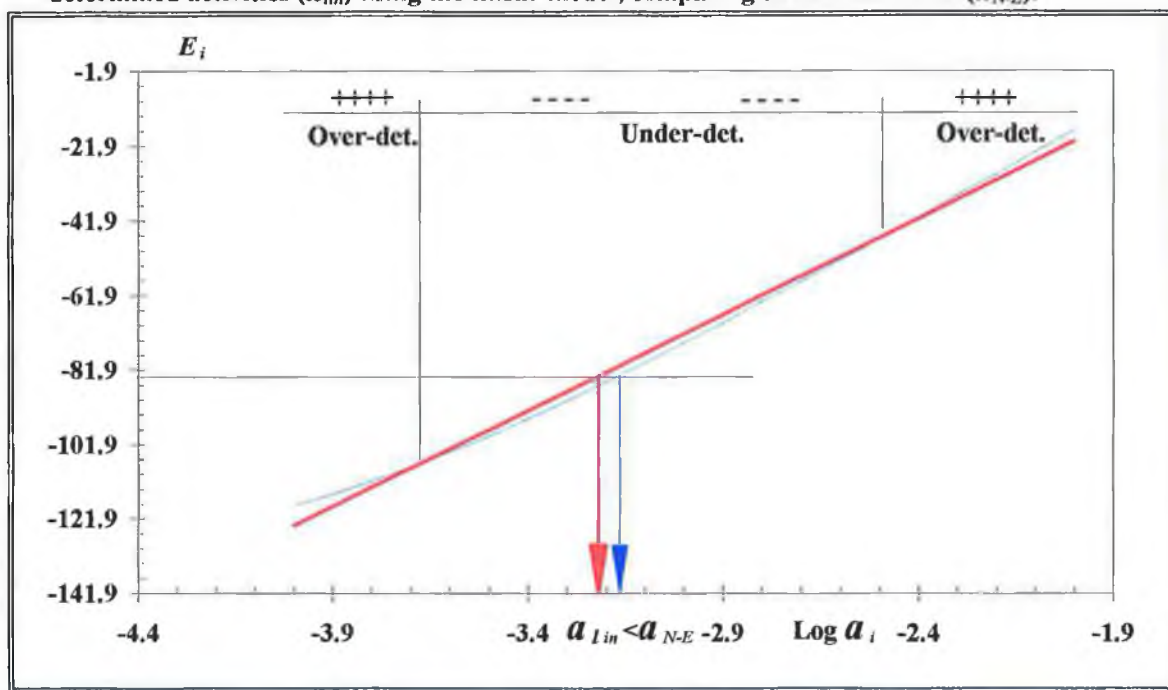
These trends are in concordance with a linear model which fits preferably at the lower range of activities to reduce as much as possible the contribution of the error in that area,

and then it varies the slope to obtain the best fit. This will also explain a reduction of the slope in the electrode model. Figure 4.5 illustrates the comparison between the ideal Nikolskii-Eisenman response (as in Figure 2.5) and its best linear fit, indicating the areas where over-determination (+) and under-determination (-) will occur, which is consistent with the behaviour trends explained above.

In addition, the primary ion concentration dependent error (a common problem associated with ISEs which arises as the contribution from the primary ion to the signal decreases compared to that of the interferents) is greatly reduced and the corrected results lie close to the ideal diagonal line along the entire concentration range investigated. A representation on the relative percentage error of the predicted activities *versus* the Relative Interferent Contribution (*RIC*), defined as:

$$RIC = \frac{\sum_l K_{jkl}^* a_{il}}{a_{ik}}$$

Eq. 4.5

shows that the relative percentage error is evenly scattered along the 0% value, showing no increasing error trend towards high *RIC* values. This suggests that the SAD model is well capable of correcting for wide variations of interferent contribution, and that this analysis technique is ideal for situations where the sample matrix can unexpectedly change from one extreme to another.

The results shown above demonstrate that real-time, automatic detection and compensation for varying concentrations of modeled interferents is possible, giving a calibration model that is inherently much more robust throughout the calibration range

chosen for the application than that given by traditional calibration methods, which

cannot cope with situations where the matrix composition may vary widely in a dynamic

manner.

Figure 4.6: Square error vs. relative interferent contribution.
The variation of the prediction error (ε) with the relative contribution of interferents (as defined in Eq. 4.5) presents a homogeneous distribution. This suggests that the SAD model can cope with wide variations of the contributions of interferents relative to the primary ion activity.
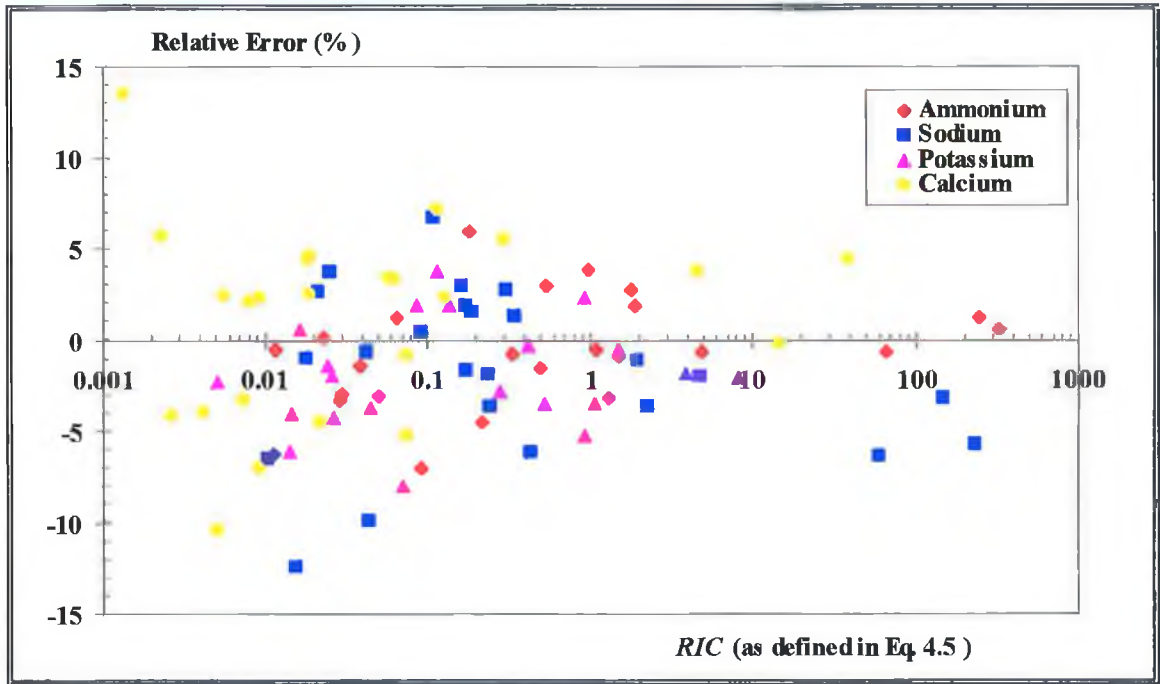
4.2.5.4 Parameter Significance in the SAD model

Figure 4.7 shows how the SIMPLEX algorithm varies the Nikolskii-Eisenman

parameters of the NH_4^+-selective electrode as it attempts to minimise the error in the

predicted activities. Initially, the more influential parameters are optimised (E_j^0 and S_j

and $K^*_{jNH_4^+K^+}$) leading to a rapid decrease in the predicted error over the first 40

iterations. In fact, after 10 iterations, the values for the standard cell potential and the

electrode slope are within 2.8% and 5% of their final values, and after 20 iterations, within 0.1% and 0.3%, respectively. With these parameters effectively set as constants, the simplex has greatly decreased the dimensionality of the search, which has been reduced to varying the sodium and calcium selectivity constants.

However, subsequent huge variations in these parameters lead to a very small reduction in the error. Hence, for this particular calibration design, these selectivity constants are not significant in comparison to the potassium selectivity constant, and hence potassium can be predicted to be the main source of error in the matrix. This type of study provides very convincing evidence of the real selectivity of an electrode in a multicomponent environment, where the matrix composition is varying significantly. Provided the characteristics of the membrane are stable, these can be expected to be much more meaningful than the data generated by the IUPAC recommended mixed solution method of assessing ISE selectivity.

These effects are also demonstrated in Table 4.2, which shows that the modeling procedure returns much more precise values for the slope and cell constant than for the selectivity constants, as these have a much greater impact on the error of the model. Furthermore, within the selectivity constants themselves, those with greater magnitude will have more influence on the final SAD model and higher accuracy in their determination is essential to obtain good prediction characteristics. Those selectivity constants with low relative values indicate low cross-response in general and low weight on the SAD model, and their wide variation may not result in significant changes in the

system's polling ability. In this particular application it seems that the most important selectivity constant parameters are those which indicate the selectivity of the NH_4^+-ISE and Na^+-ISE to potassium, and K^+-ISE to ammonium.

The relative importance of each selectivity constant in the ammonium electrode model is further examined in Figure 4.8 and Figure 4.9. In Figure 4.8, the model parameters are all maintained at their optimum values according to Table 4.2 and the effect of varying each selectivity constant in turn on the correlation coefficient of the predicted *versus* calculated NH_4^+ activities in the 24 test solutions plotted. Clearly, the larger potassium selectivity constant has a more pronounced effect than the sodium and calcium selectivity constants. As the potassium selectivity constant is increased from 10^{-3} to 10^0, the correlation coefficient improves slowly from 0.967 to a maximum of almost 0.980 at a selectivity constant of around 0.2.

These results show the importance of correcting the effect of potassium ions in the matrix on the NH_4^+-ISE if optimum results are to be achieved. Of course, gross overestimation of any of the selectivity coefficients gives too large a weighting in the calculations and hence the correlation coefficient drops sharply in all three cases for values above around 0.2. In contrast, no increase in correlation when varying the calcium and sodium selectivity constants from 10^{-3} is observed. Instead, the correlation coefficient drops sharply above 10^{-2} (sodium) and 0.1 (calcium), indicating that these parameters have little influence on the correlation of the results, provided they are not grossly over-estimated.

Figure 4.7: Variation of the electrode parameters and prediction error for the ammonium electrode during the modeling procedure.
Almost the totality of the error of model is minimised in the first forty iterations, which corresponds to the optimisation of the most influential electrode parameters.
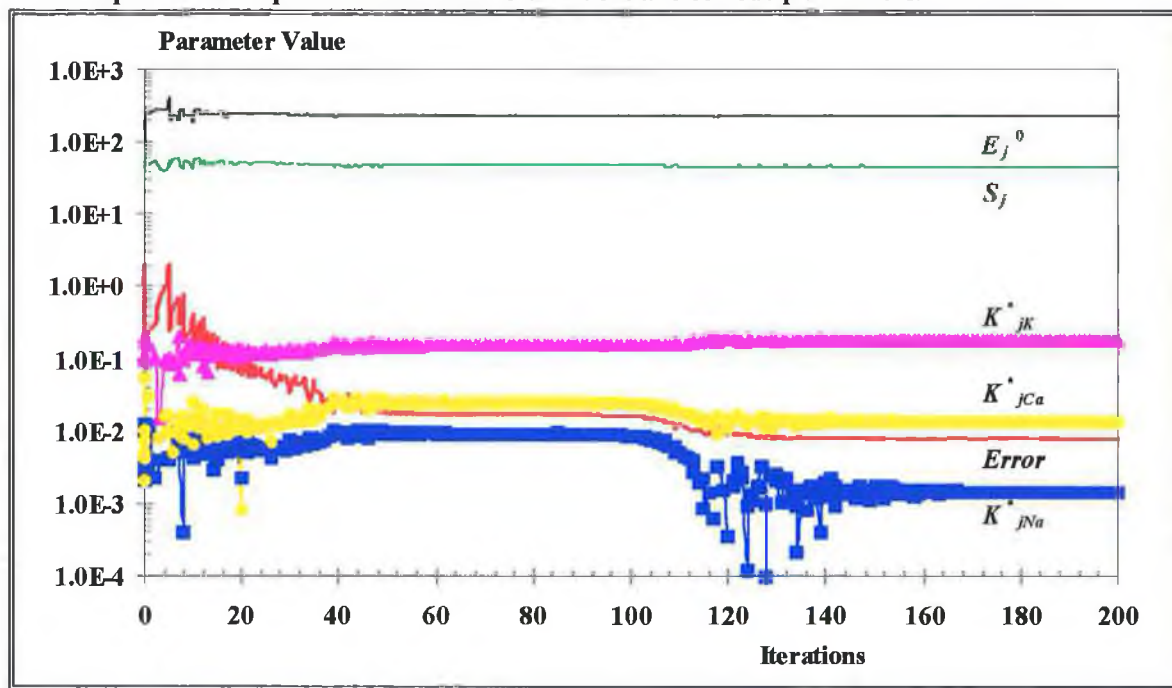
Figure 4.8: Correlation coefficient variation for the predictions of the ammonium activity in the ammonium ISE (*n*=24).
Each selectivity constant in turn is varied while the other model parameters are kept at their optimum values according to Table 4.2. The sodium and calcium selectivity constants have no effect on the correlation provided they are not over estimated confirming the selectivity of the electrode against these ions. However, the potassium selectivity constant produces a clear maximum in the correlation coefficient stating the importance of the potassium interference.
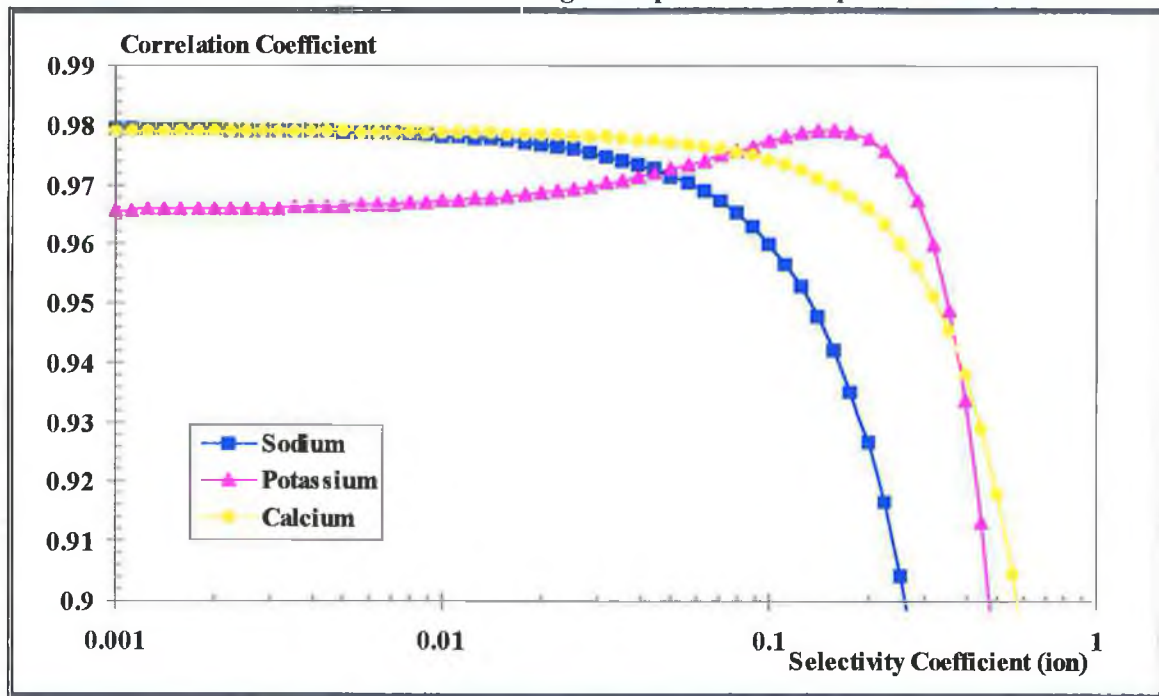
However, this gives a misleading impression when viewed in isolation. As spurious matrix responses add to the analytical signal, we can predict that the analytical data will tend to be positively biased, but still strongly correlated (see Figure 4.3). Hence examination of the effect of selectivity constant variation on the prediction error over the 24 test solutions is more informative. Figure 4.9 shows how the average relative error (defined according to Eq. 4.3; n=24) changes as each selectivity coefficient of the NH_4^+-selective electrode is varied, while maintaining the other electrode parameters at their optimum values according to Table 4.2

Figure 4.9: Variation of the average relative error of the predictions, as defined in Eq. 4.3 (n=24), of the ammonium electrode.
Each selectivity constant is varied while other electrode parameters are maintained at their optimum values. As in Figure 4.8, the sodium and potassium selectivity constants have very little effect on the prediction accuracy of the model provided they are not grossly overestimated. In contrast, the potassium selectivity coefficient must be accurately determined within a narrow range if the error is to be kept in the region of a few %.
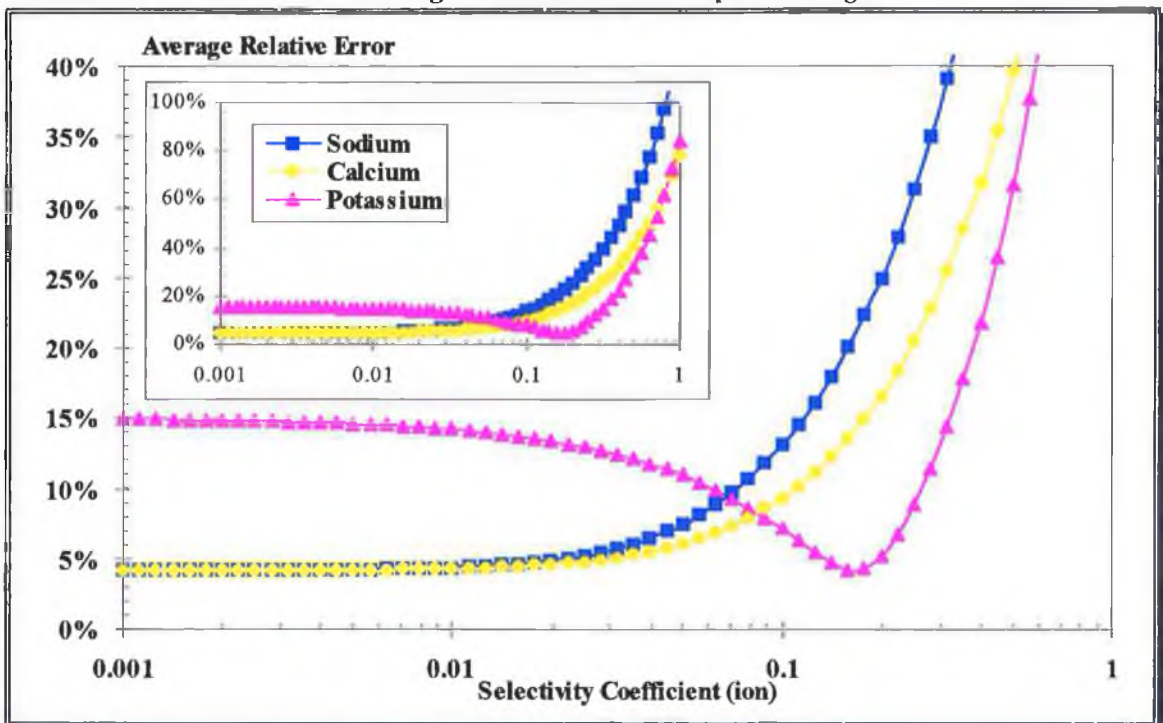
Once again, the potassium selectivity constant is seen to be the most critical. However, unlike Figure 4.8, the error is seen to rise sharply on either side of a rather narrow optimum region where the average relative error drops to less than 4%, suggesting that the potassium selectivity coefficient must be fairly precisely defined for accurate compensation of the signal. In a related manner, we can predict that variations in the potassium activity will have a similar effect on the error of the NH_4^+-selective electrode predictions unless an integrated sensing system capable of automatic decoupling and correction of interferent signals is used. The other selectivity constants once again have relatively little effect unless they are grossly over-estimated.

However, neglecting the potassium selectivity constant leads to an average relative error over the 24 solutions of around 15%, which is unacceptable for analytical purposes. Curiously, the optimum value for the potassium selectivity constant in this case is slightly different than in Figure 4.8. This is a consequence of the manner in which the data are processed, as the calculation of the correlation coefficient involves minimisation of the predicted vs. known NH_4^+ activities in the plane of the correlation line, whereas the relative error involves only a minimisation of the difference in the two data sets. From this we can also conclude that the values of the optimised selectivity constants are a function of the parameter chosen for minimisation.

Together with the other factors influencing the values of selectivity constants mentioned earlier, it leads us to the inevitable conclusion that there is no global value for a selectivity constant, but rather a value which can be treated as a constant for a more or

less limited range of conditions. However, because of the experimental design employed and removal of the charge differential problem in the Nikolskii-Eisenman equation, these limits are much broader than for conventional selectivity coefficients.

4.2.6 Conclusions

By using a FIA-SAD approach, it is possible to model accurately sensor characteristics and de-couple matrix-dependent errors from the true primary ion signal thereby greatly reducing bias and primary ion concentration dependent errors in analytical determinations with ISEs. The array approach enables accurate, multicomponent analyses to be performed, even in real-time monitoring of samples where the ion content is fluctuating widely. Provided the model characteristics remain stable, it should be possible to employ moderately selective electrodes is situations where the lack of selectivity has hitherto rendered them unusable.

Modification of the Nikolskii-Eisenman equation has enabled selectivity constants to be defined which are independent of charge differential effects. This is important for the realisation of the array model, as the model parameters can only be constants in a two-level calibration design. Some of the advantages of this approach are;

Model parameters, including *conditional* selectivity constants for ions which contribute significantly to the overall signal, can be estimated with good precision. In general, the precision in the estimation of a parameter is proportional to its importance in the final ISE model;

- These selectivity constants can be easily converted according to Eq. 3.4 to give the conventional selectivity coefficient at a particular interfering ion and primary ion activity;

- FIA enables more precise measurements of electrode responses to be made, and allows for very reproducible sampling;

- The array detector and stable model characteristics enable multicomponent analysis to be performed in real time with automatic detection and compensation for matrix variations.

These "integrated sensing systems" will allow for much more robust and reliable measurements to be performed than is possible with single sensors. Given the tremendous progress being made in nano- and micro-sensor fabrication technologies, in the controlled deposition of ordered membranes, in new surface imaging techniques (vital for quality control on the nano scale) and in the miniaturisation of instrumentation, we can look forward to new generations of intelligent sensing systems capable of returning high quality analytical data and on-line diagnosis of system performance, perhaps in the not-too-distant future.

4.3 References

[1] Commission of the European Communities. Directorate-General Environment, Nuclear Safety and Civil Protection *"European Community Environment Legislation"* Office for the Official Publications of the European Communities, Luxemberg, **1992**, *vol. 7.*

[2] Commission of the European Communities. Directorate-General Environment, Nuclear Safety and Civil Protection *"European Community Environment Legislation"* Office for the Official Publications of the European Communities, Luxemberg, **1992**, *vol. 6.*

[3] Davies, O. G.; Moody, G. J.; Thomas, J. D. R. *Analyst* **1988**, *113*, 497.

[4] Sáez de Viteri, F. J.; Diamond, D. *Analyst* **1994**, *119*, 749-758.

[5] Sáez de Viteri, F. J.; Diamond, D. *Electroanalysis* **1994**, *6*, 9-16.

[6] Weast, R. C. Ed. *"Handbook of Chemistry and Physics"*, The Chemical Rubber Co., Cleveland, Ohio, 53th ed, F-177.

[7] Diamond D., Svehla G., Seward E.M.,and McKervey M.A., *Anal. Chim. Acta.*, **1988**, *204*, 223-231.

[8] Cadogan A., Diamond D., Smyth M.R., Deasy M., McKervey M.A. and Harris S.J., *Analyst*, **1989** *114* 1551.

[9] McKervey M.A., Seward E.M., Ferguson G., Ruhl B. and Harris S.J., *J. Chem. Soc., Chem. Com.*, **1985**, 388.

[10] Morgan, E.; Burton, K. W.; Church, P. A. *Chemometrics and Intelligent Laboratory Systems* **1989**, *5*, 283.

[11] Martell, A. E. *"Stability Constants. Suplement No.1"* The Chemical Society, London, **1971**, p. 353.

[12] Gorry, P. A. *Anal. Chem.* **1990**, *62*, 570-573.

[13] Forster, R. J.; Diamond. D. *Anal. Chem.* **1992**, *64*, 1721.

[14] Diamond D.; *Anal. Chim. Acta*, **1993**, *276*, 75.

[15] Forster, R. J.; Reagan, F.; Diamond, D. *Anal. Chem.* **1991**, *63*, 876-882.

[16] Diamond, D.; Lu, J.; Chen, Q.; Wang, J. *Anal. Chim. Acta* **1993**, *281*, 629.

5. LabVIEW Graphical Programming Environment

5.1 Introduction

Since computers were invented there has been a continuous evolution of the way execution tasks are programmed so processors can understand them. From low level code like Assembly, to the higher level ones like BASIC the structure of the programme was always sequential command-oriented code. This linearity is closely related to the manner in which computers work. In contrast, object oriented code tried to push the programming structure more to the human side. Linear command lines were replaced by linear object lines, which was an improvement. But the linearity still remained.

With the development of visual object oriented languages the programmer had a new programming structure available which was more human-oriented. This eliminated the need for the programmers to design computer-wise software and enabled a more human way of programming. Objects, graphics, system diagrams or flow diagrams were amongst the new programming tools the user was provided with. These tools made programming much easier, with less need for complicated syntax or long lists of commands. Of course there is still some kind of training for prospective programmers

before being able to design programmes, but this is much reduced. With these visual programming languages, it is the computer which makes the effort to approach the structure of the human mind and thereby greatly simplifying the programming task.

By using one of these languages, G, within the development environment, a programmer is able to structure the programme in a flow diagram fashion. The environment then translates the diagram into source code so the computer microprocessor can understand the commands. Much has changed in the engineering and scientific community, specially for software programmers, with the development of these languages. In particular, LabVIEW can change dramatically the way scientists and engineers approach the development of software for their acquisition and control processes. Software controlled instruments will never be the same.

5.2 *Virtual Instruments vs. Real Instruments*

An *instrument* can be described as a tool which performs or helps to perform a particular function or task. Traditionally these tools take the form of machines or devices of various complexities which enable some kind of improvement in the realisation of a specific job. For the analytical chemist, these devices range from a simple pH meter to the most complex NMR spectrometer or chromatograph. When these instruments are designed in a stand-alone fashion, i.e. all the functions specific for that instrument (detection, data processing and/or data presentation) are solely performed by the instrument's hardware, they may be defined as *Real Instruments*.

Virtual Instruments (VIs), on the other hand are, to quote Michael Santori from the National Instruments Corporation, "instruments whose general functions and capabilities are determined in software"[1]. These VIs often meet the requirements for laboratory automation, like ease of use, intuitiveness, flexibility, error checking and analysis capabilities[2] better than their extremely expensive real instrument counterparts. Data networking and communications is another desirable feature which can easily built into laboratory VIs. Nowadays it is also very common for these virtual instruments to have some kind of graphical representation displayed on the computer's VDU which resembles the control panel of an equivalent physical or real instrument, and provides the instrument-user interface. The concept of VI was born in the early 1970s when the microprocessor technology allowed the function of an instrument to be changed by

Figure 5.1: Virtual Instruments
a) VI for basic signal acquisition and control of low level sensors/actuators with no previous signal processing or pre-treatment. b) Higher level communication is established to acquire data and control a complex instrument with built in processing characteristics.
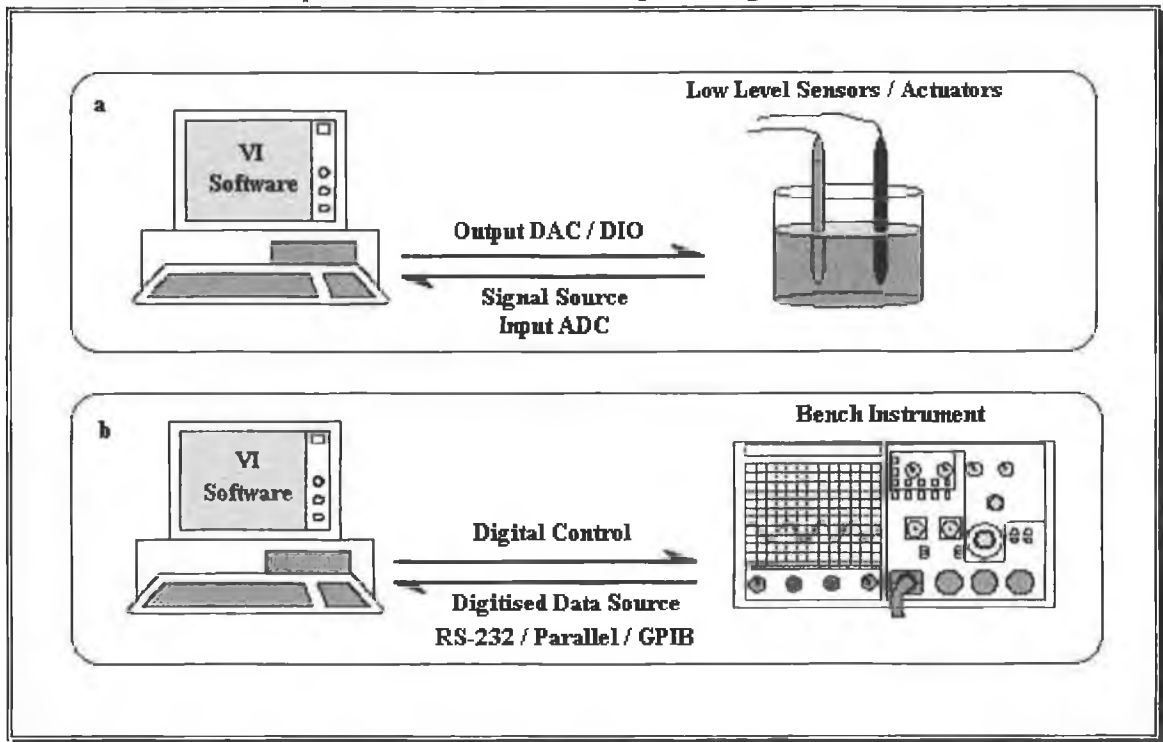
changing its software.

Figure 5.1 describes two very different VIs in terms of the level of instrumentation and control needed which probably represent the two possible extremes. The first case (Figure 5.1a) shows an instrument where the bulk of the processing is supported by the computer software. The non existence of electronic circuits for signal pre-treatment and Digital Signal Processing (DSP) or even mere signal digitisers means that the raw signal acquired *via* an I/O board will be processed by the VI software solely in a digital manner. This type of approach is typical of situations were the system to be computerised contains hi-tech sensors or actuators only, with no additional hardware.

The other extreme (Figure 5.1b) represents a virtual instrument where the electronic circuitry supports the a great number of signal pre-treatment and processing routines. Data are passed to the VI software usually through serial, parallel or GPIB communication devices and its manipulation is almost finished (if not completely) when they reach the computer. This approach corresponds to systems where data are required to be stored in digital format, or where further processing, which is not supported by the electronic circuitry, is desirable. Also, remote data logging and control, as well as "intelligent" automation or connection to a site wide communications network may be among the reasons for choosing a VI set-up.

There are a great variety of cases lying between these extremes, and the conformation of the virtual instrument will depend on the target application and the equipment available. Chapter 6 describes in detail three Virtual instruments designed for different applications,

which can be considered to belong to different points in the scale between the two cases described above.

The electronics level is where one of the main differences between both types of instruments arises. In real instruments, the hardware is specifically designed for a particular task, and in complex systems which support data processing and calculations these are implemented with electronic processors, often expensive, hardwired in the circuits. In a virtual instrument the electronic (real) support is formed by conventional computer hardware fabricated on a very large scale (more cost effective) and which is not specific of any application in particular.

The fact that different manufacturers offer the same products or similar hardware with equivalent features, and recent decreases in the cost of major components has generated a situation where the retail prices of these products has dropped dramatically, the user being the ultimate beneficiary of these circumstances. This situation does not happen with real instruments because the companies which sell these instruments usually maintain links with the customer through technical support teams which are expensive to run. This cost is returned to the company by a surcharge on the instrument price, and also on the consumables, parts and technical service directly linked to the use of such instrument, of which the company is often the only supplier. Thus, the virtual instrument approach appears as a much more cost effective user solution than the expensive high performance real instrument based solutions.

Because the virtual instrument has to rely on the computational power of the computer's microprocessor, these kind of instruments may be slower than real instruments as these may have more than one processor working in parallel to simultaneously run sub-processes, therefore reducing the system's execution time.

The speed performance of the virtual instrument can be improved by using machine code, assembly or other low level compiled languages but it is generally accepted that software driven operations execute slower than physically hardwired processes. However, one must keep in mind that software supported processes are very often much simpler and easier to implement than electronic routines which, in addition, are limited in the complexity of calculations they can physically perform. Computer microprocessors can support highly complex calculation routines which enables the development of virtual instruments which can be more comprehensive in terms of data processing or Digital Signal Processing (DSP) than real instruments. In fact, some very high performance real instruments are so limited in the functions they perform that very often the data has to be re-imported into a microcomputer for further analysis.

Even if the software execution time is lower than the required speed for a particular application, it is possible, in some cases, to delegate the instrument control to the computer hardware and, in so doing, increasing the execution performance to a degree similar to hardware speed. Many of the interfacing hardware designs for virtual instrumentation already have on-board additional processors, apart from those built-in

the host computer, which enables execution times that match, and even improve, the speed of the real instruments.

Flexibility is a term that describes another very important feature of virtual instrumentation. Because the hardware used is general purpose, the same equipment can adopt different identities depending on the software. With an operation as simple as changing the software running in the computer (and maybe some input signals) the system can be converted in a completely different instrument in a matter of minutes. Thus, the physical support, which is usually the most expensive part of an instrument, can be reused time after time for completely different applications. For example, the same hardware can be used to perform frequency analysis with Surface Acoustic Wave (SAW) devices, for FIA acquisition and control, or for testing electronic equipment. This is a great advantage for research applications, where a particular instrument is needed for short periods of time at irregular occasions. In addition, with the new micro and nanotechnology available for instrumentation, a portable notebook or laptop provided with the proper hardware and software can be the physical support for a large number of different VIs stored in the computer's hard drive.

An additional advantage of using virtual instrumentation is the possibility of accessing all the features of the computer world like compact data storage, colour printouts, networking, or telecommunications and state-of-the-art multimedia technology. Besides, one must not forget that the computer which supports the VI can still be used for any

other traditional computer applications like general office work, spreadsheets and databases.

5.3 New Trends in VI Programming

The rapid change in the world of computers over the last ten years has made very high power microcomputers readily available. This has produced a dramatic change in the way virtual instruments are designed and an even more dramatic in the way these VIs recreate the real instruments.

Probably the clearest trend since the VI first appeared is the continuous search for a higher degree of user friendliness in the software that supports the VI. A very long way has been traveled since those user unfriendly systems, barely considered as VIs[*], which could trigger the reception of data into the PC through a serial port or a GPIB card and produce a graphical display in the computer's VDU. For example, using QuickBASIC for DOS one could still select parameters and receive a visual display of data as with a real instrument, but without the support of graphical object libraries the creation of a virtual user interface was very time consuming and technically difficult.

It was not until the release of high level compilers like LabWINDOWS (Section 0) for DOS that proper Graphical User Interface (GUI) could be generated with an acceptable

---

[*] Throughout this research, Virtual Instruments are considered as instruments which present characteristic features or functions defined and implemented by software code stored in RAM memory and executed by a non-dedicated processor.

level of programming effort. Specifically designed for virtual instrumentation, its high level graphical objects allowed the programmer to create a representation of the instrument (switches, knobs & buttons) in the computer's VDU by using ready-made libraries as objects. These libraries controlled the shape and position of these objects on the screen, allowing the creation of very graphical and intuitive virtual instruments. The programme core and the graphic subroutines were still designed in traditional line code languages (QuickBASIC and QuickC), and even though the libraries did ease the burden of creating the graphics, programming and debugging the software was as laborious as for traditional languages.

WINDOWS and the general purpose visual compilers for different languages provided a graphical operating system with a ready-to-use graphical environment which enabled the creation of higher quality and homogeneous GUI for the development of virtual instrumentation. This was another step towards the generation of very user friendly and highly intuitive VIs with a realistic instrument-like user interface. But even though the improvement in graphic capability, intuitiveness and user friendliness was commendable, the complexity of the programming technique increased as the graphic objects and the programme core had to be linked *via* system subroutines. Once again, all the effort was focused on developing high quality GUI and very little on the programming side of the virtual instrumentation and much expertise was still needed for VI programming.

The graphical compiler LabVIEW from National Instruments represented an important breakthrough in this continuous trend towards increasing user friendliness, and actually

included some *programmer friendliness* in the design environment. Even from the very first interpreted release in 1986 (for Apple Macintosh), LabVIEW demonstrated how graphical programming could be as powerful as the traditional code-based languages and substantially ease the programmer's work. The latest versions of LabVIEW for WINDOWS are compiled, generating machine code which can speed up the applications up to 300% compared with the initial release[3]. It enables the design of very high quality GUI with superb graphics. The graphical programming environment, which is highly intuitive and very user friendly, provides a very good support for graphical programming, debugging and application development in general.

5.4 LabVIEW Graphical Programming for Instrumentation

LabVIEW as a graphical programming language for instrumentation was the first serious attempt to generate a programming environment which was friendly both at the user and the programmer level. Despite some initial scepticism in the graphical technique[4], favourable reviews[5,6,7,8] as well as a growing number of applications and user solution reports[9] established LabVIEW as a serious tool in the world of scientific and engineering instrumentation.

The concept of LabVIEW (Laboratory Virtual Instrument Engineering Workbench)[10] was devised by James J. Truchard and Jeffrey L. Kodosky of National Instruments,

Austin TX, USA, at a time when scientists and engineers still had to spend days working on their microcomputer controlled instruments to obtain the simplest of measurements.

They thought that in the same way that financial planners were able to program complex operations in seconds in a spreadsheet with little or no technical computer knowledge, scientists and engineers needed some similar aid to simplify the development of their test and measurement systems. Languages like BASIC and C had very good features, but the scientist had to learn the language and be a programmer before being able to be a user.

Truchard and Kodosky already had some experience with virtual instruments[1] and developed the idea that changing the software could change the system's functionality. But designing the software was not as easy as it should be. Also, the most effective systems were those that could perform tasks at different levels of complexity, allowing simple test functions at low system level and providing the option to combine these operations to conform a much more complex experimental set-up.

A hierarchy of virtual instruments where all the VIs are constructed and designed in the same way was the structural basis for a LabVIEW VI. Each of the virtual instruments had to have its own user interface so that the user could interact at low level with that particular VI by just calling it. This user interface should be a picture of the instrument's front panel, as it is probably the most intuitive graphical representation of a real instrument. The programming language also had to be as intuitive as the user interface. Existing programming languages provided, indeed, low level of intuitiveness, and Kodosky thought that the same way that business people represent data in rows and

columns the engineers represent their systems as block diagrams, and so should they while programming.

After deciding that the programming technique should be graphical and structured in a similar way to block or flow diagrams the development of the programming language G began. In designing the language, a number of serious set-backs arose when trying to represent important programming concepts, like FOR...NEXT and WHILE loops, in a graphical manner. Sequential execution of software blocks was another big problem encountered when developing the programming language which had to provide standard programming features, as a line structured language, but in a flow diagram-structured graphical code.

The software development team also ran into problems with the 512K memory limit available in the early Macintosh, as it was not enough to implement all the graphical language features that were necessary. The introduction of the Macintosh Plus with 1M RAM memory permitted the completion of the first version of LabVIEW which was released in October 1986.

Since then LabVIEW has been redesigned to compile the G language code instead of interpreting it. The newer versions improve the earlier ones in execution speed, in development features and user friendliness, and are available also for Sun Workstations and IBM PC compatibles[11,12]. One of the most important features of the last releases (LabVIEW 3.0 and 3.1 for WINDOWS) is that they are able to compile the code and generate stand-alone executable files which can run under WINDOWS in any PC with

the sufficient hardware characteristics, eliminating the need for the LabVIEW environment to be present.

5.4.1 The Programming Technique

Designing a VI with LabVIEW is very different to programming with a traditional line-code type language or some of the visual compilers for WINDOWS in which the programmer must be concerned with the correct structure of the programme and the right syntax for the commands. Software development with LabVIEW requires particular attention to the flow of data among structures, functions and subVIs and controlling the triggering of events from the VI's front panel. The programmer graphically organises blocks of code of different complexity (very often reduced to subVIs) to complete a computer programme as if it was an electronic circuit of some sort. The resulting graphical code must be able to relate the representation of the instrument in the front panel with the succession of events that occur outside the computer, in the real world.

This section does not intend, by any means, to be a programming manual for the graphical language and will only describe in general terms some of the characteristics of this graphical compiler and its utilisation. LabVIEW manuals[13] and tutorials[14], as well as dedicated literature[15] provide in-depth information about the use, at programmer's level, of the environment.

5.4.1.1 VI Front Panel

The front panel contains the graphical representation of the physical instrument. It can resemble the instrument as a copy of the controls and indicators of the instrument's panel but this is not a rule. In fact, many VIs are fictional designs of instruments which do not exist at all, and the programmers imagination, organisation skills and artistic sense do the rest. A good practice for VI front panel design is organising related functions in blocks which contain the appropriate controls and indicators.

The objects in the front panel can be actuated either from the keyboard (in a sequential mode) or with a pointer (randomly), typically a mouse. Run-time and design-time pop-up menus allow both the programmer and user to select among different options to adjust the functioning of the object to the application's needs.

For those virtual instruments which will be used as subVIs, some (or all) of the controls and indicators built in the panel can be related to terminals in the VI's icon. This icon will represent the overall VI when used in a higher hierarchy VI.

5.4.1.2 VI Code Diagram

The code diagram can be considered as the soul of the VI, as it controls and links the interaction between the user and the front panel and between the hardware and real world.

Basically, designing the software code in G involves organising a series of graphical functions, subVIs and variables in structures (Figure 5.2) and then linking them together

with "wires" to program the data flow among them. The wires are case sensitive as they automatically change colour and shape depending on the data structure and the data type they represent. Different colours for integers and real numbers, strings, booleans etc., enable easy identification of the data type being used. Different wire patterns or thicknesses will also identify clusters, arrays (and dimensions), etc. The result is a electronic circuit-like diagram which is compiled to machine code for execution.

Functions, subVIs, and diagram nodes in general support pop-up menus which allow the programmer to change the node parameters, characteristics and run-time execution features. This are also present for the objects in the front panel which allow the selection of numeric type, precision, scales, etc.

In some cases, where heavy numerical processing or special computational processes are required, or if these processes are already written in line-code languages (ANSI C), there is the possibility of linking the graphical code in G to these routines through Code

Figure 5.2: Main Programming structures in G.
a) TRUE/FALSE structure executes only one of the cases depending on the value passed to the control [?]. b) FOR...NEXT loop executes a number of times corresponding to the value input to the control N. The control [i] serves as loop index. c) Executes continuously until the value passed to the control is FALSE. [i] serves as index. d) executes all of a number of frames in sequential order. Values are not passed to other functions or structures until all the sequences are complete.
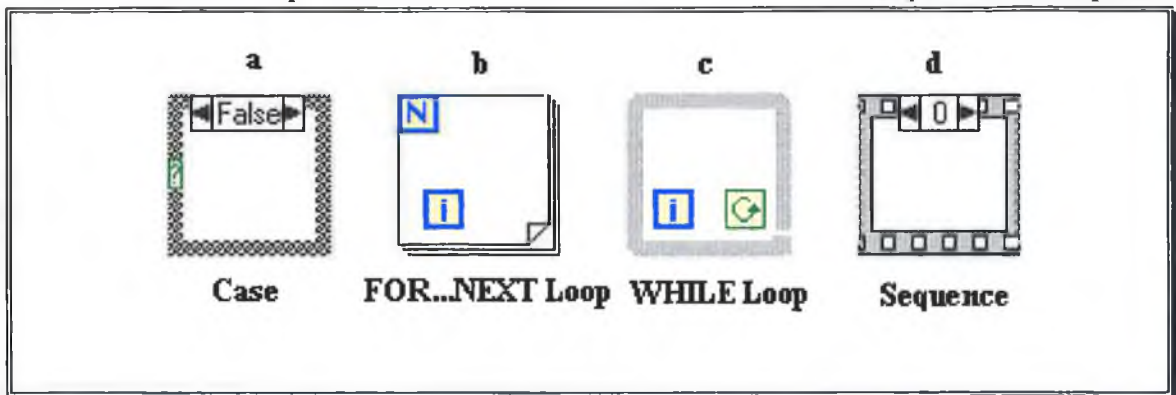
Interface Nodes (CINs). These objects in the diagram behave the same way as functions, operations and subVIs, with a number of data lines as input to the CIN's terminals, and a number of output connections as newly generated data.

5.4.1.3 VI Hierarchy Icon

The hierarchical structure of the LabVIEW applications gives this package the flexibility of using low-level VIs to perform routine check or simple functions as well as permitting the building of more complex system based in these same simpler subVIs.

This is the function of the VI icon. The input and output characteristics are represented in a square box with some text or picture to identify it. Then, the VI can be used in the code diagram of a higher order VI to perform a function or operation as a "black box", with the important difference that this box can be opened, either at design-time or at run-time, to give information about the process being executed inside.

The schematics in Figure 5.3 shows an example of the above. The front panel (A) for a VI is designed to control the functions of the peristaltic pump described in previous sections. The representations of the controls in the code diagram are wired to a subVI which controls the signal output operations (B). This subVI is loaded from the hard drive through the pop-up menu as if it was a part of the environment. The icon can either show the picture representation or the terminal connections for wiring purposes.
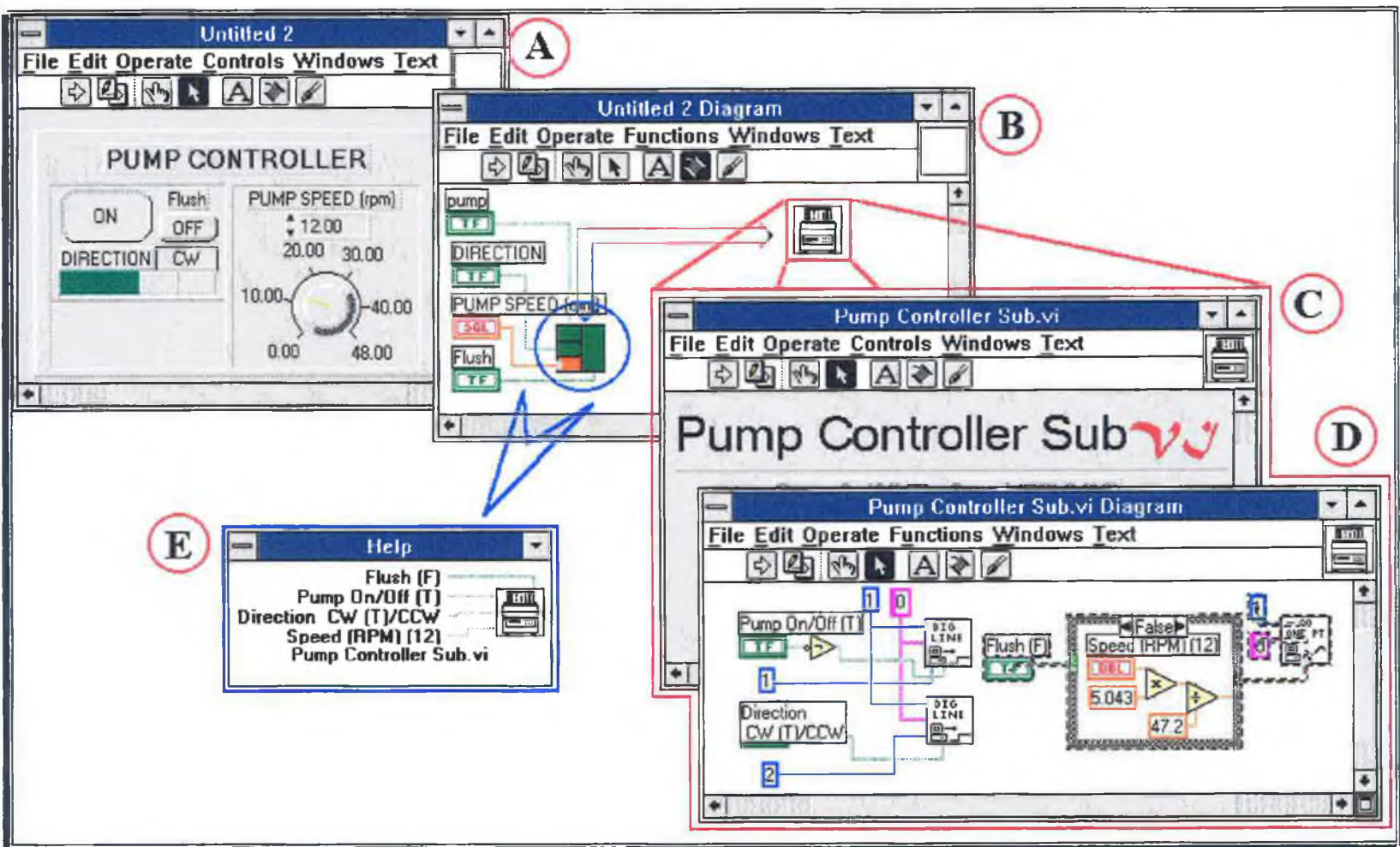
Figure 5.3: Hierarchical structure of the LabVIEW VIs.
This programming structure gives LabVIEW high flexibility and enables running the VIs independently at different levels. See text for diagram explanation.

By double-clicking on the box the subVI (C) front panel pops-up showing the controls. These are linked to the subVIs code diagram (D) which contains the graphical code for the pump control and which can be displayed by calling the diagram window. If the mouse is placed on the subVI box, the help window (E) displays the information concerning the subVI and identifies which variables, and the variable type, to be connected to the terminals.

5.4.2 The Graphical Programming Environment

The programming language G is a very high level language which needs a design support tool for software development and a translator to convert the graphic code into machine code which can be understood by the computer. These two features are only present in the full development package (run-time environment only supports translation into machine code) which runs under WINDOWS environment.

5.4.2.1 *Front Panel Design Window*

This design page appears as the active window when LabVIEW is launched and it contains the graphic objects which form the VIs GUI. During development this window shows a menu and a control bar. The menu allows the user to actuate some of the traditional WINDOWS options, and the control bar will actuate the options and functions specific for the design environment. The main features of this environment are the design windows for the VI front panel and VI code diagram, and the help window. There is also a control development tool and an editor for VI icon design

A mouse-controlled pup-up menu enables the selection of objects, controls and indicators, which will be included in the VI front panel. These objects are primarily divided into categories depending on its structure (numeric, boolean, array & cluster, graph, etc.) which present a wide variety of ready to use options. Most of them can be selected as data input (control) or data output (indicator), and they can be customised in terms of their mechanical action (switch, latch) for boolean controls or their data representation (integer, word, long word) for numeric controls and indicators. The front panel objects can also be customised in terms of appearance, scales, shape and colours. Panel decorations are also available from the menu. A editing tool is also available for the

Figure 5.4: Design-time VI front panel.
The front panel which represents the real instrument is designed by organising the different controls and indicators available in the development environment to produce a graphical interface with the user. The front panel controls the execution of the programme and also displays the information.
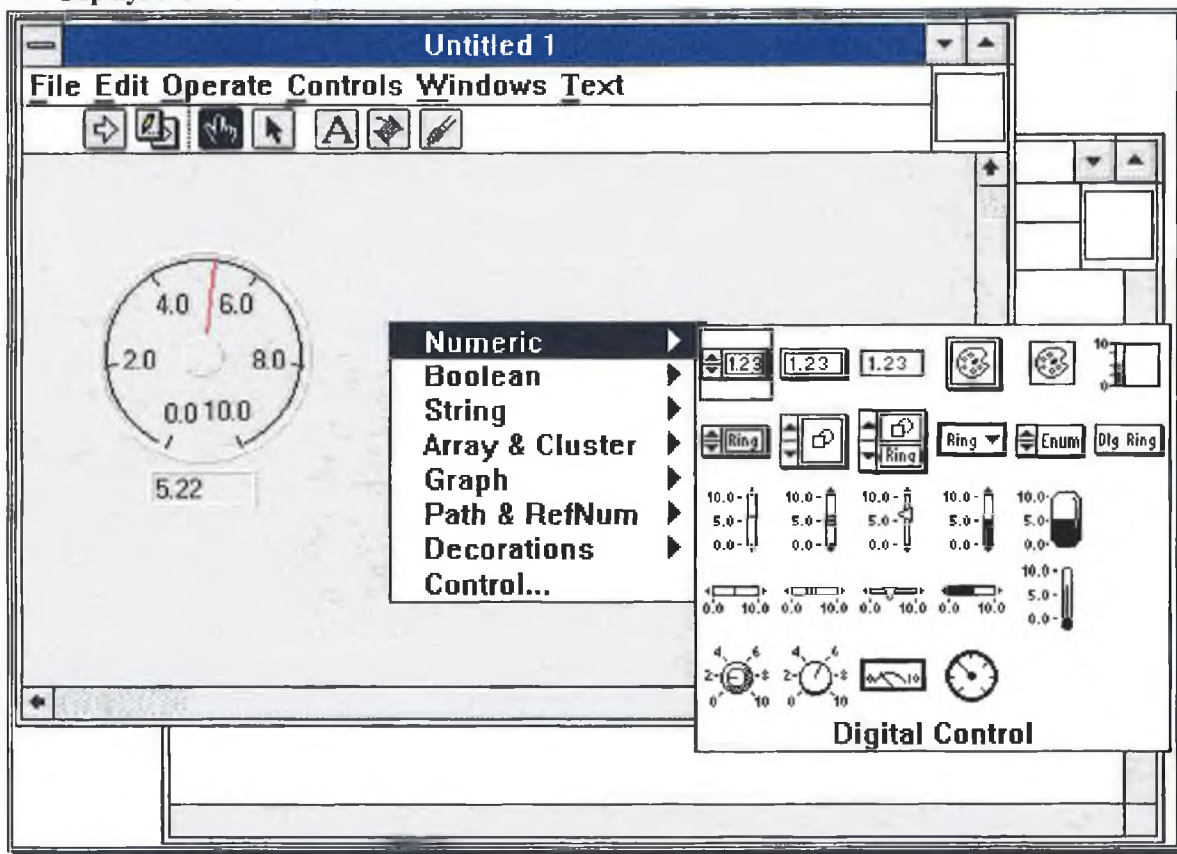
special design of controls or indicators which are not present in the standard selection. Once designed, these objects are integrated into the development environment as if they originally came with the commercial package.

Figure 5.4 shows the VI front panel during development. The pop-up menu showing the options from the numeric category gives an idea of the multi-level menus used for object selection. The window in the background is the VI's code diagram window.

The upper right corner of the panel window presents a blank square, the VI icon, which represents the whole VI when it is used as a subroutine. The characteristics and options of the VI when working as a subVI are determined and edited from the front panel activating the VI's icon. The correspondence between panel objects and icon terminals, as well as the different parameters and options available to the VI when it runs as a subVI are also edited from the front panel. The appearance of the icon can also be changed at this time with a pop-up graphical editor especially designed for this purpose.

5.4.2.2 Code Diagram Design Window

The window for designing the VI code is very similar to the one for developing the front panel in the way the functions, options and different features are used. In this case, the pop-up menu contains the structures, functions, constants and routines or subVIs which will be used for developing the code. These objects are also classified in categories, as Figure 5.5 shows, some of which come with the original development package or are included as add-ins, or developed at some stage by the user. In this last case, as it

happens with the user designed controls, the new subVIs are completely integrated in the

system and can be used in the same fashion as original or add-in functions and subVIs.

Figure 5.5: Design-time VI diagram.
The LabVIEW code is designed by connecting together functions and subVIs to produce a higher order VI or main programme. Functions and subVIs are available from the environment.
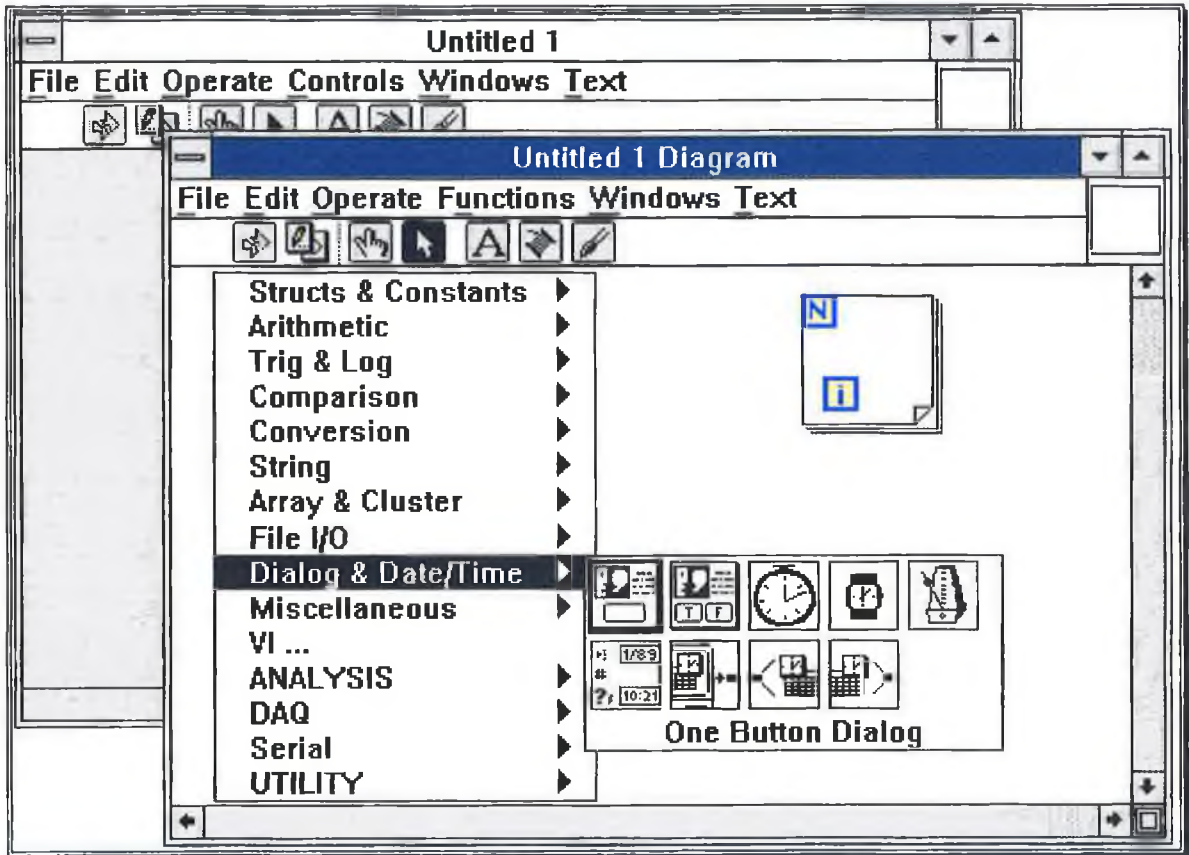
The functions selected for the software code are connected together using the "solder" tool from the icons in the control bar, which draws a "wire" through which data may pass between functions. The arrow in the same bar indicates errors in the programme. A broken arrow will tell the programmer that the code will not compile, and will also display information on the whereabouts of the errors encountered. If the arrow is solid the code is ready to execute. For debugging purposes the environment presents a series

of tools which allow step by step execution of the code, animated data flowing features and a probing system which displays the value of a particular wire at all times.

Among other characteristics, the design window features function replication, wire stretching, cut, copy and paste and other editing options.

5.4.2.3 Help Window

The LabVIEW help facility is shown as an "always-on-top" window which displays information on the functions and subVIs in the diagram window. It shows a case sensitive display of the function's features, like a general task description, options which may be available, and also a description of the functionality of each of the object's terminals and the correct type of data that must be wired to them for the function to operate properly.

Figure 5.6: Design-time Help window.
The environment help window feeds information back to the user about the function or subVI job and also the data lines the node needs connected to function properly. Different coloured lines indicate different data types.
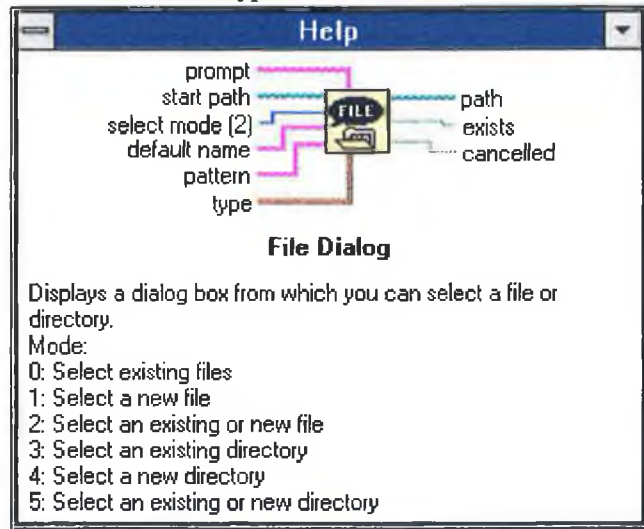
Figure 5.6 shows the help window displaying information about a subVI which features a file dialog for data save or data retrieval operations. Each of the function terminals show a description of the data and the type they accept. The terminals with the description on the left are data inputs, and those on the right are data outputs from the subVI.

The run-time help window displays information about the front panel objects and the operations they perform when actuated. This is optional and will depend on the degree of development the programmer decided at design-time.

5.4.3 Flexibility for Instrumentation and Control

The features LabVIEW designed programmes present offer high flexibility in the areas of hardware and software. The most important characteristic is the possibility to convert the hardware into completely different instrument with an operation as simple operation as loading a different programme. Even if this is a general characteristic of virtual instruments, it is accentuated in the case of LabVIEW designed VIs as they are hardware independent. In other words, a VI designed for use with a particular I/O board may be used with other I/O boards (provided they have the required functionality) simply by installing the appropriate driver for that board. In the same manner as Word for WINDOWS is independent of the printer that may be attached to the PC.

The most recent versions of LabVIEW offer the possibility of developing executable files with the compiled code which will run in a suitable computer and WINDOWS with no need for a run-time environment. As the applications can run independently, only one

development station with the LabVIEW development environment is needed per location, and the applications are allowed, by the licence agreement, to be freely distributed within the site.

The inherent hierarchical structure of the LabVIEW programmes enable the user to access and operate subVIs as main programmes. Low level system testing and debugging is much easier as the part of the system the user is interested in can be isolated. For more complex user solutions, these VIs can be organised as a subVI to create a higher order applications.

There is an extensive range of commercially available add-in LabVIEW library modules which increase the power of the basic LabVIEW design environment in terms of subVI availability. Data visualisation, data analysis, data acquisition and control or custom display toolkits are among these available add-in libraries.

With the development of new microtechnology for portable PC microcomputers like the PCMCIA plug-in acquisition boards, the notebook computer can be converted in an all purpose instrument running a whole variety of virtual instruments for different applications through the same I/O board. Hence, a standard notebook can be transformed into a simple voltage reader or a complex oscilloscope by just loading the appropriate LabVIEW application.

5.5 References

[1] Santori, M *IEEE Spectrum* Aug. **1990**, 36.

[2] Doubrava, C.; Kay, M. *International Laboratory* **1994**, *(24)*, 24-28.

[3] Mosley, j: D. *EDN* Sept. 15, **1988**, 134.

[4] Reinhardt, A. *BYTE* **1992**, *Sept.*, 63-66.

[5] McCarty, L. H. *Design News* May **1990**, 72

[6] Conquergood, S. *I&CS* January **1993**,68.

[7] Barber, J. *INTECH* **1989**, *Sept.*, p80.

[8] Johnson, K. *IEEE Spectrum* **1992**, *Oct.*, p74.

[9] *Instrumentation Newsletter* Series, National Instruments, Austin, TX, USA.

[10] Vose, G. M.; Williams, G. *BYTE* Sept. **1986**, 84.

[11] Truchard, J. *Design News* **1993**, *Apr.*, p162.

[12] Kaiser, T. *Design News* **1993**, *March*, p190.

[13] LabVIEW 3.0 manual series, National Instruments Cor., Autin, TX, USA. **1993 Ed.**

"*LabVIEW User manual*", Part No. 320534-01.

"*LabVIEW Function Reference Manual*", Part No. 320535-01.

"*LabVIEW Data Acquisition VI Reference Manual*", Part No. 320536-01.

"*LabVIEW GPIB and Serial Port VI Reference Manual*", Part No. 320537-01.

"*LabVIEW Analysis VI Reference Manual*", Part No. 320537-01.

"*LabVIEW Code Interface Reference Manual*", Part No. 320539-01.

"*LabVIEW Networking Reference Manual*", Part No. 320587-01.

[14] LabVIEW 3.0 Tutorial, National Instruments Cor., Autin, TX, USA. **1993 Ed**., Part No. 320593-01.

[15] Johnson, G. W. *"LabVIEW Graphical Programming; Practical Applications in Instrumentation and Control"* McGraw-Hill, New York, 1994.

6. LabVIEW Applications

6.1 Introduction

Almost any application which involves interfacing to instruments or devices in the physical world can benefit from the flexibility, user friendliness and power of LabVIEW. Since the first release of labVIEW in the 1980s, a continuously growing number of applications and user solutions can be found in the literature, mainly for PC and Macintosh microcomputers. Research applications for FIA[1], spectroscopy[2,3,4], polarography[5,6], electrophoresis[7] or biotechnology[8], as well as general system interfacing[9,10] and industrial solutions[11,12] have been published.

In the following sections three case studies are presented which describe virtual instrumentation designed for very different areas of application; flow-injection analysis, microdialysis and environmental monitoring.

Apart from the VIs which control I/O interfacing some other general purpose applications are also shown, which demonstrate that this different way of computer programming can be used to develop highly complex applications easily and with a very high degree of user friendliness.

6.2 Case Study I: Sensor Array Flow-Injection Analyser

This section describes improvements made on a previous version of the electrochemical sensor array instrument described in Chapter 4. This new approach takes advantage of the latest state-of-the-art hardware and software for instrumentation which enhances the flexibility of the system in terms of I/O hardware, ease of design and modifications, GUI and user friendliness[1].

Because of the programming limitations of QuickBASIC (QB), the previous version of this VI was keyboard driven, i.e. the VI functions were actuated by pressing a previously programmed key. The very low standard GUI was a consequence of the limitations of the design language available at the time, and it was limited to a simple graphic screen showing the FIA traces as they were acquired. No information about the FIA function status was displayed to the user which had to rely on other indicators like the pump's r.p.m. LCD display to calculate the flow rate, or a second "click" sound to notice that the valves in the auto injector were reset to the LOAD position.

Apart from the programming complexity of the scientific part of the VI software, the interface code to the I/O card, *via* the QuickBASIC libraries provided with the board, was very difficult and complex. The following steps were needed to properly control the card and the I/O operations;

1. Set-up Direct Access Memory (DMA) channels in the operating system for the I/O board,

2. Load and merge the card's function libraries to the QB design environment,

3. State the library routines to be used in the program, defining the arguments required for each of them,

4. Initialise routines and arguments,

5. Execute subroutines by calling and passing the right arguments with the appropriate values,

6. Read the solution argument or value handed by the routine.

In the case of analog I/O functions, the bitnumber argument (i.e. the logical number generated by the card hardware) passed by the routine had to be converted to voltage (ADC), or *vice versa* (DAC), depending on the card's hardware setup, which had to be consistent with the software definition of the routines. The I/O range of the card had to be also related to the gain used and the bitnumber type, straight binary (0 to 4095) or two's complementary (-2048 to 2047). These operations were, if not complicated, somewhat very distracting during software design

The QB VI could, because it was DOS based, run in an ENIGMA 386 SX 16 MHz PC microcomputer at a speed fast enough to match the interfacing requirements. This was probably the only advantage this VI had, but with the new high performance PC

microcomputers the software became completely obsolete. This new LabVIEW VI features all the functions the old QB software presented plus all the inherent functions and advantages of using LabVIEW as the development package.

6.2.1 System Hardware

Although the first FIA VI was designed in an ELONEX 486 66 MHz with 16 MBytes of RAM memory and a high performance 12-bit AT-MIO-16DL I/O board, when the VI was complete, debugged and tested, a WINDOWS executable application was created which would not need the LabVIEW design environment to operate. It was found that this application could run almost as fast in an ENIGMA 386 33 MHz with a 387 mathematics coprocessor and only 8 MBytes of RAM. The I/O card for this system was an AT-MIO-16H9 also from National Instruments.

The diagram in Figure 6.1 shows a schematic of the Sensor Array FIA set-up, which also illustrates linkage of the VI to commercial WINDOWS applications. The system features a Minipulse 3 peristaltic pump (Gilson Medical Electronics Inc., Middleton, WI, USA), an injector port and a SAD block for electrochemical detection as described in detail in Section 3.5.1. A PC microcomputer serves as support for the VI software and houses the plug-in acquisition card connected to the computer's bus.

A detailed diagram of the electronic circuits used for this system can be found in Appendix D.

Figure 6.1: Sensor Array FIA VI diagram.
The software programme designed in LabVIEW controls the FIA system and acquires the analytical data in standard WINDOWS format which can be imported to commercial applications for further processing. Analogue I/O is used for electrode potential reading (analogue in) and for speed pump control (analogue out). The digital ports are used for pump control and injection port actuation (digital out).
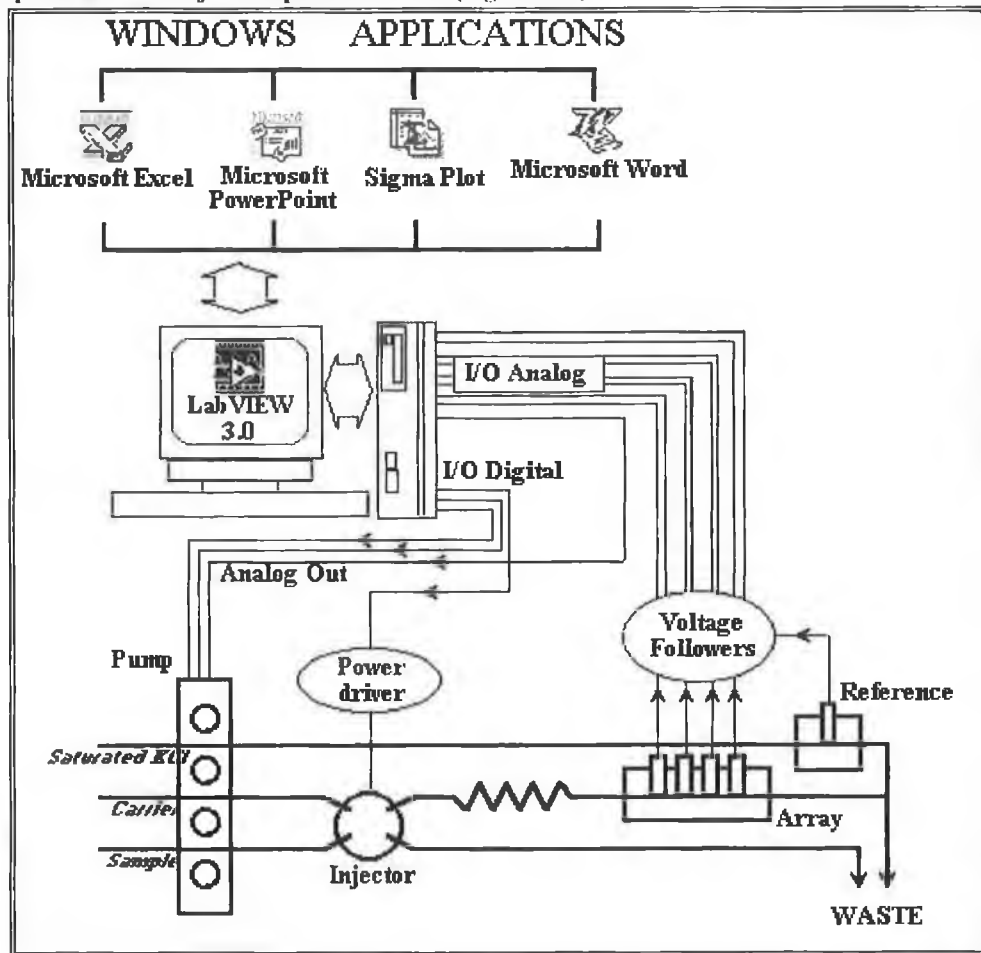
6.2.1.1 Peristaltic Pump

The pump can support up to four different flowing solutions which can be set to different

fixed flow rates using different I.D. silicon rubber tubing. It can be controlled either

manually, through RS-232 protocol or through a TTL-compatible remote port. Because

of the scarce information available on the serial control, and because the remote port was

simple to use, this approach was used for controlling the peristaltic pump. A total of

three signal pairs (2 digital HIGH/LOW and 1 analogue) are sufficient to fully control the ON/OFF, flow direction and flow rate functions, being the line low always connected to ground.

- **Flow Direction:** This function is controlled by the first signal pair, which operates the rotating direction of the pumping head. A signal of +5 volts in the line high with respect to ground will set the head rotating clockwise, sending the flow to the right of the pump. Grounding this signal the head inverts its angular velocity and the pump sends the flow to the left.

- **ON/OFF:** Line 3 (2nd pair) is in charge of the main switch of the pump. If this signal is grounded, the head rotates at a predetermined velocity. A logic +5 volts signal applied to this line stops the head motor.

- **Flow rate:** The velocity of the rotating head can be selected *via* the third pair, which also admits a global voltage difference of +5 volts between the lines high and low. In contrast to the other pairs, the applied voltage in the range 0 to 5 V is related to the angular speed of the head (0 to 48 r.p.m.). Intermediate voltage differences are accepted for particular speed selection. For example, a head velocity of 12 r.p.m. will require a related applied voltage of 1.25 volts.

6.2.1.2 Injector Port

The injector port is conformed by three 3-way solenoid valves (The Lee Company, Westbrook, CT, USA) simultaneously actuated (see Appendix B for set-up diagram).

Because the signal outputs from the card are usually low current, a power supply was used to deliver the 600 milliamps (200 mA per valve) needed to drive the autoinjector. This process was triggered from the computer through a single digital line and implemented by a quad-gated power driver integrated circuit CA 3242 E (GE Solid State, supplied by Radionics Components, Dublin, Ireland), which is required because of the low power rating of the digital I/O lines (few mA maximum).

6.2.1.3 Signal Conditioning

A second circuit for signal conditioning was designed to convert the high impedance signals from the ISEs to low impedance, reducing the possibility of environmental noise pick-up. This circuit was implemented with a series of voltage followers based on the CA 3140 AE (GE Solid State, supplied by Radionics Components, Dublin, Ireland) operational amplifiers with an overall gain of 1. The signal from each sensor is measured against a common reference electrode. This floating signal is acquired in differential mode, the signal from the ISEs being connected to the lines HIGH and the common reference to the lines LOW. A gain of 10 (input range ± 500 mV) was used which gave a measurement resolution of 0.24 mV.

6.2.2 4-Channel FIA VI

This VI controls the acquisition and remote control processes in the FIA system. Figure 6.2 shows the front panel, with the control switches on the left, and the independent channel displayed on the right. The main functions of this programme are:

- Signal acquisition. Multichannel monitoring

- System control. Pump and autoinjector actuation.

- Data display. Colour coded numerical and graphical.

- Data storage. Spreadsheet format.

Figure 6.2 shows the VI front panel during an acquisition session. The system was set to perform 10 automatic injections. The time the sample washed the injection loop was set to 30 seconds, long enough time to eliminate carry-over from high activity solutions. The reading time was set to 2.5 minutes, which allowed the signal from the sensors to return to the baseline. A fixed flow rate of 1.0 mL min^{-1} was used. The FIA traces show the response of a SAD formed by ISEs selective for lithium(1)[13], sodium, potassium and lithium(2)* (as channels 1 to 4 respectively) to a calibration solution set designed for the modeling of the response of the Na^+-ISE in an activity range focused on human plasma samples. The high and low activity levels can be appreciated in the Na^+-ISE (channel 2) as well as in the Li^+-ISE (channels 1 & 4) due to the poor selectivity these ISEs present against Na^+ ions.

Appendix E shows the code diagram for the top hierarchy VI, which controls the execution and timing for the other subVIs.

---

* The neutral carriers used for the Na^+- and K^+-selective electrodes were as described in Chapter 4. The neutral carriers for the Li^+-selective ISE(1) was a gift from Dr. David Parker, Department of Chemistry, University of Durham, Durham, U.K., and Li^+- ISE(2) was purchased from Fluka (lithium ionophore III).

6.2.2.1 Signal Acquisition

The signal from the electrodes is acquired after op-amp conditioning, in differential mode as explained in the System Hardware section. The acquisition method consists in reading independent data waves of 300 points each which are on-line processed and the average value stored in RAM. This is simultaneously run for each monitored channel, and the global overall process, repeated at a frequency of 0.5 Hz, generates the FIA traces. The system buffer is set to 8000 points, which allows continuous monitoring for over one hour before the buffer is overwritten.

The acquisition rate is software controlled, based on the computer's clock. This allows very precise control of the data sampling frequency. Besides, this feature enables the use of the VI software in computers with different architecture and speed, from the 386 DX with math processor configuration, to the fastest Pentium 66 MHz, or even higher.

6.2.2.2 System Control

The VI controls the peristaltic pump functions and the switching of the injector port. Controlling the pump from the software means sending to the I/O board the necessary instructions to generate signals compatible with the TTL-remote port available in the back of the pump. Two subVIs are accessed to implement the ON/OFF and flow direction remote options *via* digital signals which send logic TRUE/FALSE status as in the protocol explained previously.

Figure 6.2: Multichanel FIA VI.
The VI front panel is divided in two main areas. The system controls are situated at the left, which allows full control of the FIA system. On the right, independent charts show the signal traces for each of the acquired channels.
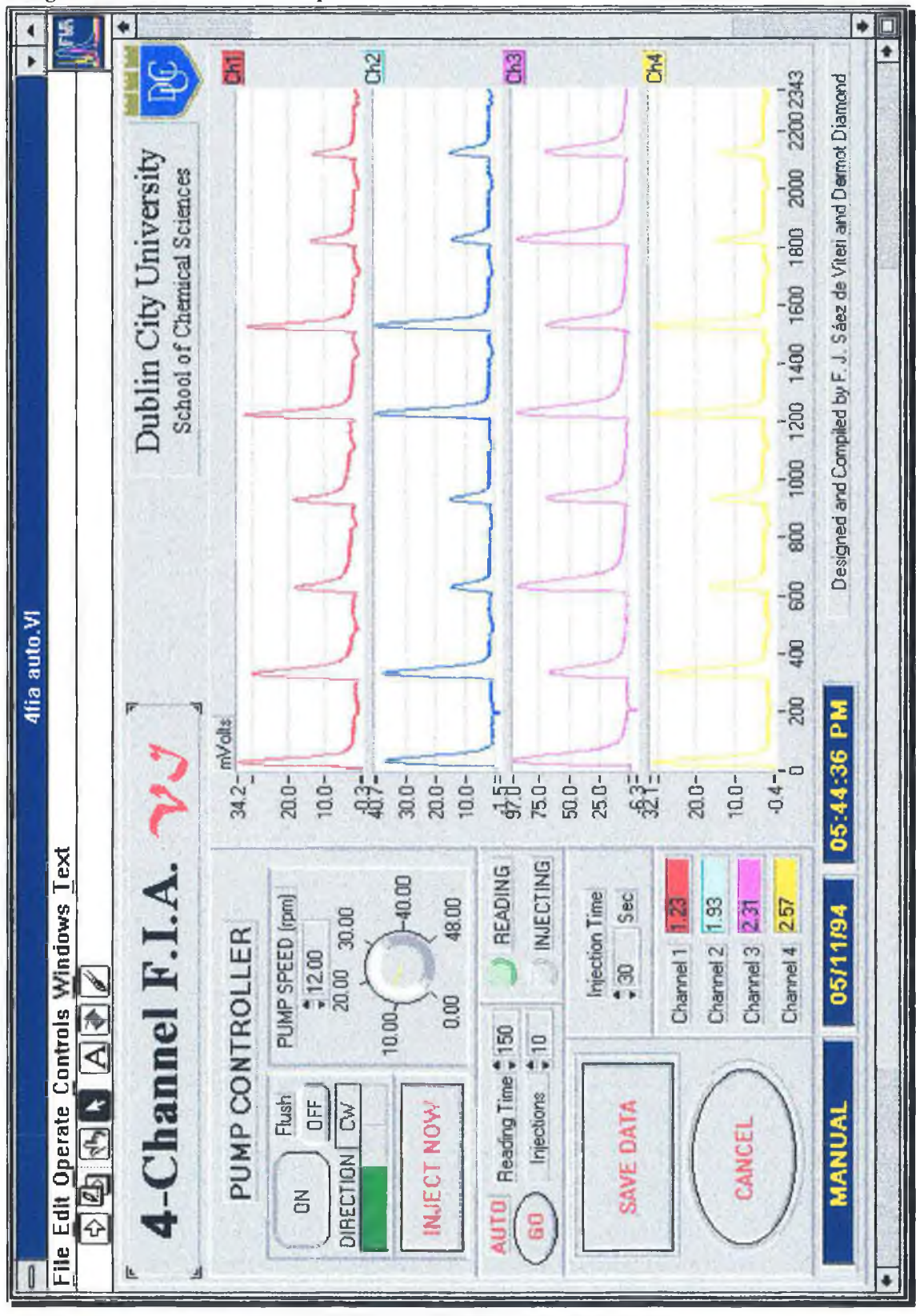
The very good linear relationship between the flow rate and the head's angular speed allows easy and precise control of the FIA flow. A typical flow rate of 1.0 mL min^{-1} (12 r.p.m.) is set as default by accessing an analogue output subVI which controls the analogue output port.

Injection port control requires only one digital out signal which actuates all three valves simultaneously through the power driver circuit. The status of the injection port (LOAD/INJECT) is controlled by the virtual instrument at all times and can be manually or automatically actuated. In the manual mode the user selects in the software when to initiate a sample injection and the duration of the sample injection. In the automatic mode the user can set parameters like the number of consecutive injections, the injection time (i.e. the time the sample is washing the injection loop) and the reading time (i.e. time between injections) as can be seen in the front panel (Figure 6.2). Control signals are updated within the main software acquisition loop, with a twice-a-second frequency.

6.2.2.3 Data Display

The data are displayed in two main ways. A numeric display gives the information of the value of the voltage input in a channel at a particular time. These data form part of a display which allows the user to graphically analyse the data input for expected features, like response peaks or baseline drift, that need to be studied over a period of time. Both data, in the numeric and in the graphical form, are related to the acquisition channel with a colour code, and they are updated as soon as the new data are acquired.

6.2.2.4 Data Storage

Data storage consists of downloading into a spreadsheet format file of the data kept in the system's RAM since the last acquisition session. The data columns, from first to fourth, correspond to channels 1 to 4 (logical channels 0 to 3) and they are separated by standard "TAB" characters. Because the acquisition rate is constant and it is not user selectable, the spacing between consecutive data is the same and there is no need for a first column containing the values for the x (time) axis. The datafiles are automatically saved into a $C:\backslash FIA$ directory and the filename is used defined, both in the name and file extension.

As an example, Figure 6.3 shows the typical Microsoft Excel window during processing of a datafile acquired and stored as mentioned above. The use of numerical and graphical display helps to easily identify and quantify points and trends in the FIA traces. The figure shows the response of a SAD to repeated injections of *LiCl* at 5×10^{-4} and 2×10^{-3} mol dm^{-3}. The position of the ISEs in the array are selective for $Li^{+}(1)$, Na^{+}, K^{-} and $Li^{+}(2)$ as described previously. Comparison of both lithium ISEs show a much smaller response of the second electrode lithium(2). This is probably caused by a higher limit of detection (LOD) for this sensor, which causes a reduction in the sensitivity as the activity levels studied approach the LOD . No response is detected for either Na^{+}- or K^{+}-ISEs.

Figure 6.3: Spreadsheet format FIA file while being processed with Microsoft EXCEL.
The availability of both graphical and numerical data facilitates analysis and graph and
report generation. Data correspond to response of a FIA-SAD system to single ion lithium
samples.
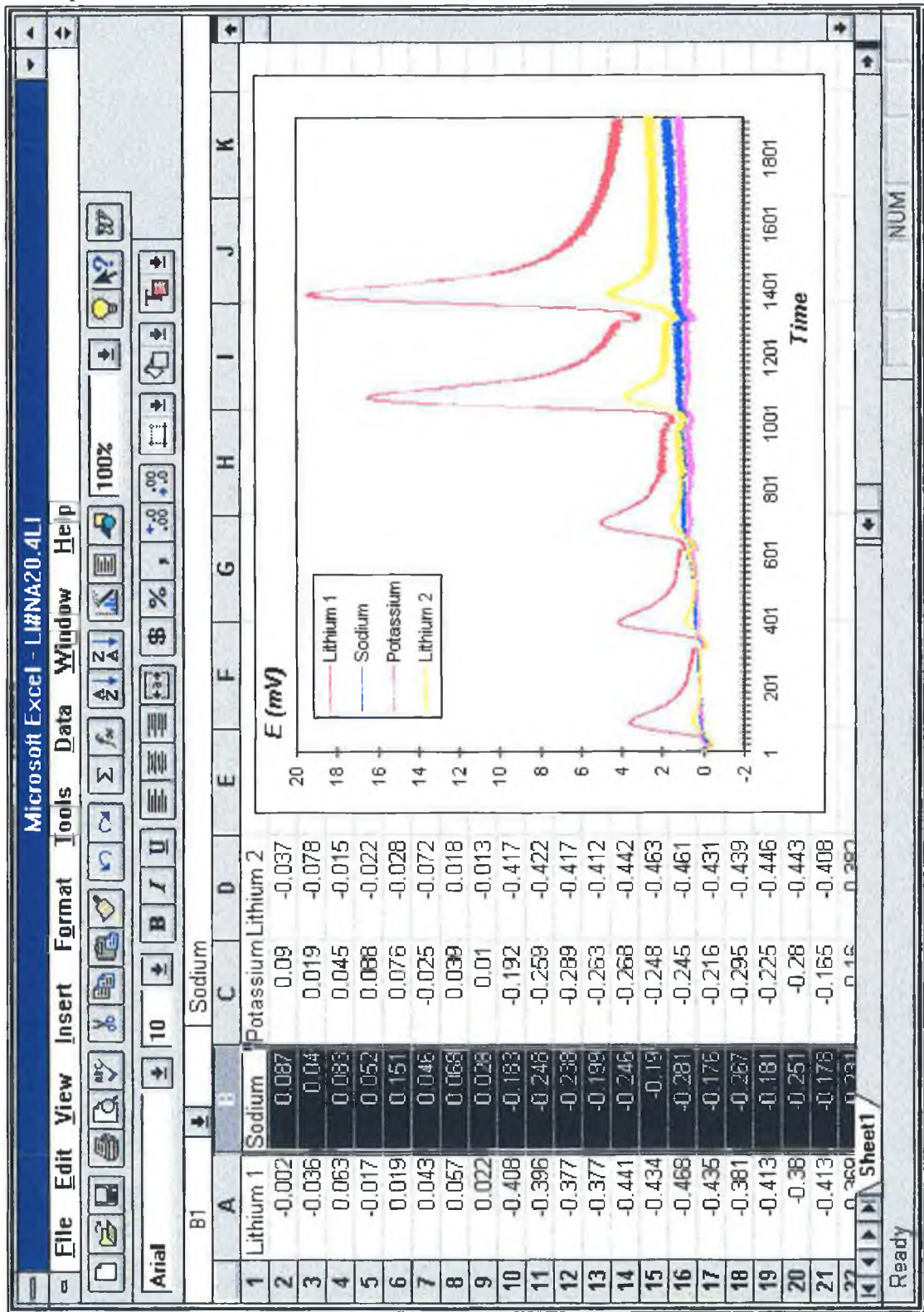
6.2.3 Peakfind VI

This VI is a component of the main FIA software dedicated to the analysis of the signal traces obtained from the SAD. The VI was designed to help the process of reading the peak heights of the electrochemical signals obtained in FIA mode.

Data are loaded into RAM using WINDOWS like menus, or typing in the path and filename of the file containing the FIA traces. The following operations are performed:

Figure 6.4: Front panel for the automatic Peakfind VI software.
The FIA traces are shown in the bottom of the screen, while the peak height data are shown in a table. This table display the information on the potential difference between the baseline and the peak maximum, and shows the position of the peak maximum in the FIA traces. A threshold value enables the programme to reject peaks which may be caused by environmental noise.
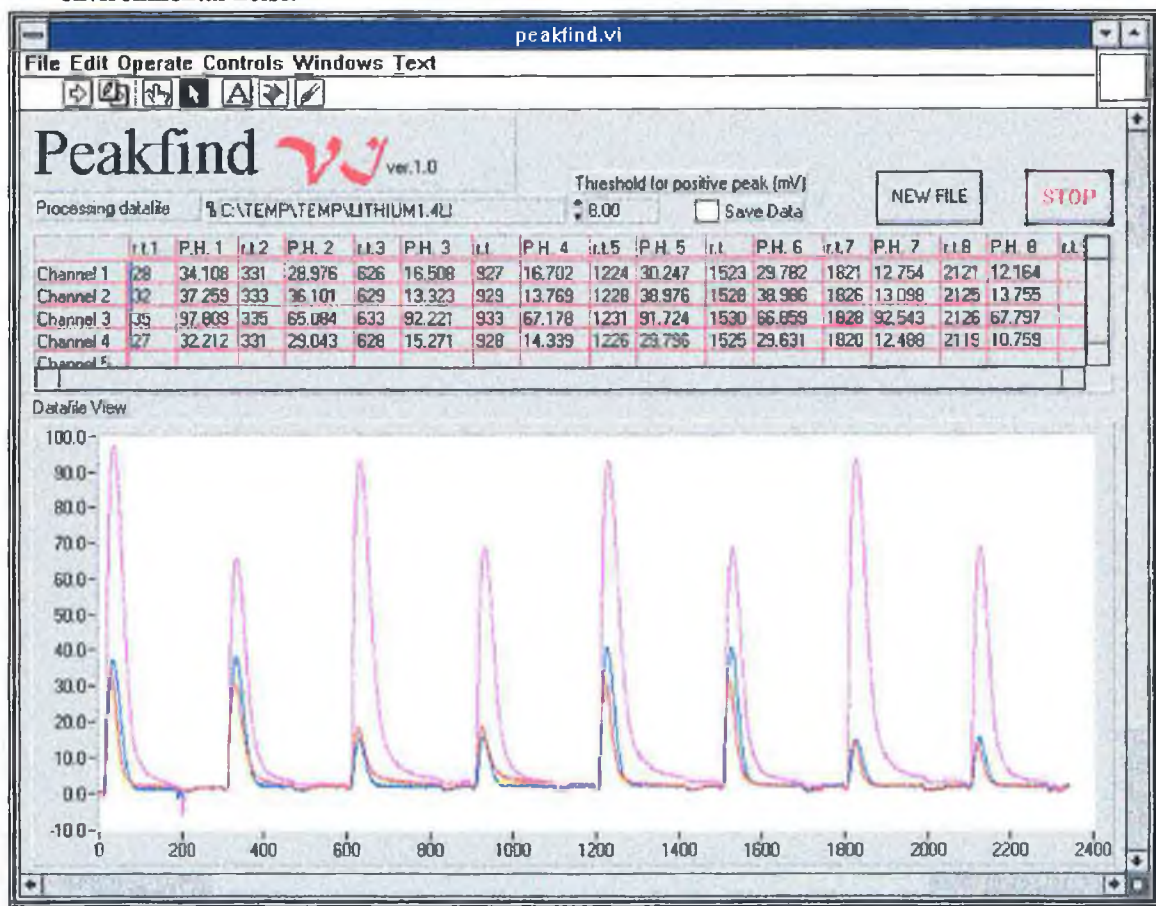
1. An incremental first derivative algorithm (Eq. 6.1) is applied to each channel and the resulting values stored in an array in RAM;

$$y_n' = \frac{y_n - y_{(n-1)}}{x_n - x_{(n-1)}}$$

<div align="right">Eq. 6.1</div>

2. The new array is searched for $y'_n=0$ values, and the x location of these points is stored separately;

3. Each $y'_n=0$ point is compared, in terms of the original electrode potential, with the previous point where the first derivative was also zero;

4. If the potential difference is higher than a user selectable threshold value, the point is marked as true peak maximum, and the position, x_n, and the peak height $(y_n-y_{(n-1)})$ is stored together in a new array.

These values are displayed in the front panel as a table containing the data for all the channels analysed. The user can request to store this table in spreadsheet format. The VI can automatically detect how many data series are in the data file, which means that it can be used to analyse traces from other sources of "peak-based" data.

Figure 6.4 illustrated the results of the procedure explained above for a datafile containing the FIA traces corresponding to the response of the SAD described in the previous section to the set of calibration solutions designed to model the Li^+-selective electrodes. Because of the high selectivity $Li^+(1)$ and $Li^+(2)$ ISEs present against potassium, high levels of the latter must be used in the calibration set so that a suitable

cross-response can be created to properly model the electrode, as explained in Section 3.4.

The routine is very simple and may fail if used in very noisy signals or if the traces present a baseline drift which is of the same order as the signals being analysed.

6.3 Case Study II: Multichannel Microdialysis System

This case is another example of the application of virtual instrumentation to scientific research, in this case biomedical analysis. The virtual instrument was designed for data acquisition and control of a microdialysis system for the simultaneous detection of glucose and lactate *in-vivo*.

A virtual instrumentation approach was identified as being necessary for this project for the following reasons;

- High precision in signal measurement needed for medical diagnosis called for a digital signal acquisition system.

- Precision in sample handling is critical so a very precise (digital) timing and control system was needed.

- For routine monitoring of lactate and glucose over extended periods (up to several days a completely automated system was required.

- As in any R&D instrument high flexibility was necessary to allow easy modifications and improvements.

- Some sort of "intelligence" was needed in the system to control a number of the instrument functions, specially operating the microdialysis pump and the flow redirection system as explained in following sections.

- The system was to be operated by non-computer specialists, and therefore there was a need for high-quality, intuitive user interface which could be mastered in a short time scale (few days).

- Microdialysis flow rates are very low (several μL min^{-1}), i.e. several orders of magnitude lower than FIA, because of the need to establish equilibrium between the sample and perfusate across the dialysis membrane in order to obtain high percentage recoveries. To obtain fast system response (few minutes), micro-tubing, micro-sensors and micro-instrumentation was required to create a micro total analytical system (μ-TAS) which obviously renders any kind of manual operation on the system impossible. This called for the use of remote signal acquisition and μ-TAS control, preferably through "intelligent" VI software.

A stand-alone microcomputer was commercially available from the manufacturers of the microdialysis pump for remote control of its functions, but at a very high cost and with poor flexibility for system alteration or enhancement. Besides, some type of digital signal acquisition was still needed which called for a computer based interface system.

Figure 6.5: Microdialysis system set-up diagram.
The microdialysis system is controlled with seven digital lines. Four of them control the pump functions and the flow system is controlled with one line per valve. An analogue output line is used to control the pump speed. Each channel from the potentiostat is monitored with one analogue input line.
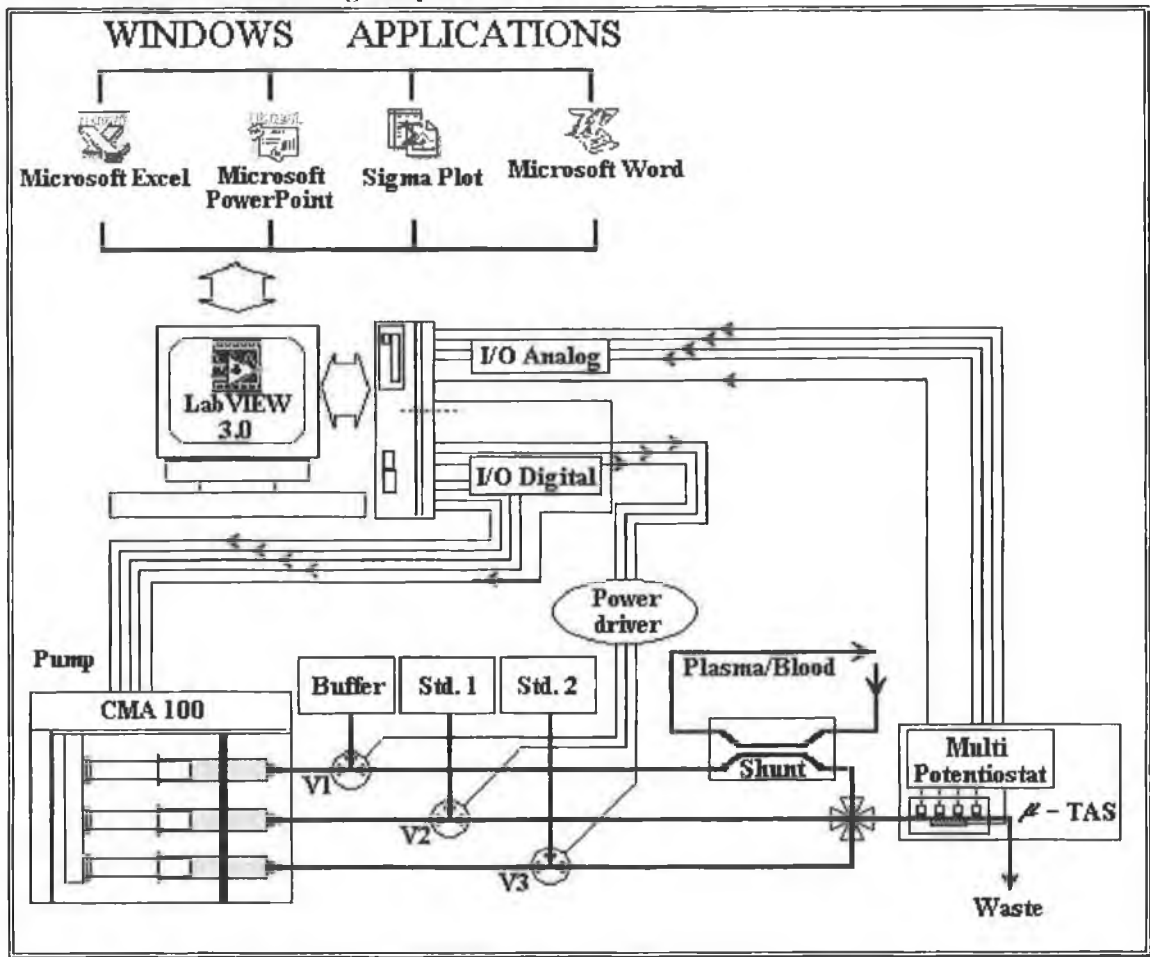
6.3.1 System Hardware

Figure 6.5 shows the set-up diagram for the virtual instrument, which comprises a microdialysis pump, a flow redirection system and a μ-TAS amperometric SAD. The whole microdialysis system was interfaced to an ELONEX 486 33 MHz PC microcomputer with 4 MBytes of RAM memory *via* an AT-MIO-16DL plug-in interface board (National Instruments, Austin, Texas, USA). A detailed diagram showing the electronic circuits of this system can be found in Appendix D.

6.3.1.1 Microdialysis Pump

The pump used to produce a continuous pulse-free high-precision flow (typically 3.0 μL min^{-1}) was a CMA 100 microdialysis syringe pump (CMA/Microdialysis AB, Stockholm, Sweden). The three pumping channels were fitted with 2.5 mL glass syringes which could give an interrupted flow for over 12 hours without refilling. The different functions of the pump could be controlled from a 15 pin TTL-compatible remote port as follows:

- **Start/Stop:** A negative logic digital signal actuates this port. Positive 5 volts (in port line 3) with respect to ground (line 1) maintains the system in stopped flow. If this line is reset to ground, the pump's motor will engage.

- **Reverse:** This feature allows the pump to function in reverse flow, which is ideal for refilling the syringes at low flow rate to avoid the formation of air bubbles. Line 13 controls this feature, being set to FALSE reverse when the line is set to ground, and TRUE reverse when the voltage is set to +5 volts.

- **Fast Feed Forward (FFF):** This function, as well as FFB, operates a secondary motor which allows fast emptying of the syringes when line 14 is set to +5 V, being disabled when the status is set to logical FALSE (ground).

- **Fast Feed Backward (FFB):** This is the opposite function to FFF with the same logic applied to line 15. TRUE (+5 V) sets it to active and FALSE (ground) disables it.

Because the above mentioned functions are not self-excluding, incompatibilities may arise if they are not properly handled. Therefore, some sort of "intelligent" managing algorithm must be used within the signal controlling device.

- **Pump Speed:** The speed of the main motor of the pump can be selected applying a voltage to line 9 of the 15 pin remote port. The input range accepted is 0 to +6.5 volts which brings the motor from full-stop to full-speed. For a 2.5 mL syringe, the range corresponds to flow rates from 0 to 250 μL min^{-1}.

Even if the pump presents very good linear relationship between the flow rate delivered and the voltage applied to line 9 at high rates (20 to 250 μL min^{-1}), this relationship cannot be extrapolated to very low flow rates, and if these are to be used, focused calibration of the flow/voltage relationship for a small window around the selected rate should be performed.

6.3.1.2 Flow Manifold

The flow redirection system is formed by three 3-way valves (The Lee Company, Westbrook, CT, USA) set-up as in Figure 6.5. As it can be appreciated from the diagram in Appendix C, the three independent flows, which are continuously being pumped forward are conducted to through the detector or redirected back to the reservoir depending on the actuation status. If a particular TRUE/FALSE valve situation is represented by 1/0 for valves 1 to 3, which correspond to buffer, high standard and low standard respectively, the following binary situations are possible:

- **Binary 000:** The buffer is pumped through the detector while both standards are redirected to their reservoirs. This position corresponds to analysis of dialisate.

- **Binary 110:** The high standard is sent though the sensor array and the other two solutions return to their respective reservoirs (for system calibration with high standard).

- **Binary 101:** Same situation than above but with the low standard.

- **Binary 100:** All three solutions are redirected to their reservoirs. This position is selected for syringe emptying or refilling.

Because only one solution should be pumped through the detector at a particular time, and to avoid incompatibility or flow mixing, the actuation device should also provide smart control of the valves.

Electronically, the valves are independently actuated *via* power drivers (based on two dual-gated CA 4232 E integrated circuits) in similar fashion as explained in previous sections. Control is achieved by three TRUE/FALSE digital signals from the I/O card and powered by an external +5 V, 1 Amp power supply.

6.3.1.3 SAD Detector

The chemical detector system consists of an array of four screen-printed amperometric enzyme biosensors selective for glucose (2 sensors) and lactate (2 sensors) fabricated by the Technical University of Vienna which are integrated in a micro-flow module designed

and manufactured by Ciba-Geigy (Basle, Switzerland). The redundancy of the electrodes gives duplicate information on the analytical sample for system diagnosis purposes, which is very important for situations where a malfunctioning detector can have catastrophic consequences (e.g. monitoring of critical patients in the ICU). Malfunctioning or dying sensors can be easily detected, providing cross-checked information and added safety in the determination of the analytes.

The biosensors are integrated in the μ-TAS which includes a 4-channel potentiostat built for this purpose by the Technical University of Vienna. The potentiostat can tune different voltages to each of the microelectrodes, and the sensitivity of the output can also be independently selected to 5, 10, 50 or 100 nA which corresponds to a full voltage output range of 1 volt. The floating signals from each sensor can be independently monitored, with respect to a common reference electrode, *via* analog input functions in the acquisition card.

Although the lowest sensitivity was selected in the potentiostat hardware (100 nA to 1 V) high precision measurements were taken by increasing the acquisition gain in the I/O board. Using a gain of 5, the voltage resolution of 0.488 mV is available, which correspond to a sensor current of 0.0488 nA.

6.3.2 Microdialysis Control System VI Software

The software design was focused on the user end (see start of Section 6.3), generating a very user friendly which could allow the operation of the system without the need of an

in-depth learning process. In general, the software is very intuitive to operate, almost completely mouse driven, and internal operation and parameter checking routines the chance for erroneous data interpretation and system malfunction. The software provides the following features to the global virtual instrument:

- Data acquisition. Variable acquisition frequency.

- Data processing. On-line noise reduction

- System control. Microdialysis pump and flow system.

- System calibration. On-line calibration

- Data display. Current/concentration colour-coded numerical and graphical.

- Data storage. Spreadsheet format.

The top hierarchy diagram for this VI software can be found in Appendix E.

6.3.2.1 Data Acquisition.

Data from the biosensors is acquired in differential mode with respect to the common reference electrode. The frequency of the data acquisition is user selectable from the main front panel. The minimum sampling period (all channels simultaneously) is two seconds (one second for the portable system described in Section 6.3.4) with a maximum of 256 seconds between acquisitions for long time monitoring purposes. This is necessary for further processing, as some commercial packages do not accept data files with more than 4000 points per series. Indicators in the front panel shows, at all times, the number of acquired points (per channel) and the acquisition period selected, which

can be modified even while acquisition is in progress. Analogue input subVIs are used to simultaneously interrogate the four AT-MIO channels monitored.

Figure 6.6 shows the front panel for the latest version of the Microdialysis Control System VI, which includes the Microdialysis File Viewer VI integrated in the main software block. The traces displayed correspond to *in-vivo* determination of glucose and lactate in greyhound dogs. These data show very good correlation between both lactate sensors, which present identical response. Glucose sensor 1 is blank to allow signal background correction. Artifacts from the system electronics can easily be identified as appearing in both types of sensors and should not be related to changes in the concentration of the species, but to some sort of current spike.

6.3.2.2 *Data Processing*

Each of the points acquired is obtained from the average of an acquisition wave consisting of 10 independently sampled data. This facilitates noise reduction leading to more consistent values from the potentiostat. The VI software re-scales the voltage signal to give the original current or, alternatively, accesses the calibration parameters to calculate the lactate/glucose concentration directly. All input channels are processed simultaneously.

Figure 6.6: Microdialysis system front panel.
The left part of the screen is dedicated for system control purposes while the right part
displays the data acquired. Two independent graphs show the data for glucose (upper) and
lactate (lower) separately, while colour coded numeric displays give information about each
of the input channels.

6.3.2.3 System Control

The AT-MIO-16DL acquisition interface board presents up to 32 digital I/O channel and 2 analogue out channel which can be used for controlling the operations of the syringe pump and the flow system.

Four digital output subVIs which control the digital port A are executed to interface the pump functions. Each port line is updated independently. The functions controlled are, as seen in the hardware section:

- Pump switch: Digital line 0; Controls ON/OFF function.

- Motor reverse: Digital line 1; Reverse feature.

- Fast feed forward: Digital line 2; Sets the secondary fast speed motor forward (fast empty).

- Fast feed backwards: Digital line 3; Starts the fast motor backwards (fast refill).

Logical algorithms designed in a purpose-built subVI to specifically control the CMA 100 microdialysis pump prevent the functions of the pump to be actuated in an incompatible manner, and actuation from the front panel is executed if and only if the requested function is possible. If this is the case, the remaining functions are set to the necessary values to avoid actuation conflict.

- A subVI was designed to hold the pump flow calibration data, computing automatically the voltage required to deliver the selected flow rate. It also

accesses a analogue output subVI which automatically controls the DAC channel 0 to produce the calculated voltage.

The solution flowing through the detector is controlled by a set of three valves arranged as Figure 6.5 as described previously. Each of the valves is actuated separately via independent lines (lines 0 to 2) of the second digital port B. The four options described in Section 6.3.1.2 and Appendix B are programmed into a subVI which "intelligently" accesses the right manifold status depending on the process being performed by the top hierarchy VI. Syringe refilling and calibration are among the processes which need the valves to be automatically controlled from the main VI.

A very important feature of the main VI software is complete independence of the actuation and acquisition functions, which allows a fast fixed system response of 2 Hz (1 Hz for the portable system) no matter what acquisition frequency has been selected by the user. With this feature, the system does not wait for the next acquisition time to refresh the data and function loops in the subVIs and main VI, allowing full user control even at very high acquisition periods.

6.3.2.4 System Calibration

A separate subVI controls the three calibration options for the microdialysis system, one of them being experimental, and the other two through previously acquired data. Sensors are assumed to present linear correlation between current and concentration in the range studied, and therefore linear regression is used to obtain the calibration data.

In the experimental calibration the subVI leads the user through the calibration steps. These are as follows:

1. Input concentration of the standards used (including % recovery factor if microdialysis is not used previous to detection) in the calibration front panel,

2. Select acquisition of either of the standards (high or low),

3. Observe the signal from detectors in the signal monitoring front panel (Figure 6.7) and allow the signal from the standards chosen to reach steady state in both glucose and lactate biosensors.

4. Once the steady-state is reached, select acquisition of the signal, which triggers data averaging. The duration of the acquisition of data for calibration is user controlled.

5. Finish data acquisition. The average of the signal during the acquisition time is passed to the calibration subroutine.

6. Repeat processes 3, 4 and 5 for the second standard.

7. Accept or reject calibration slope and intercept calculated by the calibration routine. If accepted, the system starts converting current to concentration with these new data. If rejected, system remains unmodified.

The manual input sub VI simply accepts the data supplied by the user to calculate the calibration parameters. Data can be supplied in two different formats:

Figure 6.7: Data acquisition in front panel during system calibration.
The standard being injected into the system contains glucose and lactate at 5×10^{-3} mol dm^{-3}.
Note the difference in response between both glucose sensors, which indicates an unusual low response for glucose sensor 1.
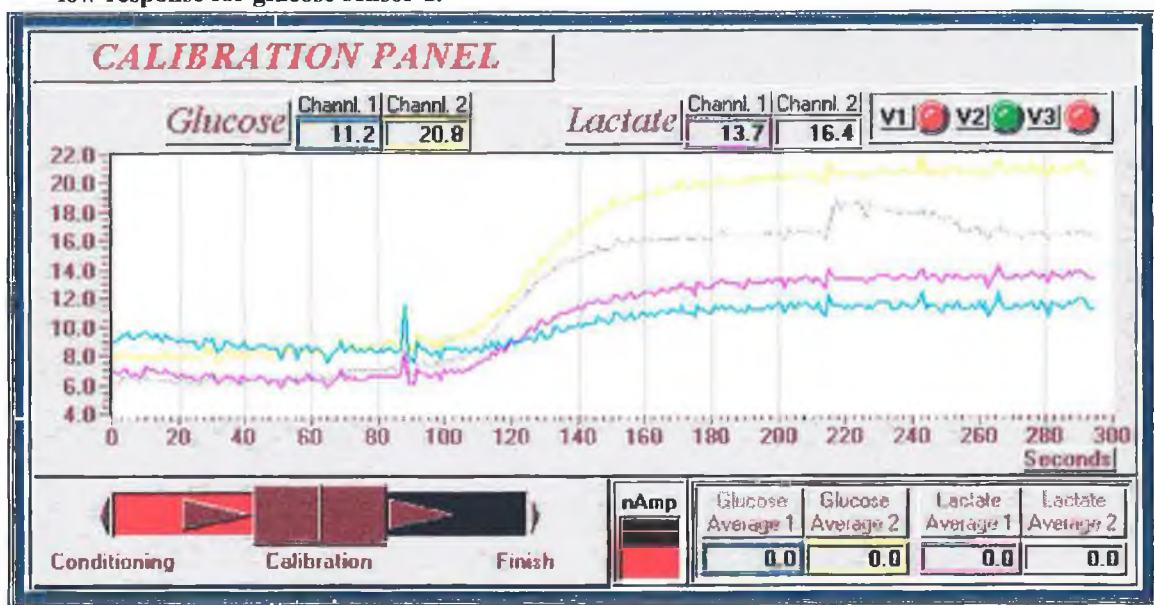
- Supply to the calibration routine the concentration levels of the high and low standards and the signal obtained for them in previous calibrations. The routine calculates automatically slope and intercept. User can also accept or reject these newly input data.

- Supply already processed calibration data in the form of slope and intercept for each of the four sensors and proceed with accept or reject as described above.

6.3.2.5 Data Display

Figure 6.6 shows the front panel of the main VI, which contains two main graphic displays for the glucose (top) and lactate (bottom) traces separately. The displays show current or concentration, depending on the data mode chosen by the user. If the concentration mode is chosen, the VI software continuously overlays in the graphs the concentration levels of the high and low standards, between which the sample concentration should be found at all times, as extrapolation may not be accurate.

Numeric displays also give updated information on the current or concentration being acquired at each instant. These data, which are not kept in memory, are updated independently from the acquisition period chosen by the user with a fixed acquisition rate at a frequency of 2 Hz (1 Hz for the portable system).

Three LED virtual indicators in the front panel of the main VI give information at all times on the switching status (red/green equals ON/OFF) of the flow manifold system.

6.3.2.6 Data Storage

After the acquisition session is finalised, and upon request of the system user, the data are stored in spreadsheet format with a file header containing the experimental conditions or system parameters and comments. The file is structured in five columns which contain the time in seconds at which the point was obtained (since the beginning of the experiment session), and the concentration detected by the Glucose 1 and Glucose 2 sensors, and Lactate 1 and Lactate 2 sensors. The time scale is necessary to properly

recover the information since the frequency can be modified while acquisition is in progress.

Calibration parameters are stored in system files after the calibration procedure is complete. These files are always retrieved when the application is launched at the beginning of a new session.

Figure 6.8: Satellite VI, Microdialysis File Viewer.
This programme allows the retrieval of data files and data display using the same structure than the acquisition programme, separating automatically the data from lactate and glucose in separate charts.
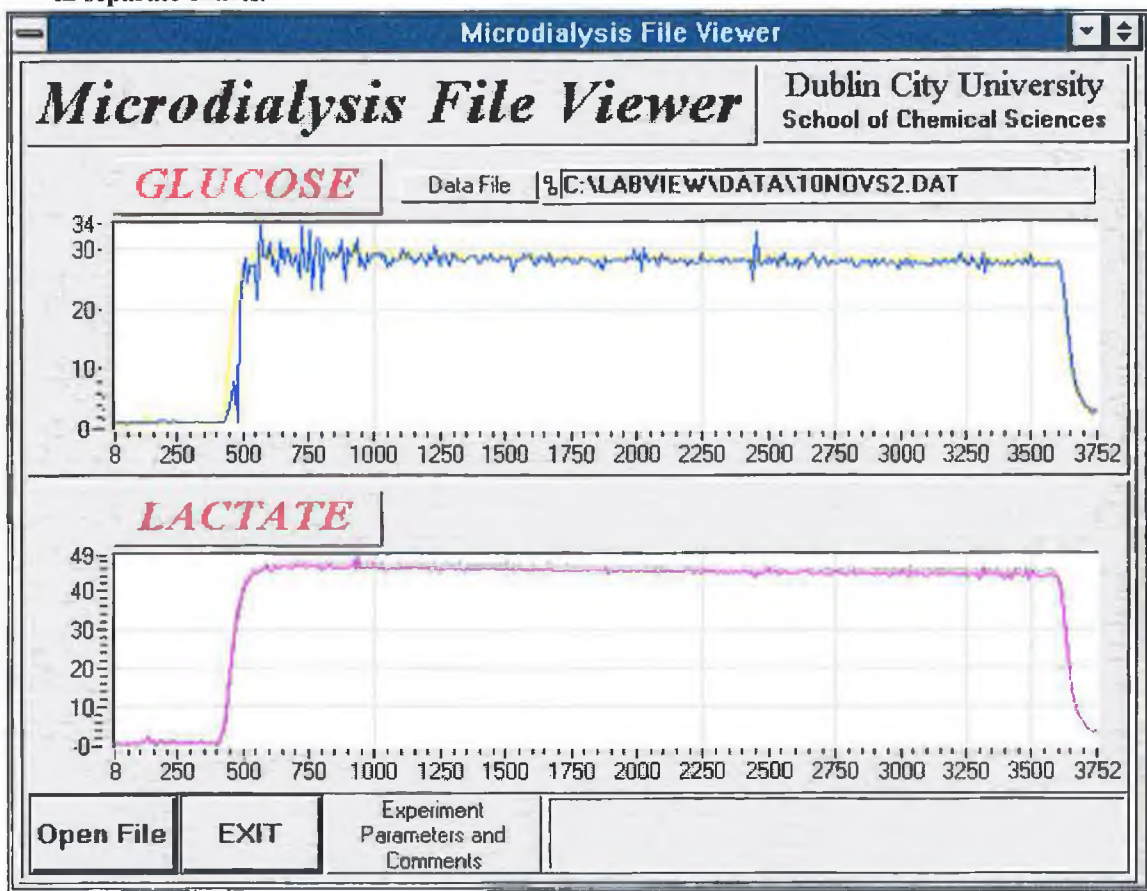
6.3.3 Microdialysis File Viewer VI Software

The software designed for this research was completed with a small application VI designed to retrieve and visualise in the computer screen data files obtained with the main microdialysis software. The programme facilitates navigation through the system with windows-like menus to select the data file to be displayed.

The VI shows the path of the data file loaded and automatically separates from the array the time scale and the two glucose traces from the lactate ones showing them in separate graphs. File headings containing experimental conditions and/or comments are also retrieved and shown in a different indicator.

Figure 6.8 shows a data file imported into File Viewer. Traces were obtained by monitoring, for over one hour, the signal (in nA) generated by the biosensors for serum samples analysed through an aminocellulose shunt of 100 mm length. It can be appreciated the good signal correlation between sensors of the same type.

On the other hand, Figure 6.9 shows a system output where, while the signal from the glucose sensors are consistent, a discrepancy in the signals from the sensors selective for lactate clearly indicates a failure in the detection system which points directly to the sensor Lactate 1 (see colour coding). In this particular case, the contradiction in the SAD response was caused by a leakage in the micro-flow array module before the sample reached sensor Lactate1.

Figure 6.9: Typical diagnosis of a system failure.
It can clearly be seen from the picture how the redundancy of the biosensors indicate a malfunction in one of the lactate electrodes (Lactate 1). In this case the problem was caused by a leakage in the flow system which prevented the sample reaching that particular sensor.
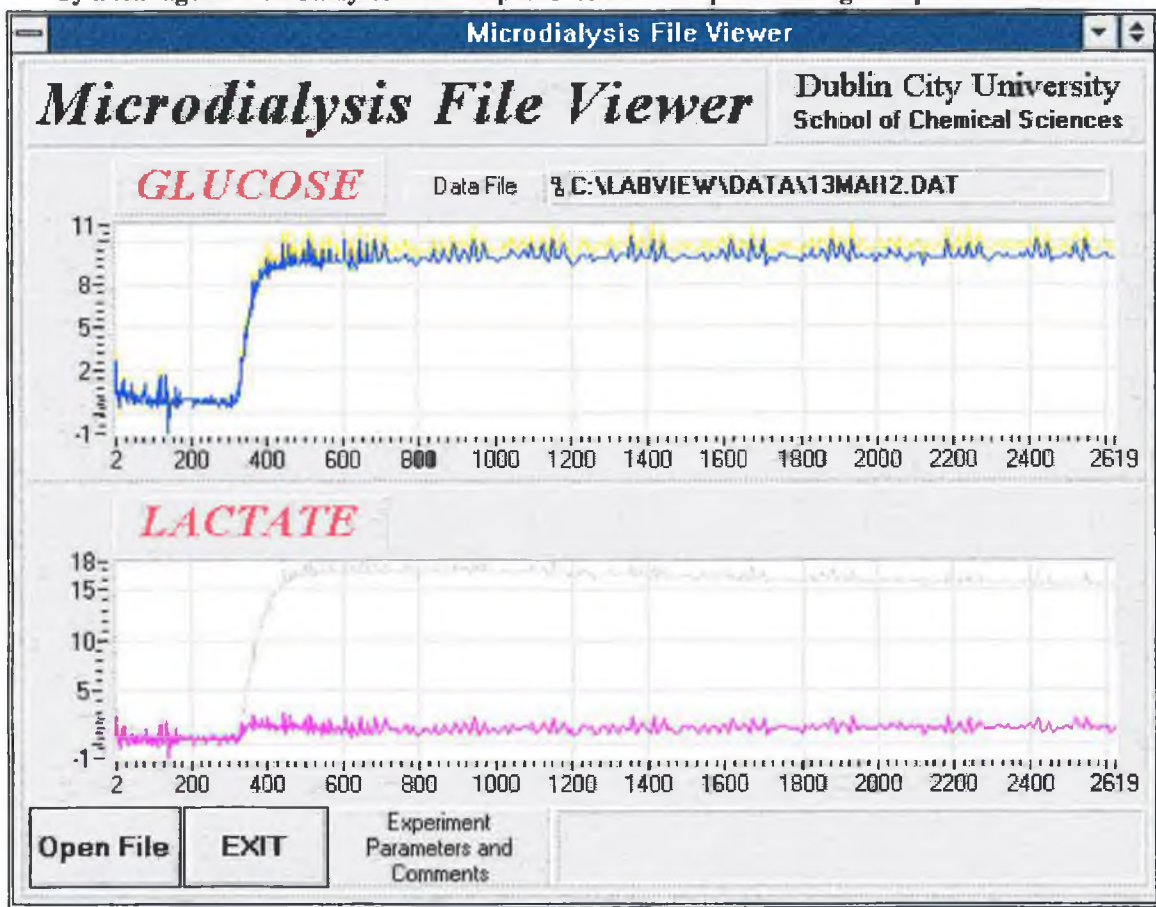
6.3.4 Portable System

In a real monitoring situation, the virtual instrument should be located as close as possible to the patient, in order to reduce sample volumes, unnecessary long tubing and increase sensor response time. Ideally the instruments should be brought to the patient's bed side and not otherwise. This may produce problems in terms space and placing a desk-top computer and instrumentation in the patients room, and specially moving and reorganising the system set-up. For this reasons, some degree of portablility was

thought to be necessary for this kind of biomedical equipment, with the final target of a compact, light, case-fitted portable monitoring system.

In order to prepare a portable microdialysis system the Microdialysis Control Software was installed in a DELL Latitude 486 50 MHz notebook computer with 16 MBytes of RAM memory. Because of the impossibility of installing a plug-in interface board inside the portable PC[*], data acquisition and control operations were implemented through a DAQPad-1200 data acquisition module from National Instruments. This external interface module is connected to the control unit *via* the parallel port which allows high communication speed and fast data transfer to/from the module. Despite the usually high compatibility of National Instruments interfacing and software products some modifications were needed to ensure a proper functioning of the microdialysis system. These lack of compatibility was originated at two different levels: VI software and Interface module hardware.

6.3.4.1 Software Problems

As described before (Section 0), the original software was designed for a desktop computer. The following problems were encountered when transferring the software to the Dell notebook:

---

[*] Although the Dell notebook supports PCMCIA technology, at the time the decision to develop the portable system was taken there were no micro card I/O devices available with analogue output functions, which were indispensable for this project.

- Middle VDU display resolution was chosen in order to increase the screen's working space. This resolution of 800x600 pixels worked perfectly in a traditional cathodic ray tube (CRT) VDU but, as the maximum resolution available in the colour Liquid Crystal Display (LCD) VDU of the Dell Latitude is 640x480 pixels, the front panel for the Microdialysis Control System virtual instrument had to be redesigned so that the entire control panel and display objects fitted the available screen resolution.

- Due to the special parallel port configuration in Dell computers, communication with the DAQPad-1200 was not established properly. The interface drivers did not recognised the notebook's printer port configuration as standard parallel protocol and the port settings had to be reconfigured so that the new parameters complied with the requirements of the Standard Parallel Centronics communications protocol. This was achieved by resetting the port configuration in the system drivers so that the DOS operating system could properly communicate with the hardware in a standard mode.

6.3.4.2 Hardware Problems

The Digital Output configuration in the AT-MIO-16DL plug-in interface board is such that the output lines are grouped in 4-line digital ports. This configuration is not compatible with the 8-line ports available in the DAQPad-1200 interface module. Therefore, the software sub VIs which control digital I/O operations had to be modified so that the portable module could be used. This modification was achieved by changing

the software controlled line size of the digital ports and using 4 lines (0 to 3) of the DAQPad-1200 DIO port A to control the pump and three lines from DIO port B (0 to 2) to control the manifold valves.

6.3.5 System Performance

Figure 6.10 shows glucose and lactate traces obtained with the microdialysis system being processed in Microsoft EXCEL version 5.0. The experiment consisted of on-line *in-vivo* monitoring of both analytes in anesthetised greyhounds. The dialysis probes consisted of a 100 mm long aminocellulose shunt with a molecular weight cut-off of 20 KDaltons.

The subject was treated with bolus injections of heparin one hour previous to the beginning of the experiment (t=-60 min) and then at hourly intervals. Five minutes after starting the monitoring process (t=5 min), the blood stream (6.0 mL min^{-1}) starts being perfused with physiological buffer, which contains low molecular weight heparin to prevent blood clotting, at a flow rate of 3.0 μL min^{-1}. Basal levels of L-lactate are soon established, and monitored for 50 minutes. At t=55 min, the subject is injected a 5x10^{-4} mol dm^{-3} L-lactate solution and then continuously infused with 2.5x10^{-3} mol dm^{-3} kgr^{-1} hr^{-1} of L-lactate until t=125 min. which produced a sharp increase of lactate levels in the subject's blood, as it can be observed in Figure 6.10, followed by a stationary phase produced by the continuous infusion of lactate. An expected decrease in the lactate levels can be observed, returning to basal concentration once the infusion process is stopped.

The dialysis process is ended at t=185 min and the monitoring process is stopped. Only the response to one lactate sensor is shown, as the signal from the redundant electrode is identical.

Throughout the above experiment, the levels of glucose in the subject's blood remains acceptably constant, as it can be appreciated from the graph in Figure 6.10. Glucose levels are only monitored by one of the biosensors, the second one being used as a blank for signal background correction.

Control measurements of both lactate and glucose on blood samples and dialysate were obtained from discrete samples taken every 15 minutes. These samples were spun down and analysed with a YSI STAT analyser. Comparison of the levels of the species in blood and perfusate seem to be in good concordance with the results given by the SAD, and also indicate that a good percentage recovery is to be expected after the dialysis process.

It can also be appreciated that the discontinuity in the signal from the sensors seems to be caused by the process of manual extraction of either blood of perfusate from the system flow, as high noise appears consistently at the same time the samples are obtained.

Figure 6.10: Mirosoft EXCEL processing microdialysis data.
On-line concentration traces obtained for glucose and lactate are in agreement with off-line analysis of the concentrations of both plasma and dyalisate obtained every 15 minutes from a YSI STAT analyser.
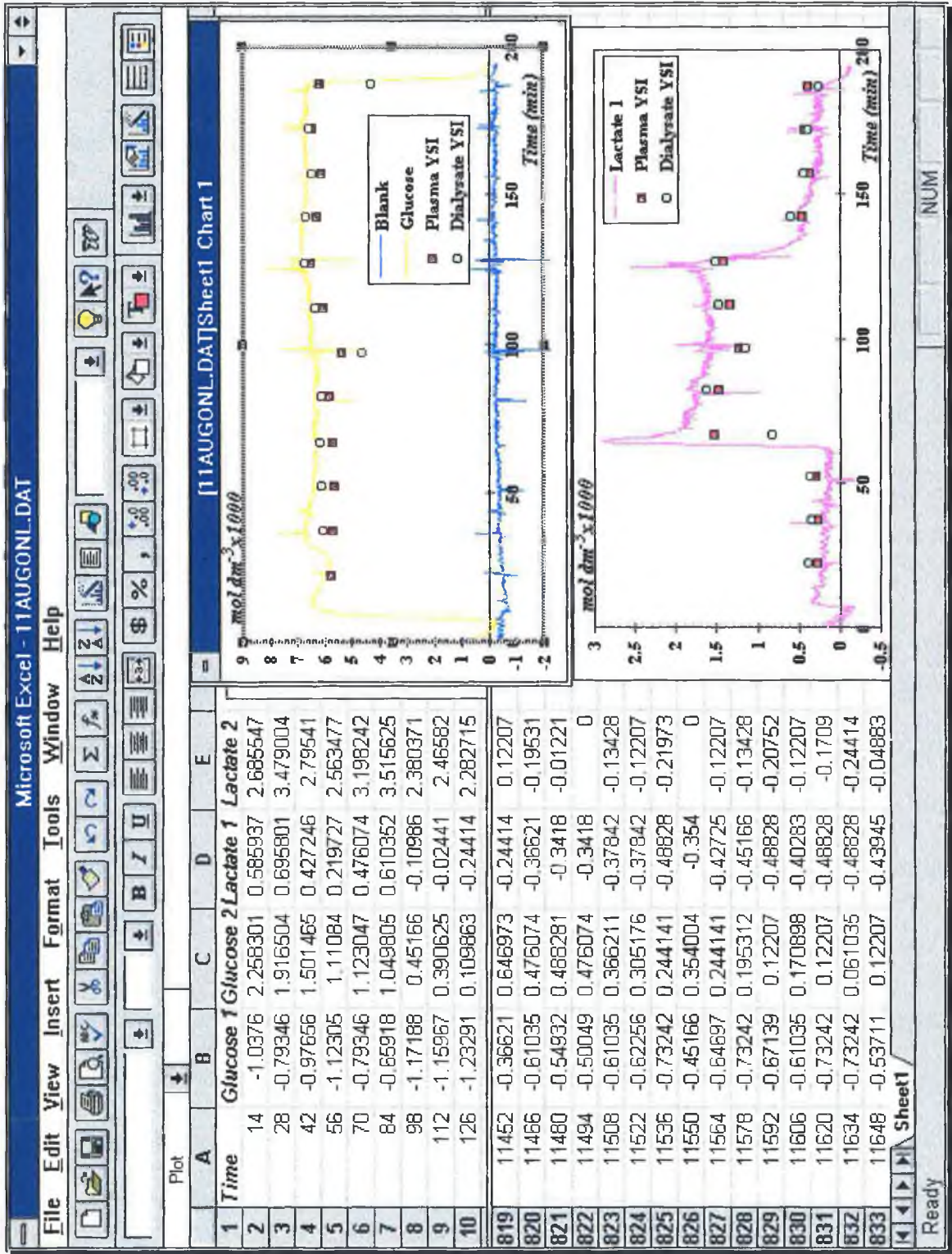
The use of virtual instrumentation for this task can clearly enhance the performance of the system in the following aspects:

- Digital data handling: Increased precision in the system measurements.

- Calibration procedures: Computer-assisted system calibration enhances the instrument accuracy.

- On-line data processing: Immediate accessibility to regularly updated data.

- Minimisation of human error in data processing through automation.

- Compact digital data storage and access to digital communication.

Figure 6.11: Environmental monitoring system set-up diagram.
The signal from a two-channel FID chromatograph is continuously acquired through the I/O card into the VI. These signals are processed and relayed to an indicator in the plant's control room. Processed data printed out in a regular basis on the system's printer.
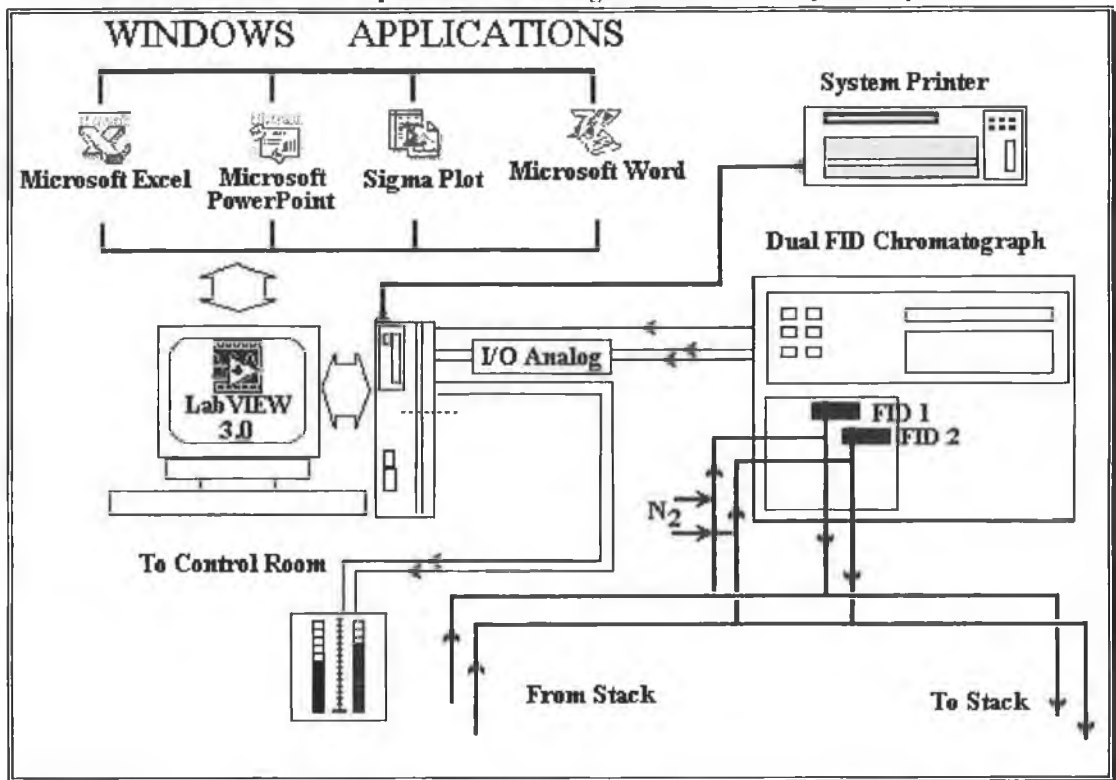
6.4.1 System Hardware

A 12-bit resolution plug-in data acquisition card (model LabPC+ from National Instruments) was used as the ADC/DAC interfacing board. The host computer was a COMPAQ 486 50 MHz PC compatible with 8 MBytes RAM memory.

The floating signal generated from the detector was input directly to the I/O card in differential mode through a breakout box. The positive and negative wires from FID 1 and FID 2 outputs were connected to the lines high and low of the ADC logical channels 0 and 1. Twisted pair shielded wire was use for these signals, and the shield earthed to the detector's ground to reduce as much as possible the high environmental noise present which, unfortunately, could only be reduced to a level of ± 2.5 mV. This high noise level was probably generated by the heavy metal pipes and manifolds, metal tanks, reservoirs and reactor, high voltage power lines nearby, and the steel structures of the building of the synthesis plant.

As the low impedance output voltage from the detector was set to a maximum 2.0 V no initial signal filtering was thought to be necessary as the signal-to-noise ratio was increased from 12 to 120 (calculated at 300 mg m^{-3} total organics emission). A maximum gain of 5 (hardware set to unipolar 0 to 10V) was used which gives the signal acquisition system an input resolution of 0.488 mV. Appendix D shows an electronics diagram showing the connections of the signals to the LabPC+ I/O channels.

6.4.1.1 Flow Manifold

The dual manifold samples the emissions at the process exhaust and at the plat's stack. PTFE tubing redirects the streams, being pumped into the environmental control room at a flow rate of 40 mL min^{-1} (3 psi) where it is mixed with nitrogen (30 mL min^{-3}) and sent to the gas chromatograph. Pressure gauges are installed to monitor the gas pressure, and a in-house manufactured system is used to adjust the flow rate of the sample/nitrogen mixture previous to analysis.

6.4.1.2 System Detector

A Varian Star 3400 CX series gas chromatograph, with a dual flame ionisation detector (FID) is used to analyse the amount of total organics in the sample. Because no separation process is needed, a null column is used, which is kept inside the chromatograph's oven at a temperature of 50 °C. The FID detectors receive a combustion mixture of air (300 mL min^{-1}) and H_2 (30 mL min^{-1}) and are maintained at 200 °C. This detector presents a linear dynamic range of 10^7 and very low output noise (max. 0.04 pA at 50 ms) which renders it ideal for monitoring systems where the analysed species may vary, unexpectedly, in a great manner.

6.4.2 Continuous Monitoring VI Software

The software for this virtual instrument was designed to perform a number of main operations on a continuous basis. All the functions, except the system calibration which

must be operator assisted, are automatic and provides a 24 hours a day stack emissions monitoring. The VI features are classified in the following categories:

- Signal acquisition. Multichannel signal wave acquisition.

- Data processing. Digital signal filtering and voltage to concentration conversion

- Signal output. Signal relayed to control room.

- Statistical data. Distribution analysis.

- Data display. Colour coding, numerical and graphical.

- System calibration. Multi-type calibration procedures.

- Data storage. Compact spreadsheet compatible ASCII storage.

- Hardcopy reports. Strip chart function and daily emissions report.

6.4.2.1 Signal Acquisition

The system was designed to allow continuous monitoring of three different channels in a differential mode with a maximum voltage range of 0 to 2 V. The number of channels active at one time is user selectable and can be easily changed by actuating the channel switch in the upper left corner of the instruments front panel (See Figure 6.12). Because the signal is low frequency, and in order not to overload the plug-in board buffer the acquisition rate was limited to 3000 inputs min^{-1}.

6.4.2.2 Data Processing

As the external environment is loaded with RF noise, an on-line digital filter was applied to the raw data to further reduce noise and to limit the global data input rate to one point per second This filter has a global effect on the half hour trace of a square wave average filter with a window size of 50 samples. The output from the filtering procedure is processed on-line in accordance to the calibration data available to the system to produce a value of the concentration of total organics (mg m^{-3}) through the stack. The voltage to concentration conversion is independent for each of the channels monitored. The concentration data are maintained in the RAM memory until the system control senses the end of the current half hour. When this occurs, the software obtains an average value for emission concentration over the last 30 minutes (typically 1800 data) and stores it in memory and in a temporary file in the computer's hard drive until midnight (24:00 hours as in the computer's hardware clock).

6.4.2.3 Signal output

The concentration value obtained at any time is rerouted to a signal generation routine which re-scales the signal (1 to 5) to produce an output voltage, through a DAC accessing subVI, being relayed to the control room of the synthesis plant, which is three floors away, and displayed in a meter. As the LabPC+ card only presents two analogue output channels this feature is only available for detectors two and three.

6.4.2.4 Statistical analysis

The average values obtained from the three channels monitored during each half hour are processed to generate a distribution table of the emission concentrations (see VI front panel, Figure 6.12). The half hour average concentration values are grouped in classes of 15 concentration units each, from 0 to 300+. When the half hour ends, the routine selects the class to which the average value belongs and increases the population number of that class by one. If the concentration average is greater or equal to 300 mg m^{-3} the population of the class 300+ (300-314) is increased. For example, an typical average value of 2 mg m^{-3} at the end of the half hour will increase the value of the first category (0 to 14) in one unit, while an unlikely average value of 400 mg m^{-3} will increase the 11th category (300+) in one unit.

6.4.2.5 Data Display

As Figure 6.12 shows, the VI front panel presents two graphic displays. The top one show the signal history of the acquired data for the current half hour and it is updated as soon as the new data point is available (typically 1 HZ). The presence of the data corresponding to a particular detector will depend solely on whether that detector is selected as active or not (see Section 6.4.2.1). Numeric displays are available which indicate, for the active channels, the signal input voltage, the concentration corresponding to that voltage and the relationship (slope) being used to convert the voltage signal to concentration.

Figure 6.12: Front panel of the Continuous Monitoring VI software..
The VI presents two graphs, one for the signal traces and a second one for the data distribution diagram. Daily data history are also available for each channel. VI controls are on the left side of the front panel. Channels are colour coded both for the controls and the indicators. Figure shows artificially induced signals corresponding to domestic ink solvents.
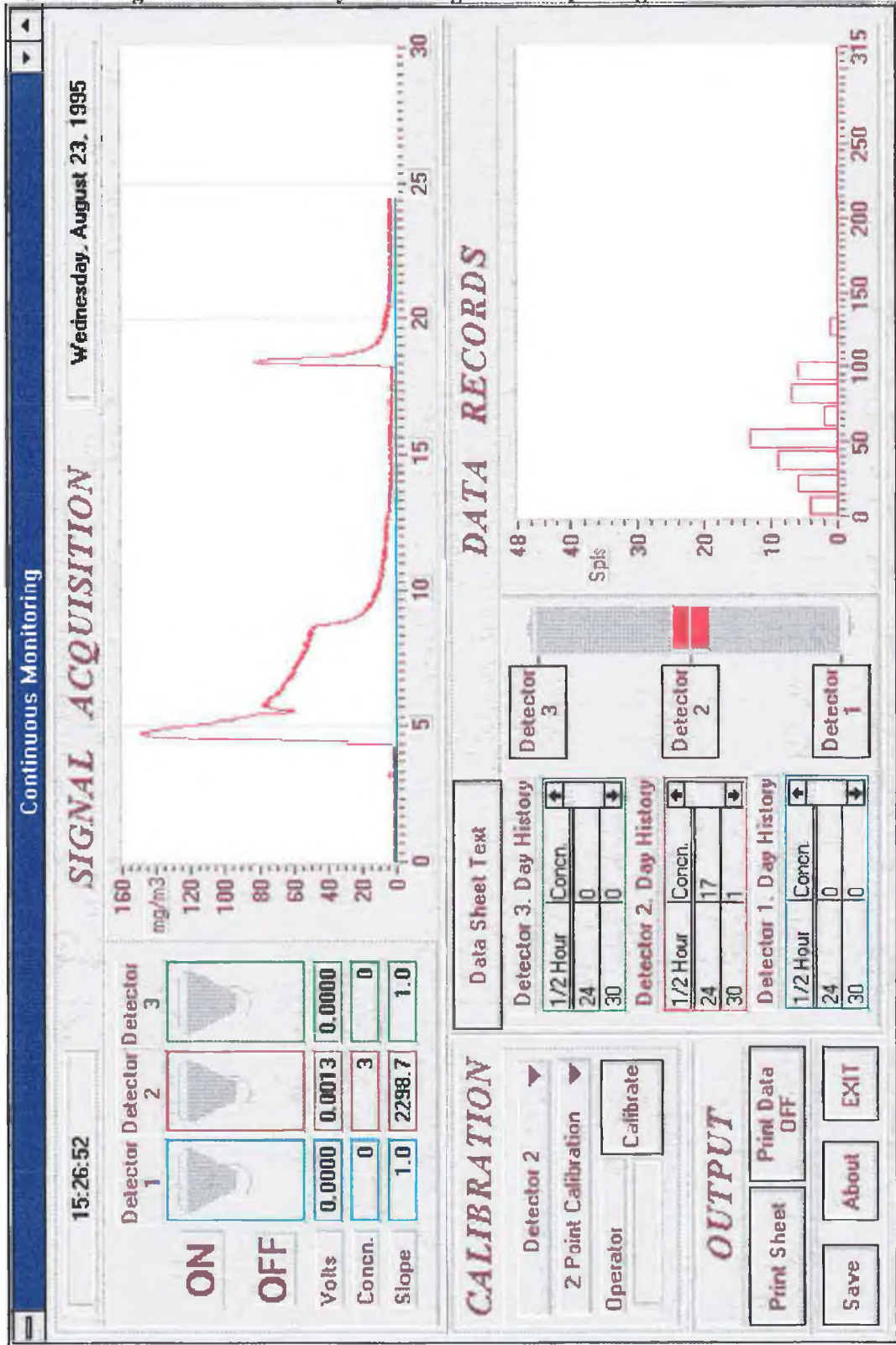
A second graphic display is available to present the statistical data for the day in course. A bar graph is shown for the selected detector (selection is independent of the main detector activation switches) showing the distribution in classes of the average emission concentration. Scrolling data tables are also available on screen which shows the average values at any half hour period of the current day.

6.4.2.6 System Calibration

When the VI is launched, it retrieves from the hard drive functioning parameters and calibration data which are stored while in operation. These calibration data can be supplied to the system by performing experimental calibrations with known standards, supplying the calibration parameters or retrieving them from previously stored data files. The following calibration options are available:

- As the FID signal is linear in the range used, two standards (high and low) can be used to calibrate the detector response. When the subroutine is initialised it acquires the signal from the detector in a stand-by mode. Once the standard has generated a stable signal in the detector, the operator actuates the acquisition mode in which the signal is acquired and processed on-line. The user decides for how long the calibration routine acquires the signal before terminating the process. The same operation is executed with the second standard to obtain the response of the FID to that particular level of organic material. The concentration of the total organics in both standards must be given to the VI. The routine

automatically calculates the regression and calibration values (see Section 6.3.2.4 for a step by step description).

- A second method is to obtain experimental response of only one standard as explained above. The second value needed for the calibration process can be obtained either by manual input, by retrieving from file or by forcing through the origin of coordinates (0,0).

- Full manual input is the third way this VI allows calibration. In the first variant the values for standard concentration and for the signal levels are manually input. In the second variant, only the values for the slope and the intercept are needed.

Figure 6.13: Continuous Monitoring calibration panel.
The initial baseline corresponds to the signal output from the detector when only carrier flows through. The solvent introduced in the flow generates a signal which is allowed to stabilise previous to data recording. The final stage shows the recovery of the system baseline.
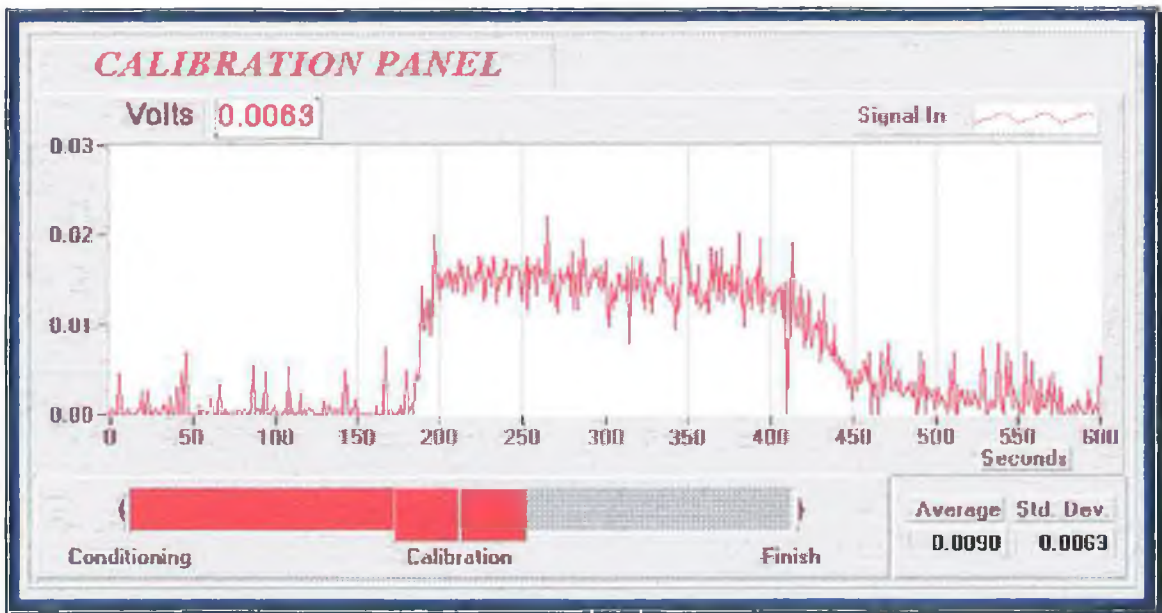
The calibration data are automatically stored in files with name and extension distinctive of the date and time and also the detector calibrated. For example, calibration data obtained for channel 2 on May 18th, at 5:00 PM will be stored under the filename *18051700.cl2*. If the data from a previous calibration process are to be used they can be retrieved from files, which are selected through WINDOWS-like menus. This is particularly useful when a number of batch processes are run in the synthesis plant and each needs different calibration parameters.

6.4.2.7 Data Storage

The collection of data obtained during the day are automatically stored in a file at 24:00 hours under a file name composed of day, month and year, *dd/mm/yy.dat*, i.e. *070894.dat* for August 7th; 1994. The file has spreadsheet format so it can be easily imported in any commercial spreadsheet package like EXCEL or Lotus 1-2-3.

Probably one of the most convenient features in data storage is the fact that the VI continuously saves the acquired data into temporary files. When this happens, a "flag" is turned on so that in the case of a power failure the system reinitialises DOS, WINDOWS and the VI software, recovering the data acquired in that day and continuing with the acquisition mode.

A series of menus designed into the system allows the user to save to a file (typically on a floppy disk) a spreadsheet containing the data obtained during the day in course. This action can be requested at any point in time.

6.4.2.8 Hardcopy Reports

An A4 page report containing the daily averages of the emission concentrations is printed out at 24:00 hours. The report may also contain details of the process in operation as well as information on the monitored channels. This report can also be generated at any point in time during the normal monitoring procedure by selecting the appropriate option in the front panel. If this is the case, printout time and a time slider indicator give information about the time the report was generated.

Figure 6.14 shows a typical report hardcopy printed out at user request at 12:45 PM of the data recorded on June 5th, 1995 during the first stage of the synthesis of the drug Piroxicam. This compound is the active component of the worldwide known medicine FELDENE which is a major once-a-day non-steroidal anti-inflammatory drug developed by Pfizer Pharmaceuticals to treat arthritis. The solvent species being released from the stack was dimethyl formamide. Data show very low concentration of solvents (in mgr m^{-3}) at both process exhaust, after solvent recuperation, and plant stack outlet with homogeneous emission values during the 24 hour monitored.

An option in the front panel also enables the operator to use the virtual instrument as if it were a chart recorder, enabling the printout of the data traces at the end of each half hour. Only the data corresponding to the active detectors appears in the printout. This is very useful when the synthesis processes are being tuned to give optimum performance.

Figure 6.14: Daily hardcopy report generated by the Continuous Monitoring VI.
The number of detectors that appear in the final printout can be selected individually by the
user. Process parameters and input channel characteristics which are set by the operator
are also displayed in the document print-out (Courtesy of Pfizer Pharmaceuticals).

OSP 2	Report Date: "Monday, June 5, 1995"			
Piroxicam I				
Printout Time	12:45		Detector 2	Detector 3
Time	1/2 Hour No.		Exhaust	Stack
0:30	1		18	1
1:00	2		18	1
1:30	3		16	1
2:00	4		16	1
2:30	5		17	1
3:00	6		16	1
3:30	7		16	1
4:00	8		16	1
4:30	9		16	1
5:00	10		15	1
5:30	11		16	1
6:00	12		15	1
6:30	13		17	1
7:00	14		15	1
7:30	15		14	1
8:00	16		16	1
8:30	17		16	1
9:00	18		16	1
9:30	19		16	1
10:00	20		15	1
10:30	21		15	1
11:00	22		15	1
11:30	23		15	1
12:00	24		15	1
12:30	25		15	1
13:00	26		15	1
13:30	27		15	1
14:00	28		15	1
14:30	29		20	1
15:00	30		19	1
15:30	31		15	2
16:00	32		24	1
16:30	33		20	1
17:00	34		17	1
17:30	35		19	1
18:00	36		18	1
18:30	37		19	1
19:00	38		19	1
19:30	39		18	1
20:00	40		16	1
20:30	41		16	1
21:00	42		17	1
21:30	43		17	1
22:00	44		17	1
22:30	45		17	1
23:00	46		15	1
23:30	47		14	1
24:00	48		15	1
Continuous Monitoring Ver. 2.1			*Pfizer Pharmaceuticals*	

6.4.3 System Performance

The virtual instrument described above is used by Pfizer Pharmaceuticals for the continuous monitoring of the emissions through the stacks of the total amount of organics after the solvent recuperation process.

The site at Ringaskiddy has three different synthesis plants, being each of them equipped with an identical Continuous Monitoring System with suitable parameters to match the synthesis characteristics of the process being carried out in the plant. The high intuitiveness of the software enables process workers, with little or no technical training in computers, to be able to operate and obtain data from the system when required for process operations.

The daily hardcopy reports are daily retrieved from the systems and filed in the environmental laboratory as proof of emissions. Datafiles are also retrieved from the system's hard drive and imported into Lotus 1-2-3 spreadsheet for WINDOWS for generation of the weekly, monthly and yearly statistics which must be reported to the Environmental Control Agency (EPA).

Figure 6.15 shows a typical Lotus spreadsheet screen during the statistical treatment and report generation process of the data provided by the monitoring system in the OSP 1 synthesis unit. An important advantage of using this kind of approach for continuous monitoring is that emissions can be traced back through the data to the day and time they happened.
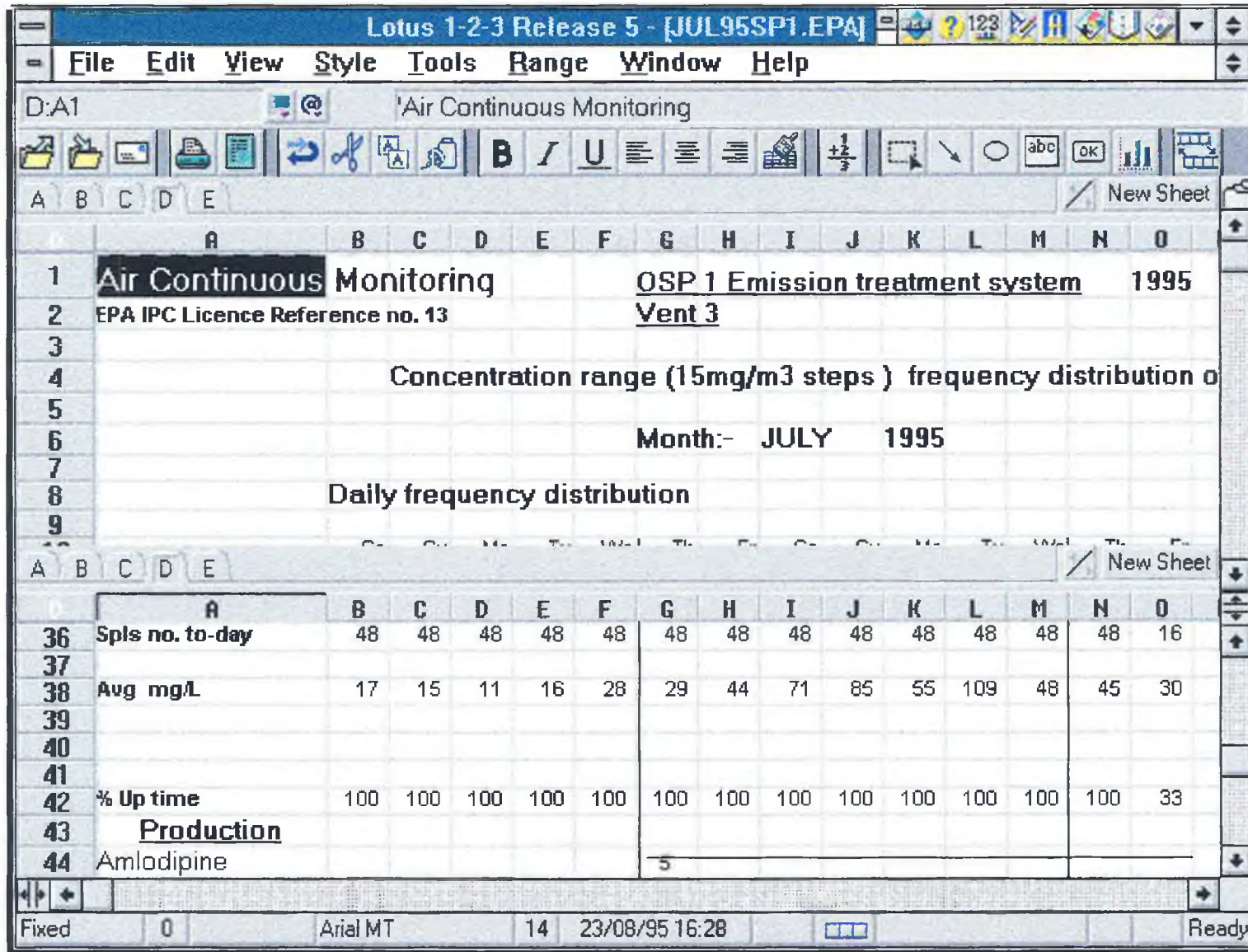
Figure 6.15: Lotus 1-2-3 for WINDOWS spreadsheet during data processing. Data obtained from the Continuous Monitoring System can be directly imported into commercial packages for further processing and report generation (Courtesy of Pfizer Pharmaceuticals).

Chapter 6: LabVIEW Applications

For example, apparent high average emissions of solvents during a particular day (109 mgr m^{-3}) can be detected on Tuesday, July 11th; 1995 (Figure 6.15). This value is a composition of the 48 samples taken at half hour intervals during that day, and retrieval of these values can help to identify whether there was a continuous moderately high emission of organics throughout the day, or if the high value was caused by a discrete event (e.g. valve/vent operation), and if so, at what time of the day this took place.

6.5 *References*

[1] Sáez de Viteri, F. J.; Diamond, D. *Anal Proc., Anal. Comm.* **1994**, *(31)*, 229-232.

[2] Wu, X.; Patterson, D. A.; Butler, L. G. *Rev. Sci. Instrum.* **1993**, *(64)*, 1235-1238.

[3] Abdel-Aal, R. E. *Meas. Sci. Technol.* **1992**, *3*, 1133-1140.

[4] Stryjewsky, W. J. *Rev. Sci. Instrm.* **1991**, *(62)*, 1921-1925.

[5] David, F.: Ouguenoune, H.; Boylos, A.; Papadopoulos, N. *Anal. Chim. Acta* **1994**, *292*, 297-304.

[6] David, F.; Papadopoulos, N. *Electroanalysis* **1991**, *3*, 721-725.

[7] Shear, J. B.; Colón, L. A.; Zare, R. N. *Anal. Chem.* **1993**, *(65)*, 3708-3712.

[8] Gregory, M. E.; Keay, P. J.; Dean, P.; Bulmer, M.; Thornhill, N. F. *J. Biotechnol.* **1994**, *33*, 233-241.

[9] Abdel-Aal, R. E. *Meas. Sci. Technol.* **1992**, *3*, 959-968.

[10] Barker, P. G. *Anal. Proc.* **1991**, *28*, p110-115.

[11] Korth, P. *EDN* **1993**, *Oct.*, 201-204.

[12] Conquergood, S. *I&CS* **1993**, *Jan.*, 68-70.

[13] Kataky, R.; Nicholson, P. E.; Parker, D.; Covington, A. K. *Analyst* **1991**, *116*, 153-140.

Appendix A: "Amoeba" QB Code

```
SUB amoeba
    mp = ndim + 1
    np = ndim
    alpha = 1!
    beta = .5
    gamma = 2!
    itmax = 10000
    mpts = ndim + 1
    iter = 0
1000 ilo = 1
    IF y(1) > y(2) THEN
        ihi = 1
        inhi = 2
    ELSE
        ihi = 2
        inhi = 1
    END IF
    FOR i = 1 TO mpts
    IF y(i) < y(ilo) THEN ilo = i
        IF y(i) > y(ihi) THEN
            inhi = ihi
            ihi = i
        ELSEIF y(i) > y(inhi) THEN
            IF i <> ihi THEN inhi = i
        END IF
    NEXT
    rtol = (y(1) + y(2) + y(3) + y(4) + y(5)) / 5
    PRINT min
    IF rtol < ftol THEN EXIT SUB
    IF iter = itmax THEN
        PRINT "Amoeba exceeding maximum
iterations"
        STOP

    END IF
    iter = iter + 1
    FOR j = 1 TO ndim
        pbar(j) = 0
    NEXT
    FOR i = 1 TO mpts
        IF i <> ihi THEN
            FOR j = 1 TO ndim
                pbar(j) = pbar(j) + p(i, j)
            NEXT
        END IF
    NEXT
    FOR j = 1 TO ndim
        pbar(j) = pbar(j) / ndim
        pr(j) = (1! + alpha) * pbar(j) - alpha *
p(ihi, j)
    NEXT
    CALL minim(pr(), min)
    ypr = min
    IF ypr <= y(ilo) THEN
        FOR j = 1 TO ndim
            prr(j) = gamma * pr(j) + (1! -
gamma) * pbar(j)
        NEXT
        CALL minim(prr(), min)
        yprr = min
        IF yprr < y(ilo) THEN
            FOR j = 1 TO ndim
                p(ihi, j) = prr(j)
            NEXT
            y(ihi) = yprr
        ELSE
            FOR j = 1 TO ndim
```

```
                p(ihi, j) = pr(j)                      FOR j = 1 TO ndim
          NEXT                                              p(ihi, j) = pr(j)
          y(ihi) = ypr                                 NEXT
      END IF                                           y(ihi) = ypr
      ELSEIF ypr >= y(inhi) THEN                  END IF
          IF ypr < y(ihi) THEN                    GOTO 1000
              FOR j = 1 TO ndim              END SUB
                  p(ihi, j) = pr(j)
              NEXT
              y(ihi) = ypr
          END IF
          FOR j = 1 TO ndim
              prr(j) = beta * p(ihi, j) + (1! - beta)
* pbar(j)
          NEXT
          CALL minim(prr(), min)
          yprr = min
          IF yprr < y(ihi) THEN
              FOR j = 1 TO ndim
                  p(ihi, j) = prr(j)
              NEXT
              y(ihi) = yprr
          ELSE
              FOR i = 1 TO mpts
                  IF i <> ilo THEN
                      FOR j = 1 TO ndim
                          pr(j) = .5 * (p(i, j) +
p(ilo, j))
                          p(i, j) = pr(j)
                      NEXT
                      CALL minim(pr(), min)
                      y(i) = min
                  END IF
              NEXT
          END IF
      ELSE
```

Appendix B: FIA Injection Port Diagram

Figure B.1: Diagram of the autoinjector used for the FIA system.
a) General tubing connections. and the alternative paths followed by sample and carrier while loading (b) or injecting.(c).
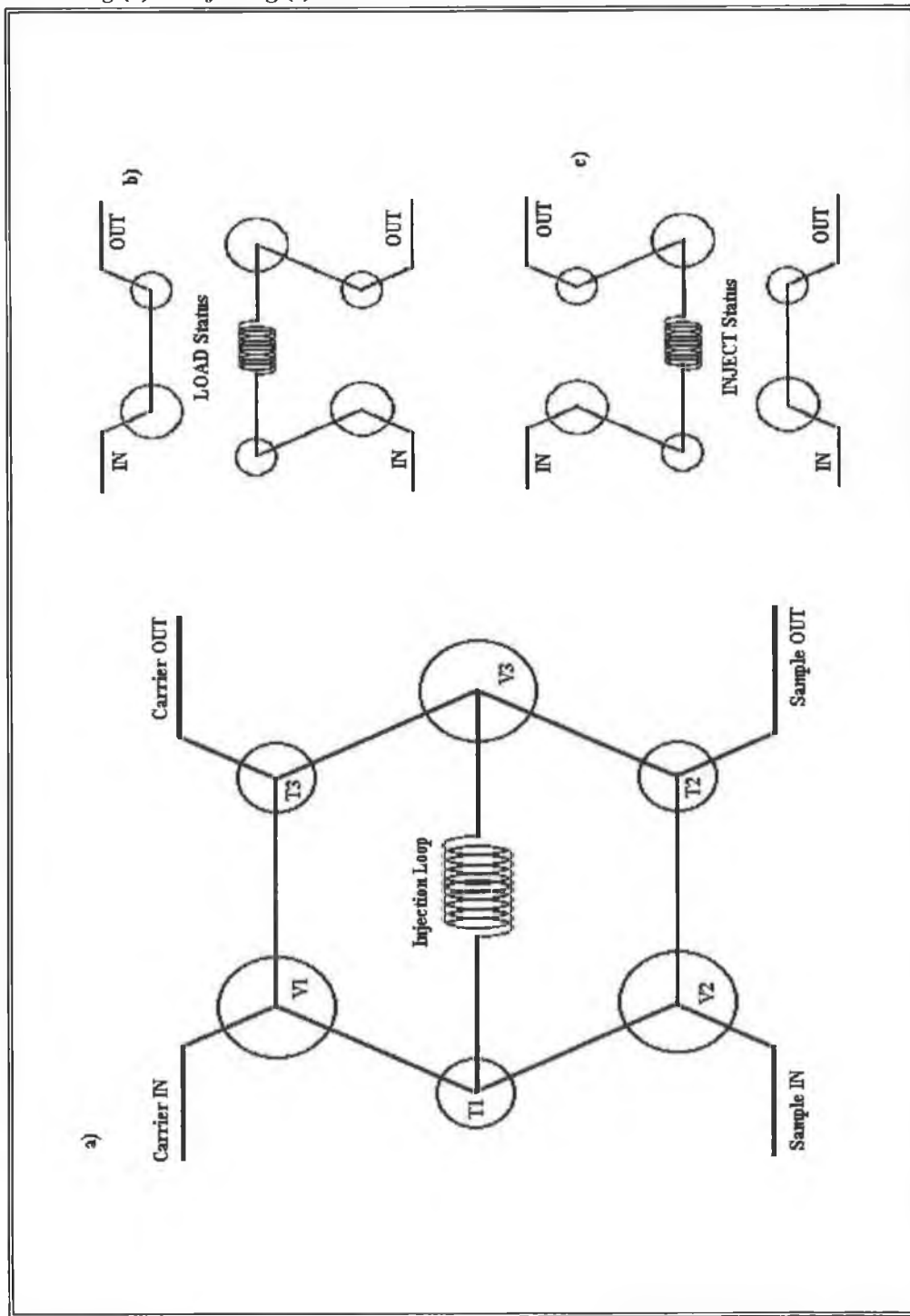
Appendix C: Microdialysis Manifold Diagram

Figure C.1: Diagram of the tubing connections in the microdialysis manifold.
a) General overview of the connections. b) Flow redirection for sample analysis. c) Calibration with the standard high. d) Calibration with the standard low. e) Syringe emptying or refilling.
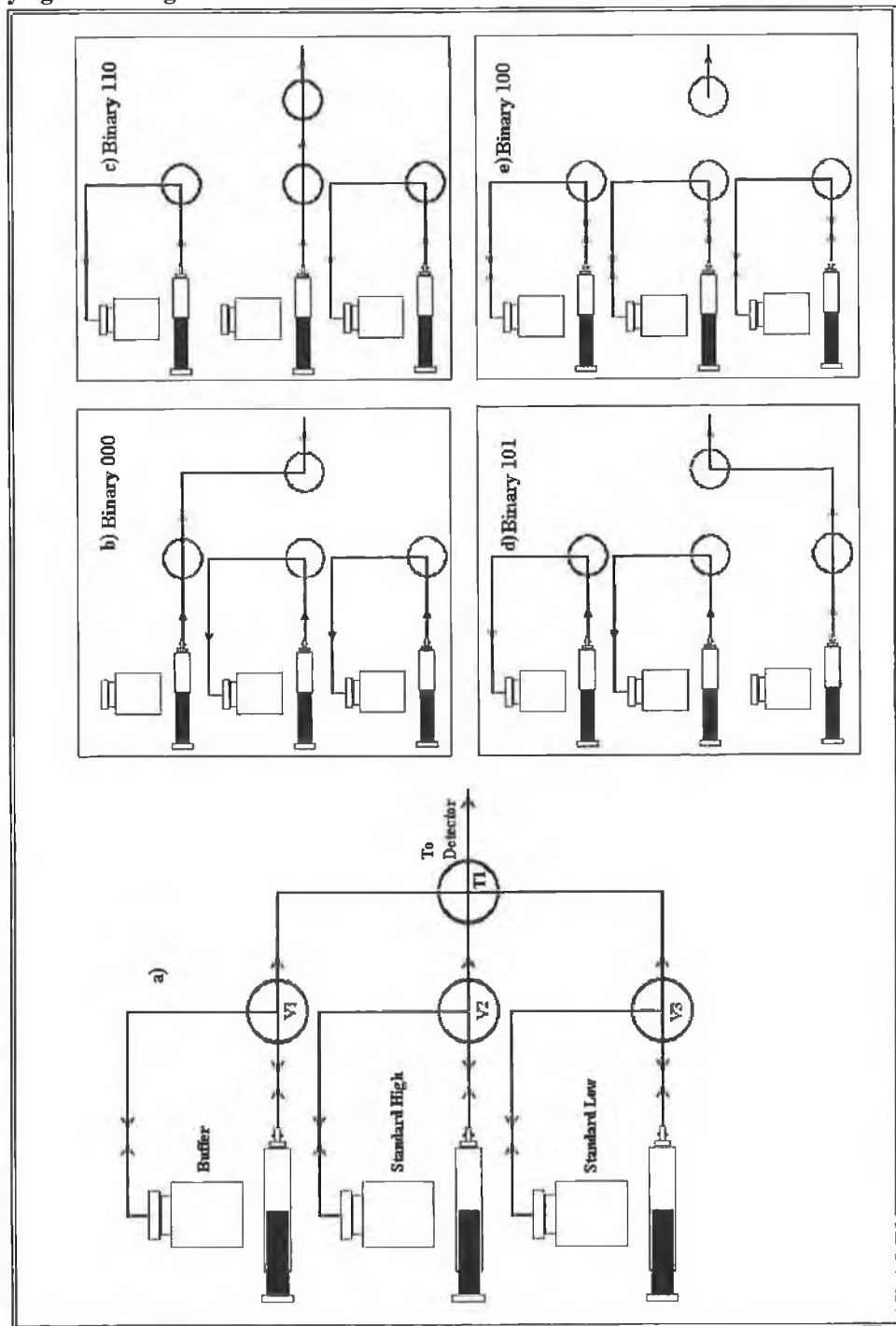
Appendix D: VI's Electronic Diagrams

Figure D.1: Electronic circuit for the FIA system in Section 6.2.
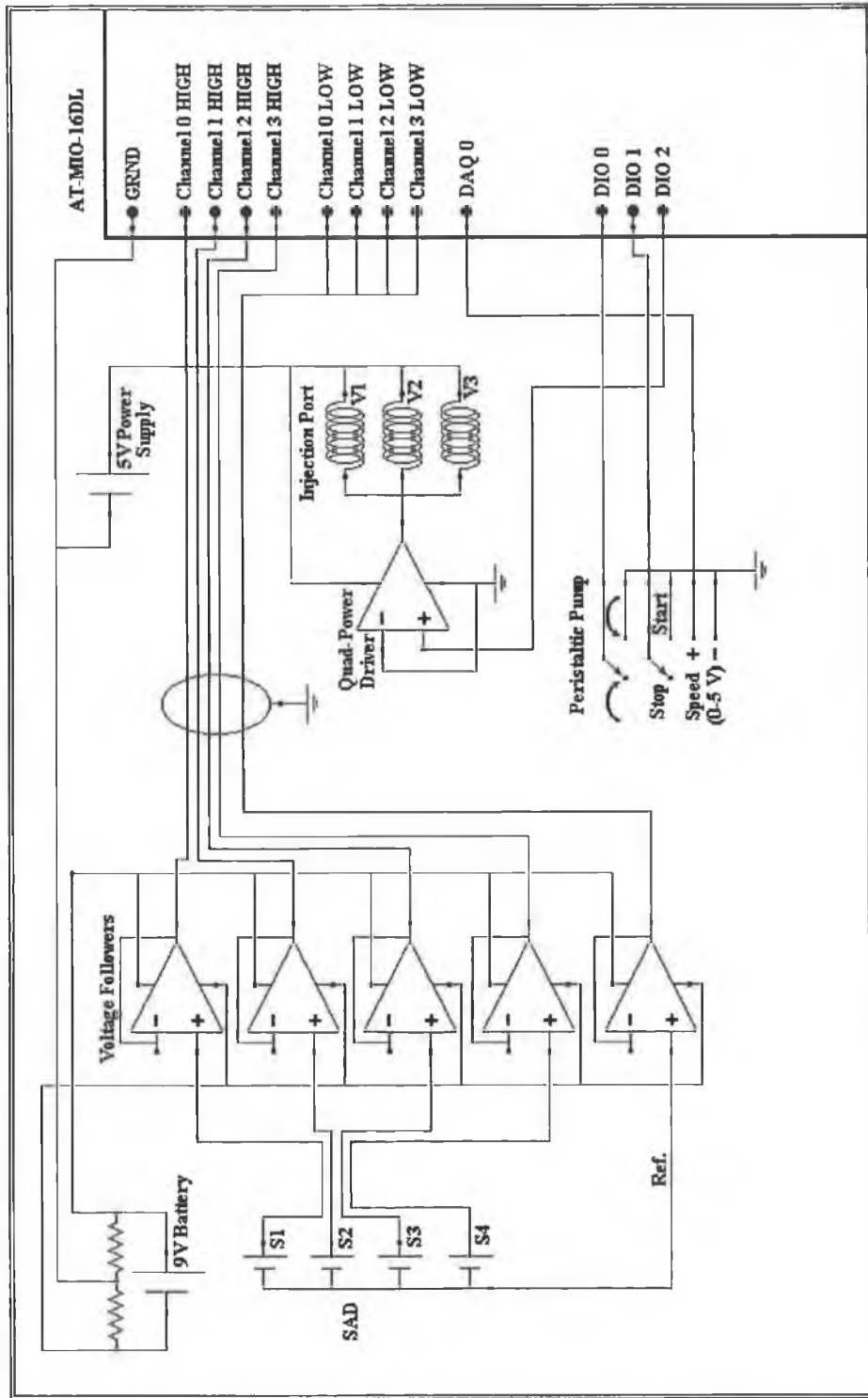
Figure D.2: Electronic diagram for the microdialysis system as described in Section 6.3.
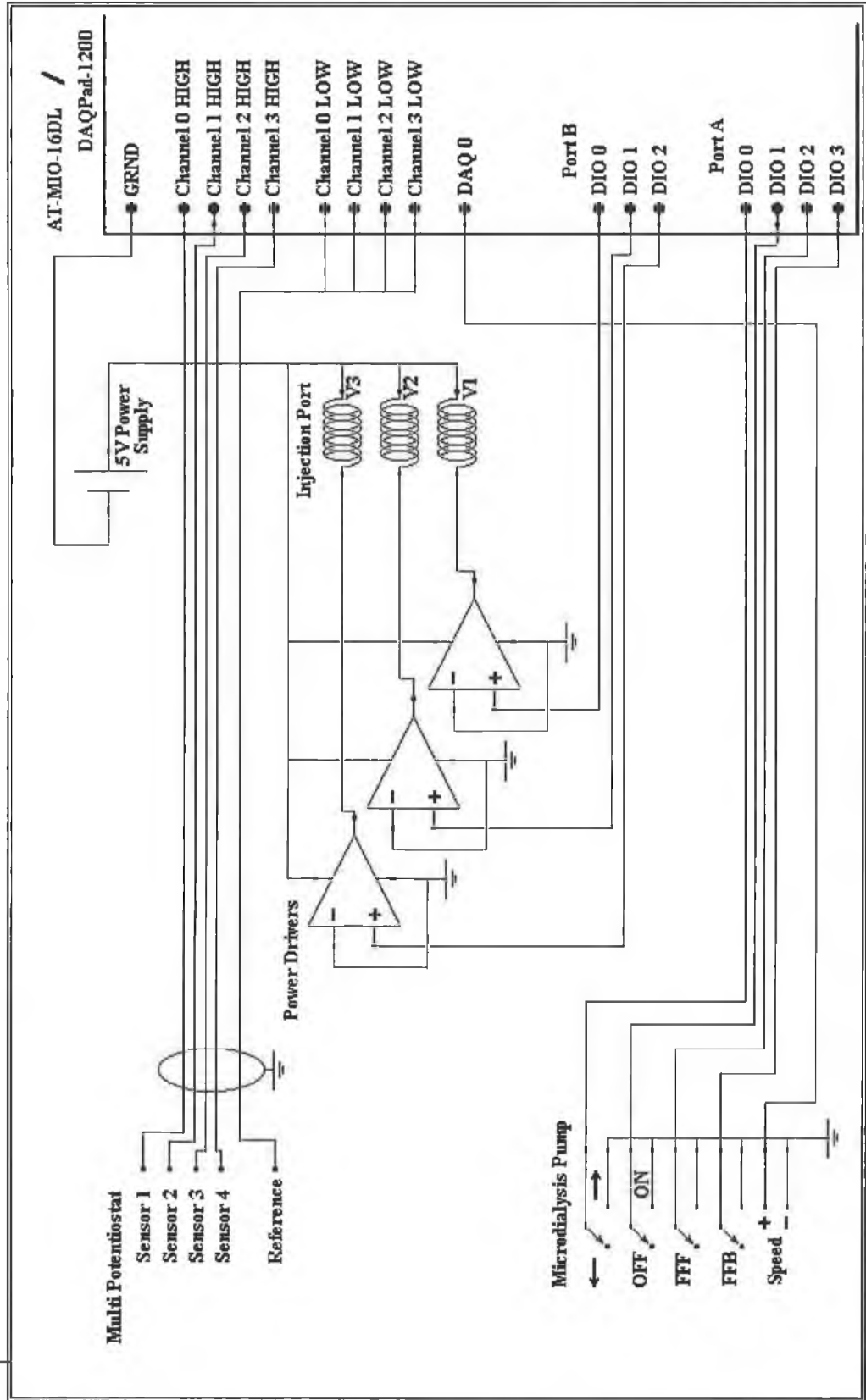
Figure D.3: Diagram of the electrical connections for the Continuous Monitoring VI (Section 6.4).
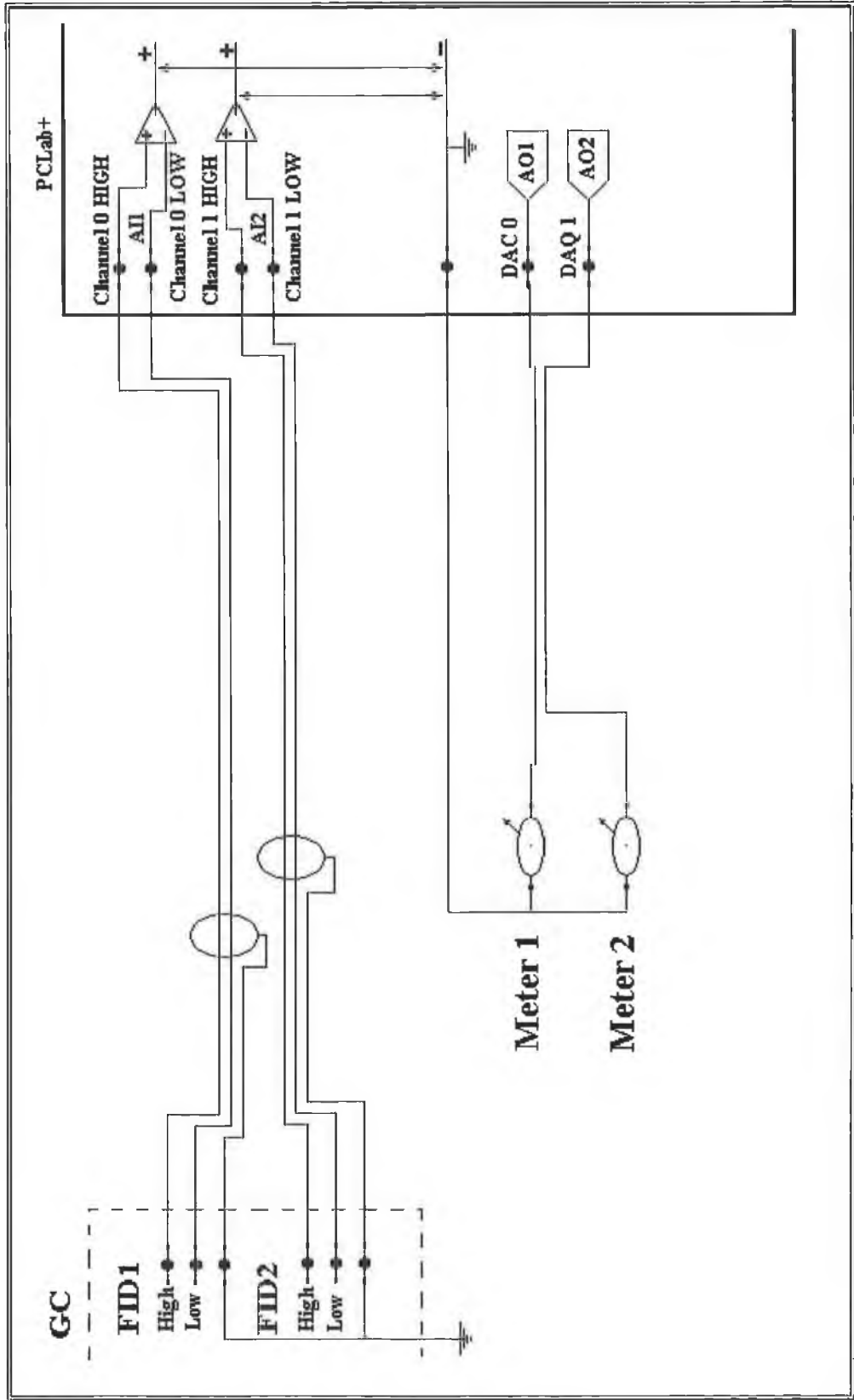
Appendix E: Top Hierarchy VI Software

Figure E.1: Top hierarchy diagram for the FIA acquisition and control software (Section 6.2).

Figure E.2: Code diagram corresponding to the Micodialysis Control System VI (Section 6.3).
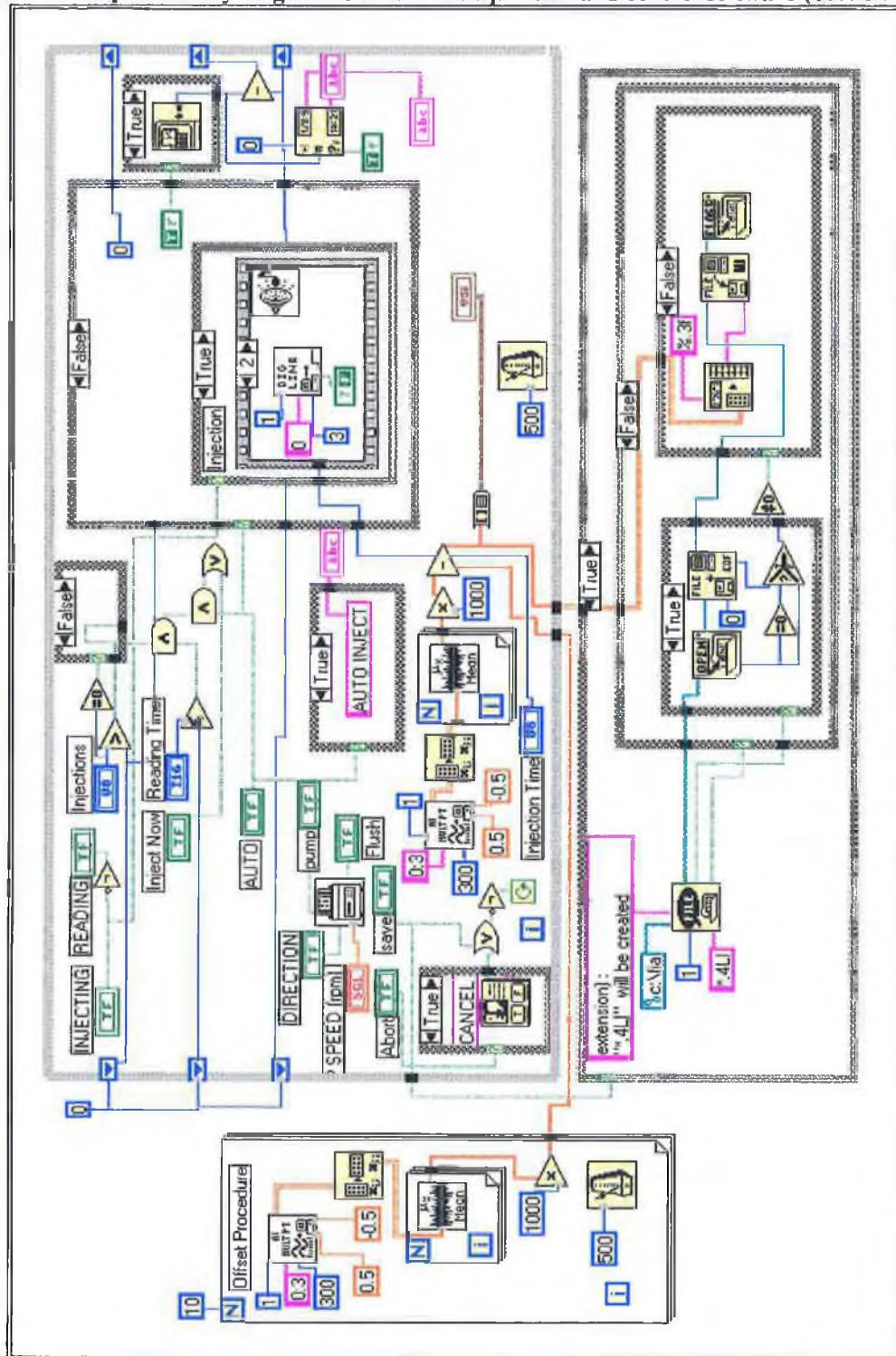
Figure E.3: Continuous Monitoring top hierarchy code diagram (Section 6.4).
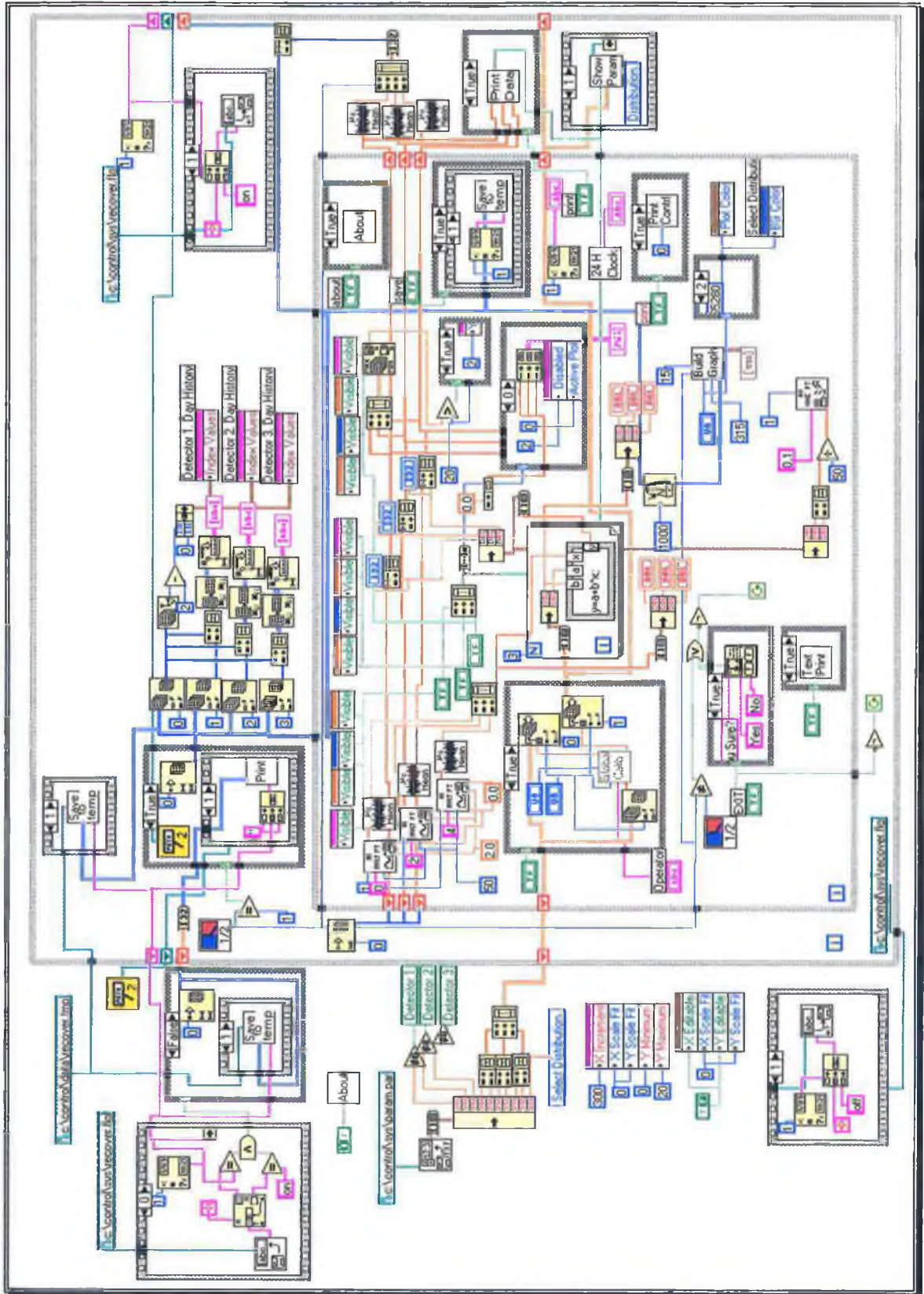
Appendix F: Data Acquisition Board Specifications

Table F.1: Specifications and connector pinouts for the AT-MIO-16 I/O card series (National Instruments).

Specifications
Typical for 25° C unless otherwise noted
Analog Input
Input Characteristics
Number of channels .... 16 single-ended or 8 differential, software selectable
Type of ADC .... Successive approximation
Resolution .... 16 bits, 1 in 65,536
Maximum sampling rate .... 100 kS/s guaranteed
Input signal ranges

Board Gain (Software Selectable)	Voltage Range (Software Selectable)	
	±10 V	0 to 10 V
1	±10 V	0 to 10 V
2	±5 V	0 to 5 V
5	±2 V	0 to 2 V
10	±1 V	0 to 1 V
20	±0.5 V	0 to 0.5 V
50	±0.2 V	0 to 0.2 V
100	±0.1V	0 to 0.1 V

Input coupling .... DC
Maximum working voltage (signal + common mode) .... Each input should remain within ±11 V of AIGND
Overvoltage protection .... ±25 V powered on, ±15 V powered off
Inputs protected .... ACH<0..15>, AISENSE
FIFO buffer size .... 512 samples
Data transfers .... DMA, interrupts, programmed I/O
DMA modes .... Single transfer, EISA demand
Configuration memory size .... 512 words
Transfer Characteristics
Relative accuracy .... ±0.75 LSB typical, ±1 LSB maximum
DNL .... ±0.5 LSB typical, ±1 LSB maximum
No missing codes .... 16 bits, guaranteed
Offset error
    Pregain error after calibration .... ±3 μV maximum
    Pregain error before calibration .... ±2.2 mV maximum
    Postgain error after calibration .... ±76 μV maximum
    Postgain error before calibration .... ±102 mV maximum
Gain error (relative to calibration reference)
    After calibration .... ± 30.5 ppm of reading maximum
    Before calibration .... ± 2,150 ppm of reading maximum
    Gain ≠ 1 with gain error adjusted to 0 at gain = 1 .... ± 200 ppm of reading
Amplifier Characteristics
Input impedance
    Normal, powered on .... 100 GΩ in parallel with 100 pF
    Powered off .... 820 Ω minimum
    Overload .... 820 Ω minimum
Input bias current .... ±1 nA
Input offset current .... ± 2 nA
CMRR (all gains) .... 107 dB typical, 94 dB minimum, DC to 60 Hz
Dynamic Characteristics
Bandwidth .... 255 kHz, all gains
Settling time, all gains and ranges

Accuracy		
±0.00076%	±0.0015%	±0.0061%
(±0.5 LSB)	(±1 LSB)	(±4 LSB)
40 μs max	20 μs max	10 μs max

System noise (including quantization error)

Gain	±10 V Range	0 to 10 V Range
1 to 10	0.6 LSB rms	0.8 LSB rms
20	0.7 LSB rms	1.1 LSB rms
50	1.1 LSB rms	2.0 LSB rms
100	2.0 LSB rms	3.8 LSB rms

Dynamic range .... 91.7 dB, ±10 V input with gain 1 to 10
Crosstalk .... -70 dB, DC to 100 kHz
Stability
Recommended warm-up time .... 15 minutes
Offset temperature coefficient
    Pregain .... ±5 μV/°C
    Postgain .... ±120 μV/°C
Gain temperature coefficient .... ±8 ppm/°C
Onboard calibration reference
    Level .... 5.000 V (±2 mV) (actual value stored in EEPROM)
    Temperature coefficient .... 2 ppm/°C maximum (10 pV/°C)
    Long-term stability .... 15 ppm/√1,000 h (75 μV/√1,000 h)
Analog Output
Output Characteristics
Number of channels .... 2,048 samples
Resolution .... 16 bits, 1 in 65,536
Maximum update rate .... 100 kS/s
Type of DAC .... Double-buffered multiplying
FIFO buffer size .... 2048 samples

Data transfers .... DMA, interrupts, programmed I/O
DMA modes .... Single transfer
Transfer Characteristics
Relative accuracy (INL)
    Bipolar range .... ±2 LSB typical, ±4 LSB maximum
    Unipolar range .... ±4 LSB typical, ±8 LSB maximum
DNL .... ±0.5 LSB max
Monotonicity .... 16 bits, guaranteed
Offset error
    After calibration .... ±305 μV maximum
    Before calibration .... ±8.15 mV maximum
Gain error (relative to internal reference)
    After calibration .... ±61 ppm maximum
    Before calibration .... ±1,820 ppm maximum
Gain error (relative to external reference) .... ±1,500 ppm, not adjustable
Voltage Output
Ranges .... ±10 V, or 0 to 10 V, software selectable
Output coupling .... DC
Output impedance .... 0.3 Ω
Current drive .... ±5 mA maximum
Load impedance .... 2 kΩ min, 1,000 pf maximum
Protection .... Short-circuit protected
Power-on state .... 0 V (±5 mV)
External reference input
    Range .... ±18 V
    Overvoltage protection .... ±30 V, powered on or off
    Input impedance .... 10 kΩ
    Bandwidth (-3 dB) .... DC to 300 kHz
Dynamic Characteristics
Settling time to ±0.003% FSR for 20 V step ... 10 μs
Slew rate .... 5 V/μs
Noise .... 50 μV rms, DC to 1 MHz
Stability
Offset temperature coefficient .... 50 μV/°C
Gain temperature coefficient
    Internal reference .... ±7.3 ppm/°C
    External reference .... ±7.3 ppm/°C
Onboard calibration reference level .... 5.000 V (±2 mV) (actual value stored in EEPROM)
Temperature coefficient .... ±2 ppm/°C maximum
Long-term stability .... ±15 ppm/√1,000 h
Digital I/O
Number of channels .... 8 I/O
Compatibility .... TTL
Digital logic levels

Level	Minimum	Maximum
Input low voltage	0 V	0.8 V
Input high voltage	2.0 V	6.0 V
Input low current (V_{in}=0.8 V)	—	-250 pA
Input high current (V_{in}=2.4 V)	—	250 pA
Output low voltage (I_{out}= 24 mA)	—	0.5 V
Output high voltage (I_{out}= -2.6 mA)	2.4 V	—

Power-on state .... Tri-state
Data transfers .... Programmed I/O
Timing I/O
Number of channels .... 3 counter/timers, 1 frequency scaler
Resolution
    Counter/timers .... 16 bits
    Frequency scalers .... 4 bits
Compatibility .... TTL, gate and source pulled high with 4.7 kΩ resistors
Base clocks available .... 5 MHz, 1 MHz, 100 kHz, 10 kHz, 1 kHz, and 100 Hz
Base clock accuracy .... ±0.01%
Maximum source frequency .... 6.897 MHz
Minimum source pulse duration .... 70 ns
Minimum gate pulse duration .... 145 ns
Data transfers .... Programmed I/O
Triggers
Digital Trigger
Compatibility .... TTL
Response .... Falling edge
Pulse width .... 50 ns minimum
RTSI
Trigger lines 7
Clock skew .... 6 ns typ, 21 ns maximum
Serial links .... 1 full-duplex
Serial transfer rate .... 10 Mb/s
Bus Interface .... Slave
Power Requirement
+5 VDC (±5%) .... 2.0 A
Power available on rear connector .... +4.65 V to +5.25 V at 1 A
Physical
Dimensions .... 33.8 by 11.4 cm (13.3 by 4.5 in.)
I/O connector .... 68-pin male SCSI-II type or 50-pin male
Environment
Component operating temperature .... 0° to 55° C
Component storage temperature .... -55° to 150° C
Relative humidity .... 5% to 90% noncondensing

AT-MIO-16D I/O Connector Pin Assignment

AT-MIO-16 I/O Connector

Table F.2: Specifications and connector pinouts for the DAQPad-1200 I/O module (National Instruments).

Specifications
Typical for 25° C unless otherwise noted
Analog Input
Input Characteristics
Number of channels .... 8 single-ended, 4 differential, software selectable
Type of ADC.. Successive-approximation
Resolution .... 12 bits, 1 in 4,096
Maximum single-channel sampling rate............................ 100 kS/s in EPP mode, 25 kS/s with standard Centronics port
Input signal ranges

Gain (Software Selectable)	Analog Input Signal Range (Software Selectable)	
	±5 V	**0 to 10 V**
1	±5 V	0 to 10 V
2	±2.5 V	0 to 5 V
5	±1 V	0 to 2 V
10	±500 mV	0 to 1 V
20	±250 mV	0 to 500 mV
50	±100 mV	0 to 200 mV
100	±50 mV	0 to 100 mV

Input coupling .... DC
Maximum working voltage (signal + common mode) ...... Average of inputs should remain within 7 V of ground
Overvoltage protection .... ±42 V powered on or off
Inputs protected .... ACH <0 . .7>
FIFO buffer size .... 2,048 samples
Data transfers .... Interrupts, programmed I/O
Transfer Characteristics
Relative accuracy .... ±0.5 LSB typical, ±1.5 LSB maximum
INL... ±0.5 LSB typical, ±1.0 LSB maximum
DNL.. ±0.5 LSB typical, ±1.0 LSB maximum
No missing codes .... 12 bits, guaranteed
Offset error (after calibration) .... ±(0.06 µV + 0.2 mV/gain) maximum
Gain error (relative to calibration reference) .... ±0.020% of reading maximum
Amplifier Characteristics
Input impedance
Normal powered on .... 1 MΩ in parallel with 5 pF
Powered off.. 4.7 kΩ in parallel with 5 pF
Overload... 4.7 kΩ in parallel with 5 pF
Input bias current... ±60 pA typical, 200 pA maximum
Input offset current .... ±20 pA typical, 100 pA maximum
CMRR

Gain	CMRR DC to 60 Hz
1	60 dB
2	66 dB
5 to 100	74 dB

Dynamic Characteristics
Analog input bandwidth   Settling time to full-scale step   System noise (including quantization error)

Gain	Single-Channel Bandwidth
1 to 10	400 kHz
20	200 kHz
50	80 kHz
100	40 kHz

Gain	Settling Time to 0.012% (±0.5 LSB) accuracy
1-10	12 µs
20	16 µs typical, 18 µs maximum
50	18 µs typical, 25 µs maximum
100	40 µs

Gain	Dither Off	Dither On
1 to 50	0.3 LSBrms	0.6 LSBrms
100	0.6 LSBrms	0.8 LS Brms

Stability
Recommended warm-up time... 15 minutes
Offset temperature coefficient.. ±(20 + 100/gain) µV/°C
Gain temperature coefficient... ±50 ppm/°C
Analog Output
Output Characteristics
Number of channels.. 2 voltage
Resolution .... 12 bits, 1 in 4,096
Maximum update rate .... 8 kS/s in EPP mode, 4 kS/s with standard Centronics port
Type of DAC... Double-buffered
Data transfers .... Interrupts, programmed I/O
Transfer Characteristics
Relative accuracy (INL).. ±0.25 LSB typical, ±0.5 LSB maximum
DNL.. ±0.25 LSB typical, ±0.75 LSB maximum
Monotonicity .... 12 bits, guaranteed
Offset error (after calibration) .... ±0.2 mV maximum
Gain error (after calibration) .... ±0.004% of reading maximum
Voltage Output
Ranges .... 0 to 10 V, ±5 V, software selectable
Output coupling .... DC
Output impedance... 0.2 Ω
Current drive .... ±2 mA maximum
Protection.. Short circuit to ground
Power-on state .... 0 V in bipolar mode, 5 V in unipolar mode
Dynamic Characteristics
Settling time to 0.012% FSR.. 6 µs for 10 V step
Slew rate.. 10 V/µs

Stability

Offset temperature coefficient .... ±60 µV/°C

Gain temperature coefficient .... ±10 ppm/°C

Digital I/O

Number of channels 24

Compatibility .... TTL.

Digital logic levels

Level	Minimum	Maximum
Input low voltage	0 V	0.8 V
Input high voltage	2.0 V	5 V
Input low current (V_{in} = 0.8 V)	–	-10 µA
Input high current (V_{in} = 2.4 V)	–	10 µA
Output low voltage (I_{out}= 1.7 mA)	–	0.45 V
Output high voltage (I_{out}= -200 µA)	2.4 V	–

Darlington drive output current (Ports B and C only)

(R_{EXT}=750 Ω, V_{EXT}=1.5 V) .... -1 mA minimum, -4 mA maximum

Handshaking .... 3-wire, 2 ports

Power-on state .... Inputs

Data transfers .... Programmed I/O, interrupts

Timing I/O

Number of channels .... 3 counter/timers

Resolution counter/timers .... 16 bits

Compatibility .... TTL, counter gate and clock inputs are pulled up with 10 kΩ resistors onboard

Base clocks available .... 2 MHz

Base clock accuracy 0.001%

Maximum source frequency .... 8 MHz

Minimum source pulse duration .... 60 ns

Minimum gate pulse duration .... 50 ns

Physical

Dimensions .... 14.6 by 21.3 by 3.8 cm (5.8 by 8.4 by 1.5 in.)

Weight .... 0.77 kg (1.7 lb)

I/O connectors

parallel port .... two 25-pin female D-sub connectors

I/O connector .... 50-pin male DIN C front I/O connector

Parallel port

Type .... EPP and Centronics

Throughput .... 180 kHz

Power Requirements

Voltage .... 9 to 42 VDC

Power .... 250 µA at 12 VDC

BP-1 Rechargeable Battery Pack

Output .... 12 V, 3.2 Ah

Run time with DAQPad-1200 .... 11 h

Dimensions .... 14.6 by 21.3 by 3.8 cm (5.8 by 8.4 by 1.5 in.)

Weight .... 1.92 kg (4 lb 3.5 oz)

Environment

Operating temperature .... 0° to 50° C

Storage temperature .... -55° to 150° C

Relative humidity .... 5% to 90% noncondensing

ACH0	1	2	ACH1
ACH2	3	4	ACH3
ACH4	5	6	ACH5
ACH6	7	8	ACH7
AI SENSE/AI GND	9	10	DAC0OUT
Analog Ground	11	12	DAC1OUT
Digital Ground	13	14	PA0
PA1	15	16	PA2
PA3	17	18	PA4
PA5	19	20	PA6
PA7	21	22	PB0
PB1	23	24	PB2
PB3	25	26	PB4
PB5	27	28	PB6
PB7	29	30	PC0
PC1	31	32	PC2
PC3	33	34	PC4
PC5	35	36	PC6
PC7	37	38	EXTTRIG
EXTUPDATE*	39	40	EXTCONV*
OUTB0	41	42	GATB0
OUTB1	43	44	GATB1
CLKB1	45	46	OUTB2
GATB2	47	48	CLKB2
+5V	49	50	Digital Ground

DAQPad-1200 I/O Connector

Table F.3: Specifications and connector pinouts for the Lab-PC+ I/O board (National Instruments).

Specifications

Typical for 25° C unless otherwise noted
Analog Input
Input Characteristics
Number of channels .... 8 single-ended or 4 differential, jumper selectable
Type of ADC .... Successive approximation
Resolution .... 12 bits, 1 in 4,096
Maximum sampling rate.. 83 kS/s
Input signal ranges

Board Gain (Software Selectable)	Board Range (Jumper Selectable)	
	±5 V	0 to 10 V
1	±5 V	0 to 10 V
2	±2.5 V	0 to 5 V
5	±1 V	0 to 2 V
10	±0.5 V	0 to 1 V
20	±0.25 V	0 to 0.5 V
50	±0.1 V	0 to 0.2 V
100	±0.05V	0 to 0.1 V

Input coupling .... DC
Overvoltage protection .... ±45 V powered on, ±45 V powered off
   Inputs protected... ACH<0..7>
FIFO buffer size... 512 samples
Data transfers .... DMA, interrupts, programmed I/O
DMA modes.. Single transfer
Transfer Characteristics
Relative accuracy.. ±1.0 LSB typical, ±1.5 LSB maximum
DNL.. ±0.5 LSB typical, ±1 LSB maximum
No missing codes .... 12 bits, guaranteed
Offset error
   Pregain error after calibration................................ Adjustable to 0 V
   Postgain error after calibration .... Adjustable to 0 V
Gain error (relative to calibration reference)
   After calibration... Adjustable to 0%
   Before calibration .... ±0.76% of reading (7,600 ppm) maximum
   Gain ≠ 1 with gain error adjusted to 0 at gain = 1 ..... ±0.5% of reading (500 ppm) maximum
Amplifier Characteristics
Input impedance... 0.1 GΩ in parallel with 45 pF
Input bias current... 150 pA
CMRR

Gain	CMRR at 60 Hz
1	75 dB
100	105 dB

Dynamic Characteristics
Bandwidth (-3 dB)... 400 kHz for gain = 1, 40 kHz for gain = 100
Settling time to full-scale step   System noise

Gain	Accuracy ±0.02% (±1 LSB)
≤10	14 µs
20, 50	20 µs
100	33 µs

Gain	±5 V Range
1	0.3 LSB rms
100	0.6 LSB rms

Stability
Recommended warm-up time....................................... 15 minutes
Offset temperature coefficient
   Pregain .... 450 µV/°C
   Postgain .... 10 µV/°C
Gain temperature coefficient .... ±50 ppm/°C
Analog Output
Output Characteristics
Number of channels 2
Resolution .... 12 bits, 1 in 4,096

Type of DAC		Double-buffered multiplying
Data transfers		Interrupts, programmed I/O

Transfer Characteristics

Relative accuracy (INL) bipolar range		±0.25 LSB typical, ±0.5 LSB maximum
DNL		±0.25 LSB typical, ±0.75 LSB maximum
Monotonicity		12 bits, guaranteed

Offset error

After calibration		Adjustable to 0 V
Before calibration		±37 mV maximum

Gain error (relative to internal reference)

After calibration		Adjustable to 0%
Before calibration		±0.5% of reading (3,900 ppm) maximum

Voltage Output

Ranges		±5 V, or 0 to 10 V, jumper selectable
Output coupling		DC
Output impedance		0.2 Ω maximum
Current drive		±2 mA maximum
Protection		Short to AGND
Power-on state		0 V for ±5 V range, 5 V for 0 to 10 V range

Dynamic Characteristics

Settling time to 0.012% FSR for 10 V step		7 μs
Slew rate		10 V/μs

Stability

Offset temperature coefficient		±30 μV/°C
Gain temperature coefficient internal reference		±10 ppm/°C

Digital I/O

Number of channels		24
Compatibility		TTL

Digital logic levels

Level	Minimum	Maximum
Input low voltage	0 V	0.8 V
Input high voltage	2.0 V	5 V
Input low current (V_{in}=0.8 V)	—	-10 pA
Input high current (V_{in}=2.4 V)	—	10 μA
Output low voltage (Iout = 1.7 mA)	—	0.45 V
Output high voltage	2.4 V	—

Darlington drive output current (Ports B and C only)

(R_{EXT}=750Ω, V_{EXT}=1.5 V)		1.0 mA minimum -40 mA maximum
Handshaking		3-wire (requires 1 port)
Power-on state		Configured as input
Data transfers		Interrupt, programmed I/O

Timing I/O

Number of channels		3 counter/timers
Resolution		16 bits
Compatibility		TTL, gate and source pulled high with 4.7 kΩ resistors
Base clocks available		2 MHz
Base clock accuracy		0.01%
Maximum source frequency		8 MHz
Minimum source pulse duration		60 ns
Minimum gate pulse duration		50 ns
Data transfers		Programmed I/O

Triggers

Digital Trigger

Compatibility		TTL
Response		Rising edge
Pulse width		250 ns

Bus Interface		Slave

Power Requirement

+5 VDC (±10%)		180 mA
+12 VDC (±5%)		80 mA
-12 VDC (±5%)		50 mA

Physical

Dimensions		16.5 by 9.9 cm (6.5 by 3.9 in.)
I/O connector		50-pin male

Environment

Operating temperature		0° to 70° C
Storage temperature		-55° to 150° C
Relative humidity		5% to 90% noncondensing

ACH0	1	2	ACH1
ACH2	3	4	ACH3
ACH4	5	6	ACH5
ACH6	7	8	ACH7
AISENSE/AIGND	9	10	DAC0OUT
Analog Ground	11	12	DAC1OUT
Digital Ground	13	14	PA0
PA1	15	16	PA2
PA3	17	18	PA4
PA5	19	20	PA6
PA7	21	22	PB0
PB1	23	24	PB2
PB3	25	26	PB4
PB5	27	28	PB6
PB7	29	30	PC0
PC1	31	32	PC2
PC3	33	34	PC4
PC5	35	36	PC6
PC7	37	38	EXTTRIG
EXTUPDATE*	39	40	EXTCONV*
OUTB0	41	42	GATB0
OUTB1	43	44	GATB1
CLKB1	45	46	OUTB2
GATB2	47	48	CLKB2
+5V	49	50	Digital Ground

Lab-PC+ I/O Connector

Table F.4: Specifications and connector pinouts for the RTI-815 acquisition board (Analog Devices).

SPECIFICATIONS

ANALOG INPUT SPECIFICATIONS

Number of Input Channels [2]	16 single-ended, 16 pseudo-differential, or 8 differential inputs. Expandable to 32 single-ended, 32 pseudo-differential, or 16 differential input channels using the Multiplexer Expansion Kit (ADI Part Number OA10)
A/D Resolution	12 bits (4096 counts)
A/D Ranges [2]	0 to +10 V, ±5 V, ±10 V (gain = 1)
A/D Input Codes [2]	Binary, two's complement
Instrumentation Amplifier Gain Ranges	1, 10, 100, 500 V/V (software selectable)

A/D Conversion Time [3]

(Converter only)	Typical	Maximum
RTI-800 and RTI-815	25 μs	35 μs
RTI-800-A and RTI-815-A	12 μs	15 μs
RTI-800-F and RTI-815-F	8 μs	9 μs

System Throughput [4]

RTI-800 and RTI-815	31.2 kHz
RTI-800-A and RTI-815-A	50.0 kHz
RTI-800-F and RTI-815-F (Rev 3.0)	66.6 kHz
RTI-800-F and RTI-815-F (Rev 4.0)	91.0 kHz

Measurement Accuracy	±0.02% of full-scale range (10 V) ±0.03% of full-scale range (1 V) ±0.12% of full-scale range (100 mv) ±0.25% of full-scale range (20 mV)
Input Overvoltage Protection	35 V (powered), ±20 V (unpowered)
Input Impedance	>10⁶ ohms
Input Bias Current	±20 nA
Common Mode Voltage (CMV) (Includes Signal Voltage)	±10 V min.
Common Mode Rejection (CMR)	80 dB [5]
Linearity	±1/2LSB
Differential Nonlinearity	±1LSB max.
Temperature Coefficients Gain	±30 ppm/ C of full-scale range (10 V) ±100 ppm/ C of full-scale range (20 mV)
Offset	±10 ppm/ C of full-scale range (10 V) ±100 ppm/ C of full-scale range (20 mV)

ANALOG OUTPUT SPECIFICATIONS (RTI-815 ONLY)

Number of Output Channels	2
Output Voltage Ranges [2]	0 to +10 V, ±10 V @ 2 mA
D/A Resolution	12 bits (4096 counts)
Analog Output Accuracy	±0.02%
D/A Input Codes [2]	Binary, two's complement
Differential Nonlinearity [6]	±1LSB max.
Output Settling Time (Converter Only)	20 μs (to ±1/2LSB, +10 V step)
Temperature Coefficients Gain Offset	±15 ppm/ C of full-scale range ±25 μV/ C
Output Protection	Short-to-ground, continuous

DIGITAL I/O SPECIFICATIONS

Digital I/O	8-bit digital input port and 8-bit digital output port, polarity inverted for solid-state relay I/O subsystem compatibility (active low)
Input/Output Configuration	TTL-compatible
Input Signal Levels	V_{IH} = 2.0 V min. V_{IL} = 0.8 V max. I_{IH} = 20 μA, Vi = 2.7 V I_{IL} = -0.4 mA max.
Output Signal Levels	V_{OH} = 2.7 V min. V_{OL} = 0.5 V max. I_{OH} = -0.4 μA max. I_{OL} = 8 mA max.

TIME-RELATED DIGITAL I/O SPECIFICATIONS

Number of Counter/Timer Channels [7]	3
Modes of Operation	Event counting, frequency measurment, pulse output, time proportional outputs
Event Counting Maximum Count Rate Range	100 kHz 65,531 (16 bits)

Frequency Measurement
Frequency Range   0 to 100 kHz
Gate Time   1 μs to 655.35 s (programmable)
Resolution   16 bits

Pulse Output (Single Pulse)
Pulse Range   2 μs to 655.35 s (programmable)
Resolution   16 bits

Time Proportional Outputs
Duty Cycle Range   0 to 100%
Period Range   1 μs to 655.35 s (programmable)

Time Base Accuracy   ±0.01%

Input/Output Configuration   TTL-compatible

A/D PACER CLOCK SPECIFICATIONS
Number of Channels [8]   1

Use   Time-based triggering for A/D conversions

Resolution   5 decades of 16-bit resolution

Period Range   3 μs to 655.35 s

SYSTEM CONFIGURATION SPECIFICATIONS
Bus Resource Utilization   Occupies one long slot in the IBM expansion bus

Address   DIP switch selectable I/O locations (16 consecutive bytes in 512 byte block 200H to 3FCH)

Data Acquisition Modes   High speed scan and collect A/D conversions require availability of DMA and interrupt. Polled status does not require this resource

Compatibility   IBM, Compaq, or other IBM-compatible backplane

PHYSICAL/ENVIRONMENTAL SPECIFICATIONS
I/O Connector
Digital I/O (J1)   34-pin male ribbon connector
Analog I/O (J2)   50-pin male ribbon connector

Dimensions
(including connector)   4.2 in. (10.6 cm) x 13.1 in. (33.2 cm) x 1 in. (2.54 cm)

Operating Temperature Range   0 to +70 C

Storage Temperature Range   –25 to +85 C

Relative Humidity   Up to 90% (non-condensing)

POWER
Power Consumption   +5 V @ 1.1 A

Connector J1 Pin Assignments

Pin	Function	Pin	Function
1	+5V	2	N/C
3	DIGITAL OUTPUT 0/MODULE 0	4	DIGITAL INPUT 0/MODULE 8
5	DIGITAL OUTPUT 1/MODULE 1	6	DIGITAL INPUT 1/MODULE 9
7	DIGITAL OUTPUT 2/MODULE 2	8	DIGITAL INPUT 2/MODULE 10
9	DIGITAL OUTPUT 3/MODULE 3	10	DIGITAL INPUT 3/MODULE 11
11	DIGITAL OUTPUT 4/MODULE 4	12	DIGITAL INPUT 4/MODULE 12
13	DIGITAL OUTPUT 5/MODULE 5	14	DIGITAL INPUT 5/MODULE 13
15	DIGITAL OUTPUT 6/MODULE 6	16	DIGITAL INPUT 6/MODULE 14
17	DIGITAL OUTPUT 7/MODULE 7	18	DIGITAL INPUT 7/MODULE 15
19	DIGITAL COMMON	20	DIGITAL COMMON
21	INPUT 0 (COUNTER/TIMER)	22	INPUT 2 (COUNTER/TIMER)
23	GATE 0 (COUNTER/TIMER)	24	GATE 2 (COUNTER/TIMER)
25	OUTPUT 0 (COUNTER/TIMER)	26	OUTPUT 2 (COUNTER/TIMER)
27	INPUT 1 (COUNTER/TIMER)	28	FREQ OUTPUT (COUNTER/TIMER)
29	GATE 1 (COUNTER/TIMER)	30	DIGITAL COMMON
31	OUTPUT 1 (COUNTER/TIMER)	32	DIGITAL COMMON
33	DIGITAL COMMON	34	DIGITAL COMMON

Connector J2 Pin Assignments

Pin	Function	Pin	Function
1	ANALOG COMMON	2	ANALOG COMMON
3	CHANNEL 0 (CHANNEL 0 HIGH)	4	CHANNEL 16 (CHANNEL 8 HIGH)
5	CHANNEL 1 (CHANNEL 1 HIGH)	6	CHANNEL 17 (CHANNEL 9 HIGH)
7	CHANNEL 2 (CHANNEL 2 HIGH)	8	CHANNEL 18 (CHANNEL 10 HIGH)
9	CHANNEL 3 (CHANNEL 3 HIGH)	10	CHANNEL 19 (CHANNEL 11 HIGH)
11	CHANNEL 4 (CHANNEL 4 HIGH)	12	CHANNEL 20 (CHANNEL 12 HIGH)
13	CHANNEL 5 (CHANNEL 5 HIGH)	14	CHANNEL 21 (CHANNEL 13 HIGH)
15	CHANNEL 6 (CHANNEL 6 HIGH)	16	CHANNEL 22 (CHANNEL 14 HIGH)
17	CHANNEL 7 (CHANNEL 7 HIGH)	18	CHANNEL 23 (CHANNEL 15 HIGH)
19	CHANNEL 8 (CHANNEL 0 LOW)	20	CHANNEL 24 (CHANNEL 8 LOW)
21	CHANNEL 9 (CHANNEL 1 LOW)	22	CHANNEL 25 (CHANNEL 9 LOW)
23	CHANNEL 10 (CHANNEL 2 LOW)	24	CHANNEL 26 (CHANNEL 10 LOW)
25	CHANNEL 11 (CHANNEL 3 LOW)	26	CHANNEL 27 (CHANNEL 11 LOW)
27	CHANNEL 12 (CHANNEL 4 LOW)	28	CHANNEL 28 (CHANNEL 12 LOW)
29	CHANNEL 13 (CHANNEL 5 LOW)	30	CHANNEL 29 (CHANNEL 13 LOW)
31	CHANNEL 14 (CHANNEL 6 LOW)	32	CHANNEL 30 (CHANNEL 14 LOW)
33	CHANNEL 15 (CHANNEL 7 LOW)	34	CHANNEL 31 (CHANNEL 15 LOW)
35	INPUT SENSE*	36	ANALOG COMMON
37	ANALOG COMMON	38	ANALOG COMMON
39	ANALOG OUTPUT 0	40	ANALOG OUTPUT 1
41	OUTPUT SENSE 0	42	OUTPUT SENSE 1
43	ANALOG OUTPUT COMMON	44	ANALOG OUTPUT COMMON
45	DIGITAL COMMON	46	DIGITAL COMMON
47	EXTERNAL CONVERT COMMAND	48	EXTERNAL TRIGGER
49	EXTERNAL CLOCK	50	DIGITAL COMMON